



University of HUDDERSFIELD

University of Huddersfield Repository

Bell, Andrew

Towards an integrated strategy for effective machine tool probing

Original Citation

Bell, Andrew (2021) Towards an integrated strategy for effective machine tool probing. Masters thesis, University of Huddersfield.

This version is available at <http://eprints.hud.ac.uk/id/eprint/35653/>

The University Repository is a digital collection of the research output of the University, available on Open Access. Copyright and Moral Rights for the items on this site are retained by the individual author and/or other copyright owners. Users may access full items free of charge; copies of full text items generally can be reproduced, displayed or performed and given to third parties in any format or medium for personal research or study, educational or not-for-profit purposes without prior permission or charge, provided:

- The authors, title and full bibliographic details is credited in any copy;
- A hyperlink and/or URL is included for the original metadata page; and
- The content is not changed in any way.

For more information, including our policy and submission procedure, please contact the Repository Team at: E.mailbox@hud.ac.uk.

<http://eprints.hud.ac.uk/>

Towards an integrated strategy for effective machine tool probing

Andrew Bell

A dissertation submitted to the University of Huddersfield in partial
Fulfilment of the requirements for the degree of
MSc by Research

April 2021

Abstract

Spindle-mounted probing systems on machine tools have become commonplace within manufacturing industry over the last ten years. On-machine probing (OMP) is often used as an automatic way of finding workpiece offsets on machine tools to allow better repeatability and more automated procedures. In more advanced engineering OMP may be used for in-process gauging, error correction or even final pass-off. They therefore form part of the measurement process that defines the overall quality control chain.

When used in production the probing system, and the machine that carries them, is subjected to harsh and variable conditions that are not experienced in a metrology room. This includes undergoing tool change routines, being affected by changing thermal conditions and contaminated by cutting debris. Unlike a traceable quality control department there is also the possibility of comparatively poor calibration techniques as this is considered a machine tool function. As a result, many companies do not use their OMP effectively, either because of a lack of understanding of capability or mistrust in the results due to a lack of understanding of uncertainties.

This research has provided the building blocks for a “bottom up” strategy to analyse influencing factors for OMP to enable end users to get reliable results with the lowest uncertainty for the desired function. Crucially, the research assumes different tolerance requirements for various functions that can be performed with such a probing system in order to avoid recommending onerous pre-requisite procedures where they are not needed.

The influencing factors for OMP are identified through literature review and a failure mode analysis conducted with experts from industry and academia. The magnitudes of the key factors and effects are then analysed through stated system specifications or experimentation on example machines. However, the dissertation concluded that all machine tools behave differently, and have different accuracy requirements. The main outcome of this work is, therefore, to determine which tests and checks are pre-requisite for OMP on any machine, depending upon their intended use. Ultimately, though, the work concludes that the unpredictability of thermal behaviour is likely to cause the greatest problems for on-machine probing, with a full understanding being required for reproducibility of measurement results from a machine tool.

Acknowledgements

I would like to express my thanks to my supervisors Professor Andrew Longstaff and Dr Simon Fletcher for the opportunity, encouragement, and advice throughout this study. My background is as a time-served machine tool programmer and user and more latterly an applications engineer. Undertaking this research project has opened my eyes to the rigour required in academic projects and I am grateful for the patience they have shown in helping me through the process.

I am grateful too to Machine Tool Technologies Ltd. for the training program delivered by them in collaboration with the University of Huddersfield. This gave me the grounding in the use of machine tool calibration instruments and understanding of measurement uncertainties that led to me undertaking this in-depth project.

Most importantly, thanks to my wife and children for their patience and support while I have been mastering the art of research and academic report writing.

Table of Contents

Abstract	i
Acknowledgements	ii
List of Acronyms.....	xv
Chapter 1 Introduction.....	1
1.1 Probing on machine tools.....	1
1.2 Machine tool accuracy	3
1.3 Relationship to coordinate measuring machines.....	4
1.4 Conformance.....	5
1.5 Timeliness.....	5
1.6 Summary.....	6
Chapter 2 Literature Review.....	6
2.1 Process Foundation	8
2.1.1 Machine tool thermal influences	9
2.1.2 Machine tool configurations.....	12
2.1.3 Machine tool geometry	13
2.1.4 Machine tool axis errors.....	14
2.1.5 Non-rigid errors.....	16
2.1.6 Errors of motion	17
2.1.7 Machine tool Calibration	17
2.1.8 Machine tool Calibration Equipment	17
2.1.8.1 Engineers Squares and straightedges for geometry.....	17
2.1.8.1.1 Square	18
2.1.8.1.2 Straight edge.....	19
2.1.8.2 Laser interferometer.....	20
2.1.8.3 XM60 multi-axis calibrator.....	23

2.1.8.4	Interferometer Environmental compensation.....	25
2.1.8.5	ETALON / laser tracers	26
2.1.8.6	Laser tracker.....	27
2.1.8.7	On-machine probing of artefacts.....	28
2.1.9	Machine geometric monitoring.....	28
2.1.9.1	Ball bar	29
2.1.10	Spindle/tool interface.....	31
2.1.10.1	HSK 69893	32
2.1.10.2	SK Din73381	32
2.1.11	Foundation process summary	32
2.2	Process setting layer	33
2.2.1	Probe errors.....	33
2.2.1.1	Stylus length.....	34
2.2.1.2	Hysteresis	34
2.2.2	Probe condition.....	34
2.2.3	Initial probe set up	34
2.2.4	Probe Calibration.....	34
2.2.4.1	Automatic calibration	35
2.2.4.2	Electronic system latency.....	35
2.2.5	Human error	35
2.2.6	Clamping	35
2.3	Methods of failure analysis.....	35
2.3.1	FMEA characteristics.....	36
2.3.2	FMEA prioritisation	36
2.4	Project Aim.....	39
2.5	Research Objectives	39
2.6	Scope.....	39
2.6.1	Machine tools	39
2.6.2	Probing function (workpiece/tool measurement).....	40
2.6.3	Workpiece interaction method (Tactile/non-contact).....	40
2.6.4	Probing strategy (Discrete-point/scanning).....	40
2.6.5	Thermal errors and modelling.....	40
2.7	Methodology.....	41

2.7.1	Background knowledge and informal influences.....	41
2.7.2	Formal methodology	41
2.7.2.1	Objective 1 & 2.....	41
2.7.2.2	Objective 3	42
2.7.2.3	Objective 4	42
2.8	Contributions	42
2.9	Summary.....	42
Chapter 3	On-machine probing FMEA	44
3.1	Methodology.....	44
3.2	Measurement modes for on-machine probing.....	45
3.2.1	Evaluating the machine	45
3.2.1.1	Machine geometric error measurement	45
3.2.1.2	Machine thermal error measurement.....	45
3.2.2	Part setting	46
3.2.2.1	Fixture location	46
3.2.2.2	Fixture orientation	46
3.2.2.3	Stock size check.....	46
3.2.2.4	Part location.....	46
3.2.2.5	Part orientation.....	47
3.2.3	In-process/post-process	47
3.2.3.1	Tool breakage.....	47
3.2.3.2	Re-datum during operation	47
3.2.3.3	Measure-cut.....	47
3.2.3.4	Final inspection	48
3.3	Failure Modes: Definition of “success” and “failure” for OMP	48
3.3.1	No results from probe (Failure to take a measurement)	49
3.3.2	Unacceptable measurement cycle time.....	49
3.3.3	A measurement is taken but the uncertainty unacceptably reduces the conformance zone.....	50
3.3.4	Bad measurement	50
3.4	Failure Mode Effects	51
3.5	Mechanisms (causes) of failure.....	52
3.6	Discussion.....	57

3.7	Summary.....	58
Chapter 4	Proposed framework	60
4.1	Key performance indicators.....	60
4.2	Framework	61
4.2.1	Initial approach	61
4.2.2	Final Approach	63
4.3	Down selection of machine tool quantification tests	65
4.3.1	Geometry tests	65
4.3.1.1	Straightness of linear motion errors and angular deviations of linear motions.....	65
4.3.1.2	Squareness between linear motions.....	65
4.3.2	Linear position error of linear motion tests.....	66
4.3.3	Angular errors of linear axes.....	66
4.3.4	Spindle Checks.....	66
4.3.4.1	Parallelism between the spindle axis and Z-Axis motion.....	66
4.3.4.2	Spindle Run Out	67
4.3.4.3	Tool-change repeatability	67
4.3.5	Machine tool thermal stability and effects	67
4.3.5.1	Environmental - ETVE.....	67
4.3.5.2	Spindle thermal distortion evaluation	68
4.3.5.3	Axis thermal distortion evaluation.....	68
4.3.5.4	Effects of spindle heat expansion on cold tools.	69
4.3.6	Alternative approach – gauge capability study	69
4.4	Machine tool benchmark monitoring	69
4.5	Creation of enabling part-programs.....	69
4.6	Summary.....	70
Chapter 5	Testing and discussion of results.....	71
5.1	Part program design.....	72
5.1.1	Part program structure – Example Repeatability of	72
5.2	Probing systems tests	74
5.2.1	Repeatability of probing	74
5.2.1.1	Z Axis single point with minimum movement	74
5.2.1.2	Z Axis single point with full stroke in Z.....	75
5.2.2	Effect of probe calibration	78

5.2.2.1	Measurement with uncalibrated probe.....	78
5.2.2.2	Measurement with calibrated probe.....	79
5.2.2.3	Repeatability of probe calibration	81
5.2.3	Effect of surface contamination (coolant).....	85
5.3	Machine geometric error influences	89
5.3.1	Effect of tool change repeatability.....	89
5.3.1.1	Tool change repeatability	90
5.3.2	Geometric error measurements.....	91
5.3.2.1	Y Axis XM60 geometric error graphs	91
5.3.2.2	X Axis XM60 geometric error graphs	92
5.3.2.3	Z Axis XM60 geometric error graphs.....	94
5.3.2.4	Geometric error graph comparisons.....	94
5.3.3	Ball bar results.....	99
5.3.3.1	XY Plane.....	99
5.3.3.2	History graphs from Machine D.....	103
5.3.4	Effect of calibration vs probing location	104
5.4	Thermal influences.....	114
5.4.1	Laser testing.....	116
5.4.2	Probing testing.....	120
5.4.2.1	Description of analysis	120
5.4.3	Typical temperature profile	122
5.5	Temperature and probing analysis.....	127
5.5.1	Probing when the machine has just been switched on (cold state)	127
5.5.1.1	Simulated machining from cold.....	127
5.5.1.2	Test performed on Machine B	130
5.5.2	Probing with only machine self-warming.....	133
5.5.2.1	Test performed on Machine B	135
5.5.3	Probing influenced by axis and spindle heating.....	137
5.5.4	Probing after simulated machining cycle	139
5.5.5	Probing after machining cycle with coolant.....	139
5.6	Discussion and summary	140
Chapter 6	Conclusions and further work	142
6.1	Discussion.....	142

6.2	Summary and conclusions	143
6.3	Further work.....	145
6.3.1	In-depth investigation of geometry and thermal effects	145
6.3.2	Other machine configurations.....	145
6.3.3	Expansion of the logic and “industrialising” the process	145
6.3.4	Tool measurement probes.....	146
6.3.5	Artefact.....	146
	References.....	146
	Appendix A Test list for a 3-axis machine.....	153
	Appendix B Machine descriptions.....	154
B.1	Machine A Cincinnati	154
B.2	Machine B Robodrill	154
B.3	Machine C Geiss.....	154
B.4	Machine D Hurco	155
B.5	Machine E Huron VX10.....	155
B.6	Machine F Hermle C22	155
	Appendix C Part programs.....	156
C.1	Main variable Probing Program.....	156
C.2	Probing Subroutine	168
C.3	Machining Positions	172
C.4	Axis Heating.....	172
C.5	Z Repeat	173
C.6	Z repeat with tool change.....	175
C.7	Probe Calibrate 19mm ring	177
C.8	Probe Calibrate 44mm ring	180
	Appendix D Failure mechanisms in probing.....	184
	Appendix E Probe calibration repeatability data	185
E.1	44 mm diameter ring	185
E.2	19 mm diameter ring	191

Table of Figures

Figure 1 Typical machine tool probes from a) Heidenhain [8], b) Renishaw [3]	2
Figure 2 Typical machine tool with probe systems	3
Figure 3 Different modelling approaches for machine tool accuracy [12].....	4
Figure 4 Influence of measurement uncertainty on zone where conformance is verified – modified from [16].....	5
Figure 5 Renishaw Productivity Process Pyramid™ [18]	7
Figure 6 manufacturing process timeline [19].....	8
Figure 7 DMU210 cooling fluid routing [28]	10
Figure 8 Linear positioning plot dominated by thermal expansion and showing drift	11
Figure 9 Cyclic error of chiller coming on and off	11
Figure 10 The twelve possible configurations of 3-axis vertical spindle machining centre [31]	13
Figure 11 “Angular and linear error motions of a component commanded to move along a (nominal) straight line trajectory parallel to the x-axis” [22].....	15
Figure 12 Angular errors affecting linear position [44].....	16
Figure 13 Various engineers squares and working faces [44].....	18
Figure 14 Effect of straightness on squareness measurement	19
Figure 15 Schematic of straight edge artefact supported on Airy points [46]	20
Figure 16 XL80 Optics L-R linear position, angular, straightness [courtesy Renishaw plc].....	21
Figure 17 Linear positioning optic set up [44].....	21
Figure 18 Typical XL80 linear positioning measurement set up	22
Figure 19 Renishaw XM60 on a machine.....	23
Figure 20 Comparison of linear positioning error measured in continuous and quasi-static measurement modes [40]	24
Figure 21 Renishaw EC10 (a) environmental compensation unit and (b) air temperature sensor	26
Figure 22 Multilateration and GPS [60]	27
Figure 23 Inora SRS [67].....	28
Figure 24 QC20w ball bar [69]	30

Figure 25 Typical ball bar set up	31
Figure 26 steep taper and hollow taper contact areas [71].....	32
Figure 27 Ten steps for an FMEA [84]	44
Figure 28 Mind map diagram of modes of operation for on-machine probes	45
Figure 29 Mind map diagram of failure modes for on-machine probing	49
Figure 30 Mind map diagram of failure effects	51
Figure 31 Top-level mind map of failure mechanisms when probing	52
Figure 32 Mechanisms - factory environment	53
Figure 33 Mechanisms – machine	54
Figure 34 Mechanisms – fixture	54
Figure 35 Mechanisms – workpiece.....	55
Figure 36 Mechanisms – location.....	55
Figure 37 Mechanisms – probe/stylus.....	56
Figure 38 Mechanisms – operator.....	56
Figure 39 Mechanisms – probing program.....	57
Figure 40 Mechanisms – analysis and reaction	57
Figure 41 Overall top-down approach	62
Figure 42: Proposed framework for an example mode of operation.....	64
Figure 43 a 44 mm setting ring gauge on the table of Machine A	71
Figure 44 Data graph for Z surface touch points with minimal Z axis movement	75
Figure 45 Data graph for Z surface touch points with 300mm Z axis movement.....	76
Figure 46 temperature graph 300mm Z movement.....	77
Figure 47: Temperature graph Z 300 mm movement – selected sensors.....	77
Figure 48 Ring gauge measurement with outdated calibration parameters (a) table of values, (b) deviation in the X- and Y-axis directions (c) polar plot.....	79
Figure 49 Ring gauge measurement with newly created calibration parameters (a) table of values, (b) deviation in the X- and Y-axis directions (c) polar plot	80
Figure 50 Ring gauge set up on Machine A	82
Figure 51 Summary of repeated results from 44 mm diameter ring	83
Figure 52 Temperature readings during measurement of 44 mm diameter ring	84
Figure 53 Summary of repeated results from 19 mm diameter ring	84

Figure 54 Temperature readings during measurement of 19 mm diameter ring	85
Figure 55 Graph showing change in Z surface measurement from coolant contamination.....	86
Figure 56 Z surface probe Line 1 -20 / +20 point Graph	87
Figure 57 Z surface probe Line 2 -20 / +20 point graph	87
Figure 58 Ring gauge with coolant held within dammed area (blu-tack)	88
Figure 59 Z surface probe - effect of coolant.....	88
Figure 60 Tool change repeatability graph	90
Figure 61 Tool change temperature graph.....	91
Figure 62 Y axis combined 6DoF graphs	92
Figure 63 X Axis combined 6DoF graphs 3 axis vertical machining centre	93
Figure 64 Z Axis combined 6DoF graphs	94
Figure 65 X Axis combined 6DoF graphs 3 axis vertical machining centre (Machine A)	95
Figure 66 Y Axis combined 6DoF graphs large gantry machine (Machine C).....	96
Figure 67 Y Axis combined 6DoF graphs 5 axis vertical machining centre (Machine D)	97
Figure 68 Y Axis combined 6DoF graphs 3 axis vertical machining centre (Machine E)	98
Figure 69 YRX graph from Figure 68 (Machine E).....	98
Figure 70 X Axis combined 6DoF graphs 5 axis vertical machining centre (Machine F)	99
Figure 71 ball bar graph XY 2500mm/min (Machine A).....	100
Figure 72 ball bar graph XY 250mm/min (Machine A).....	101
Figure 73 ball bar graph ZX 2500mm (Machine A)	102
Figure 74 ball bar graph ZX 250mm (Machine A)	102
Figure 75 XY plane circularity (Machine D).....	103
Figure 76 Positional deviation history graph (Machine D).....	104
Figure 77 Measurement order of ring gauges	105
Figure 78 G55 datum positions for each ring gauge	105
Figure 79 Measured error magnitude position 1X	107
Figure 80 Measured error magnitude position 2X	108

Figure 81 Measured error magnitude position 3X	109
Figure 82 Measured error magnitude position 1A	110
Figure 83 Measured error magnitude position 4Y	111
Figure 84 Measured error magnitude position 5Y	112
Figure 85 Measured error magnitude position 1Y	113
Figure 86 Summary chart of error magnitudes with standard deviation calculated	114
Figure 87 Assembly of the machine (view 1) [26].....	115
Figure 88 Assembly of the machine view 2 [26].....	115
Figure 89 X-axis heating test using laser on Machine B.....	117
Figure 90 Y-axis heating test using laser on Machine B.....	118
Figure 91 Z-axis heating test using laser on Machine B.....	119
Figure 92 Probing points for thermal tests.....	120
Figure 93 Label convention for probing spheres	121
Figure 94 Legend used for probe analysis	122
Figure 95 Ambient temperature graph.....	122
Figure 96 Legend used on following temperature graphs (unless otherwise given)	124
Figure 97 Temperature profile of machine over a 21-day period in February.....	125
Figure 98 Comparison of axis and spindle motor temperatures	126
Figure 99 Comparison of different sensors on the Z-axis.....	126
Figure 100 Comparison of spindle temperatures with ambient temperature inside the machine.....	127
Figure 101 Three-day graph of temperature (simulated machining)	128
Figure 102 Probing from cold start (area of interest A).....	129
Figure 103 Repeat of test the following day (area of interest B).....	130
Figure 104 Probing from cold on Machine B	131
Figure 105 Z-axis error on Machine B (from cold start).....	132
Figure 106 Y-axis error on Machine B (from cold start).....	132
Figure 107 Results for Machine A with Z-axis self-heating already completed	133
Figure 108 Second half of the test (failed).....	134
Figure 109 Approximated reconstruction of the test data showing missing data	134
Figure 110 Approximated reconstructed data	135

Figure 111 Machine B simulated cycle after self-heating	136
Figure 112 Z-axis error on Machine B	136
Figure 113 Effect of axis heating only (spindle only running from 6.5hours onwards)	137
Figure 114 Selected temperatures during “no spindle” test.....	138
Figure 115 Simulated cycle without spindle	138
Figure 116 Simulated machining cycle.....	139
Figure 117 Machining cycle with coolant.....	140
Figure 118 Mind map showing the different failure mechanisms in probing	184

Tables

Table 1 Renishaw OMP600 accuracy chart [72]	33
Table 2 Guidelines for severity ranking in design/product FMEAs [79]	37
Table 3 Guidelines for severity ranking in process/production FMEA [79]	38
Table 4 Mapping of failure modes to modes of operation.....	51
Table 5 Definition of conditions for framework	61
Table 6 Location of sensors on Machine A during analysis.....	123

List of Acronyms

CAD	Computer Aided Design
CAM	Computer Aided Manufacturing
CMM	Coordinate Measuring Machine
CNC	Computer Numerical Control
CTE	Coefficient of Thermal Expansion
DTI	Dial Test Indicator
OMP	On-machine Probing
OMM	On-machine measurement
PPP	Productive Process Pyramid™ [1]
QC20w	Renishaw wireless ball bar
SPOS	Spindle Positioning mode (Used in Sinumerik controllers)
XL80	Renishaw axis laser interferometer
XM60	Renishaw multi-axis laser calibrator

Chapter 1 Introduction

1.1 Probing on machine tools

Before the mid-1970s machine tools were predominantly used for metal cutting, and mostly controlled by manual methods. Operators would know where the part was located in the machine's volume and would be able to move the cutting tool to the correct positions through apprentice-trained skills. But as computer numerically controlled (CNC) machines started to take over the work of the manual machines, engineers soon realized that an accurate and repeatable part position would be needed for CNC machines to manufacture consistently accurate parts automatically.

Although mechanical probes had been used within coordinate metrology since the 1950s, the first electronic touch trigger probe was invented in 1972 [1]. Sir David McMurtry [2], who later went on to be cofounder of Renishaw plc [3], created the electronic touch trigger probe while working at Rolls-Royce plc [4], to be used for the measurement of small-bore tubes as part of the Olympus engine development process [5]. After the inception of the electronic touch trigger probe this quickly led to the replacement of the mechanical probes previously deployed on coordinate measuring machines (CMMs). This later led to deployment on CNC machine tool spindles, thus allowing CNC machine tools to accurately locate parts within the working volume through an automatic part program.

In 2021, Renishaw plc is a global supplier of machine tool probing systems employing 1000s of staff worldwide. However, other companies, including Blum-Novotest [6], Marposs [7], Heidenhain [8] and M&H [9] also producing part and tool probing systems (see Figure 1 for examples). In 2018, Future Market Insights [10] forecast a US\$75.6 Bn market valuation for machine tool touch probes (sic.) by 2028. Their analysis is that the main suppliers will continue to dominate the market, but demand will be driven by more automation.

Unlike the mid-1970s, many modern machine tools now come with machine tool probing systems as standard equipment and almost all machine tool suppliers offer probing as an option. Although these systems are prevalent in many machine shops around the world, it has been established through both personal experience and interactions with industrial partners that there is a tendency for them to be inefficiently or incorrectly used. This is not a fault of the technology but can be due to a combination of issues such as, lack of knowledge of the system's capability and a reliance on older historically proven methods.

Probe heads have been developed so that they are intrinsically very accurate, with advances such as strain gauge technology making the repeatability of the probe unit submicron [11]. This allows the possibility of measurements on machines to reach the accuracy levels of quality systems instruments, or machines such as CMMs. It is important to consider, though, that the probe head is just one small part of the measurement system. Although the probe head may have submicron repeatability the machine that carries it may not.

With modern manufacturing methods and advances in electronics, today's probes are not only extremely accurate but also very durable to enable them to work within the machine tool's harsh environment. Although probe heads are produced by different manufacturers, they are often very similar in appearance (see Figure 1). For the purposes of this dissertation, This research will investigate this type of spindle-mounted workpiece probe, as shown on a machine in the University of Huddersfield workshop in Figure 2. Tool setting probes, also seen on the machine in Figure 2, are less common and consideration of them would expand the dissertation greatly.

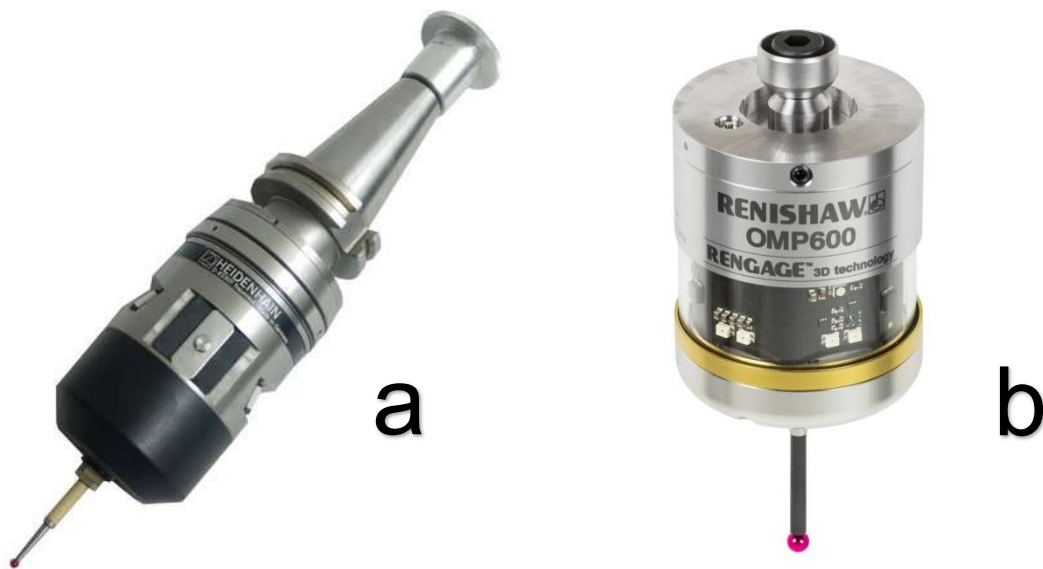


Figure 1 Typical machine tool probes from a) Heidenhain [8], b) Renishaw [3]

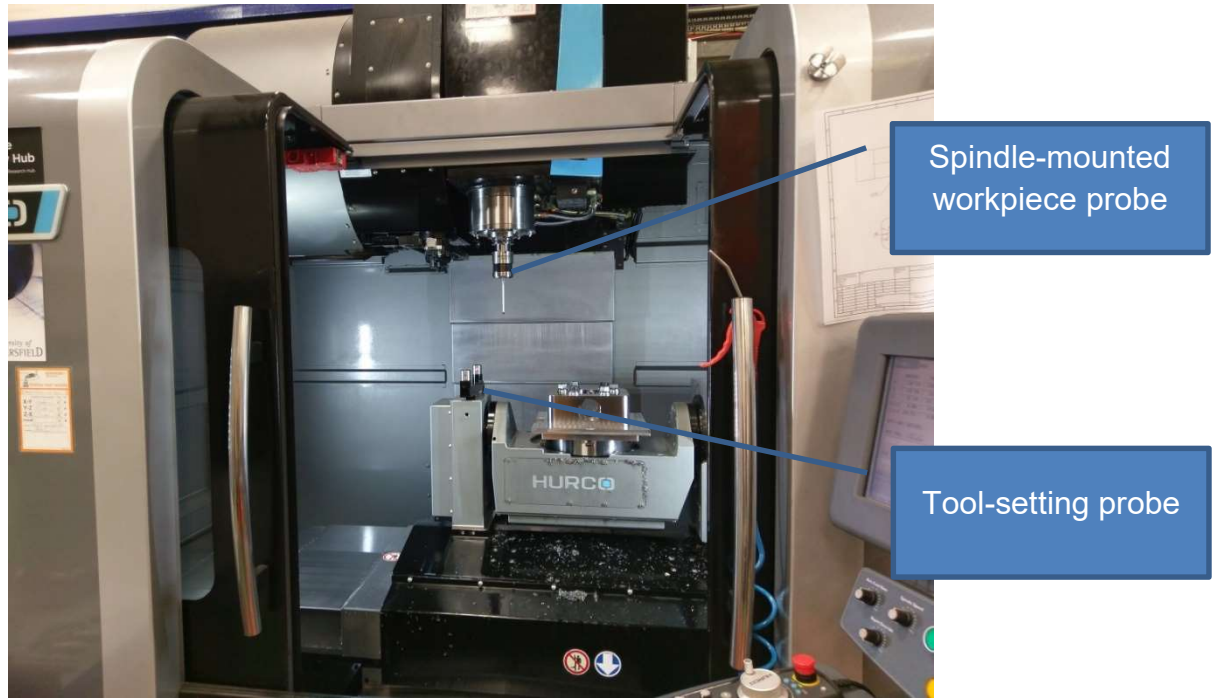


Figure 2 Typical machine tool with probe systems

1.2 Machine tool accuracy

The main focus of this dissertation will be on characterising the accuracy of the machine tool that carries the probing system. Historically, machine tools have been sold in terms of the resolution of their encoders or accuracy of each axis. Longstaff et. al. [12] describe this as being linear positioning error only and contrast it with the more complete “5-axis volumetric” rigid-body error that better describes the machine (Figure 3). However, the authors also draw attention to the need for understanding thermal, non-rigid and control errors during motion.

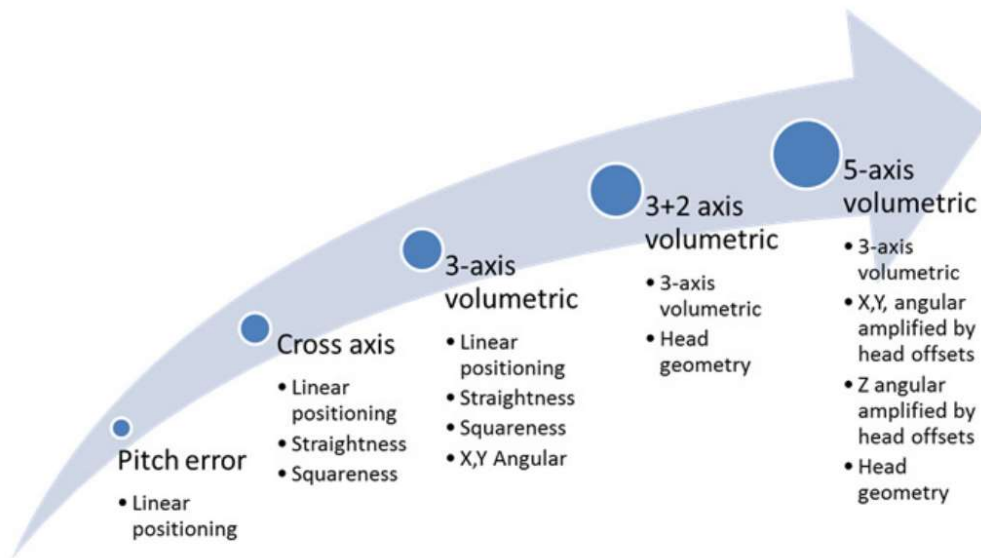


Figure 3 Different modelling approaches for machine tool accuracy [12]

Experience has shown that most machine tool users do not analyse their machines to this level but rather “engineer out” accuracy issues by modification of the process or part program. This approach loses some of the benefits of CNC and automation, by relying on the experience of the skilled operators along with interruptions to production. Similarly, not knowing these errors will contaminate any probing measurements. While probing to re-reference (re-datum) can help avoid unknown errors, they would compromise the use of on-machine probing (OMP) for in-process or final measurements.

One global machine tool end-user has privately quoted up to 90% of their machines as not being regularly calibrated during service. In this context, control of their on-machine measurement processes is severely compromised. The same manufacturer stated that 100% of their metrology equipment is regularly calibrated and traceable.

1.3 Relationship to coordinate measuring machines

In terms of standardisation of machine tool probes, ISO 230-10:2016 covers “Determination of the measuring performance of probing systems of numerically controlled machine tools”. However, it states in the introduction that, “*The results of these tests do not reflect on the performance of the machine tool used as a coordinate measuring machine (CMM). Such performance involves traceability issues, and it is intended that they be evaluated according to ISO 10360-2 and ISO 10360-5.*” [13] These latter two standards were written for CMMs and, although they provide valuable reference, they are not directly applicable due to the different influencing factors in a machine tool and its operating environment. In fact, a preliminary proposal has been put forward to create a new international standard for using “Machine Tools as

Coordinate Measuring Machines” and the outcome of this dissertation will contribute towards influencing its development.

1.4 Conformance

The “conformance zone” is “*that part of the design tolerance that remains after the uncertainty of measurement has been considered*” [14, 15, 16]. Figure 4 shows how the design specification has an upper and lower tolerance, but that conformity is guaranteed only for that portion where it is not impinged by the uncertainty. This is a crucial concept for on-machine measurement (OMM) since the uncertainty is often not well-qualified and therefore the conformance zone cannot be well-determined.

The main thrust of this dissertation is to provide guidelines for assessing machine accuracy so that the influencing factors are sufficiently well understood to be able to ensure conformity for a given mode of operation of the probe. It is a first step, so does not seek to provide a full, formal uncertainty analysis due to the complexity of that challenge.

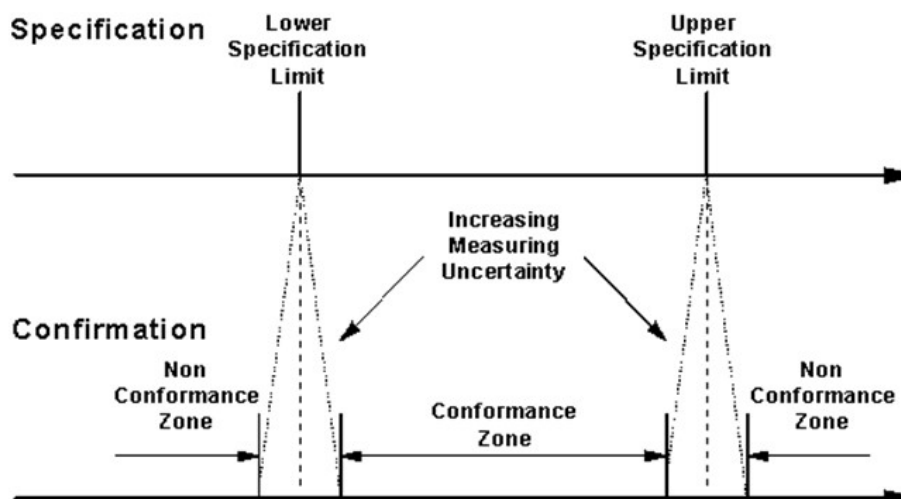


Figure 4 Influence of measurement uncertainty on zone where conformance is verified – modified from [16]

1.5 Timeliness

The timeliness of this project comes from the growing prevalence of probing systems on machine tools. The following quote comes from a market analyst:

"More and more companies are using technologically advanced CNC machining with pre-programmed computer software, required for dictating the movement of machinery and tools in manufacturing units and development of highly intricate models and components. This has subsequently led to a rise in implementation of machine tool touch probe technology in lathe, milling, laser, grinding, and welding machines.

CNC machining has made a huge difference in the metal processing industry by increasing efficiency and reducing cycle time and material wastage”, Principal Analyst, Industrial Automation, Future Market Insights [10].

Because of this growing prevalence of probing systems, the project reported in this dissertation is required now to address the underlying processes that should be undertaken before using such devices for different activities.

Verma [17] emphasises the need for automated on-machine inspection, stating through a Process Failure Mode and Effects Analysis (PFMEA) that on precision manufactured parts in the aero-engine manufacturing sector, *“the in-process measurement operation [is] the high-risk area for a potential failure to occur.”*

1.6 Summary

This brief introduction has explained that on-machine probing is an important, yet underused element of automated CNC machine tools. While forecasts show that the availability of probes is set to rise, the work in this dissertation will provide a way of determining what pre-requisites are required for different uses of a probing system, an example which is provided in Chapter 4

Chapter 2 will conduct a review of relevant literature to understand what systems are available and some of the influencing factors that need to be considered.

Chapter 2 Literature Review

The Renishaw productive process pyramid™ [18] (PPP) has been used as a convenient structure for this literature review. It is a well-established process control framework that can be applied to manufacturing processes, with machine tool probing at the heart of the pyramid. Although aimed at promoting Renishaw’s own products, the framework provides a solid foundation that can be attributed to any machine tool user looking to achieve accurate and repeatable probing results.

Of the four layers of the pyramid (Figure 5), probing could be used in any of the layers, although in manufacturing probing is much more widely attributed to the “process setting” and in “in-process control” layers. Within this project the application of probing in the “Process Foundation” layer will also be looked at in more detail and opportunities for “final pass-off” in the “post-process monitoring” layer will be considered as a significant driver to the research.

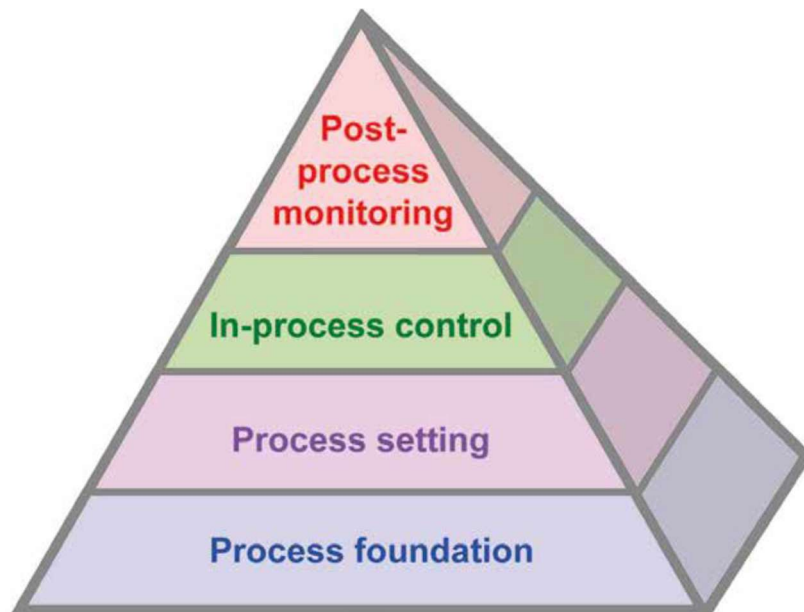


Figure 5 Renishaw Productivity Process Pyramid™ [18]

The four layers are regarded as preventative, predictive, active, and informative from the bottom layer upwards. The PPP has since been refined as a process flow (Figure 6), additionally breaking down the levels as “in advance”, “just before”, “during” and “after”.

The process foundation layer is something that is quite often overlooked by companies when utilising machine tool probes. This first level of the pyramid is classed as preventative and is an extremely important part of the whole framework process and something that should not be ignored, without this foundation, significant waste is incurred in trying to “engineer out” problems otherwise hidden. However, it also creates a requirement for some quite in-depth and time-consuming measurements, this reduces the time available for cutting and minimising the intrusiveness of this activity is therefore vital.

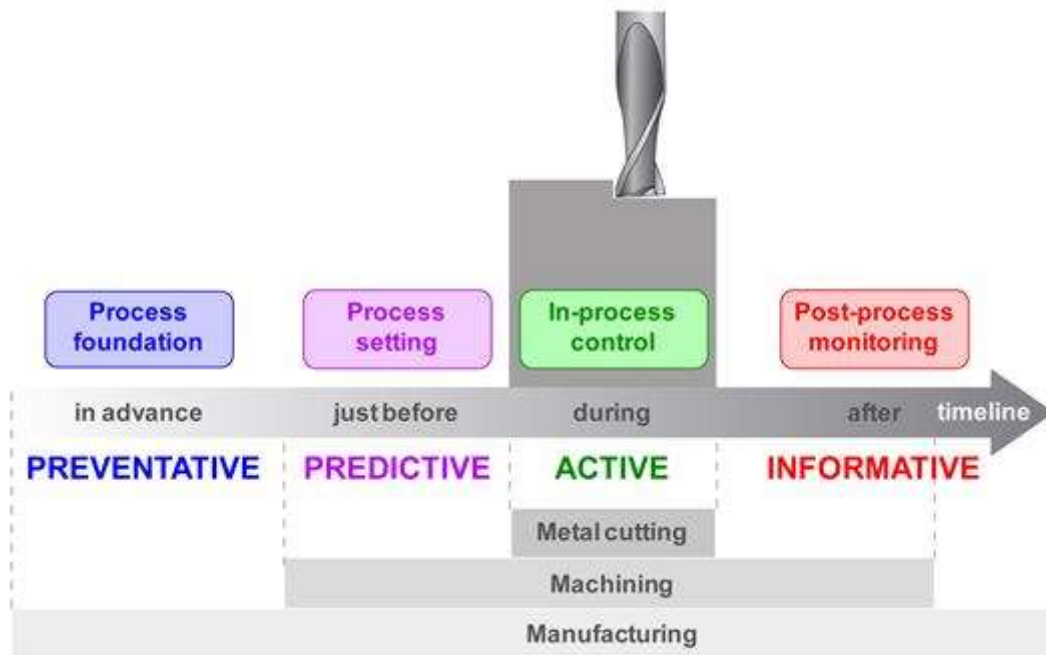


Figure 6 manufacturing process timeline [19]

Renishaw suggest that for any kind of on-machine probing (OMP) to give confident and traceable results, the machine condition optimisation process foundation [20] is an essential element.

This research will look more closely at the process foundation and process setting layers with respect to its influence on how probing might be also used in the subsequent layers.

2.1 Process Foundation

The majority of modern manufacturing machine tools will contain at least one linear axis, but more commonly they will have between three and five. In mill-turn or other complex machines, they could have many more. The Fanuc Series 30i-model B controller for instance has the ability to control 24 axes simultaneously with a maximum number of 72 feed axes and 14 spindles [21].

Machine tool axes have six degrees of freedom each, couple with offsets between axes these are known as the Geometric errors. Based on the indicated degrees of freedom in the standard ISO 230-1:2014 [22] and discussed by Ibaraki *et al* [23] there are 21 geometric errors on a 3-axis machine and 36 on a 5-axis machine. To quantify these errors a process of calibration or verification is performed.

Machine tool axis calibration sits within the process foundation layer and enables the performance and condition of the machine tool to be established. Schwenke *et al.* [24] in their review paper have described the various machine tool errors and the methods of their measurement. The key contributors that fall within the process foundation layer

and influence the effectiveness of on-machine tool probing are summarised in the following sections.

2.1.1 Machine tool thermal influences

Today there is a better understanding of the need to keep machine tools and their operating environment thermally stable than say 20 years ago, but there are still a large number of machine shops that are not temperature controlled, meaning they are not in a thermally stable environment. This means the ambient temperature can change significantly over the day, or in some cases even in the time it takes to complete a machining operation. This, coupled with localised heat from the spindle, axis motors, ball-screw and frictional movements of the machine tool, heat generated from the cutting action itself, etc. means that the machine structure can expand, contract and bend, changing the shape significantly [25].

A low budget machine fitted with a glass scale as the axis position feedback system should be able to position an axis to within 10 μm of its intended target [26]. Due to the increased accuracy of the base machine, this now means that thermal issues are seen to be the largest contributor to any geometry error on a machined component; Mayr *et al* estimate this to be as high as 75% [25]. Although the thermal influences are now considered the dominant error source, it should always be looked at in context. For instance, a machine with very well set up thermal compensation or a machine in a temperature-controlled environment may bring this figure much lower and highlight the geometry or axis compensation errors whereas a machine with no thermal compensations in an environment with large temperature swings could see this figure rise higher.

Manufacturers employ various methods in an attempt to manage the thermal variations and keep the machine tool and its machining operation in a thermally stable condition. Spindle chillers [26] that keep liquid at a set temperature and pump it through channels in the spindle housing along with cooled electrical cabinets are all now commonplace on many machine tools. Some of the methods used for cooling are explored by Patil and Mudholkar [27]. Some higher-precision machines have now utilised a similar system on axis motors, linear rails and ball screws. All these systems are designed to help keep the thermal influences to a minimum.

Figure 7 shows the cooling system routing on a DMG DMU210 5 axis machining centre [28], temperature-controlled fluid can be seen in blue routed through the balls crews, linear rails and motor jackets.

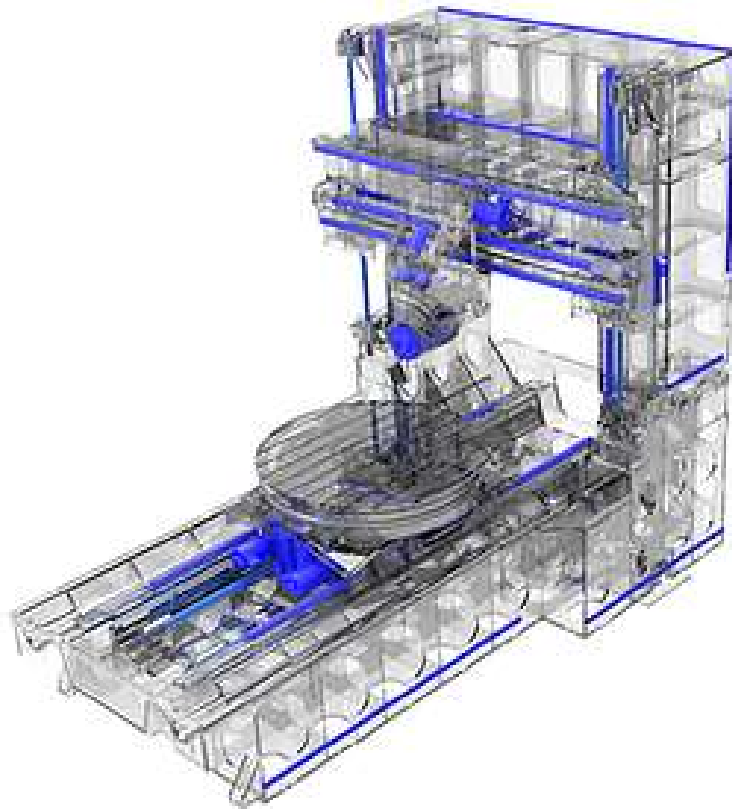


Figure 7 DMU210 cooling fluid routing [28]

Manufacturers expend a lot of resource to improving thermal errors, with some systems able to cope with temperature fluctuations very well. However, it is not uncommon for these systems to over-compensate in some situations and exaggerate the very errors they are trying to control.

For example, the linear positioning graph in Figure 8 shows an axis linear positioning error (see section 2.1.4) dominated by thermal drift. Figure 9 shows the positional deviation of a machine axis fitted with glass scales and an air purge, designed to keep the scales clean of debris. The air purge was connected to a chiller unit. As the ambient temperature rises the chiller unit comes on and cools the air being fed to the machine, causing the scales to cool. When the chiller reaches its lower setpoint temperature it switches off and the scale starts to warm again. This causes the cyclic error of contraction and expansion shown in Figure 9. These two graphs, taken by researchers within our research group, are only two of many such examples on machines operating in industry.

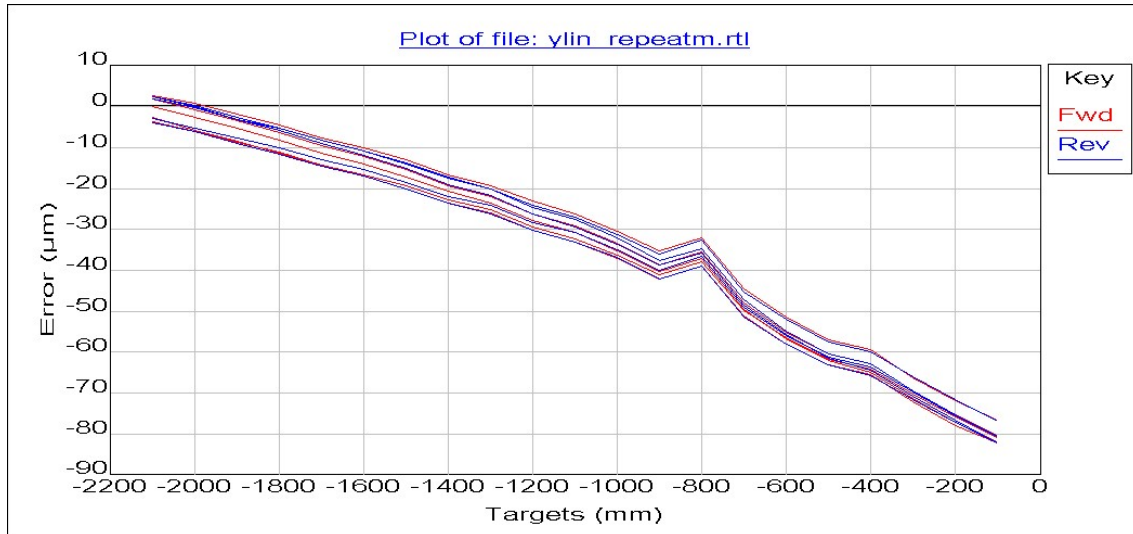


Figure 8 Linear positioning plot dominated by thermal expansion and showing drift

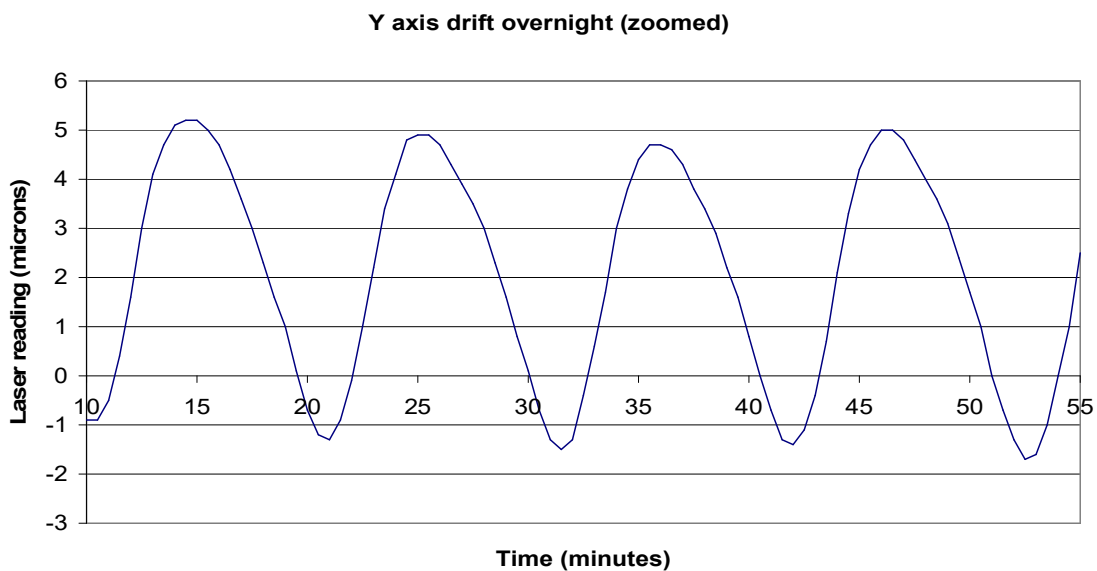


Figure 9 Cyclic error of chiller coming on and off

Thermal errors and their influence on the measurement data are something that cannot be ignored when implementing on-machine probing. When evaluating whether a machine is suitable for measuring to a certain tolerance, the thermal performance must be established. Two machines which look very similar can behave very differently. These errors will be investigated in greater detail in the research phase of this document. The way in which probing could be used to map these errors will also be explored.

2.1.2 Machine tool configurations

There are many variants of machine tools within modern production facilities, these can broadly be reduced to two very distinct types, namely subtractive and additive [29]. This research project will only consider subtractive process machine tools.

Within the subtractive sector, more commonly known as metal cutting machines, there are many different machine configurations, but the majority will fall into the category of having either a vertical or horizontal spindle [30]. On a milling machine, the spindle holds the rotating tool; on a lathe the spindle holds the rotating workpiece. More complex multitasking machines may have variants of both horizontal and vertical spindles and may combine both milling and turning operations. Such machines are called “mill turns” or “turn mills.” [31, 80]

ISO 10791-3:1998 [31] describes twelve possible configurations for a 3-axis vertical spindle machining centre. The configuration of the machine is important in both machining and probing since the errors that are experienced are affected by the construction and interaction between axes. For example, Figure 10.01 shows a machine where the component is moved by two of the axes, whereas Figure 10.11 is a “fixed-bed” where the component remains stationary. The latter, in principle, could machine a workpiece of any given weight without affecting the performance, whereas the former will change behaviour depending upon how much the workpiece weighs. These aspects need to be considered as the different errors are described in the remainder of this section.

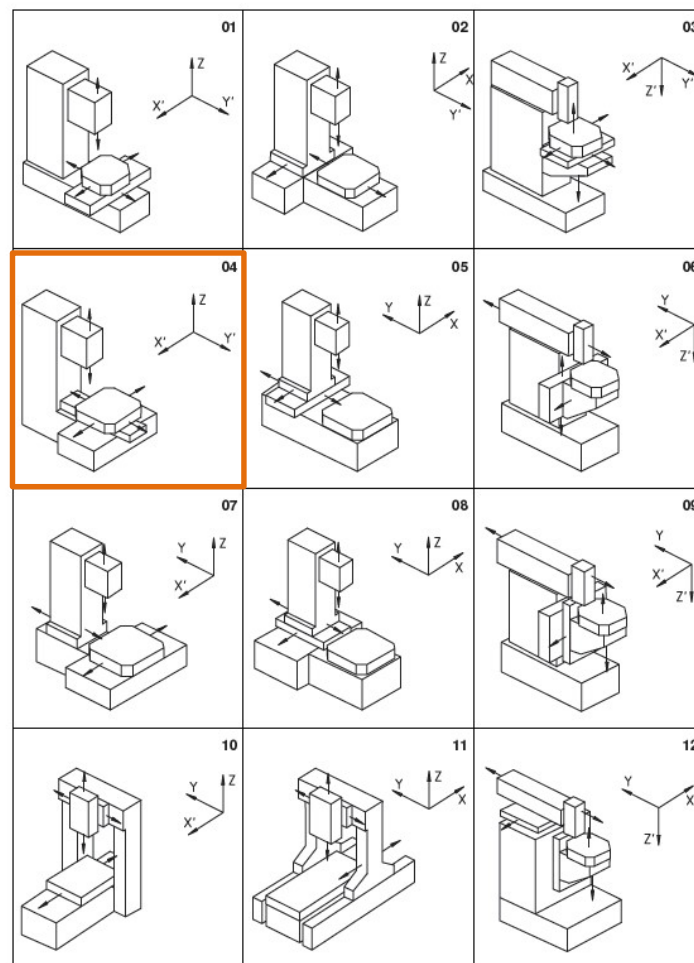


Figure 10 The twelve possible configurations of 3-axis vertical spindle machining centre [31]

The overall ISO 10791 standard series covers the test conditions for both horizontal and vertical spindle machining centres, these standards rely heavily on the general principles of measurement described in ISO 230-1:2012 [22] and reference it throughout. Where the ISO 10791 series differs to ISO 230-1:2012 is that it also “establishes the tolerances or maximum acceptable values” for all the geometric errors.

The main test machines in this dissertation, Machine A and Machine B (see Appendix B), are the C-frame configuration show in in Figure 10.04 and highlighted in orange.

2.1.3 Machine tool geometry

Geometric errors or kinematic errors are the rigid-body errors that are inherited from the manufacturing process of the individual components that make up the machine tool through to the errors in the final build process where these components are mated together. These errors are termed “quasi-static” since they exist when the machine is not moving. They can change over time and with use. These errors determine the

machine's basic geometric accuracy in terms of the squareness of the axes to each other, the straightness and parallelism of the guide rails and ball screws and the flatness of component mounting surfaces.

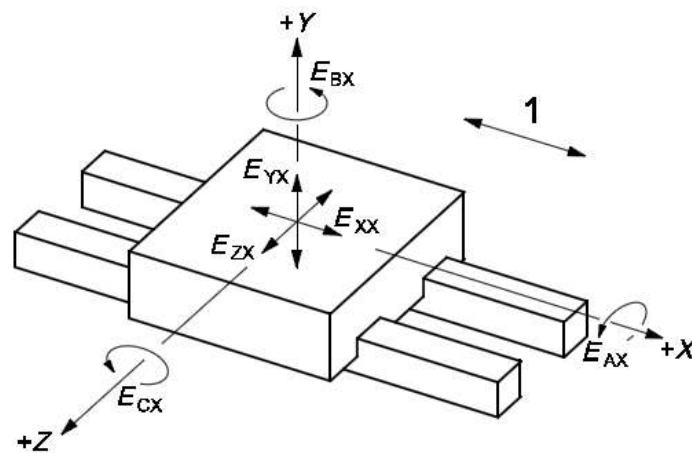
Geometric errors cannot be easily and cost-effectively removed, normally requiring the machine tool to be broken down and the errors remedied by remanufacturing or by reseating of the components. They can however be compensated with advanced compensation [24] but this will never truly remove any angular irregularities. These errors could have a significant impact on any probing results recorded in any location other than where probe calibration takes place.

The standard ISO 230-1:2012 [22] covers the testing and quantifying of the geometric errors of the built machine tool. It is important to recognise that these tests are conducted on "*machines operating under no-load or quasi-static conditions.*" Therefore, geometric errors could present differently when the weight of fixtures and component stock are placed on the machine. However, standards are always a compromise agreed by committee; the ideal for geometric testing in relation to machine tool probing would be for the machine to be tested with all the fixturing and stock in place. This would be impractical, for a "standard," since it could not account for the variety of products that might be manufactured and for the ever-changing state of the machine due to stock material being machined away.

Where the standard is particularly applicable is that the forces during probing are, unlike cutting, close to zero-load.

2.1.4 Machine tool axis errors

Machine tool axis errors are the position-dependant errors of each axis which determine the positional accuracy of the system. Position-dependent means that the magnitude of the error could change depending on the position of the axis within its stroke. Each linear axis is subject to six degrees of freedom [22] relating to six error components, one linear positioning error, two perpendicular translation (straightness) errors, and three angular errors. These are colloquially known as Linear position, Horizontal and Vertical straightness, Roll, Pitch and Yaw. In ISO 230-1:2012 the terminology of how these errors are reported has been standardised and can be seen in Figure 11

**Key**

- 1 X-axis commanded linear motion
- E_{AX} angular error motion around A-axis (roll)
- E_{BX} angular error motion around B-axis (yaw)
- E_{CX} angular error motion around C-axis (pitch)
- E_{XX} linear positioning error motion of X-axis; positioning deviations of X-axis
- E_{YX} straightness error motion in Y-axis direction
- E_{ZX} straightness error motion in Z-axis direction

Figure 11 “Angular and linear error motions of a component commanded to move along a (nominal) straight line trajectory parallel to the x-axis” [22]

The ideal path for a single machine tool linear axis would be a perfectly straight line reaching every programmed position exactly. In reality, the inherent errors in the machine tool's manufactured components and build will cause deviations from the ideal path, leading to positional errors in the relationship between the tool tip and workpiece. This is a function of the errors of motion, described above, and the position of the other machine axes. Figure 12 shows an angular error, E_{BX} , having (a) no effect when the Z-axis is retracted, but (b) error in the X-axis direction as the Z-axis amplifies the error.

Several researchers have published models on the effect of the axis errors in terms of a homogeneous transformation matrix (HTM) [32], axial model [33], etc. These models are used for error prediction [34,35] or compensation [36, 37, 38]. Figure 12 (c) shows how a linear-axis-only compensation is applied by moving the X-axis an equal, but opposite amount to the calculated error.

Positional deviations are therefore a result of an angular influence as well as any error in linear position feedback.

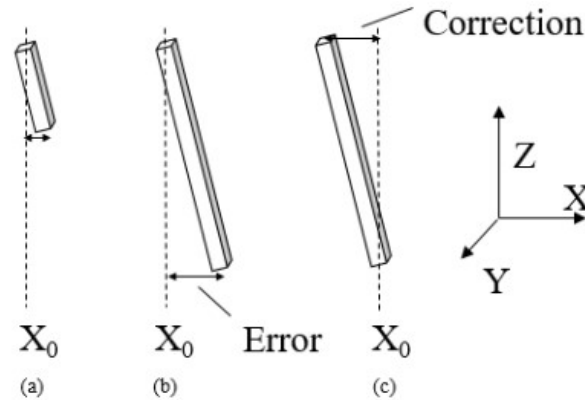


Figure 12 Angular errors affecting linear position [44]

The axis errors could influence any results obtained by machine tool probing; this is particularly relevant when the errors at the positions of measurement are significantly different from the errors at the positions of probe calibration. This effect must be based upon the configuration. For example, “Roll” of the spindle (Z-axis) on the machine shown in Figure 10.04 is not amplified on a 3-axis machine where the tool or probe is collinear with the centre of the spindle, so the effect is negligible. However, if the probe is mounted orthogonally, or a 5-axis head is mounted on the end of the ram, then the roll error will be amplified.

Reviewing the existing literature shows that this has been considered for machining, relative to the absolute machine coordinate system, but not in the “relative” coordinates with respect to the location of any probe calibration artefact or with respect to datum positions established and revisited during the manufacturing process.

2.1.5 Non-rigid errors

The weight of the axis and any combined weight placed upon it can have a significant influence, especially on large machines [39]. The configuration of the machine axes (section 2.1.2) can have a significant impact in the expected geometric errors. Specifically in the way the geometry errors manifest themselves as an error on the manufactured component. For instance, a machine with a large component on a moving table with a fixed position spindle may react differently to a machine with the same component on a fixed table and moving spindle. This could have a significant effect on any probing results if two components of the same geometry were manufactured on two differently configured machines.

Although important on large machines, further investigation of this aspect will not be considered in this dissertation since the machines under test have small volumes and rigid construction, so the effects will be negligible when compared to the other factors.

2.1.6 Errors of motion

Errors of motion are those errors additional to the quasi-static ones which derive from the movement of the machine tool axes, for instance clearance between the parts in the drive train of the axis can create backlash; as an axis changes direction clearance between a rack and gear or balls crew and nut will lead to a loss of motion. It is important to remember that backlash is a mechanical phenomenon, however when the electronic components (motors, drives, compensation) of the machine tool are added this will become reversal. These errors are discussed in more detail by Ford [38] and Miller et al [40]. Although these errors can impact probing, the effect on the measurements are generally mitigated by always probing at the same speed.

2.1.7 Machine tool Calibration

The National Physical Laboratory (NPL) Introduction to Measurement and Metrology course [41] states *“Calibration, is the comparison of an instrument, artefact or reference against a more accurate one, along with the application of any necessary corrections, to ensure that it is fit for purpose.”*

The most common form of machine tool axis calibration, and by many considered the minimum requirement, is what has become known colloquially as “lasering.” This is the use of a laser measuring device to measure the error components of a linear axis. How many are measured is often down to the availability of equipment and expertise, but the linear positioning errors (EXX, EYY, EZZ) can now be commonly acquired. It is worth noting that these are only three of the 21 error sources reported by Ibaraki [23]. The principle of measurement is often laser interferometry. Once these error components have been mapped a decision will be made on whether the axis needs to be maintained / repaired or compensated to bring the errors within an acceptable specification.

In simpler terms the machine tool axis position is compared against the highly accurate laser reference and any positional deviation is the error.

2.1.8 Machine tool Calibration Equipment

When conducting machine tool calibration there are a wide variety of measurement equipment and artefacts that can be used, this section will give a brief description of the main pieces of equipment being used within this research project but will also consider measurement devices usually associated with larger volume machines and emerging measurement technologies.

2.1.8.1 *Engineers Squares and straightedges for geometry*

Engineering squares, cylindrical squares, and straight edges (Figure 13) are used as the surface reference when used in conjunction with a relevant measurement system, like a dial test indicator (DTI) [42] for instance. To be used for traceable measurements, the artefacts should be manufactured in accordance with BS

939:2007 [43] and a calibration certificate be present stating the tolerances of flatness and straightness for straight edges, and for squares the flatness, straightness, and squareness to each other of the designated working faces.

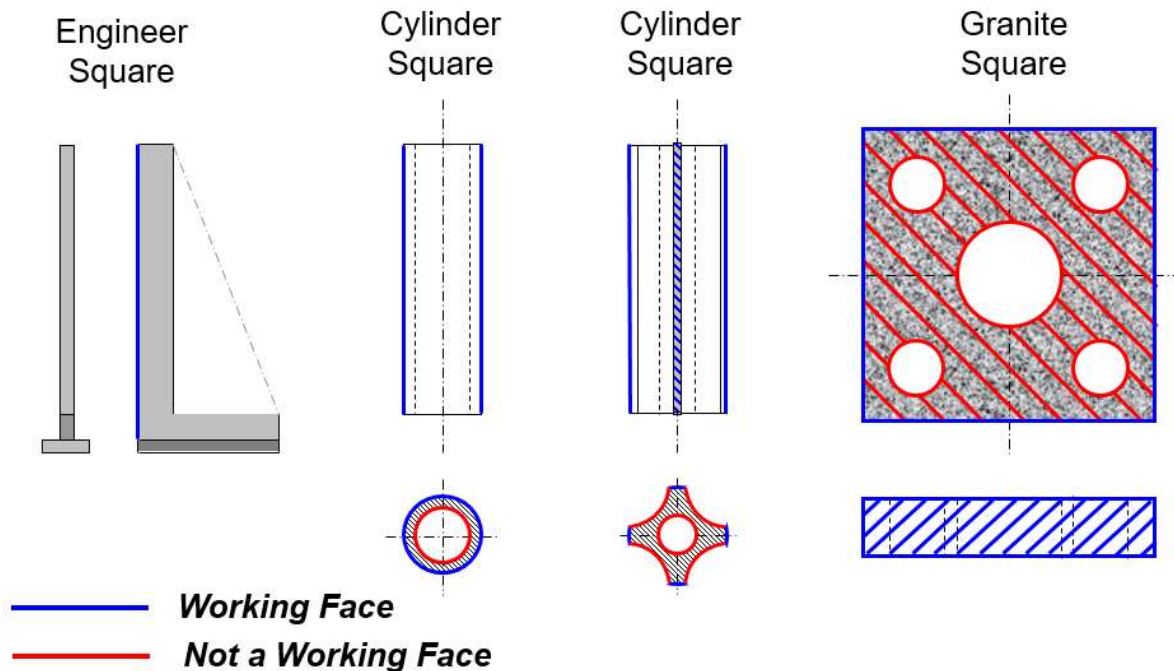


Figure 13 Various engineers squares and working faces [44]

The differing properties of engineering squares, cylindrical squares and straight edges used in machine tool metrology are discussed in the following subsections.

2.1.8.1.1 Square

Precision squares do not actually have to be square and can also be triangular (tri-square). But by definition will always have a minimum of two master faces square to each other (nominally at 90°).

A true square can be used for the checking of verticality, straightness, parallelism, and the squareness between any two axes, whereas tri-squares cannot be used for the measurement of parallelism.

Squares are manufactured in a range of sizes and accuracy grades and will often be made from granite (diabase) as this is much lighter than the steel or cast-iron equivalent and will not be subject to the surface corrosion issues of the latter. As a large square can be extremely heavy, holes will often be created to allow lifting and manoeuvring of the artefacts with the added benefit of removing weight.

The master faces of a square will be marked with an individual number or letter to distinguish them from one another. These will be marked on the square itself and listed on the calibration certificate along with the calibration values that show the deviation from the nominal 90° to each other. The designation of individual markings allows the

error between the measured faces to be referenced against the calibration square; this in turn allows the reference error to be removed from the squareness measurement to give the residual squareness error.

Measurement of axis squareness is complicated by contamination from axis straightness. Figure 14 shows that if an axis is not straight it will create, for example, the bowing shape on the top and right-hand side of the square when under measurement. If only two points were taken on each of these two working faces, which is very common practice, then the chosen location of these would greatly influence the squareness value. Taking more points on each face, to generate a best-fit linear approximation, is not attractive in terms of added machine downtime while taking the readings.



Figure 14 Effect of straightness on squareness measurement

This discussion on some of the detail of squareness measurement is to highlight the complexity of this one measurement, as an example, as a reason why the foundation layer measurements are so often ignored by companies.

2.1.8.1.2 Straight edge

Straight edges are primarily used within machine tool geometry for checking the straightness and flatness of the axes (mainly guiderail straightness's). All straight edges will have at least one master face that has a straightness value calibrated back to traceable standards.

Due to the ratio of a straight edge's length to width, it is important when sitting the straightedge in position that the artefact is supported on the Airy points [45, 46] as indicated in Figure 15. These are two points calculated along the artefacts length, symmetrically about the straight edge's centreline to minimise deflection due to gravity (sag).

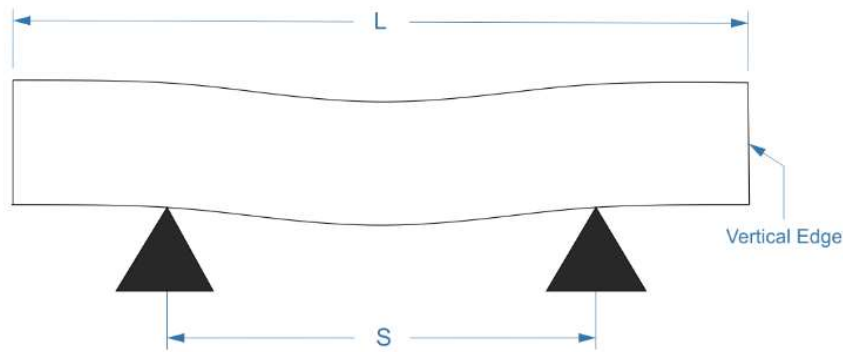


Figure 15 Schematic of straight edge artefact supported on Airy points [46]

S= the distance between the supports

L= the length of the artefact

$$s = \frac{L}{\sqrt{3}} \quad \text{--- (1)}$$

So if the straight edge is 1m long the calculation would be

$$\frac{1000 \text{ mm}}{\sqrt{3}} = 577 \text{ mm}$$

Meaning Distance s would be 577 mm

A straight edge will never be perfectly straight, so to remove the influence of the artefact errors it can be rotated 180° about its length and the measurements repeated. This is known as the reversal technique [47], but naturally almost doubles the time for taking a straightness measurement.

Again, the inclusion of this description is to highlight by example the rigour required for achieving measurements with low uncertainty.

2.1.8.2 *Laser interferometer*

The XL80 [48] is a laser interferometer manufactured by Renishaw PLC. Other manufacturers produce similar interferometer-based instruments but the XL80 is discussed as it is available within the university. The system is capable of measuring five of the six degrees of freedom (Roll being unable to be measured) by using different optic set ups, linear positioning, pitch and yaw angular errors and horizontal and vertical straightness.



Figure 16 XL80 Optics L-R linear position, angular, straightness [courtesy Renishaw plc]

The laser interferometer works by splitting the beam from the laser head into two and measuring the difference between the return beam from the stationary and moving optics, as there will be an incremental difference between the two beams when they are recombined (interfere) [44]. Figure 17 shows the beam being split and the relevant beam paths and Figure 18 shows a typical machine tool laser set up.

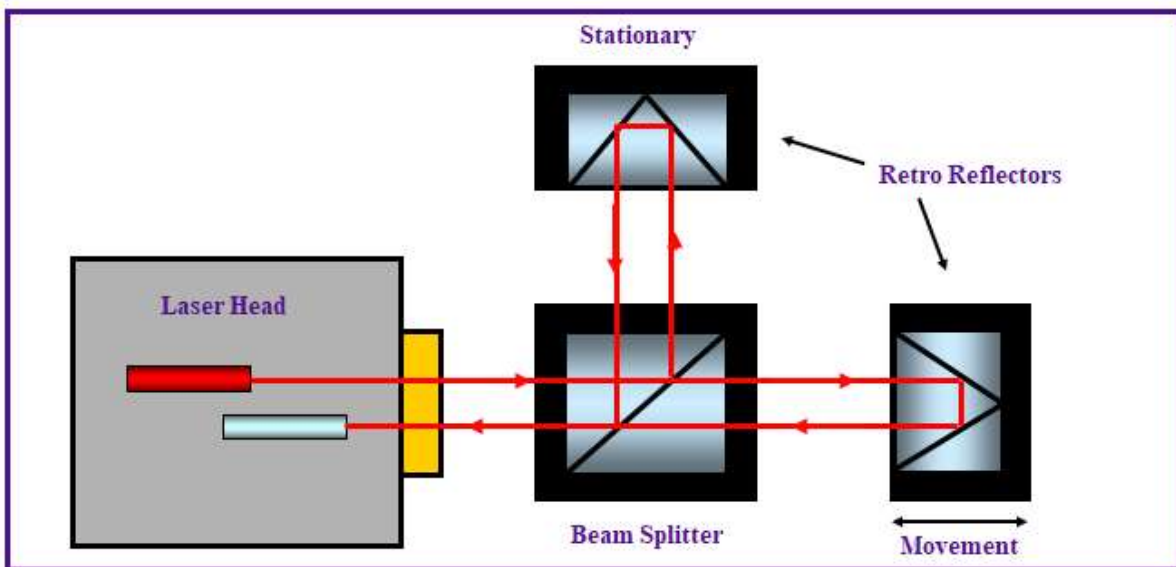


Figure 17 Linear positioning optic set up [44]

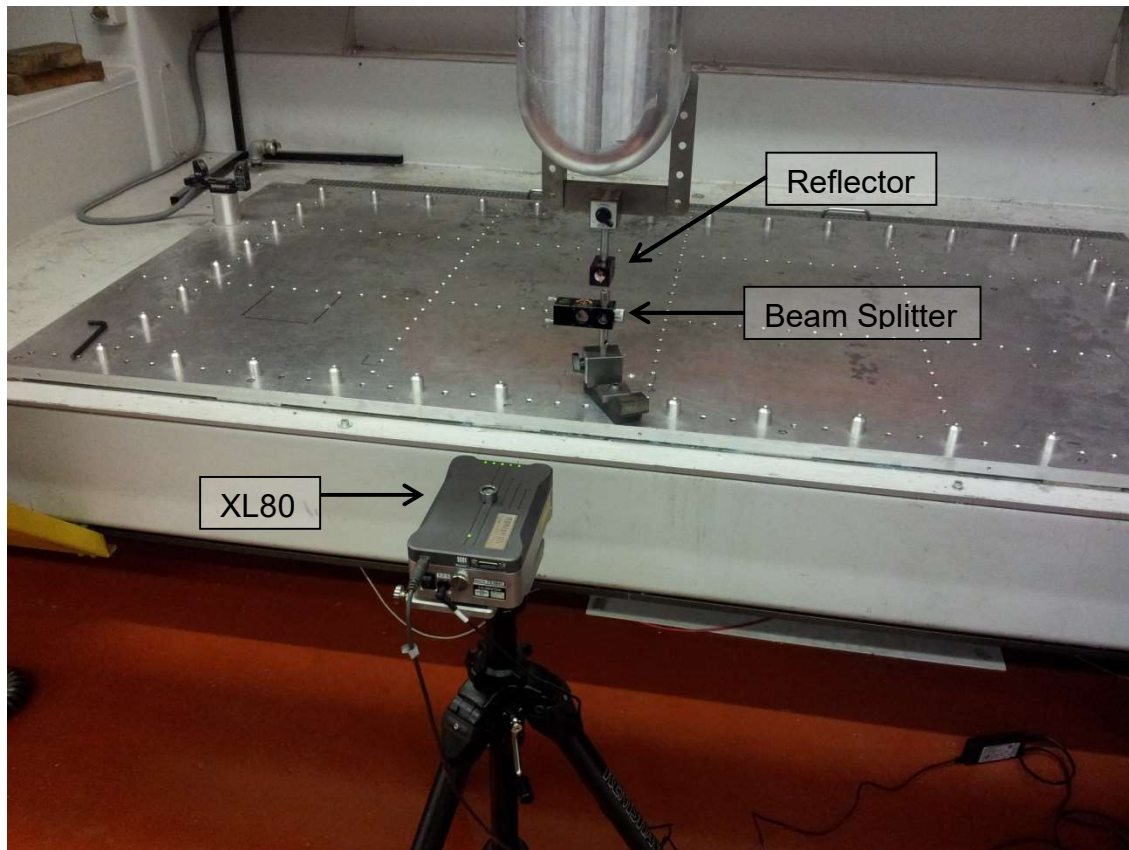


Figure 18 Typical XL80 linear positioning measurement set up

The system uses the same XC80 [48] environmental compensation unit and temperature sensors to compensate for the environmental effects on the laser beam wavelength.

Measurements are taken by moving from one target to another and pausing. The method of test for linear positioning errors (EXX, EYY, EZZ) is described in ISO 230-2:2014 [49]. The standard calls for a minimum of five targets per metre, but in practice more points than this are needed to adequately map the axis errors [40]. When using a laser for the other geometric errors, such as angular and straightness, it is common practice to apply the same target spacing. The caveat to that is where manual data capture is needed, when fewer targets are used for convenience.

One of the largest drawbacks of this system compared to the XM60 mentioned in 2.1.8.3 below is the inability to measure all error components in “one shot”. For example, all the different error components have to have different optic set ups to complete the measurement, meaning that all measurements are completed in different environmental conditions.

2.1.8.3 *XM60 multi-axis calibrator*

The Renishaw XM60 Multi degree of freedom calibrator is a measurement device that uses the combination of a laser interferometer and a quad sensor to enable the measurement of all six degrees of freedom of a linear axis in one measurement cycle. Figure 19 shows the system mounted on a machine as part of this research work, with the launch unit mounted on the table on the right and received unit attached to the spindle on the left.

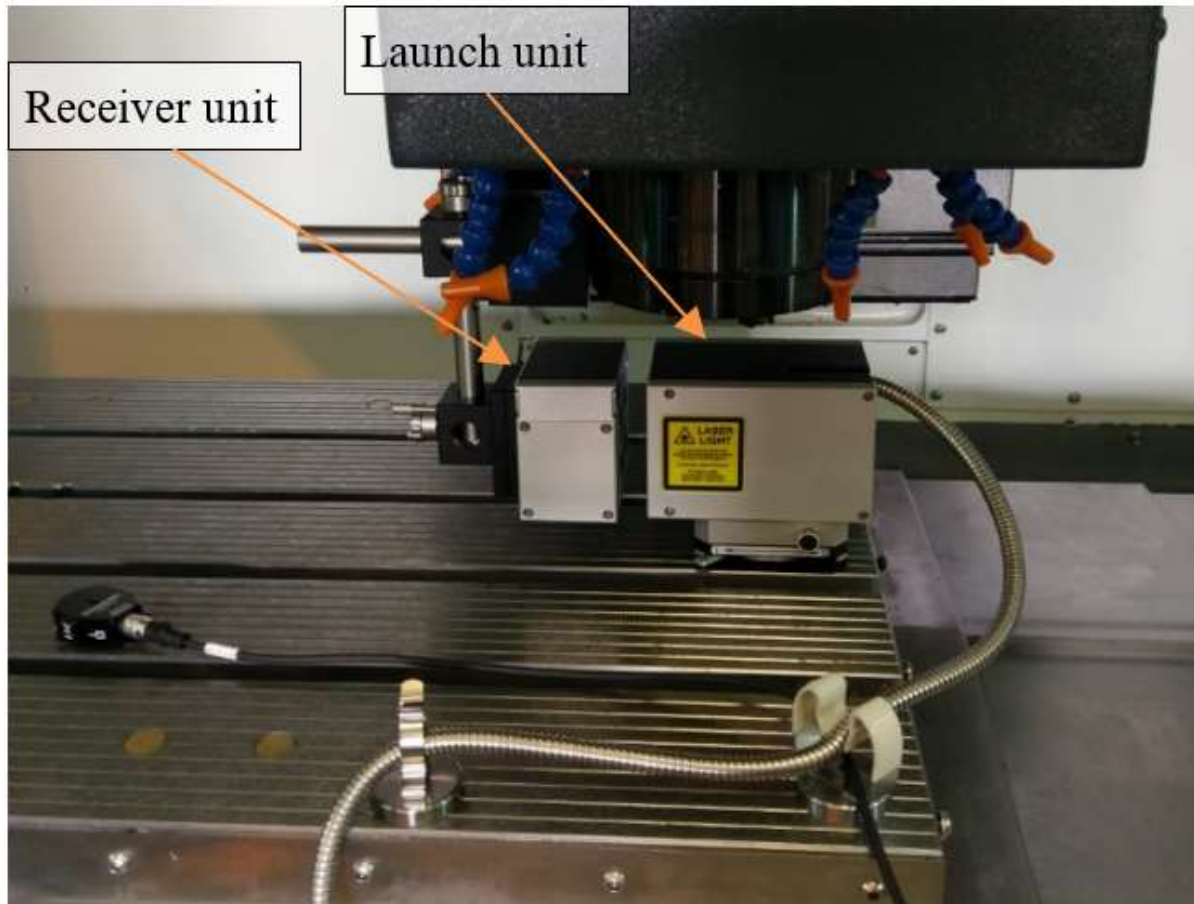


Figure 19 Renishaw XM60 on a machine

As discussed in 2.1.4, the positioning error is partly a function of the angular errors. When using a system that is only capable of measuring one axis error in a measurement run, the different data sets gathered from multiple set ups and due to the extra time needed to complete the separate measurements, the possible contamination from the changing environmental conditions, can lead to uncertainties when evaluating all the errors as a whole [50].

Measurement of all six error components simultaneously, not only speeds up the measurement time but improves the quality of the data by the fact that all the errors are recorded in the same time period under the exact same conditions. The results

can then be confidently evaluated as a whole, due to there being none of the issues related to different data files recorded separately.

The XM60 measuring system consists of several parts; the main components are the Laser unit, Launch unit, Reflector, XC80 environmental compensator and ambient and material temperature.

The laser unit by definition is where the laser source itself is contained; this is a Helium-Neon (HeNe) laser tube, Similar to that used in the XL-80. The laser source is separated from the launch unit, a design utilised to make the launch unit compact and to protect the measurement optics from any laser induced thermal effects.

The laser beam is fed through fibre optics in an umbilical cord from the laser unit into the launch unit where it is split into three beams. These beams use interferometry to measure the linear position, the pitch angle and yaw angle. Besides the interferometry splitters, the launch unit houses a light-emitting diode that creates a fourth beam to measure the two straightness and roll errors.

Miller et al. [40] describe new research into the use of the XM60 in “continuous motion measurement” mode. This can be used to identify errors that are otherwise missed, due to “aliasing” when taking measurements in the standard quasi-static measurement mode (see section 4.3.2).

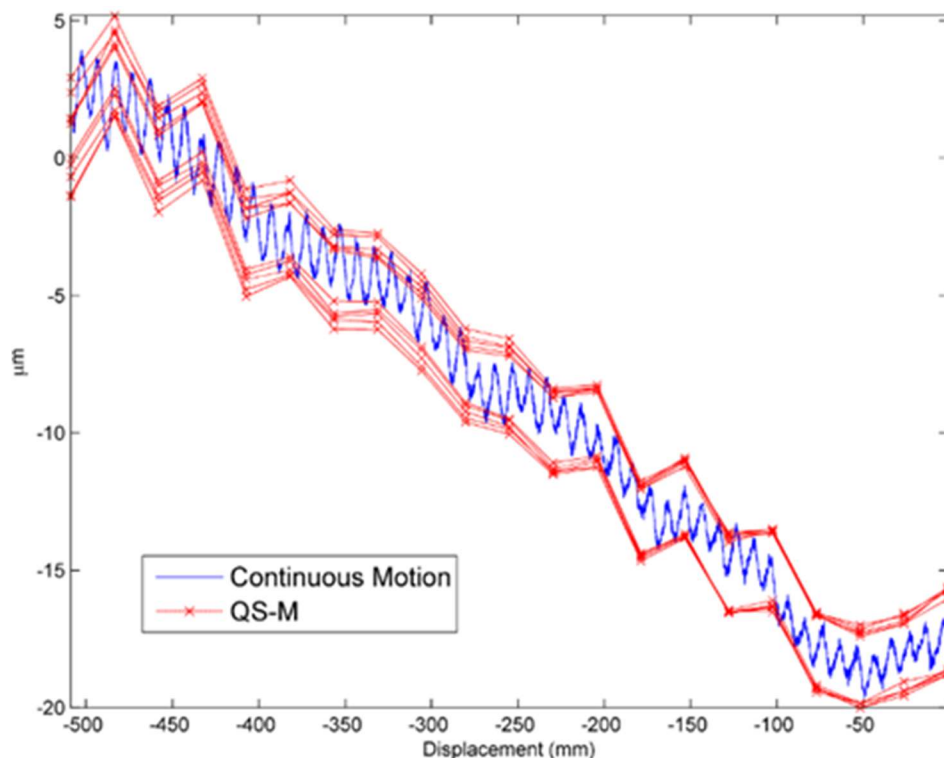


Figure 20 Comparison of linear positioning error measured in continuous and quasi-static measurement modes [40]

The methodology of this type of calibrator is for the launch unit to represent the workpiece and the reflector head unit to represent the tool allowing for all measurements to replicate the tool to workpiece relationship.

The advantages of this system, and the close working relationship between the University and the manufacturer during the research and development phase of the product, meant that this was chosen for the measurements in this project.

2.1.8.4 *Interferometer Environmental compensation*

Measurements taken using a laser interferometer rely on the wavelength of light as the reference. Ideally, but impractically, laser measurements should be taken in a vacuum. For position measurement the change in reading can therefore be either due to a change in wave path (desired measurement) or in the refractive index of the air through which it passes (uncertainty in the measurement) [51].

In real-world conditions, the laser measurements must be compensated for changes in the environment. The air temperature, air pressure, and relative humidity all influence the wavelength of the laser beam. The Edlén equations [52] are used to correct these effects. Birch and Downs published an improvement on the equation to take into account the effect of carbon dioxide composition in the air [53, 54], but the overall impact on uncertainty is not significant in machine tool calibration and is not measured.

A measurement unit, such as the Renishaw EC10 (Figure 21a) is used to capture the air pressure and relative humidity. An attached air temperature sensor (Figure 21b) feeds directly back into the unit.

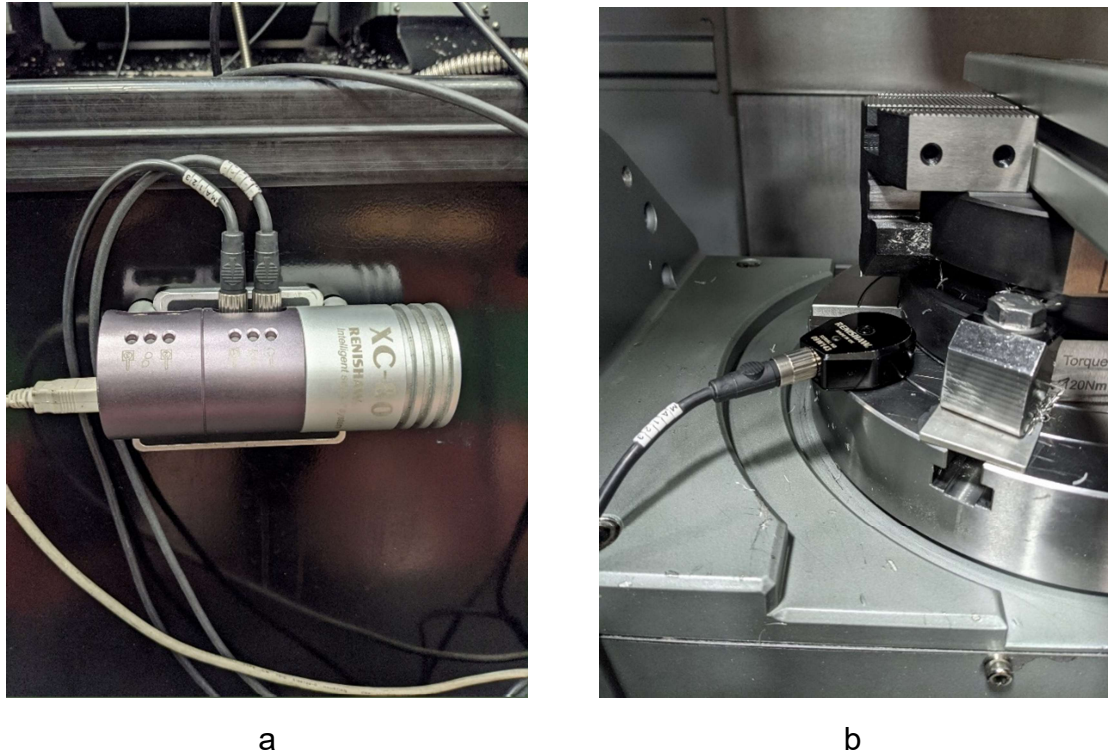


Figure 21 Renishaw EC10 (a) environmental compensation unit and (b) air temperature sensor

The unit also permits the use of up to three material temperature sensors. These do not correct for uncertainty due to the refractive index of air. Instead, they may be used to measure the temperature of the structure under test and can either be used to record measurement conditions or scale any position measurement by a factor of the coefficient of thermal expansion (CTE) of the object under test.

2.1.8.5 *ETALON / laser tracers*

The Etalon [55] laser tracer uses a laser interferometer with $0.001\mu\text{m}$ resolution to measure machine tool axes up to 20m in distance. Laser tracers mainly differ from the more typical laser interferometer like the Renishaw XL80, which can only measure points along one in line axis at a time, in that once the laser tracer has locked onto the cat eye style reflector [56] it can then automatically follow the path it takes through a multitude of axes positions recording points in X, Y and Z.

The use of a pair of rotary axes and a highly accurate reference sphere placed at the centre of rotation of these axes enables the laser tracer to rotate the beam and track the reflector to any location; the only limiting factor being that the cat eye stays within the angular range to reflect the beam back and have direct line-of-sight. A typical cat eye laser acceptance angle (the angle at which the laser beam can enter the reflector and be returned) can vary between 30° and 45° but with the advent of the new range of super cat eyes [57] this can now be as much as 75°

The methodology of calibrating a machine tool using a laser tracer revolves around the system of multilateration [58], using the same principles as GPS systems [59] measurements are taken from different locations within the working volume; this would usually be a minimum of four different locations.

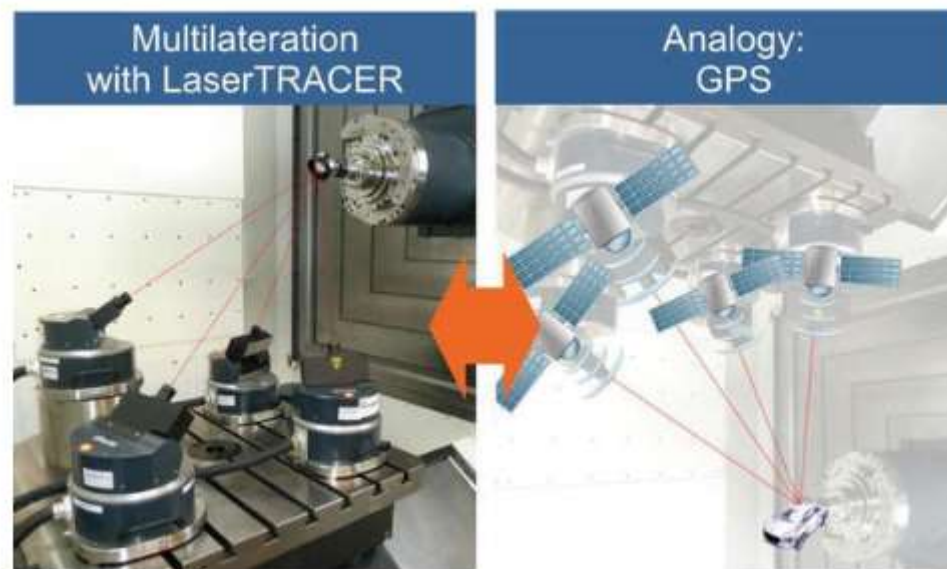


Figure 22 Multilateration and GPS [60]

The laser tracer is placed in the first position and then locks its laser beam on to a retro reflector (usually placed in the spindle), the machine tool then follows a pre-programmed path through the working volume stopping at set points along the way to take static measurements. Once the defined path has been completed the tracer is moved to the second position and the measurements repeated and so on until the minimum number of locations have been measured and the required amount of data has been captured. Software is then used to derive spatial positional data so that an assessment of the machines volumetric accuracy can be made.

The use of laser tracers for machine tool calibration can be time consuming and adding in the high cost of the hardware and software, means they are more suited to large volume machines where the high financial cost of non-conformance of larger components would give better financial benefit, but saying this, they give unrivalled accuracy in volumetric measurement and should not be excluded if available.

2.1.8.6 *Laser tracker*

Since the inception of laser trackers [61, 62] during the late 1980s these measurement devices have mostly been utilised for component and feature measurement in product verification, but as accuracy has increased they have become more prominent in the measurement and calibration of machine tools and more recently robots.

As with a laser tracer the tracker needs an unobstructed view of the retroreflector target to return the beam and calculate the measurement. As well as the cat eye style reflector the most common type of laser tracker target is the spherically mounted retroreflector (SMR) [56]

Insphere BASELINE [63] utilises a laser tracker to perform multilateration and infer the geometric errors from the combination of length measurements. On a large machine with rotary table this can be done relatively efficiently, since the laser can be moved by the machine as well as the optic. On smaller machines, or ones without rotary tables, the access issues can be problematic.

2.1.8.7 *On-machine probing of artefacts*

Erkan, Mayer and Dupont [64] describe a method of assessing the distortion of a machine's geometry by probing a 3D reconfigurable ball artefact. Zimmermann and Ibaraki [65] propose a method utilising the spindle probe and uncalibrated cylindrical artefact. Choi, Min, and Lee [66] proposed a cube artefact. Inora Spatial Reference System [67] utilises several calibrated, interlocking lengths to form a pyramid. In each of these cases, the availability and relatively automated data gathering from spindle-mounted probing is perceived as a convenient and efficient method of data gathering.

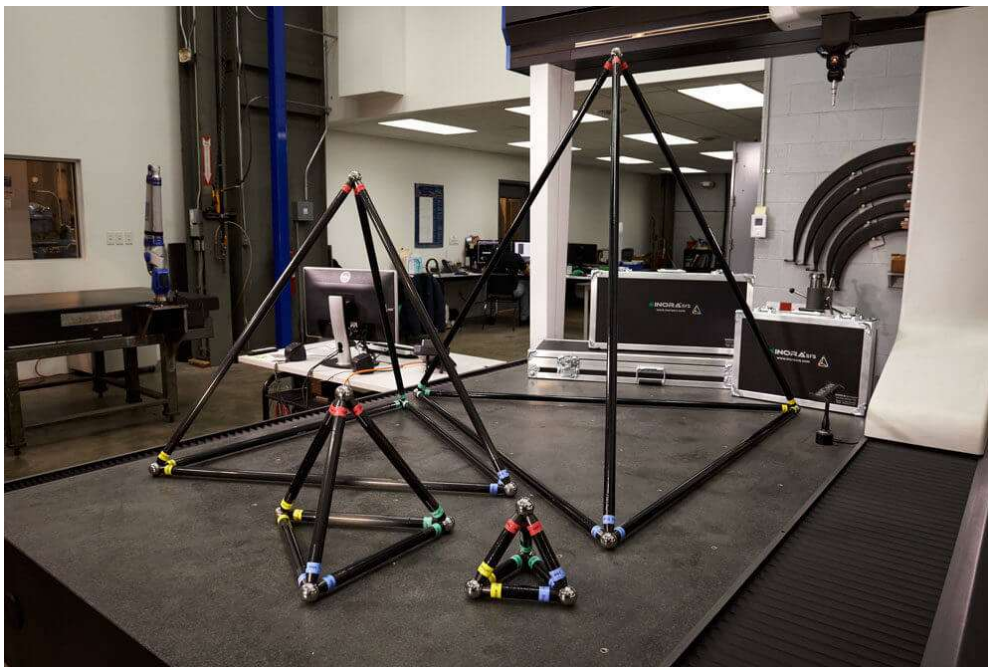


Figure 23 Inora SRS [67]

2.1.9 **Machine geometric monitoring**

After all the linear axis errors have been mapped, and if not found to be within acceptable limits, either repaired or compensated for, the next stage would be to create a benchmark that can quickly and easily be referred to. A benchmark set of

results could be obtained by running something as simple as a ball bar test. This would create a baseline set of results from a test that can be run in a short space of time with minimal impact on any production and at set intervals. The main advantage of this type of test is that they can be completed relatively quickly utilising personnel with limited experience, but there are rules that have to be adhered to if future comparable results are to be obtained. For instance, Parkinson and Longstaff discuss in their paper optimisation of machine tool error mapping using automated planning [50] in the context of minimising either the uncertainties or time for measurement. Extrapolating from this, it is evident that the monitoring tests should be run with conditions as close to the original benchmark data capture conditions as possible.

Having calibrated and benchmarked the errors, through the calibration techniques described in section 2.1.7, the machine should continue to be monitored at regular intervals. A calibration of a machine tool, like all calibrations, is only valid at the time it is completed. Over time wear will occur between moving parts and collisions will quickly degrade the performance of the machine tool.

This along with the ever-changing environmental conditions ranging from temperature and humidity and even the possibility of the foundations changing due to the effects of the differing water table levels, means that without regular monitoring of the machine tool, any changes in the errors between full calibration intervals could go unnoticed.

2.1.9.1 *Ball bar*

A telescoping ball bar by its name is typically a bar with one ball on each end. One ball is fixed and the other is attached to a linear transducer within the system housing to measure displacement. For this research the Renishaw QC20w ball bar system has been utilised [68]. The system transmits data wirelessly to the pc meaning there is no trailing of cables to compromise the measurement or getting in the way of closing guard doors



Figure 24 QC20w ball bar [69]

Unlike the XL80 and XM60 measurements that take points statically along a machine tool axis the ball bar takes a dynamic measurement of two axes at the same time. This is done by commanding a circular movement around a fixed centre point

The method of operation consists of two balls held magnetically within cups situated on the machine bed or fixture and on a part of the spindle housing; a circular movement is then commanded through a CNC program around the centre point of the fixed cup. As the machine rotates around the fixed cup any deviation from the programmed path is captured by the linear displacement sensor and recorded. If the ball bar has been calibrated before the test on the calibrator supplied, then the length of the bar is known and along with the federate the software can calculate the deviation values.

Figure 25 Shows a typical XY plane measurement set up on a 3-axis machine tool

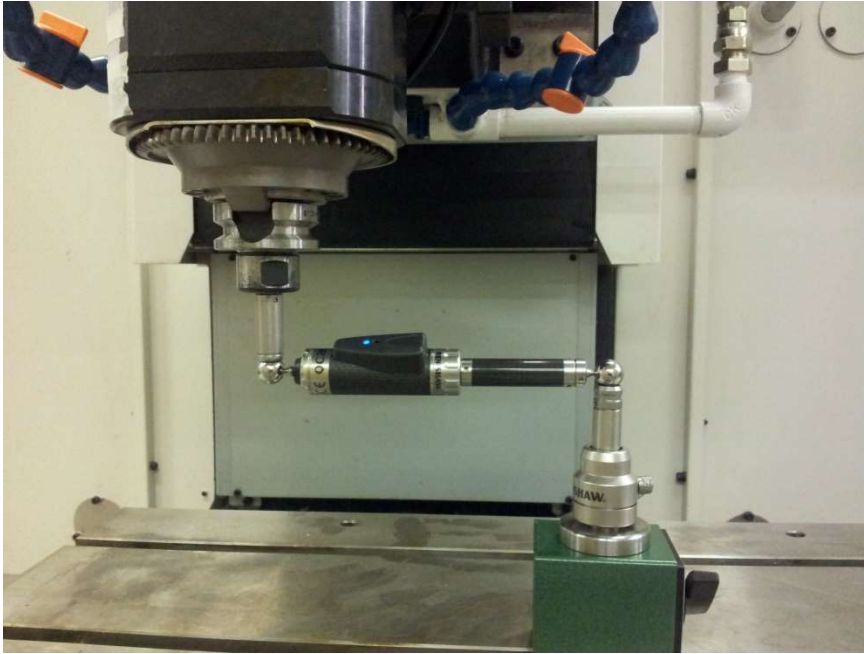


Figure 25 Typical ball bar set up

The test is relatively fast and can be completed by personnel with very little experience, making it appealing to industrial users, but care should be taken if using as a diagnosis tool and individual error measurements derived from the data should always be backed up by a more in-depth test before corrective action takes place.

Within the ball bar software there is also the option to create a history graph of all measurements as they are taken; this makes a ball bar an ideal tool for benchmarking machines. Measurements can be taken at designated periods and referred to the original readings to highlight any changes in performance.

2.1.10 Spindle/tool interface

An often-overlooked aspect of a machine is the interface between the tool and spindle. This has particular importance for probing systems, where the orientation of the probe and repeatability of the interface is of critical importance.

The tool-holder interface will normally fit into one of two categories, hollow taper (HSK), and steep taper (CAT, ISO, DIN and MAS BT). Steep taper-style holders will normally only contact on the tapered cylindrical shank (Big Daishowa Big Plus being the exception [70]) while hollow taper shank give the added rigidity and repeatability of face and taper contact. Figure 26 gives a brief description of the main differences and shows the main area of tool to spindle interface contact areas.

STEEP TAPER VERSUS HSK

Steep Taper (ISO, BT, CAT)

- Relatively poor stiffness
- Poor axial accuracy
- Not suitable for high speeds (outside clamping)
- Large mass and large stroke
- Widespread

Hollow Cup Taper (HSK)

- Excellent static and dynamic stiffness
- Excellent axial and radial accuracy
- Excellent suitability for high speeds (inside clamping)
- Low mass and stroke

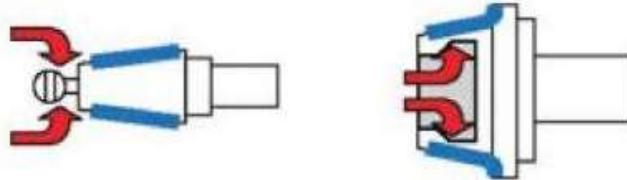


Figure 26 steep taper and hollow taper contact areas [71]

2.1.10.1 HSK 69893

HSK [71] type tool holders, or to give them their correct name Hohlschaftkegel, are hollow-shank type holders with face-and-taper contact. This gives the tool holders greater accuracy and repeatability during tool changes than the steep-taper SK tool holder range, especially in the Z axis due to the face contact with the spindle nose. The face-and-taper contact prevents the toolholders from suffering the tool suck up mentioned in section 5.3.1

These tool holders are covered under the German DIN 69893 series of standards. However, the key characteristics are freely available from the individual tool holder manufacturer's websites.

2.1.10.2 SK Din73381

SK [71] tool holders are part of the steep taper family of tool holders and are produced in a range of sizes. They are very similar in dimensions to BT tool holders but with subtle differences. These types of holders are not usually face and taper so can suffer from the tool suck up phenomenon mentioned in section 5.3.1. Due to the long length of taper and the tolerances associated with the angle these tool holders are deemed to not provide the same level of accuracy as HSK holders

2.1.11 Foundation process summary

Within this section the process foundation layer of the PPP has been examined. The main pieces of equipment that are needed for calibration have been discussed, along with the key areas that need to be quantified before efficient on-machine probing can begin to take place. This review has identified the need to clearly consider this layer as part of an integrated strategy for on-machine probing. It has also identified the key

technology (Renishaw XL80, Renishaw QC20w and Renishaw XM60) that will be used for testing the machine geometry.

2.2 Process setting layer

The second layer of the pyramid is the process setting layer and focuses on the predictive controls that are put in place before metal cutting begins; these include tool setting, part setting and machine setting.

As the main focus of this research is on the part probe, It will concentrate mainly on the machine and part setting areas of this layer, and not the tool setting.

The use of automated machine probes removes the ambiguity and non-reproducibility of manual machine tool setting. Rather than deskilling the operation it allows resources to be placed where most needed. Having said this, if the rules of the foundation layer have not been observed then data acquired using these means cannot be trusted and may be inferior to that of an experienced operator performing manual tasks.

2.2.1 Probe errors

The stated accuracy for an omp600 Renishaw touch trigger probe is given in Table 1. The figures only relate to the probing unit itself once it has been calibrated and ignoring inaccuracies in the machine tool geometry.

Sense directions	$\pm X, \pm Y, +Z$
Unidirectional repeatability	0.25 μm – 50 mm stylus length) 0.35 μm – 100 mm stylus length
X, Y (2D) form measurement deviation	$\pm 0.25 \mu\text{m}$ – 50 mm stylus length $\pm 0.25 \mu\text{m}$ – 100 mm stylus length
X, Y, Z (3D) form measurement deviation	$\pm 1.00 \mu\text{m}$ – 50 mm stylus length $\pm 1.75 \mu\text{m}$ – 100 mm stylus length

Table 1 Renishaw OMP600 accuracy chart [72]

2.2.1.1 *Stylus length*

Tool probe manufacturers will usually recommend a maximum length of stylus, due to the forces involved with triggering the probe. The length of the stylus can change how the stylus bends during operation, as can be seen above in the 3d form measurement Table 1, the accuracy changes by $0.75\mu\text{m}$ with a 50mm longer stylus.

Gaska et al [73] discuss this in more detail, and although their research is based around CMM probe styli some of this is applicable to machine tool probes.

2.2.1.2 *Hysteresis*

Hysteresis within the kinematic structure of the probe is something that is inherent when a change in direction of the probe touch happens and is not usually considered when creating probing routines. Wozniak and Meczynska [74] looked at this in detail and concluded that the styli length and speed of measurement had a direct impact on the level of hysteresis, a longer styli increasing hysteresis and a decrease in measurement speed led to an increase in hysteresis.

Although the hysteresis effect was small, around $1\mu\text{m}$, this could be a large percentage effect on a tight tolerance measurement. Also, by using a specially built measurement stage to activate the probe, the hysteresis of the whole probing system was not considered.

2.2.2 **Probe condition**

No literature has been found due to probe condition factors relating to on-machine probing.

2.2.3 **Initial probe set up**

Before the probe can be used it will have to be married to the correct tool interface and the initial set up completed. This could involve centering the ruby runout to within a set tolerance and decision made whether to use a preprogrammed CNC command to switch the probe on and off or for the probe to time out and switch off after a certain amount of time. The installation guide for the Renishaw RMP60 [75] recommends this should be within $+2.5\mu\text{m}/-2.5\mu\text{m}$.

Although centering the ruby is recommended, the calibration should remove any offsets from the measurements, meaning as long as the probe is used in the orientation it is calibrated this should not have a detrimental effect.

2.2.4 **Probe Calibration**

Due to inaccuracies in the manufacture and assembly of the probe system and the tool spindle interface connection all probing systems should be calibrated before use on the machine. Calibration will map the deviations of the stylus tip from the Centre line of the machine tool spindle in the X and Y axis and also the ruby tip radius at the

intervals required. A macro used within a CNC program provided by the machine tool builder, or the probe manufacturer enables measurement of an artefact (ring gauge or sphere) that will update parameters within the controller. These parameters will be called anytime a probing cycle is used.

Every time the condition of the probe changes calibration should be repeated

2.2.4.1 *Automatic calibration*

Some machines run automatic calibration routines where the position of the artefact is fixed, this position could change due to thermal deviation, or in a worst-case scenario a collision.

2.2.4.2 *Electronic system latency*

The principle of operation for a probing system is to send a signal to the controller when the probe has triggered to record the axis positions. This happens while the axis is in motion and therefore any latency can influence the time at which the value is recorded. This will be discussed further in section 5.2.2.3

2.2.5 *Human error*

No literature has been found due to human factors relating to on-machine probing. This aspect is touched upon in chapter 3.5

2.2.6 *Clamping*

Large thin-walled parts can deform while machining or under the load of the clamping to hold the component in place. Machining company RUAG discusses the merits of machining, and on machine inspecting while clamped under the same loads [91]. Having run benchmark tests they have proved this method to repeat “within a couple of microns” of CMM results, though they do not provide the actual value.

2.3 *Methods of failure analysis*

There are many different methods of analysing product, design or system failure. Cristea and Constantinescu [7693] list several, and then concentrate on the relative merits of the two methods of failure analysis that were considered for this project, based upon the approaches taken by the industrial partners.

Fault Tree Analysis (FTA) [77] uses a top-down approach to identify potential failures and represent these as a flow-diagram of events and Boolean “gates”. Transfer symbols are used to connect different processes FTAs. The failures are classified by the severity of the failure, with greater attention being given to parts of the tree with greatest severity.

Failure Mode and Effects Analysis (FMEA) is in many ways the opposite. Key aspects of an FMEA are given in the European Standard EN IEC 60812:2018 [78]. It looks at all possible ways in which a system can fail (the failure modes) and creates a register

which allows users to work backwards towards the failure cause, often called the initiating fault or event.

Utilising both methods would result in a lot of duplication, so FMEA was chosen to conform to the prevailing approach from our industrial partners.

2.3.1 FMEA characteristics

The standard [table F.2] requires the following information for each failure:

- Step of process
- Function
- Failure mode
- Failure effect
- Failure mechanism
- Failure cause

For this project the heading will be used to define the problem and formalise the knowledge of the experts who contributed to it.

Additionally, the following mitigation factors will be included either as part of the FMEA exercise (Chapter 3), or by the framework produced in this project (Chapter 4):

- Possible Detection
- Possible Prevention

2.3.2 FMEA prioritisation

“Failure modes may be prioritized according to their importance. The prioritization can be based on a ranking of the severity alone, or this can be combined with other measures of importance.” [78]. It is important to note that the standard allows the flexibility to apply quantified values for prioritisation where they are useful but does not require them in all cases. The standards define “severity, occurrence and detectability (SOD)” and assign the risk priority number (RPN) as:

$$RPN = S \times O \times D \quad \text{_____ (2)}$$

Table 2 shows an example guideline for assigning “severity” scores used for a product or design, while Table 3 provides the same for a process.

Category (Product)	Criteria: Severity of Effect (Effect on Product)	Rank
Failure to Meet Safety or Regulatory Requirements	Potential failure mode affects safe operation or regulatory requirements, without warning	10
	Potential failure mode affects safe operation or regulatory requirements, with warning	9
Loss or Degradation of Primary Function	Loss of primary function	8
	Degradation of primary function	7
Loss or Degradation of Secondary Function	Loss of secondary function	6
	Degradation of secondary function	5
Annoyance	Item operable, but with annoyance noticed by >75% of customers	4
	Item operable, but with annoyance noticed by 50% of customers	3
	Item operable, but with annoyance noticed by <25% of customers	2
No Effect	No noticeable effect.	1

Table 2 Guidelines for severity ranking in design/product FMEAs [79]

Category (Product/Process)	Criteria: Severity of Effect on Product	Criteria: Severity of Effect on Process	Rank
Failure to Meet Safety or Regulatory Requirements	Potential failure mode affects safe operation or regulatory requirements,	Potential safety-related effect on machine or assembly operator, without warning	10
	Potential failure mode affects safe operation or regulatory requirements,	Potential safety-related effect on machine or assembly operator, with warning	9
Loss or Degradation of Primary Function / Line disruption	Loss of primary function	> 50% of product may need to be scrapped. Line shutdown	8
	Degradation of primary function	< 50% of the production run may need to be scrapped. Decreased line speed	7
Loss or Degradation of Secondary Function / Re-work out of station	Loss of secondary function	> 50% of production run may need to be reworked off line	6
	Degradation of secondary function	< 50% of production run may need to be reworked off line	5
Annoyance / Re- work in station	Item operable, but with annoyance noticed by >75% of customers	> 50% of production run may need to be reworked in station	4
	Item operable, but with annoyance noticed by 50% of customers	< 50% of production run may need to be reworked in- station	3
	Item operable, but with annoyance noticed by <25% of customers	Slight inconvenience to operation or operator	2
No Effect	No noticeable effect	No noticeable effect	1

Table 3 Guidelines for severity ranking in process/production FMEA [79]

Although the ultimate aim of on-machine probing is to improve the product, the FMEA conducted in this project will be applied only to the process, the design FMEA would relate to the design of the machine tool or probe, where the mitigations would be design changes to these systems. In many cases, the severity cannot be generalised, so becomes part of the framework. Two examples where this applies are:

1. Accuracy-related failure modes in probing will relate to amount of the conformance zone (section 1.4) that would be transgressed by the failure, the value or consequence, etc.
2. Time-related failure modes will relate to the impact on production time/productivity.
 - a. For a process with a high throughput of hundreds of components per day the severity is likely to be very high for even a small delay. This is likely, though not guaranteed, to be less significant where the cycle time for a part is several hours.

- b. Likewise, where an operator is always present with the machine an interruption due to detectable probe failure can be quickly rectified, whereas in lights-out automated production this could effectively halt all overnight production.

2.4 Project Aim

The aim of this project is to create a bottom-up strategy for minimising uncertainty for practical on-machine measurements, giving machine tool users a solid foundation for confident and appropriate use of machine tool probes.

2.5 Research Objectives

The aim will be met through the following research objectives:

- Obj 1. Determine the influencing factors that cause failures or create uncertainties in on-machine probing.
- Obj 2. Categorise the different uses of probing on machines to provide sufficient nuance that it can be applied in practical, industrial use.
- Obj 3. Create a framework for correct use of probing, including pre-requisites before measurement.
- Obj 4. By literature review or experiment, show the relative magnitudes of the most critical influencing factors to prove the need for the produced framework.

2.6 Scope

2.6.1 Machine tools

Taking the scope of machine tools from ISO230-1:2012, machines considered in this dissertation are “power-driven machines, which can be used for machining metal, wood, etc., by the removal of chips or swarf material or by plastic deformation. It does not cover power-driven portable hand tools.” [22]. Furthermore, **the dissertation only covers milling machines controlled by computer numerical control (CNC)**, since the probing systems under investigation are used to update controller offsets automatically or for further numerical processing. In practical terms, it is unlikely that this dissertation would apply to woodworking, where tolerances are generally much wider. However, the framework developed could easily be adopted in such industries if required.

As a point of interest, the research group was approached by a company manufacturing granite kitchen worktops using a large CNC machine who did consider adopting probing to reduce waste and increase productivity. There is, therefore, anecdotal evidence that these systems may become even more ubiquitous in the future.

2.6.2 Probing function (workpiece/tool measurement)

On-machine probing can be broadly split into probing of the workpiece (using a spindle-mounted probe) and probing of the tool for length and diameter. **This dissertation considers the spindle-mounted workpiece probing system.** Further work is recommended to understand more fully the influence when used in combination with tool-probing systems.

2.6.3 Workpiece interaction method (Tactile/non-contact)

Probing technology is broadly split into tactile systems (based on a stylus tip contacting the surface of the object under measurement) or non-contact using optical methods. Non-contact systems, such as the Hexagon LS-C-5.8 Machine Tool Laser Sensor [80], have only recently entered the market. **This dissertation analyses tactile touch-trigger and strain-gauge probing systems.** This is because these systems are prevalent on current machines in industry and were available for testing. However, it is only the uncertainty and calibration of the optical probe that would require inclusion within the framework developed in this dissertation. Further work is recommended to analyse optical probes more thoroughly for application in machine tools.

2.6.4 Probing strategy (Discrete point/scanning)

Recent developments have led to tactile machine tool probes with scanning capability, such as the Renishaw SPRINT [81]. These bring into play additional errors of motion and control. **This dissertation considers discrete-point measurement,** since the adoption of scanning probing systems is beyond the requirements of most industrial applications at present. Scanning by tactile or optical means will emerge as a more rapid method of data collection in the future if the cost of integration can be sufficiently low. However, international standards for quantifying the influencing factors also require development. It is recommended that further work be undertaken to develop the framework presented in this dissertation to accommodate scanning technology.

2.6.5 Thermal errors and modelling

The literature review has revealed the large amount of work being undertaken to create and validate thermal error models for machine tools. **This dissertation acknowledges the need for quantifying thermal influences but does not seek to create a new thermal error model.** Chapter 5 includes some representative thermal tests, which form part of the prerequisites for reliable probing defined in Chapter 4. This data will be used by other researchers to generate thermal error and compensation models, which ultimately can be deployed to reduce this source of uncertainty.

2.7 Methodology

2.7.1 Background knowledge and informal influences

The authors background knowledge to this subject comes from over three decades of experience as a CNC machinist and then manufacturing cell supervisor in industry. In those roles I learned the required principles of good measurement and how it applies on machine tools. The work I undertook was highly specialist precision engineering and required that I learned about new technology and how it could be applied to improve process flow and overall quality. Since 2012 I have been a Machine Tool applications Engineer at the University of Huddersfield, where I have been able to get much more in-depth understanding of machine tool accuracy and the tools needed to measure them. During this time, I have worked on projects at over thirty different manufacturing companies and spoken to machine operators, maintenance engineers and production engineers. I have also supported a number of academic projects including research council projects and projects with industry, PhD researchers and MSc students. This learning has formalised my approach to experiments and testing. All research and test results presented in this dissertation have been undertaken by myself and not presented elsewhere, unless otherwise referenced.

Much of this research has therefore been influenced by frequent observation of real industrial practice over the years before and during these studies. While the remainder of this work follows a more formal, academic methodology, it would be misleading not to acknowledge the foundational awareness of industry practice that has come from these informal interactions.

2.7.2 Formal methodology

2.7.2.1 *Objective 1 & 2*

DETERMINE THE INFLUENCING FACTORS THAT CAUSE FAILURES OR CREATE UNCERTAINTIES IN ON-MACHINE PROBING.

CATEGORISE THE DIFFERENT USES OF PROBING ON MACHINES TO PROVIDE SUFFICIENT NUANCE THAT IT CAN BE APPLIED IN PRACTICAL, INDUSTRIAL USE.

The project is based upon a literature review using academic texts found through the University Library, academic publishing houses and general search engines. It also relies heavily on industrial references, such as user manuals, training material and other resources from manufacturers of probing systems, machine tool suppliers and end-user case studies. Particular reference is given to standards published under “ISO/TC 39/SC2 Test conditions for metal cutting machine tools” which cover aspects of machine tool effects on accuracy performance.

This was then supplemented by performing a formal Failure Modes and Effects Analysis (FMEA), working with industry partners who are using machine tool probing

systems to provide detailed information and grade importance of failure modes and effects under different modes of operation (Chapter 3).

2.7.2.2 *Objective 3*

CREATE A FRAMEWORK FOR CORRECT USE OF PROBING, INCLUDING PRE-REQUISITES BEFORE MEASUREMENT.

The framework is created in Chapter 4, based upon the previous two objectives. It has been constructed as a flow chart, with appropriate decision points and flexible entry of variables (e.g., tolerance values) to make it generally applicable across manufacturing, rather than answering a single case-study.

2.7.2.3 *Objective 4*

BY LITERATURE REVIEW OR EXPERIMENT, SHOW THE RELATIVE MAGNITUDES OF THE MOST CRITICAL INFLUENCING FACTORS TO PROVE THE NEED FOR THE PRODUCED FRAMEWORK.

The most critical aspects of the FMEA were validated by literature or measurement for the probing system and machine which carries it (Chapter 5).

To achieve this, tests were designed and run to check the reliability and repeatability of the probing system as a whole, including all the inherent errors of the machine tool, tool probing system, and environment. These were broken down into machine tool geometric and thermal measurement strategies that were designed and conducted to determine the optimum volume that needs to be measured to provide good probing results (Chapter 5).

2.8 Contributions

The concept for the test artefact used during thermal tests (Chapter 5) arose during a project to develop the iTEC thermal compensation system with Dapatech PTE. Ltd. and Renishaw plc. Similarly, the cycles used for evidence of thermal influences on probing are based on those developed by the author during the project.

Moschos Papananias thesis [82] describes in detail the work undertaken to compare the results of on-machine probing against CMM measurements and flexible gauging. During this work all the machine tool probing routines and programs were written by me, and some of the issues highlighted by this work gave rise to this research.

MATLAB programs have been developed within the research group over many years to analyse temperature and probing data. These functions were developed and executed for me by colleagues within the team to contribute to the data analysis in Chapter 5 of this dissertation. All data and interpretation are my own.

2.9 Summary

This literature review has identified the Renishaw productive process pyramid as a clear way of breaking down the steps from the process foundation to products setting,

in-process control and post-process monitoring. Adopting this structure enabled the remaining literature review to broaden beyond the scope of the pyramid, while retaining focus around its key aims at each level. Considerable volume is given to the methods of measurement for the foundation layer and better understanding the probing systems themselves. Inherently probes are repeatable and accurate, but the machines which carry them, and processes used to operate them, have a significant number of potential weaknesses.

This chapter provides both the aim and four research objectives. It also recognises the large area in which this dissertation sits, so considerable thought has gone into describing and limiting the scope to set realistic expectations, based upon the papers and standards.

The methodology has been described, acknowledging the influence and value of the informal knowledge that has been acquired in the lead up to this project. Many aspects of on-machine probing have sensitive commercial consequences; so much of the input from practitioners must necessarily remain confidential.

The reviewed literature was important to determine the direction of the project, but also to contribute to how the framework would be created. A brief review of methods of generating such frameworks has led to an approach of using an FMEA informed by both the review, informal and experiential knowledge as well as more formal brainstorm with experts. This process will be described in the next chapter.

Chapter 3 On-machine probing FMEA

Failure Mode and Effects Analysis (FMEA) is a method of inductive reasoning used to identify causes of failure and their effects [83]. This method was chosen to analyse the problem and narrow down the large number of influences to the most significant for this project.

3.1 Methodology

The FMEA was conducted in 2019 using knowledge gained from the literature review and experts from academia and industry. The industrial experts included maintenance engineers from a machine tool service company, machine operators and production engineers. The FMEA was reviewed in both 2020 and 2021 considering findings during this project.

Critically, the FMEA was also informed by informal discussions with industrial practitioners. For example, one manufacturing facility has a sign on their machines, “Machine probe to be calibrated weekly”. However, in discussion with the operator it was evident that no probe recalibration had taken place for several months, with the perception from operators that this did not make a difference.

The general steps for an FMEA are given in Figure 27. In this project steps 1, 2, 3 and 8 were undertaken by the panel. The “severity, occurrence and detectability” (SOD) parameters were in some cases included as part of this exercise, though as explained in section 2.3.2 this has been omitted due to the generalised nature of the FMEA.

Step 1	Review the process or product.
Step 2	Brainstorm potential failure modes.
Step 3	List potential effects of each failure mode.
Step 4	Assign a severity ranking for each effect.
Step 5	Assign an occurrence ranking for each failure mode.
Step 6	Assign a detection ranking for each failure mode and/or effect.
Step 7	Calculate the risk priority number for each effect.
Step 8	Prioritize the failure modes for action.
Step 9	Take action to eliminate or reduce the high-risk failure modes.
Step 10	Calculate the resulting RPN as the failure modes are reduced or eliminated.

Figure 27 Ten steps for an FMEA [84]

3.2 Measurement modes for on-machine probing

Initially, the uses of on-machine probing were listed in accordance with the literature review and a “brainstorm” with the experts involved. Each has a different purpose, a likely different frequency of use and different effects. These are summarised in

Figure 28 and described in the subsections below.

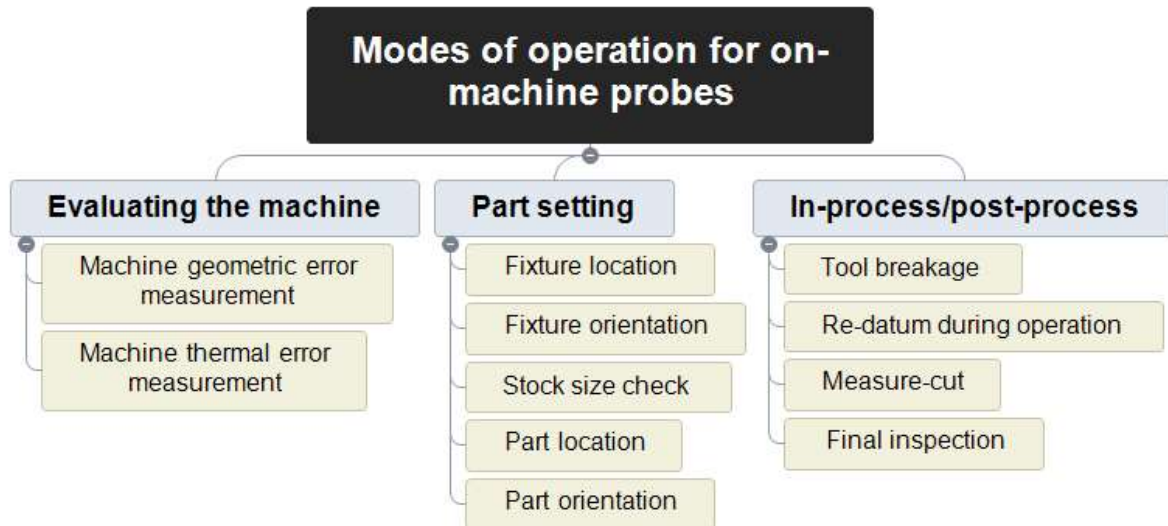


Figure 28 Mind map diagram of modes of operation for on-machine probes

3.2.1 Evaluating the machine

3.2.1.1 *Machine geometric error measurement*

As discussed in section 2.1.8.7, probing of machine artefacts can be used to determine the geometric errors and, in some cases, compensate them. The purpose is to make the machine cut material more accurately. Therefore, if the probe induces errors into the evaluation of the machine it will consequently make the machine worse. Full geometric error measurements are generally only occasionally carried out (perhaps every year) though some very automated measurements, for example to update the rotary axis offsets, might be run as regularly as every day or before each finishing cut.

3.2.1.2 *Machine thermal error measurement*

Probing of artefacts can be undertaken to see change due to thermal influences. For a duty-cycle thermal model (e.g., spindle run-time) only the probing data is required. By also monitoring temperature at key points while undertaking this operation and temperature-based thermal model can be created. Models are generally developed from large data sets, so uncertainty of individual readings is likely to be compensated by averaging or curve-fitting of the data. Repeatability is the most important attribute of a probe for this type of work as the measurement datum will be set at the start of

the test and incremental changes will be logged. The geometric errors of the machine also do not influence the measurement for the same reason, but the axis repeatability is the limiting factor in the quality of the data.

3.2.2 Part setting

3.2.2.1 Fixture location

Fixtures can be simply devices for holding a part while being machined. In this case the location of the fixture may need to be known only for collision avoidance (setting zones which the machine cannot enter), for automated part-loading, etc. Any required accuracy of part location would come from probing the part itself. In this case, the requirements for probe performance for locating the fixture would be relatively low.

Alternatively, fixtures can include their own datum features and repeatable part location. In this way, a component can be loaded into the fixture and machining can commence without any further need for establishing the workpiece coordinate system; the coordinate system is defined by the fixture. In this case the probe would require the levels of performance needed for finding part offsets or possibly even higher, since the reliance on finding a fixture once and using it many times could be construed as carrying higher risk of consequential failure than finding each part where only one component at a time is at risk

3.2.2.2 Fixture orientation

The considerations for orientation of the fixture are the same as for location. However, the two are separated because the numeric tolerance might be more stringent on one than the other.

3.2.2.3 Stock size check

Probing check to ensure the correct stock size is loaded, pre-empting costly tooling breakage from oversize stock, or lost time through machining of parts from undersized stock. Generally, it would be expected that this has low performance requirements of the probe, since the stock will necessarily be larger than the final machined part. This cannot be guaranteed; as machines become more repeatable and manufacturing becomes more reproducible the stock part can become closer to “near-net” meaning there is less excess material, thus potentially increasing the demands on the probe for this mode of operation; inaccuracies in the probing system could falsely reject a part as undersized or start work on one that is undersized.

3.2.2.4 Part location

Probing to locate a part within the working volume and align the part datum with the machine coordinates. A similar argument can be made as for stock size check, though probably with a greater amount of performance required for part location. As per the

previous discussion, the level of performance required may depend on the amount of spare material and where it is a roughing or finishing operation.

3.2.2.5 *Part orientation*

Square stock or part machined components may need to be aligned parallel to an axis, or more importantly to a part programme. It would be expected to have similar requirements to part location, though as with the fixture location or orientation may have tighter requirements so they have been separated for this analysis.

3.2.3 *In-process/post-process*

Parts can be checked for size either before finishing or at the end of a cycle for conformance. The performance of the probing system will depend upon the resultant action. If a part is to undergo a machining operation, then clearly the tolerance of the part will in some way inform the levels required of the probing system (refer to the conformance zone in section 1.4). Another consideration, for post-process monitoring, is that control decisions on machine parameters or overall production could be made on the statistical process control (SPC) values generated by the OMP. Therefore, consideration must be given not just to the quality of the data for decisions on an individual part, but on the entire plant maintenance structure.

3.2.3.1 *Tool breakage*

The probe can be used for checking that a tool is not left broken in a hole. This is not commonly done, due to the measurement time, but if an on-machine tool setter, or tool breakage checker, are used and identify a broken tool then the spindle-mounted probing can be used to identify whether any damaged tool remains in the hole before undertaking the next operation, such as tapping.

Probe accuracy, repeatability and uncertainty can be low as the operation is only looking for an obstruction.

3.2.3.2 *Re-datum during operation*

Re-datuming is used to keep control of, for example, changing thermal errors, tool wear, etc. The performance requirement will be linked to the general in-process tolerances.

3.2.3.3 *Measure-cut*

This is often used for updating part or tool offsets but can also be used for iteratively machining by taking a roughing cut, probing, then taking a semi-finishing cut and making final updates before finishing. Taking extra cuts takes more time, but for high-value components it is better to leave “metal on” by stopping the cut short than trying to take it all off at once and scrapping the part.

Companies who are adopting “lights out” manufacturing, where the machine tool runs without operator intervention overnight, are likely to use this method to ensure that time is not wasted on operations that have not successfully completed.

3.2.3.4 *Final inspection*

While the majority of users would send completed components to inspection departments to check conformance before despatch, there is a growing desire to avoid this bottleneck, especially on large parts. The performance of the probing system must therefore match the requirements of the quality department in terms of repeatability, reproducibility, uncertainty and traceability. Depending upon the demands of the component this might be a relatively wide tolerance, but for some manufacturer this is where the greatest burden would lie, but possibly greatest returns could be achieved.

3.3 **Failure Modes: Definition of “success” and “failure” for OMP**

In the context of this analysis, a decision was made through discussions with industrial partners and ourselves that success would be defined as:

- a good measurement,**
- with appropriate level of uncertainty,**
- taken in a timely manner.**

The first brainstorm exercise created a long list of failures when probing. However, subsequent reflection allowed these to be rationalised to only four modes of failure (Figure 29) which are considered in the following subsections. This process of refining the failure modes was undertaken with great care to preserve the nuance in the failure effects and mechanisms (sections 3.4 and 3.5) while simplifying the failure modes.

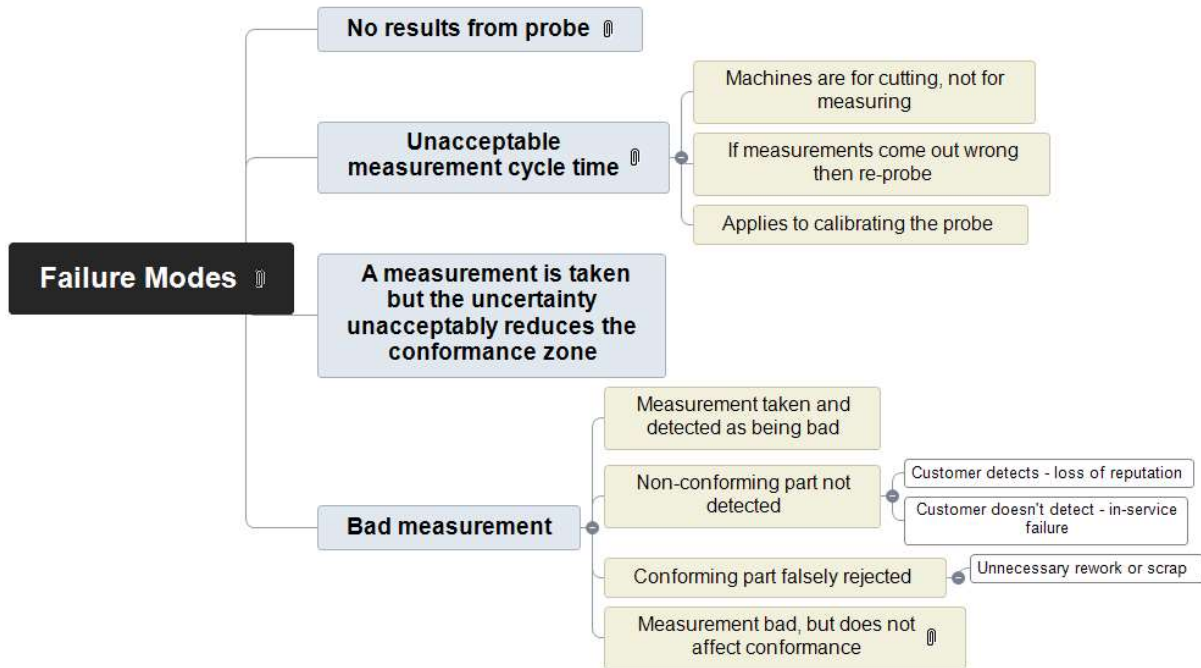


Figure 29 Mind map diagram of failure modes for on-machine probing

3.3.1 No results from probe (Failure to take a measurement)

Whichever mode of operation, it is self-evident that a result must be supplied. This failure should very quickly be noticed if the probe did not return a result or faulted due to a false trigger or battery failure. This would cause the controller to cease operations and display a warning to the operator. However, if the process were “lights out” with no operator in front of the machine then the delay could be much longer – not until the morning shift started.

3.3.2 Unacceptable measurement cycle time

Machines are only “making money when the spindle is running” is a phrase that is often heard; sometimes a probing routine can have a long cycle time. On low-value parts a long cycle time that takes longer to measure than it takes to make the part would be deemed unacceptable. However, this does not universally apply and should be challenged. It applies when the machine tool is the bottleneck process, or where an operator must be dedicated entirely to a machine, etc. However, where this is not the case, greater savings could be made by reducing the need for subsequent inspection and rework steps [94]. Therefore, the point at which this cycle time becomes “unacceptable” will vary from process to process.

3.3.3 A measurement is taken but the uncertainty unacceptably reduces the conformance zone

A measurement is taken but the uncertainty unacceptably reduces the conformance zone

3.3.4 Bad measurement

This failure from a bad measurement can manifest in one of two ways:

1. A bad measurement is taken and is detected as being “bad” data

In this case an appropriate response would be for the operator or controller to cease operations and validate why a bad measurement was produced: debris in the component, broken styli, or program error. Unless there is an automatic response to the detected bad data a delay is likely to be caused, affecting productivity, but there should be no additional consequences.

Alternatively, the response may be inappropriate, such as ignoring the result. In this case, this could lead to consequential damage to the part or further quality control or delay issues downstream of the process.

2. A bad measurement is taken and is not detected
 - i. A bad measurement is taken and gives an undetected false positive
 - ii. A bad measurement is taken and gives an undetected false negative
 - iii. A bad measurement is taken, not affecting conformance decision (perhaps affects SPC)

The mapping of failure modes to modes of operation is given in **Table 4** on a scale from zero to five in terms of how much a failure mode would have affected a mode of operation. For example, tool breakage detection is not a measurement as such, so is unaffected by the “measurement” uncertainty and scored zero. Final inspection requires a good understanding of the uncertainty so rated five. This table was derived according to the methodology provided in 3.1.

Failure Mode	Applies to										
	Machine geometric error measurement	Machine thermal	Fixture location	Fixture orientation	Stock size check	Part location	Part orientation	Tool breakage	Re-datum during machining	Measure-cut	Final inspection
No result	1	1	1	1	1	1	1	1	1	1	1
Unacceptable cycle time	1	1	2	2	2	2	2	1	3	4	5
Too high uncertainty	3	3	2	2	1	3	3	0	4	4	5
Bad measurement	3	3	2	2	1	2	2	2	4	4	5

Table 4 Mapping of failure modes to modes of operation

3.4 Failure Mode Effects

The FMEA effects were similarly broken down into generic failure effects in terms of damage to the machine or operator, loss of production or increased production time or damage/scrap of parts. They are provided in Figure 30 and discussed in the context of possible root cause in sections 3.5 and 3.6.

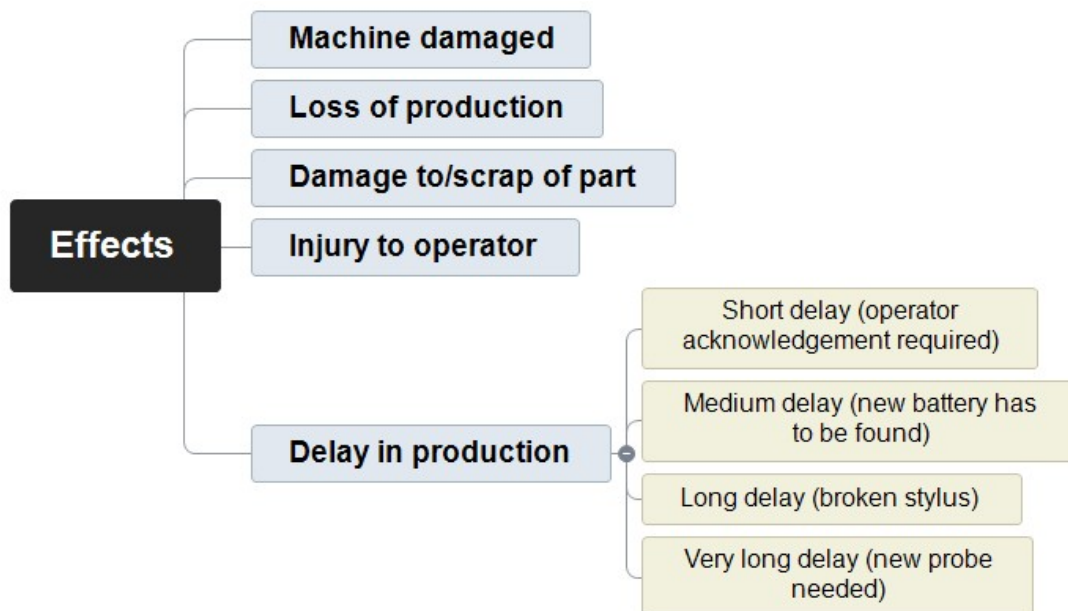


Figure 30 Mind map diagram of failure effects

3.5 Mechanisms (causes) of failure

The causes of failure were initially broken down into their main classifications, as shown in Figure 31. The approach was to linearly build from the factory and machine through process hardware, procedures, tools and software to final results and reactions. The fully expanded map is a typical root cause analysis shown as a fishbone diagram, provided in Appendix D as Figure 118

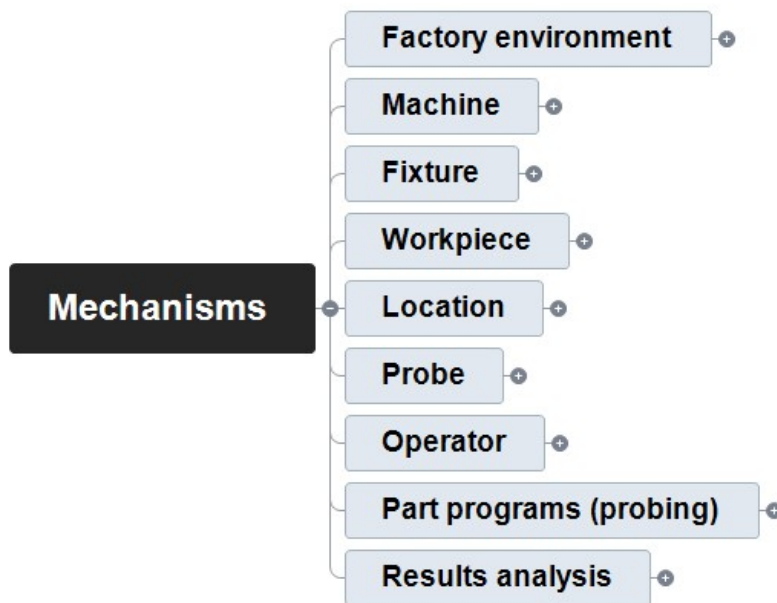


Figure 31 Top-level mind map of failure mechanisms when probing

The remaining figures in this section (Figure 32 to Figure 40) summarise the key mechanisms. They will not be individually addressed in this dissertation, since each point crystallises several issues and effects that would lead to a failure mode.

The factory environment (Figure 32) has a direct impact on the machine and therefore the probing. Research work took us to a facility where a press was operating on a machine close to a milling process where surface finish was paramount, and vibrations were transferred through the floor from the press to the milling machine. Another example is on a machine where tidal effects cause the foundations to move. Possible impacts on probing are false readings or no reading through mis-triggering.

Similarly, one facility revealed that a measuring machine had been accidentally struck by a forklift truck. Having a no-blame culture, this incident was reported, and remedial action taken. However, in a less enlightened facility this could have been missed, causing bad readings to be taken and emphasising the need for regular monitoring through tools such as a ball bar or artefact probing.

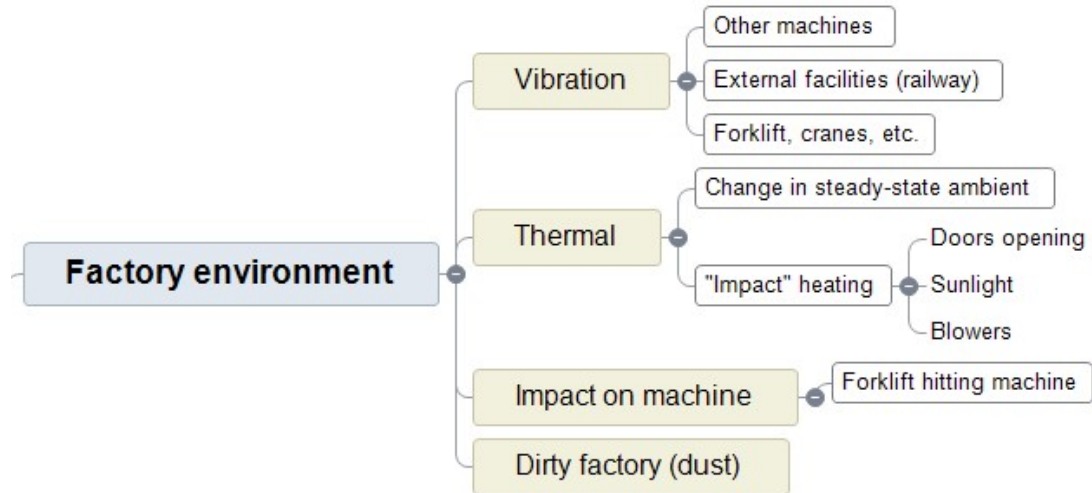


Figure 32 Mechanisms - factory environment

Many of the machine factors (Figure 33) have already been discussed in Chapter 2. An undetected bad measurement caused by machine errors could lead to too much material being removed on a finishing cut, causing delays, or scrapping a part. The geometric (quasi-static mode) and thermal influences are considered to be the main influencing factors from the literature review but have also been seen to have wide variation in magnitude from our research activities. These errors will therefore be carried forward to the investigation in Chapter 5.

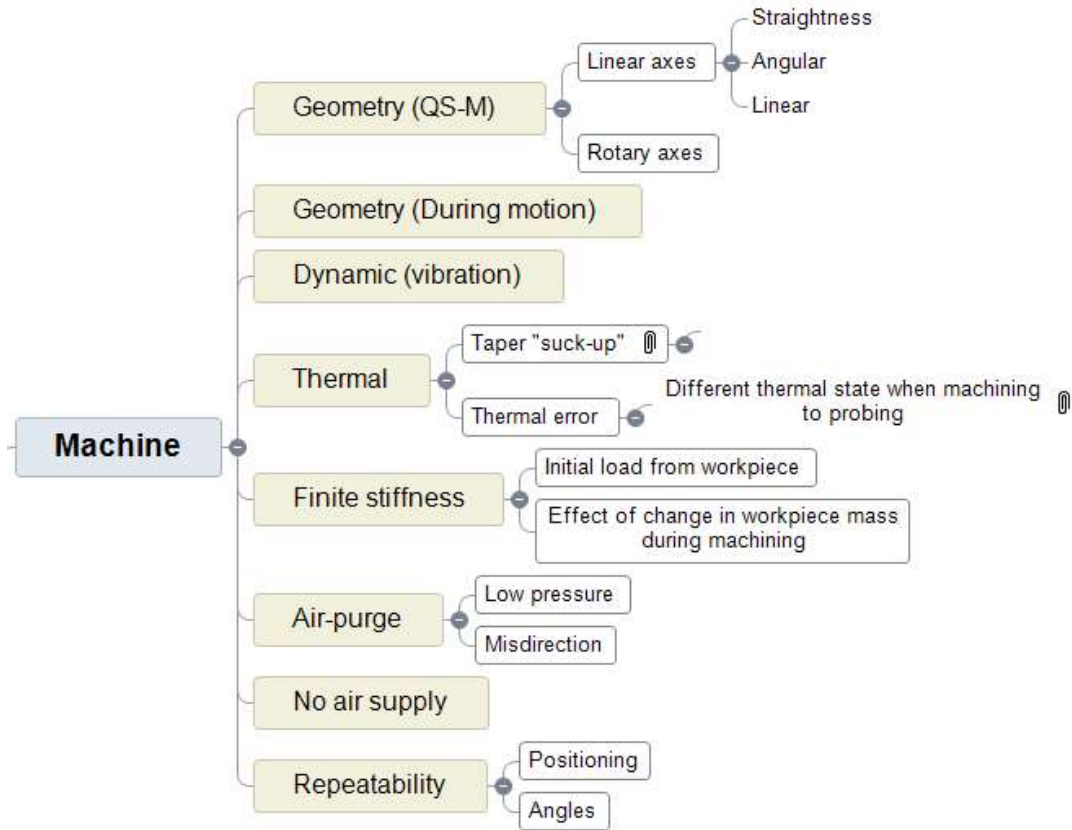


Figure 33 Mechanisms – machine

The fixture (Figure 34) can have a large effect on components, especially thin-walled parts, where clamping forces, and spring-back after machining, can have a significant effect. If the fixture is used for datuming the part, then it becomes part of the measurement thread.

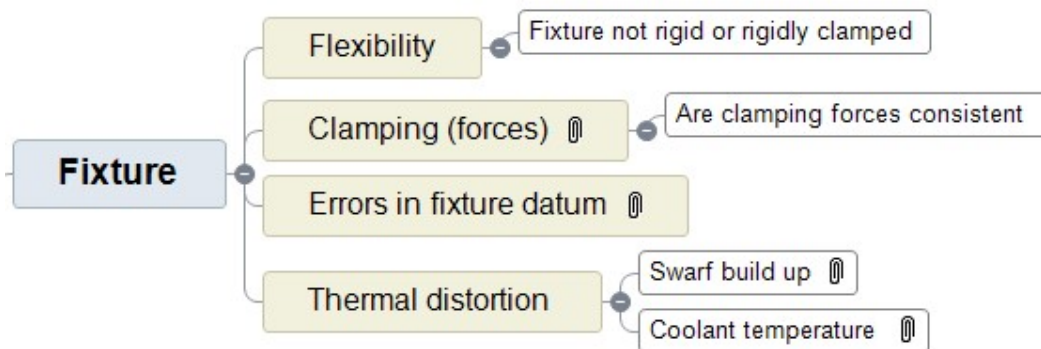


Figure 34 Mechanisms – fixture

Probing of the workpiece (Figure 35) is influenced by the surface being probed. Unlike a CMM, machine tools are harsh environments where cutting fluids, swarf (cutting chips) and heat build-up can all affect measurements.

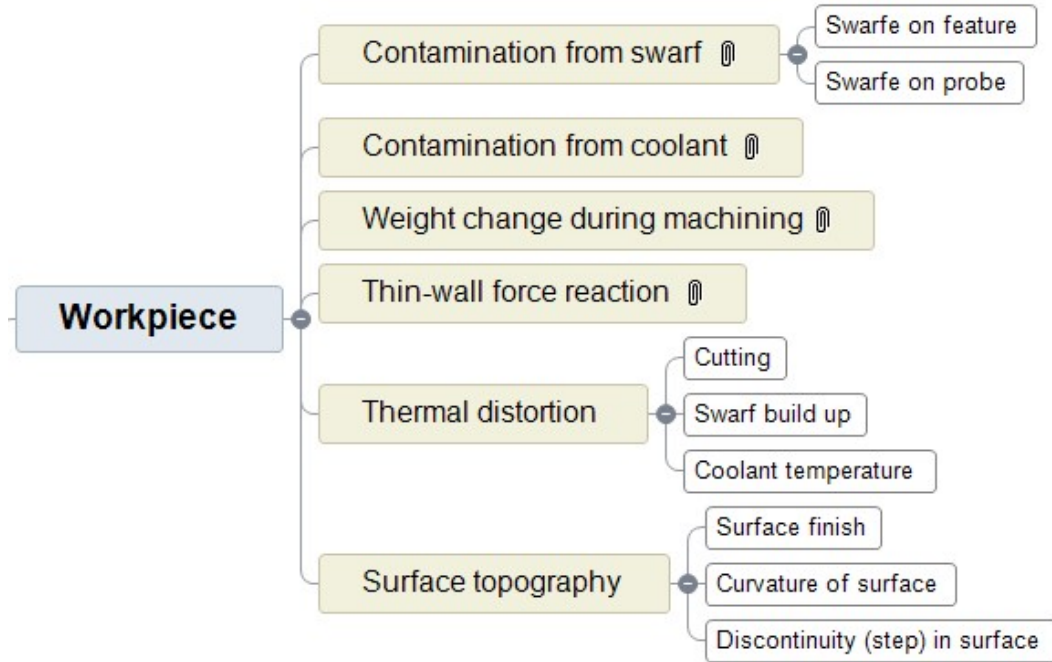


Figure 35 Mechanisms – workpiece

The “location” mechanisms (Figure 36) will be discussed in more detail in Chapter 4 and Chapter 5. They are not the root cause but are being considered as one of the key pathways to creating a failure mode because of the effect of geometric errors.

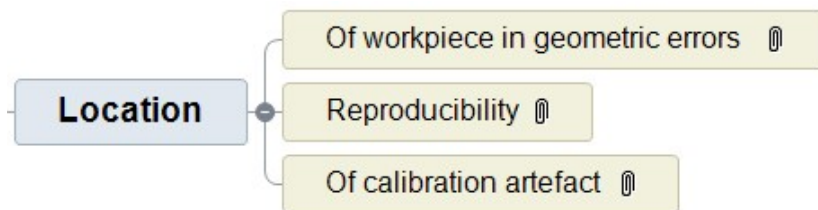


Figure 36 Mechanisms – location

Although probes have very impressive specifications, as noted in Chapter 2, aspects of the probe in use and maintenance can have an influence (Figure 37). One machine builder, responding to a call-out due to rectify a faulty probe, reported that upon attending the company it was found that the stylus had not been screwed in sufficiently tightly, thus giving bad readings. From testing conducted by this research group, the battery can fail at an inopportune time, causing no result to be available. As noted in 3.3.1, this could cause a considerable delay if operating “lights-out”.

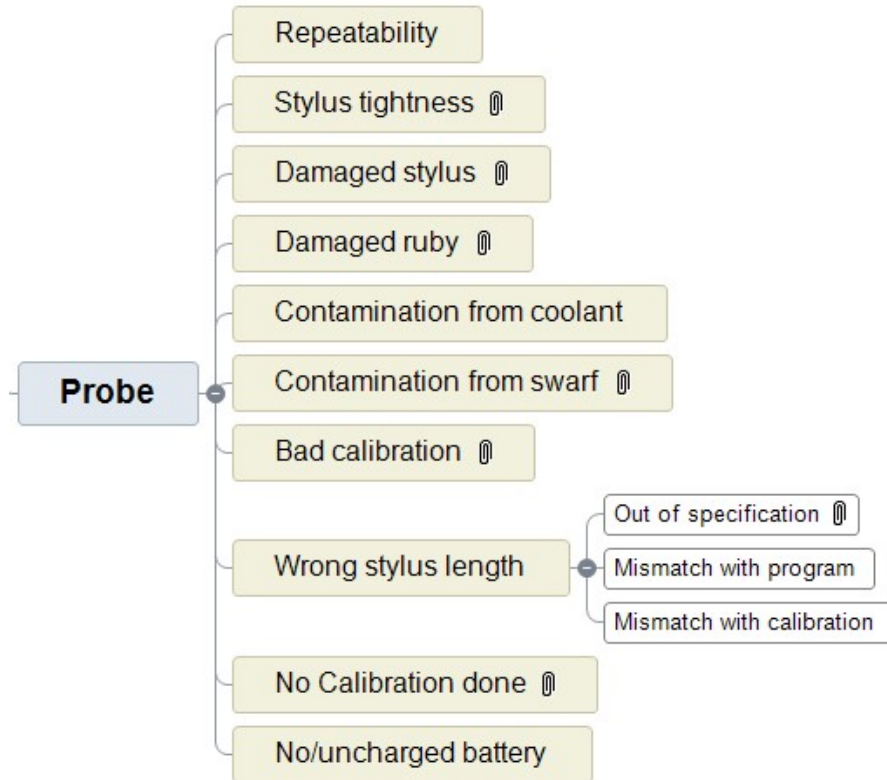


Figure 37 Mechanisms – probe/stylus

Care has been taken when considering the operator as a “cause” of failure (Figure 38). For example, selecting the wrong program could be considered an operator-generated failure. However, this could equally be assigned as an error of the procedures. Likewise, feed rate override (the ability to change to a percentage of the programmed feedrate through a panel-mounted potentiometer) can be itself overridden by programming practice to force the override selector to be ignored.

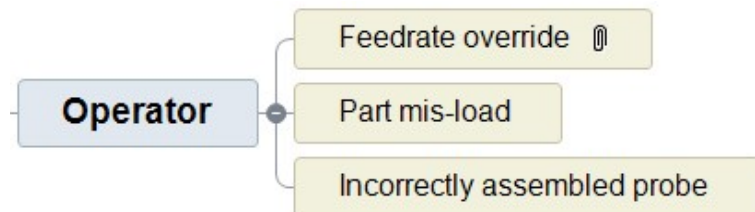


Figure 38 Mechanisms – operator

The software for probing (Figure 39) can also play a part in erroneous reading (fast feed rate, insufficient points), delays in production (slow feed rate, too many points), incorrect macro (subprogram) calls, etc. “Safe moves” are used to move the probe within the working volume when there is a risk of collision. However, they are slower than when moving the machine at rapid. It requires judicious programming to ensure safe operation while minimising the time lost in moving slowly.

Damage to the machine or injury to the operator from the probe itself at first seems unlikely. However, a member of the panel reported an incident where a probe had been in the spindle when a command of several thousand revolutions per minute was mistakenly commanded. The resultant force caused the battery to be ejected through the probe housing, causing irreparable damage to the probe. If there were sufficient force, then the battery could have caused damage to the machine or to the tools in the open carousel.

More likely scenarios include mis-programming of the probe, such as not using safe moves, or misloading of the part could lead to a collision between the probe and the machine or fixture. Sufficient force could damage the spindle holding the probe, which is often the weakest part on a machine.

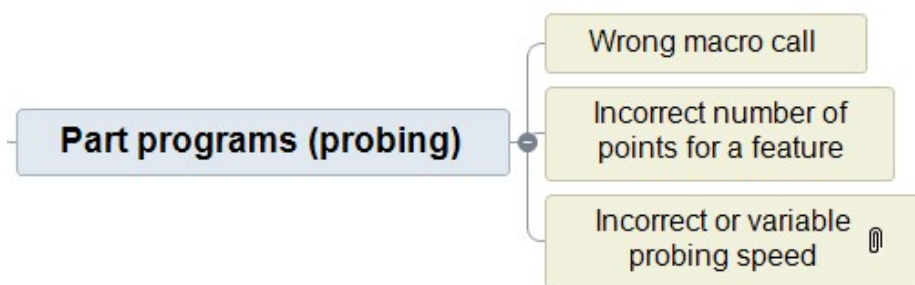


Figure 39 Mechanisms – probing program

The analysis and reaction can in itself have multiple causes of failure, from miscalculation and rounding errors in algorithms to incorrectly chosen tolerances (when considering the conformance zone). Poorly chosen response actions are very common. Experience seen in industrial workshops is that a bad, or out-of-tolerance, readings can be flagged up to the operator, who can then effectively “OK” the message and allow the process to continue. There is no fault attached to the validity of the probing results, but the overall result is a failure of the implementation of the probing system to provide a suitable and useful result.

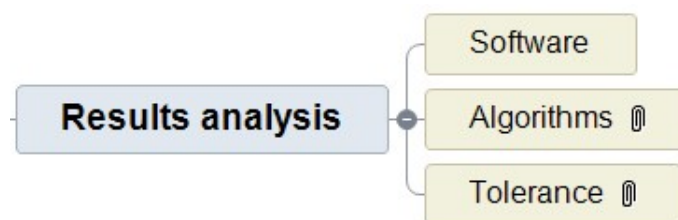


Figure 40 Mechanisms – analysis and reaction

3.6 Discussion

The FMEA process provided the breakdown of the causes of failure as it applies to the modes of operation previously devised. In consultation (formal and informal) the

breakdown has been validated both by agreement with those consulted and by anecdotal evidence from several practitioners (end users, production managers, maintenance engineers and probing suppliers). It would be foolhardy to claim that the list of effects and mechanisms is exhaustive, but it covers sufficient of the main factors to provide the basis of the framework.

Part of the issue with formalising procedures for supporting probing is that very often the failure does not immediately arise from a *potential* mechanism.

For example, one company has a procedure whereby the probes on the machine tool should be calibrated at the start of every working week, but due to the pressures of production this is not done by the operators. Through informal conversations this has been found to be far more common than might be thought. In this company, the probes are only used for locating the stock in the volume of the machine and not for measuring any features so although the procedure is not adhered to, the operators feel there is not an issue. In fact, one could argue that the procedure itself has been put in place without consideration for the impact on production. If there is no value in taking time to calibrate the probe, then the principles of “lean” manufacturing mean that step (wasted time) should be removed. The knock-on effect of mandating a “pointless” step is that if the company next wish to exploit further opportunities for the probe, then the culture will not permit that advance.

The other aspect is that in some circumstances a company might be “getting away with” omitting a step; just because you don’t measure something it doesn’t mean it is bad, it just means that you are not in control. If the factors and risks are known then a company can decide to operate conservatively, taking all necessary measures, or at risk. This statement is not pejorative; taking a calculated risk is sensible in business. The purpose of this dissertation is to be able to document and highlight the risk so the owner of a machine with probing can make an informed judgement.

3.7 Summary

This chapter has defined the different modes of operation for the use of on-machine probes. It also defined the “failure” of a probing system in terms of “no data” and “bad data” as well as excessive time required to use the system. These formed the foundation for the FMEA to understand the influencing factors in each case. The contributors provided anecdotal (anonymised) examples to support some of the items listed, which have been discussed in this chapter. They also provided information (indicative tolerances) on the requirements for each mode of operation. Since the tolerance values provided were only indicative it is not considered informative to present them in this dissertation. Each tolerance is very much set on a case-by-case judgement depending upon the value of the product throughput of parts, etc. Therefore, a more comprehensive study would be needed to provide values that would not be misleading to other researchers.

This analysis, classification and interpretations provides a backbone for better application of on-machine probing. In itself, it provides a list of considerations that should be made before using on-machine probing.

Many factors and failures were highlighted during this exercise, so it was decided to focus the scope on the factors affecting accuracy. Chapter 4 will produce a framework based on the machine tool factors related to accuracy, repeatability, and reproducibility of the probing. Chapter 5 will provide experimental data to show some of the effects of the important factors related to the machine and probe that were identified during this FMEA.

Chapter 4 Proposed framework

The literature review of the process foundation clearly identifies that due to the errors of the machine tool axes, the use of on-machine probing for measurement purposes should not take place until the influencing errors have been established. Once understood a decision can be made on whether they are within acceptable limits to proceed. However, as described in section 2.1, much of that exercise is time-consuming and requires skilled personnel. Therefore, it would be impractical to force all users of probes to undertake the full gamut of testing if they are only using the probe for stock-sizing or roughly locating a part before roughing operations.

4.1 Key performance indicators

The key performance indicators (KPIs) for the accuracy performance of the machine as a probing system are the measurement accuracy, repeatability, and reproducibility. They are defined by the international vocabulary of metrology - Basic and general concepts and associated terms (VIM) [85]:

Measurement accuracy: *“closeness of agreement between a measured quantity value and a true quantity value of a measurand”* and “NOTE 1: The concept ‘measurement accuracy’ is not a quantity and is not given a numerical quantity value. A measurement is said to be more accurate when it offers a smaller measurement error.” [VIM 2.13] [85]

Therefore, it should be noted that where a system is asked to meet an “accuracy” requirement, what is really meant is that numerically the measurement error must be less than a defined tolerance.

Repeatability condition of measurement: *“condition of measurement, out of a set of conditions that includes the same measurement procedure, same operators, same measuring system, same operating conditions and same location, and replicate measurements on the same or similar objects over a short period of time”* [VIM.2.20] [85]

Measurement repeatability: *“measurement precision under a set of repeatability conditions of measurement”* [VIM 2.21] [85]

Reproducibility condition of measurement: *“condition of measurement, out of a set of conditions that includes different locations, operators, measuring systems, and replicate measurements on the same or similar objects”* [VIM 2.24] [85]

Measurement reproducibility: *“measurement precision under reproducibility conditions of measurement”* [VIM 2.25] [85]

4.2 Framework

Within the following section a framework of tests for benchmarking the machine tool against the three KPIs will be proposed, that will allow the errors affecting on-machine probing to be quantified. This would enable an estimate of the measurement uncertainty when probing to be made. This would then allow an informed decision on how on-machine measurement can be used on a particular machine. For example, it may limit use to establishing datums, or may only be useful for monitoring changes, but not for full verification. The modes of operation provided in section 3.2 will be used as the guideline.

4.2.1 Initial approach

The initial approach was to look at the problem as a top-down review. If you establish the performance of your machine, then you can determine for which modes of operation it is capable. Figure 41 shows a high-level overview of this strategy, where measurements of the machine are taken and then the machine is classified as meeting conditions A to D (as defined in **Table 5**) for each mode of operation in turn.

Condition	Meaning
A	Machine out of tolerance for measurement; probing can only be used as an indicator
B	Repeatability is within tolerance
C	Accuracy achieved; Measurement Error is within tolerance
D	Reproducibility is within tolerance over a defined range of conditions

Table 5 Definition of conditions for framework

The tolerance database for each mode of operation can then be easily tailored depending upon factors such as the value of a product being manufactured, required throughput, available capacity for downtime, etc. Furthermore, the framework can be expanded for additional KPIs in the future.

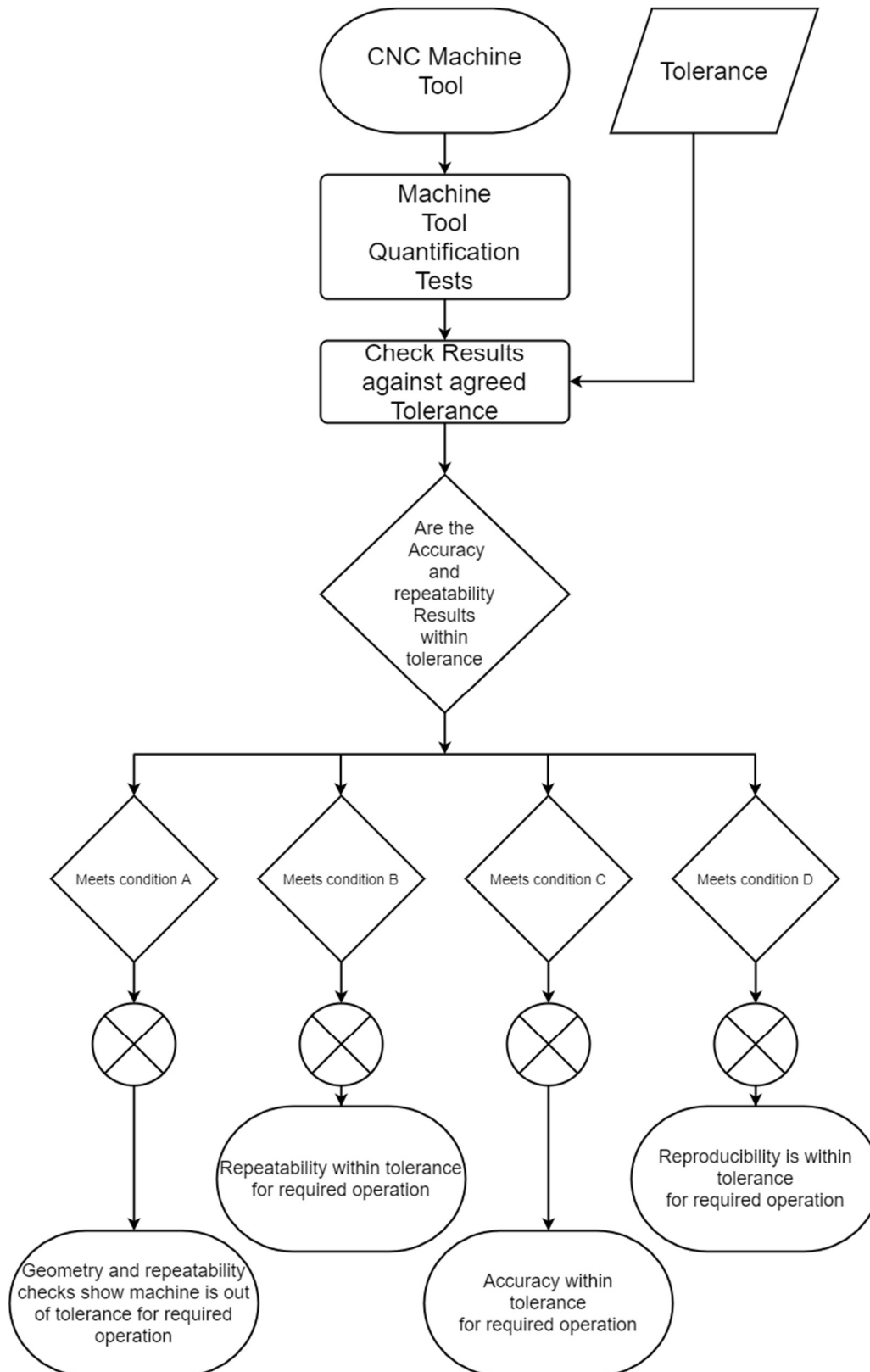


Figure 41 Overall top-down approach

4.2.2 Final Approach

The drawback of the initial approach was that it did not consider the commercial implications of having to undertake all the measurements to be able to populate the decision tree. Therefore, a new approach was taken, building up from the bare minimum where a probe/machine system does not require high performance. Complexity can then be increased as more demanding modes of operation are required. The same tolerance approach can be used as given in **Table 5**.

Tolerances are not just on an individual item? For example, there would be tolerances on repeatability, accuracy, and reproducibility for the 21 error sources, position-dependent and position independent thermal error, amount of tool-change non-repeatability, etc. In fact, each mode of operation can have a tolerance set against any test in section 4.3 or Chapter 5, or can have “not applicable” assigned against those which don’t matter for that mode of operation.

Even with this approach waste was identified; measurements would be taken only for the mode of operation under investigation. There was no “lookahead” to take advantage of where a machine user would like to be with the system. Additionally, the approach did not consider what improvements could be made to the machine at each stage.

Figure 42 provides a revised approach which includes an iterative loop for improving quality of both the repeatability and accuracy of the machine. The reproducibility loop has been omitted from the diagram for clarity.

Now, the data taken from the first instance can be interrogated at each stage, but if modes of operation with higher demands are required, they can be accommodated by analysing the same data plus any additional data required. If the system has not passed the less demanding tolerances, then the process does not pass on to the next level, so time is not wasted acquiring data for that eventuality.

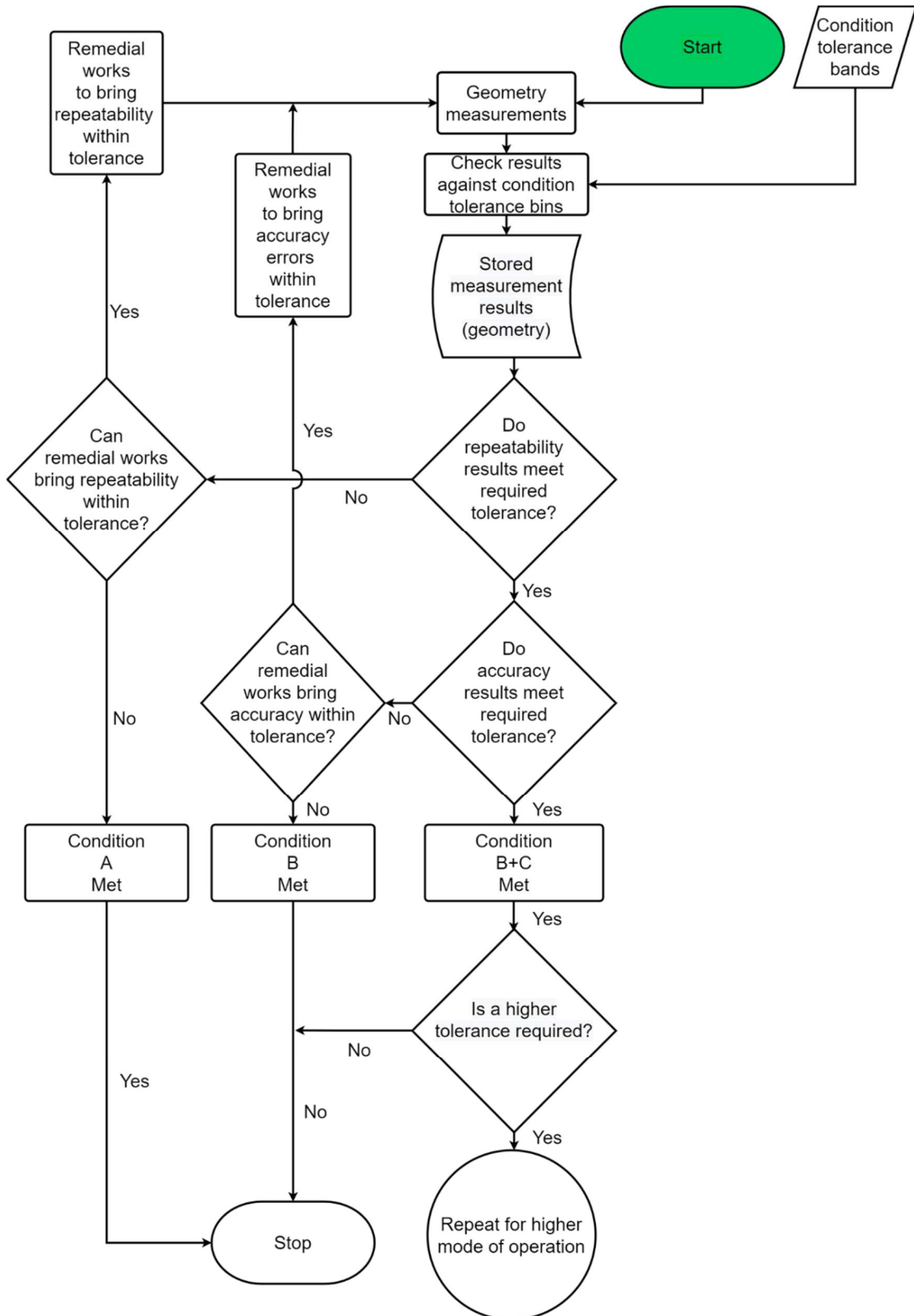


Figure 42: Proposed framework for an example mode of operation

4.3 Down selection of machine tool quantification tests

This section discusses the quantification tests, informed by the literature review, that are required to support the decision-making process above.

These tests are generically applicable to a wide range of machine configurations. Examples of these tests are provided in Chapter 5 for a C-frame type vertical spindle machine tool (VMC) similar to Figure 10 (04) and can be applicable to either a 3-axis or trunnion-mounted 5-axis machine tool.

Tests will be conducted utilising rapid machine tool verification methods, meaning there can be some deviation from the ISO standard tests, in order to minimise downtime of the machine and still allow traceable measurements to the applicable standard.

4.3.1 Geometry tests

4.3.1.1 *Straightness of linear motion errors and angular deviations of linear motions.*

ISO 10791-2:2001 proposes the use of a granite straight edge and dial test indicator be used on each axis in turn to measure the straightness of its linear motion, and precision levels (or inclinometers) for the measurement of the angular deviations. Due to advances in technology of machine tool metrology instruments, as discussed in Section 2.1.8.3, these measurements can also be completed at the same time as the linear position tests (section 4.3.2) using the Renishaw XM60 multi-axis calibrator. This has the additional advantage of being able to measure over a distance of up to 4 m, whereas a straight edge of that length would be very expensive and difficult to manage.

In this project the Renishaw XM60 will be exclusively used for gathering straightness data, although the framework would allow for alternative methods.

4.3.1.2 *Squareness between linear motions*

Measurement of the squareness between two axes is normally carried out using a DTI measuring on either a granite square or cylindrical square, as discussed in section 2.1.8.1. It can also be measured using the on-machine probe instead of a DTI.

The following errors should be ascertained using ISO 10791-2 as a guide

1. squareness between Z-axis motion and the X-axis motion
2. squareness between Z-axis motion and the Y-axis motion
3. squareness between X-axis motion and the Y-axis motion

The evaluation of squareness is significantly affected by the axis straightness (see Figure 14). Best practice is to consider that a squareness measurement is essentially made up of two straightness measurements at a nominal angle of 90° to each other.

At present, the Renishaw XM60 is not capable of directly measuring squareness. Squareness can be measured with a standard laser interferometer, such as the Renishaw XL80, using straightness optics and an optical square. This, though, is a time-consuming process and although a valid testing method will not be applicable to this research.

In this project, squareness values will be obtained using a telescopic ball bar. In this case the measurement is inferred, rather than directly measured, but the method is efficient and can be undertaken by machine operators.

4.3.2 Linear position error of linear motion tests

Standard methods use a laser interferometer, such as the Renishaw XL80, to measure this axis error.

The Renishaw XM60 multi-axis calibrator or similar device, allowing the capture of the six degrees of freedom, can be used to establish the linear axis errors of the machine tool. The measurement equipment should provide traceability back to international standards. An important factor is the number and distribution of targets to sufficiently map the axis errors. As reported by Miller et al. [40] the minimum number of points required by ISO230-2:2014 [49] is not necessarily sufficient to describe the axis errors.

In this project the Renishaw XM60 will be used for capturing the linear positioning error.

4.3.3 Angular errors of linear axes

The small angular deviations of a linear axis are normally measured using gravity-based inclinometers or optics on a laser interferometer. The former can only work on measurements where gravity can assist (i.e., they cannot do the “yaw” of a horizontal axis such as EBX in Figure 11 or “roll” of a vertical axis) and the latter cannot do measurements about the axis of the laser beam (i.e. “roll” of an axis).

In this project the Renishaw XM60 will be used to capture the angular errors at the same time as the linear positioning and straightness errors.

4.3.4 Spindle Checks

4.3.4.1 *Parallelism between the spindle axis and Z-Axis motion*

Using a calibrated test mandrel located in the machine spindle and Dial test indicator, the following errors should be quantified using the procedure set out in ISO 230-2:2014 clause 10.1.3.

1. Parallelism between the spindle axis and Z-Axis motion in the YZ plane
2. Parallelism between the spindle axis and Z-Axis motion in the XZ plane

A minimum of five readings should be recorded for each of the two end positions on the mandrel. The spindle should be rotated 180° and the test repeated. Rotating the spindle 180° and repeating the measurements isolates and removes any errors within the measurement artefact (test mandrel) from the actual test measurement readings. This is known as the Donaldson reversal technique [86]

Although standards exist to ensure procedures are followed and measurements by different companies or personnel can be compared, they are always a compromise and improvements can be made if the original intent is still adhered to. By completing several measurements on the test mandrel rather than one, an average can be taken of the readings, it is important though to make sure any reversal error is removed at the two extremes of the measurement before returning in the opposite direction.

4.3.4.2 *Spindle Run Out*

Spindle runout can be tested using a DTI measuring a calibrated dummy tool or in the taper of the spindle itself. It is also possible to measure it with some machine-mounted tool measurement devices, such as the Blum LC50-DIGILOG [87] rather than a DTI.

4.3.4.3 *Tool-change repeatability*

The repeatability of the machine tool spindle clamping mechanism after tool changes, independent of the spindle thermal influences, can be undertaken by using either a dummy tool and DTI or on-machine tool measurement device.

In this project the probe itself will be used to evaluate tool-change repeatability by measuring the same artefact several times (at least ten) without tool-change and then the same number of times with a tool-change cycle in between probing. To try to reduce cross-contamination with thermally induced errors, the amount of axis movement should be similar for both sets of tests.

4.3.5 **Machine tool thermal stability and effects**

4.3.5.1 *Environmental - ETVE*

ISO 230-3:2007 defines an ETVE test as “*designed to reveal the effects of environmental temperature changes on the machine and to estimate the thermally induced error during other performance measurements.*” Generally speaking, if the influence of the environmental effects on the machine tool are measured, it can be estimated how any change in temperature will affect future test results.

The ETVE test can be conducted following the procedure set out in the relevant ISO standard. The Lion Precision spindle error analyser (SEA) [88] or similar NDT sensor nest can be used to conduct the test.

Thermal testing is, by its nature, a time-consuming process. Therefore, this project will consider both the technical need and commercial impact to assist with recommending the most appropriate course of action.

Despite many years of using an SEA for this type of test, this project will use the on-machine probing of an artefact for the analysis of ETVE. This allows automation of the process, which can be run automatically, or semi-automatically whenever the machine is idle.

4.3.5.2 *Spindle thermal distortion evaluation*

In a temperature-controlled room, a machine might be assumed to be thermally stable, but being in a stable environment does not remove the need to monitor the thermal behaviour of the machine tool components such as motors, drives and axes.

For the spindle thermal distortion evaluation, a suitable test mandrel is normally inserted into the rotating part of the spindle. A fixture containing five linear displacement sensors, such as the SEA mentioned above, is suitably fixed on the table to surround the mandrel with two each of the sensors in alignment with the X and Y axes and one sensor in the Z axis direction.

Despite many years of using an SEA for this type of test, as with the ETVE, this project will use the on-machine probing of an artefact for the analysis of spindle heating. This allows automation of the process, which can then include duty cycles with axis movements as part of the same program as the spindle excitation. This cannot be conveniently achieved with an SEA because of obstruction to axis movement by the sensors.

The standard BS ISO 230-3:2007 [89] details two types of test for spindle thermal distortion evaluation and offers that either can be used with agreement from all parties involved.

The two tests are

1. A constant spindle speed run through the whole of the test
2. Variable speed spectrum, where the spindle speed is run at different speeds for specified lengths of time with short stops added intermittently.

For both tests it is suggested that they should be ended when “*the distortion change during the last 60 min is less than 15 % of the maximum distortion registered over the first hour of the test.*”

As this research is interested in the behaviour of the machine under operation, rather than quantifying the machine for a thermal model, a representative variable speed spectrum duty cycle is chosen as being the most useful test.

4.3.5.3 *Axis thermal distortion evaluation*

Axis heating tests of an individual axes can be performed using laser measurement similar to the standard measurement for geometric errors, but with a period of excitation (rapid traverse of the axis) between measurements. An example of this process using a Renishaw XL80 will be given in section 5.4.1. However, the majority of the thermal testing will again use artefact probing.

4.3.5.4 *Effects of spindle heat expansion on cold tools.*

Temperature differentials cause distortion. An often-overlooked aspect is how the probe reacts when a probe at “ambient” temperature is taken from the tool carousel and placed in a warm spindle. This can be tested by undertaking the tool-change repeatability tests (section 4.3.4.3) under cold and warm spindle conditions.

4.3.6 **Alternative approach – gauge capability study**

An alternative approach would be to conduct a gauge capability or gauge R&R (repeatability and reproducibility) study [97].

This approach is appropriate when similar products are made in a similar manner in similar locations on the machine. However, it is not useful where a probing system is being used for a wide variety of tasks, or a machine is used for a wide variety of parts. Another drawback is that such a study tends not to be diagnostic, in terms of being able to correct the machine to make improvements. If there is wear the whole R&R would need repeating regularly. This is likely to be more intrusive than checking the individual contributors to change.

4.4 **Machine tool benchmark monitoring**

Different methods of monitoring any change in machine performance have been proposed and reviewed in Chapter 2. Future systems may rely more on signals and sensors permanently active on the machine, but at present the analytics are not sufficiently mature to be able to discern micron-level changes in repeatability, accuracy, or reproducibility. Therefore, an example of how a Renishaw QC20w telescopic ball bar can be used to track performance is provided in section 5.3.3.

4.5 **Creation of enabling part-programs**

All suppliers of machine tool probes will supply their own macros that can be imported into a program to enable probing on the machine. Many CNC controller manufacturers and some machine builders also provide their own, alternative routines.

Due to the wide range of testing undertaken within research this project embraces the research group’s policy of creating parametric machine tool part programs. While not unique, normal practice in industry is to modify programs according to need. The philosophy brought to this work is to provide a section at the start of a part program that holds a set of variables to change the cycle. Allied with the probe macros, this can become an extremely powerful tool, which should become part of the approach to probing to gain most benefit.

An explanation of the approach being put into practice is given in section 5.1 and several example programs are provided in Appendix C.

4.6 Summary

This chapter has proposed a decision-making framework focussed on the accuracy-related mechanisms that lead to the probing failure modes. Essentially, the framework diagrams presented concentrate on the contribution from the machine tool. It seeks to break down the tolerance requirements of repeatability, accuracy, and reproducibility for each of the modes of operation identified in 3.2. It provides an approach that could then be replicated for other failure mechanisms.

The remainder of the chapter then described the machine testing that is required to support this decision process and the possible tools that can be used. It also explains which of the options will be used for the work in this dissertation. The next chapter will report some of the testing undertaken in support of this approach.

Chapter 5 Testing and discussion of results

In this chapter, simple artefacts have been chosen to highlight the effect of the key components of the framework described in Chapter 4. For the initial testing, setting ring gauges (Figure 43) were used as simple, traceable objects.

Two Steel gauges were chosen, nominal 44mm and nominal 19mm, these were first measured on a coordinate measuring machine to check conformance before probe measurements were conducted on the machine tool. Although in some tests, i.e., single point Z surface, only one ring gauge was used.

The measurement routine is an important part of using a probe correctly, but this work did not go into this aspect in detail, since it is a large topic on its own. Where possible, guidelines from NPL's "Good Practice Guide 41: CMM Measurement Strategies" [90] were used. However, limitations in the macros on the CNC machine in some cases prevented this.



Figure 43 a 44 mm setting ring gauge on the table of Machine A

Testing of this nature never presents data of interest if only a single machine is considered. Therefore, in this chapter results from several machines have been included. The basic description of all the machines is combined in Appendix B for ease of reference. Names and ownership of the machines have been anonymised due to commercial sensitivity. Nevertheless, it is fair to say that all machines used in this study are standard, commercial offerings designed for production manufacturing. The

majority of the probing results are performed on Machine A (see Appendix B.1), which was dedicated to this project.

5.1 Part program design

The project requires several similar tests. A method of parametric programming was adopted and developed for all the testing in this chapter. The following example, used to provide the results in section 5.2.1, gives a breakdown of this programming approach. The following example is for a SIEMENS Sinumerik controller, but a similar approach with different syntax is used on machines with a FANUC controller.

5.1.1 Part program structure – Example Repeatability of

A comment line indicates the use of the program:

```
;THIS PROGRAM REPEATS THE Z MEASUREMENT AND WRITES THE VALUES TO FILE
```

The constants, which define the specific test, are then listed at the top of the program. It is therefore convenient, once the program has been tested, simply to change these values. In this case, the number of measurements and dwell time between measurements is defined. In other programs the constants might be feed rate, spindle speed, etc.:

```
DEF REAL repeats = 200 ;no of repeat measurements
DEF REAL wait = 5. ; no of seconds between measurements
```

The variables are then defined below a comment line of asterisks, to indicate no further modification should take place:

```
;*****
DEF REAL zero = 0
DEF REAL hourstart
DEF REAL minstart
DEF REAL secstart
;*****
```

The method of recording to file is common for all testing to ensure efficient and consistent analysis in either Excel or MATLAB.

```
EXTERN FWRITE (STRING[160],STRING[200])
DEF STRING[200] msgtxt=" "
DEF STRING[160] FNAME="Z_DATA_1"
msgtxt=<<"DATE"<<" "<<"START"<<" "<<"ZPOS"
FWRITE (FNAME,msgtxt)
```

The test (in this case probing) is then conducted. The use of “LABEL” keywords allows loops:

```
G17 T21
```

```
M6
G40 G90
G55 G0 X0 Y0
Z100
SPOS=0
M75;turns probe on
G04F0.5
L9800
R26=5 R9=5000
L9810
LABEL10:
```

All test data is traceable to the file database, with start time recorded for correlation with other data, such as temperature from the independent on-machine condition monitoring system. In this case it is only the start of each single probing cycle, but for some programs each result would come from several measurements and both the start and end time would be recorded.

```
;store measurement start time
hourstart=$A_HOUR
minstart=$A_MINUTE
secstart=$A_SECOND
```

This is an example of a probing subprogram. In this case it is the L9811 (XYZ single surface measure) subprogram from Renishaw, whose action is defined by setting the R Values in the controller (R26 is for the Z Axis for X axis use R24 and for Y axis use R25). In this program R26 tells us the position of the surface to be probed.

```
R26=0
L9811
```

The data is then stored in the format:

12/3/21 9:47:6 0.0334

```
msgtxt=<<$A_DAY<<"/"<<$A_MONTH<<"/"<<$A_YEAR<<"
"<<(hourstart)<<":"<<(minstart)<<":"<<(secstart)<<"
"<<((ROUND(RENC[37]*10000))/10000)
FWRITE(FNAME,msgtxt)
```

The R value can also be used to tell the probe what position to move to, in the next section of the program the Z axis now moves to Z5.0 (R26) in protected move mode L9810 (protected positioning routine). When the machine tool is moving in protected positioning mode, all the axes will stop moving if the probe is triggered, hence protecting the probe from damage. Although it is important to remember this only

works if the stylus is triggered and on the majority of probes the main body is not protected from damage.

```
R26=5
```

```
L9810
```

It then waits for the time defined by the constant before going round the loop to LABEL 10, assuming that it has not hit the maximum number of cycles.

```
G04F=wait
```

```
repeats=repeats-1
```

```
IF repeats>0 GOTOB LABEL10
```

The program then “tidies up” ready for the next test and terminates.

```
R26=100 R9=5000
```

```
L9810
```

```
M75
```

```
M5
```

```
M30
```

5.2 Probing systems tests

The probing system tests were designed to test the complete system of environment, machine tool and probe individually and with all the accumulated errors and electronic issues associated with it.

5.2.1 Repeatability of probing

5.2.1.1 *Z Axis single point with minimum movement*

This test was conducted on Machine A to find the repeatability of the system probing a single point in the Z Axis, with minimal axis movement between touches.

The machine had been left powered up for over four hours prior to the test to allow for the machine to become thermally stable within its environment. The reason for leaving the machine powered on is that when the motors are active, they lose heat energy into the machine structure. As machine tools are designed for precise positioning, as soon as the drives become active the control loop will command the motors to make small movements to return the axis to the command position in response to any disturbance. For the Z-axis, in particular, this is a response to the brake being released and the axis motor having to work against gravity. The effect of this on the machine accuracy is analysed in further detail in Section 5.4.

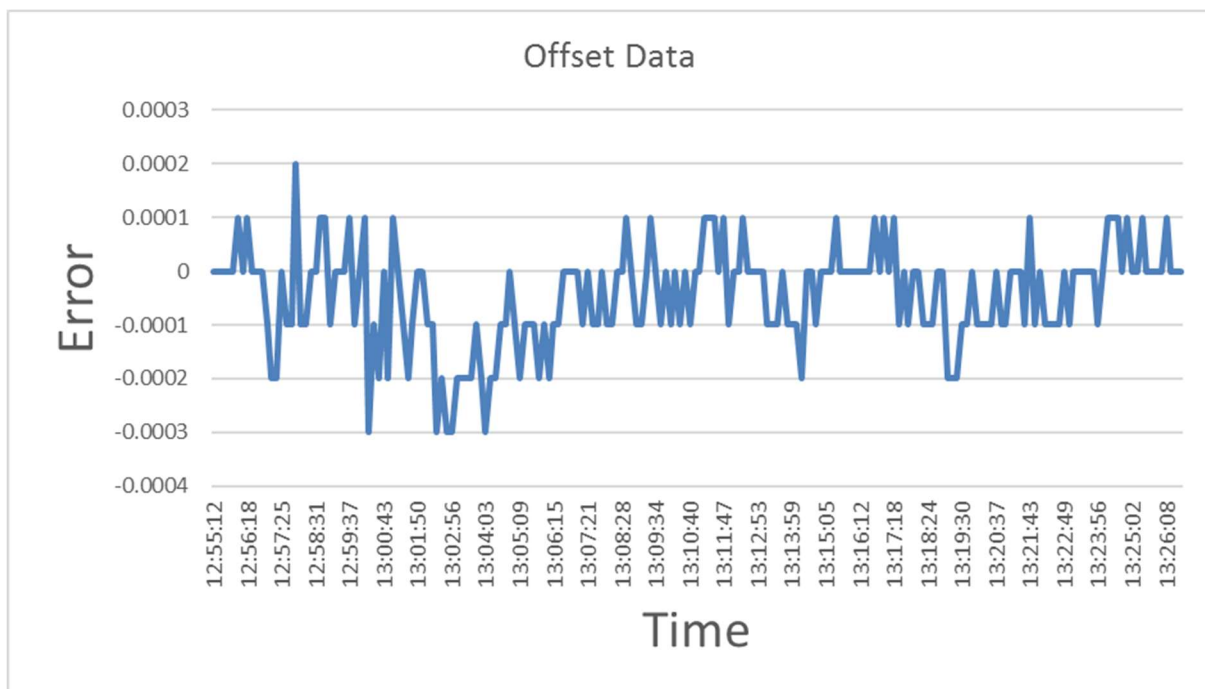
With only a small axis movement and the machine being already thermally stable, the probing deviation is only affected by the probe and axis measuring system repeatability.

The probing operation starts at 5 mm above the ring gauge, it then feeds down taking a point on the top surface of the ring gauge and records the position to file, the axis then returns the probe back to 5 mm above the surface and waits for 5 seconds before repeating the operation, this was repeated 200 times.

The probe remains switched on through the whole operation, does not re-datum or re-orientate the probe at any point.

The program, Z_REPEAT_DATAWRITE.MPF for this operation is shown in section 5.1.1, all subsequent programs will be shown in Appendix C.

The results for this test (Figure 44) shows a range of 0.5µm. Considering that the stated repeatability for this probe in the Z axis is 0.35 µm this shows excellent repeatability for the combined system. The machine has a glass linear scale and excellent control loop, as evidenced by the results. However, the design of test means that the machine is only making very small moves.



Mean	-0.0000450000
STD Dev	0.0000936750
Range	0.0005

Figure 44 Data graph for Z surface touch points with minimal Z axis movement

5.2.1.2 Z Axis single point with full stroke in Z

Having previously tested the repeatability using a minimal axis stroke in section 5.2.1.1 the test was rerun using a much longer axis stroke (distance). The probe now returns

to Z 300 mm above the ring gauge surface and waits for 60 seconds between taking each Z surface point.

As can be seen in Figure 45, there is now a displacement of 3.5 μm when probing with the longer approach stroke. It does however appear from the graph that the machine has not stabilised by the end of the test, so there can be an expectation the Z error will be greater than 3.5 μm if the test were continued.

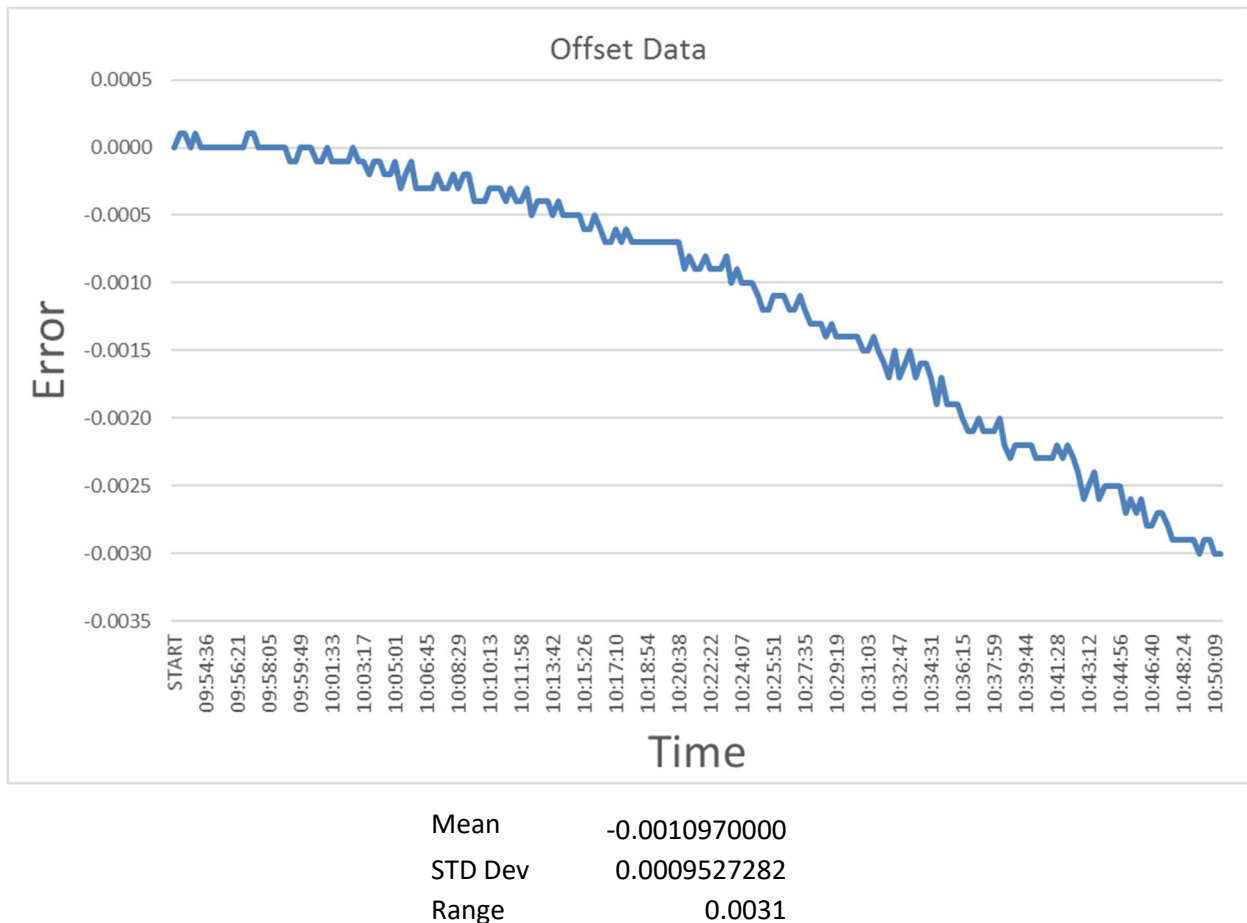


Figure 45 Data graph for Z surface touch points with 300mm Z axis movement

Looking at the associated temperature graph in Figure 46 It can be seen that the spindle motor temperature (green trace) rises while the other sensors (there are 38) broadly stay the same. This graph is only provided for context at this stage. The location of the sensors is given in section 5.4.3.

Figure 47, however, focuses on only four of the sensors and shows that the spindle motor temperature rises by 7 °C over the test duration. Section 5.4 will show evidence that this correlation between temperature and change in probe values does indeed have a causal relationship on this configuration of machine.

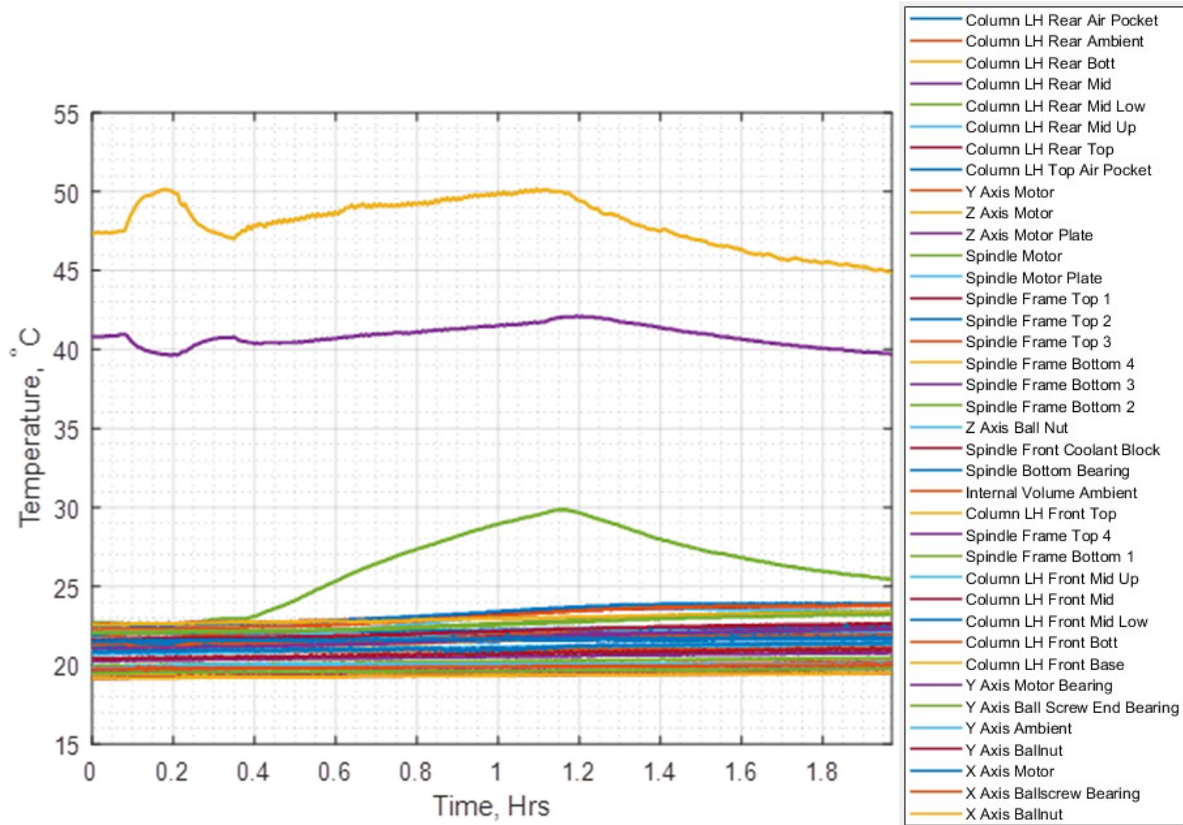


Figure 46 temperature graph 300mm Z movement

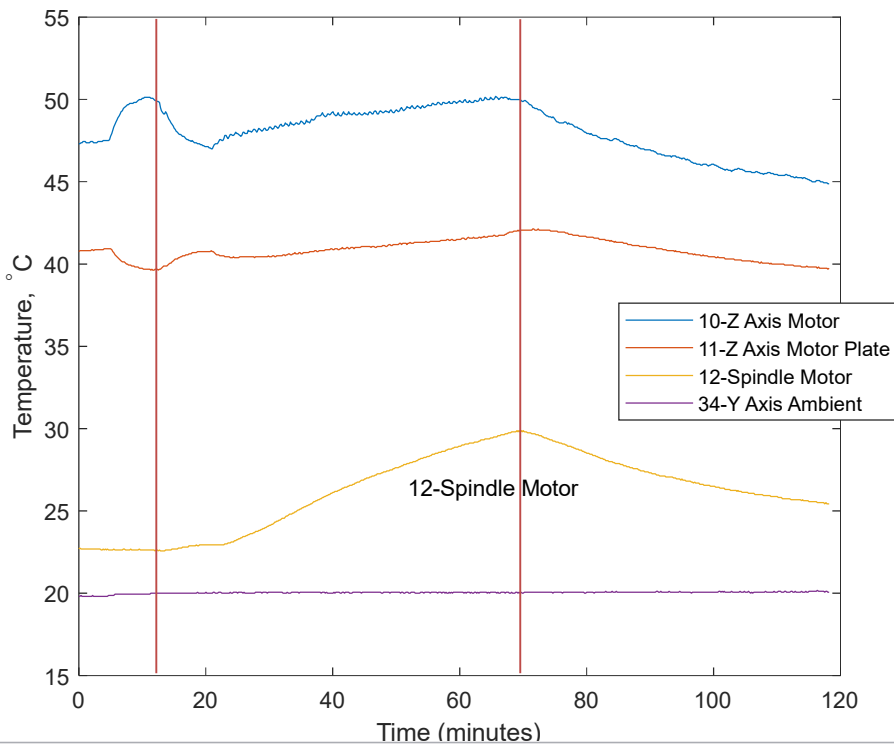


Figure 47: Temperature graph Z 300 mm movement – selected sensors

5.2.2 Effect of probe calibration

In the following sections 5.2.2.1, 5.2.2.2 graphs will show the effect of measuring an artefact with a probe that has not been calibrated for some time and a newly calibrated probe respectively. To a metrologist, the importance of calibrating the probe system would be widely known, but for a company manufacturing parts where “time is money” may not be so keen to spend unproductive time calibrating a machine tool probe on a machine tool. Running the same test with an outdated calibration and newly conducted calibration quickly shows the differences in the errors.

5.2.2.1 *Measurement with uncalibrated probe*

Figure 48 shows the errors measured on a calibrated ring gauge with an old calibration. The calibration cycle had been run approximately one month before the test. Errors of up to 7.5 μm can be seen in the table of figures (a).

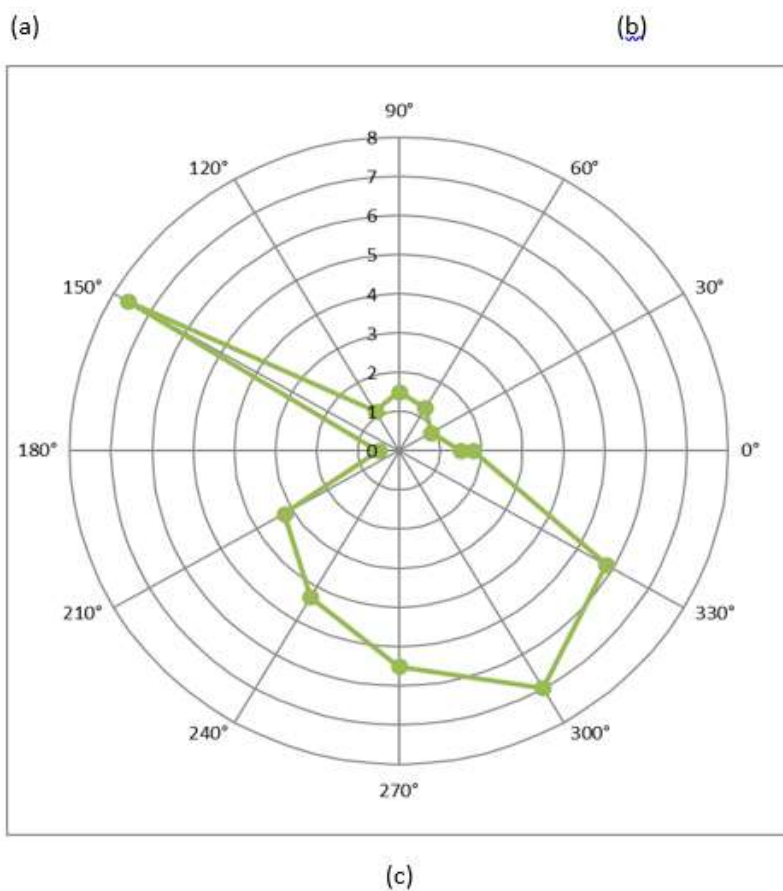
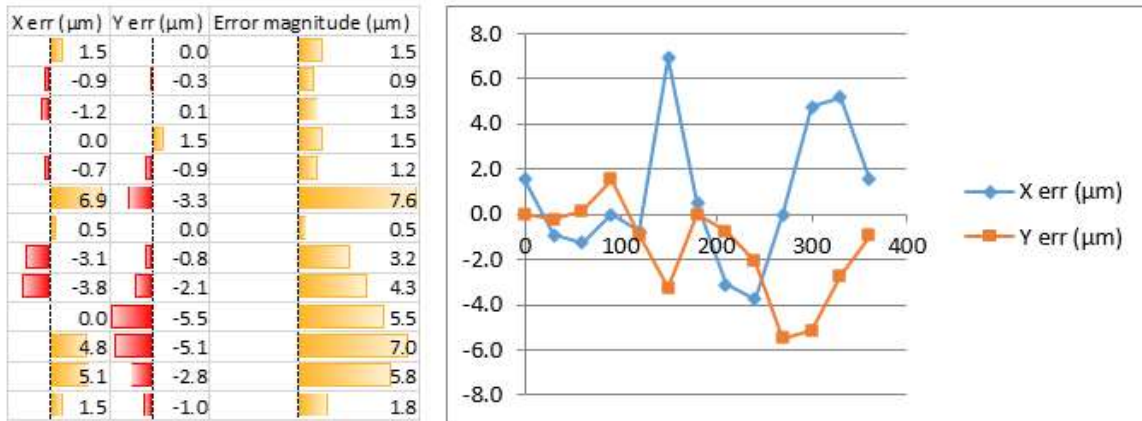
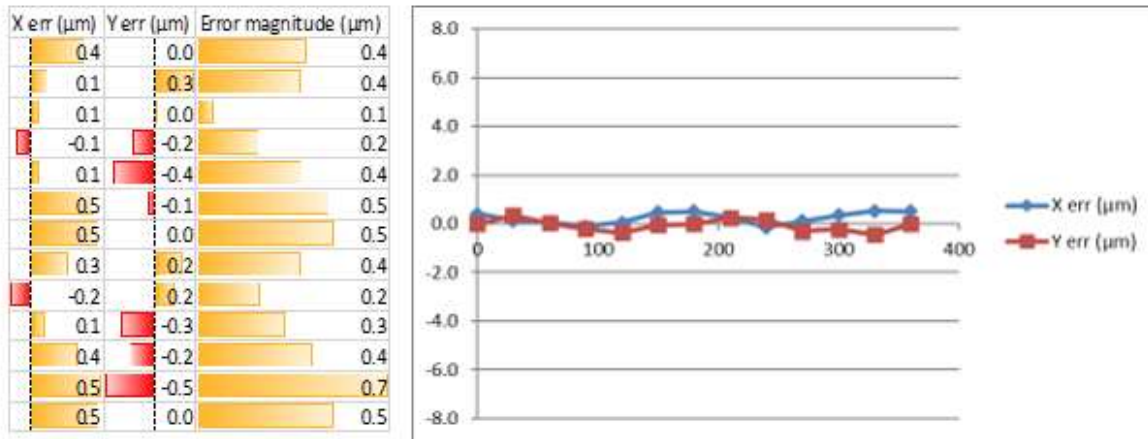


Figure 48 Ring gauge measurement with outdated calibration parameters (a) table of values, (b) deviation in the X- and Y-axis directions (c) polar plot

5.2.2.2 Measurement with calibrated probe

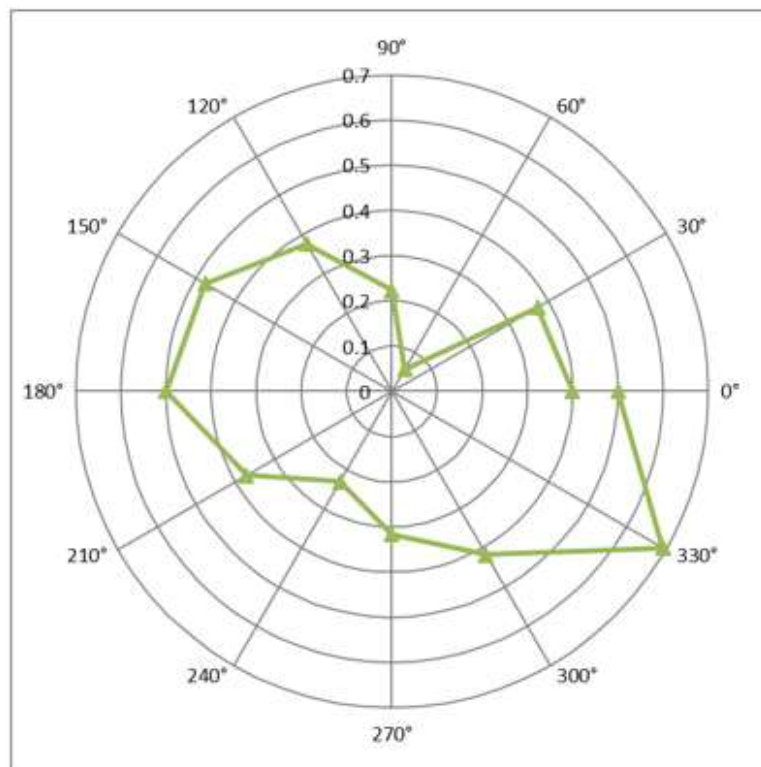
Figure 49 shows the same ring gauge measured after the probe has been calibrated. There has been an order of magnitude improvement.

30-degree angles were chosen for the measurements in the ring gauge as these are the vector angles used to calibrate the probe ruby radius in the probe manufacturer's cycles



(a)

(b)



(c)

Figure 49 Ring gauge measurement with newly created calibration parameters (a) table of values, (b) deviation in the X- and Y-axis directions (c) polar plot

5.2.2.3 *Repeatability of probe calibration*

Although highly repeatable in isolation, when placed in the machine tool the probe will need calibrating to align the stylus touch points to the machine kinematics. On a typical 3-axis machining centre, using either a ring gauge or sphere as the calibrated artefact, a CNC program is run that will then measure the centreline offset of the stylus touch point quadrants to the spindle centreline in the X and Y axis and the ruby radius. The program will then measure the stylus ruby radius at set angular intervals around the circumference of the artefact. All this is done at a defined feed rate so the program can calculate the pre-travel (the time it takes from the ruby hitting the surface to triggering the stop command in the controller and recording the axis positions).

One of the main factors influencing pre travel is the feed rate of the axis, with this in mind it has to be said that it is important that the probe is used to datum or measure at the same feed rate that was used for calibration.

The latency of the response from the time of probe trigger to the machine capturing the axis positions can also affect probe accuracy. It is unlikely that this will change over time, but in principle could change with degradation of the electrical contacts and cabling. Nevertheless, even if it occurs, this is a long-term drift that would be mitigated by regular recalibration at the intended probing speed.

The CNC programs are written using defined macros provided by either the probe manufacturer or the machine tool manufacturer; these macros ensure a set cycle is run and that the calibration data is the stored in the correct variables within the controller.

To enable a test to find the repeatability of the probe calibration a program, using the probe manufacturers macros, was created to run a calibration cycle on an artefact and output the recorded data to file. Although the machine manufacturer can provide their own probing macros, testing of any differences between machine manufacturer and probe manufacturer was deemed to be outside the scope of this research.

The tests were run on two differing sizes of measurement artefacts that had been previously measured on a CMM, namely a ring gauge of nominal diameter 44 mm and a smaller ring gauge Nominal diameter 19 mm. For each test, the calibration routine was run 100 times in succession with the feed rate constant and low, to avoid excessive generation of heat. The tests took 2 hours 15 minutes and 2 hours 1 minute respectively.



Figure 50 Ring gauge set up on Machine A

The results of the calibration tests are provided in Appendix E. The results are summarised in Figure 51 for the 44 mm diameter ring gauge and Figure 53 for the 19 mm diameter ring gauge. XSTYLUSOS and YSTYLUSOS are the stylus offsets in the X- and Y-axis directions respectively. XR and YR are the ruby radius calculated in the X- and Y-axis directions respectively (at 0° and 90°) and the remaining values are at 30° intervals, as indicated by their names.

It is clear from these results that ruby diameter measurement is consistent to less than 1 μm for all angles around each ring gauge. There is a very slight difference in the mean size between the two gauges, but at only $\pm 1 \mu\text{m}$ it is within the uncertainty of the test.

There is a small, but observable trend in the readings for the stylus offsets (as highlighted in Figure 51 and Figure 53). This is almost 4 μm for the larger gauge and 1 μm for the smaller. This is the most pronounced error once again and, as has been previously mentioned, this correlates to the thermal measurements seen in the temperature graphs in Figure 52 and Figure 54 respectively. In each graph red lines have been placed to indicate the start of each ring probing routine. Again, it will be shown in section 5.4 evidence that this correlation between temperature and change in probe values does indeed have a causal relationship on this configuration of machine.

This error is the centreline to spindle offset in the Y direction and its influence will greatly depend on how measurements are being taken in relation to when the probe was calibrated. With this probe on this machine, if the probe were calibrated on the machine when warm and then a datum set, a measurement made only two hours later could include approximately 4 µm shift in the Y axis direction. For measurements taken from a datum on a fixture, this has the potential to double to 8 µm if, say, the datum was on the Y-positive side of the ruby and then the measurement on the Y-negative side of the ruby.













	Trend	Mean (mm)	Range (microns)	Std Dev (microns)
XSTYLUSOS		-0.010	0.900	0.236
YSTYLUSOS		-0.006	3.700	1.022
XR		2.993	0.200	0.056
YR		2.992	0.300	0.065
30R		2.993	0.500	0.104
60R		2.992	0.400	0.096
120R		2.992	0.500	0.100
150R		2.993	0.500	0.091
210R		2.993	0.400	0.079
240R		2.992	0.400	0.095
300R		2.992	0.600	0.117
330R		2.993	0.600	0.110

Figure 51 Summary of repeated results from 44 mm diameter ring

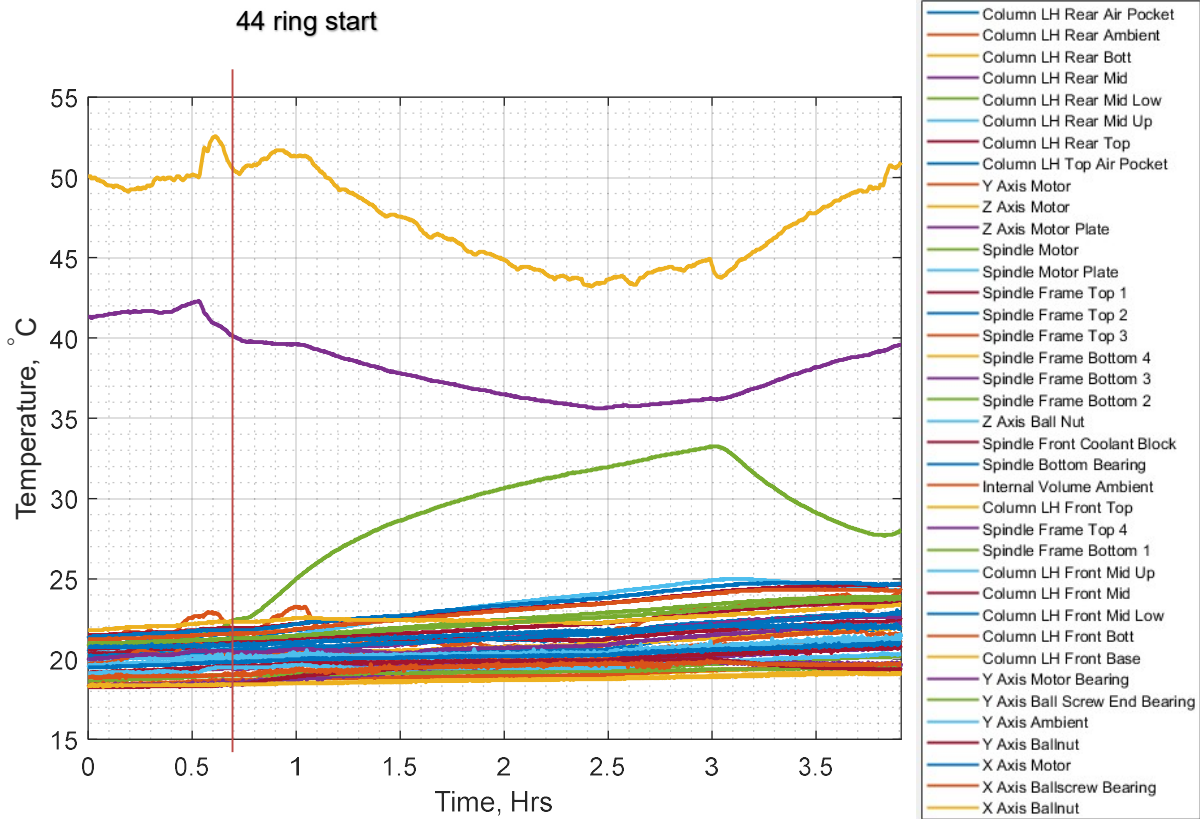


Figure 52 Temperature readings during measurement of 44 mm diameter ring

	Trend	Mean (mm)	Range (microns)	Std Dev (microns)
XSTYLUSOS		-0.008	0.600	0.108
YSTYLUSOS		-0.005	1.200	0.289
XR		2.991	0.400	0.067
YR		2.991	0.200	0.054
30R		2.991	0.500	0.077
60R		2.991	0.400	0.080
120R		2.991	0.600	0.100
150R		2.991	0.500	0.102
210R		2.991	0.400	0.084
240R		2.991	0.400	0.067
300R		2.991	0.400	0.082
330R		2.991	0.400	0.091

Figure 53 Summary of repeated results from 19 mm diameter ring

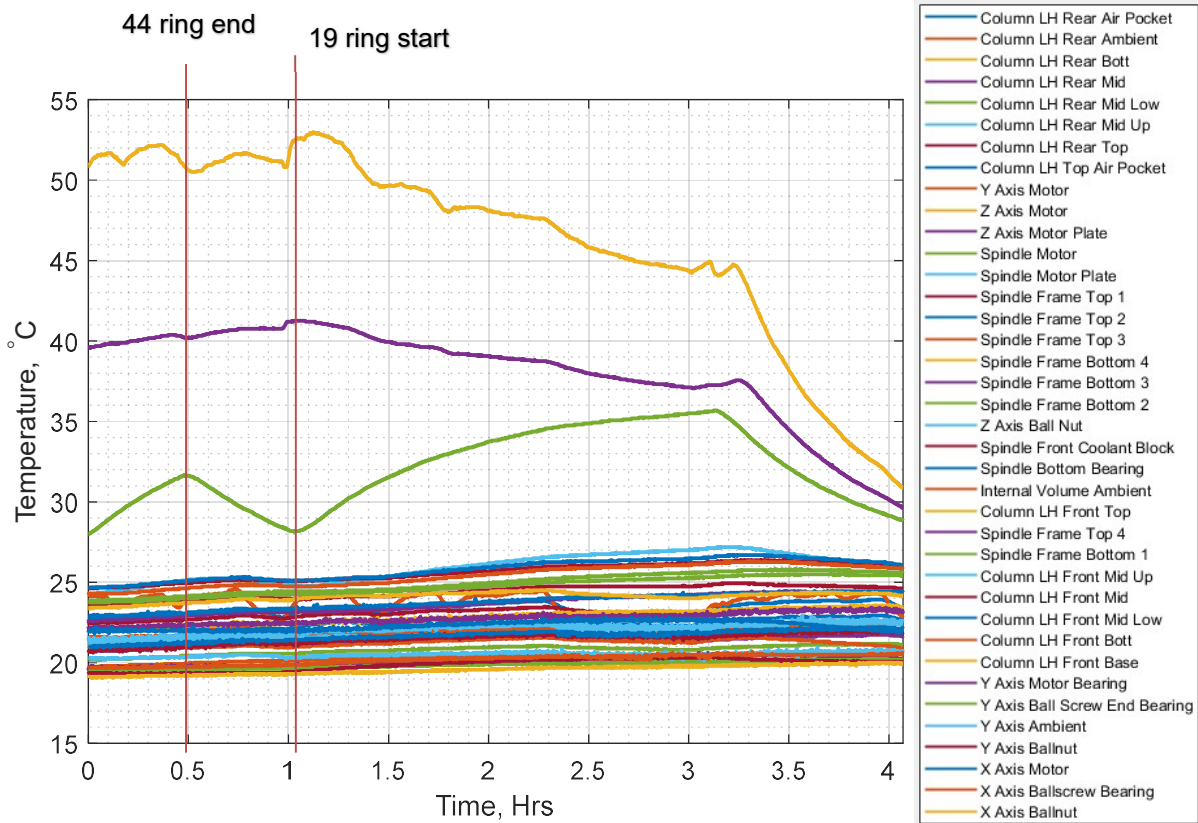


Figure 54 Temperature readings during measurement of 19 mm diameter ring

5.2.3 Effect of surface contamination (coolant)

Probing on a machine tool will often take place in the harshest of environments, unlike on a CMM where the parts and working area will be clean and free from contaminants. Within the machine tool there will often be swarf, debris and coolants with varying degrees of viscosity. These could create uncertainties within the measurements obtained, that could lead to “no measurement” wasted time or “bad measurement” that would possibly go undetected as a bad measurement.

A test was run, again using the surface of the ring gauge, to determine if coolant left sitting on the surface of the component could influence the measurement taken.

The program Z_REPEAT_DATAWRITE.MPF used in 5.2.1.1 was utilised for the test, with the only change being the name of the data file where the data was recorded.

The machine had again been left under power for a number of hours previous to the test to achieve as much thermal stability as possible.

200 points were measured with a five second delay between probe points with the ring clean and dry. This part was run twice, meaning two sets of 200 points were recorded.

The coolant was then switched on covering the ring gauge and table area of the machine with coolant; this was run for five seconds. The coolant was switched off and then the measurements re-run, again taking two sets of 200 points.

The area was then dried and cleaned, and the two cycles repeated, two sets of 200 points dry, two sets of 200 points wet.

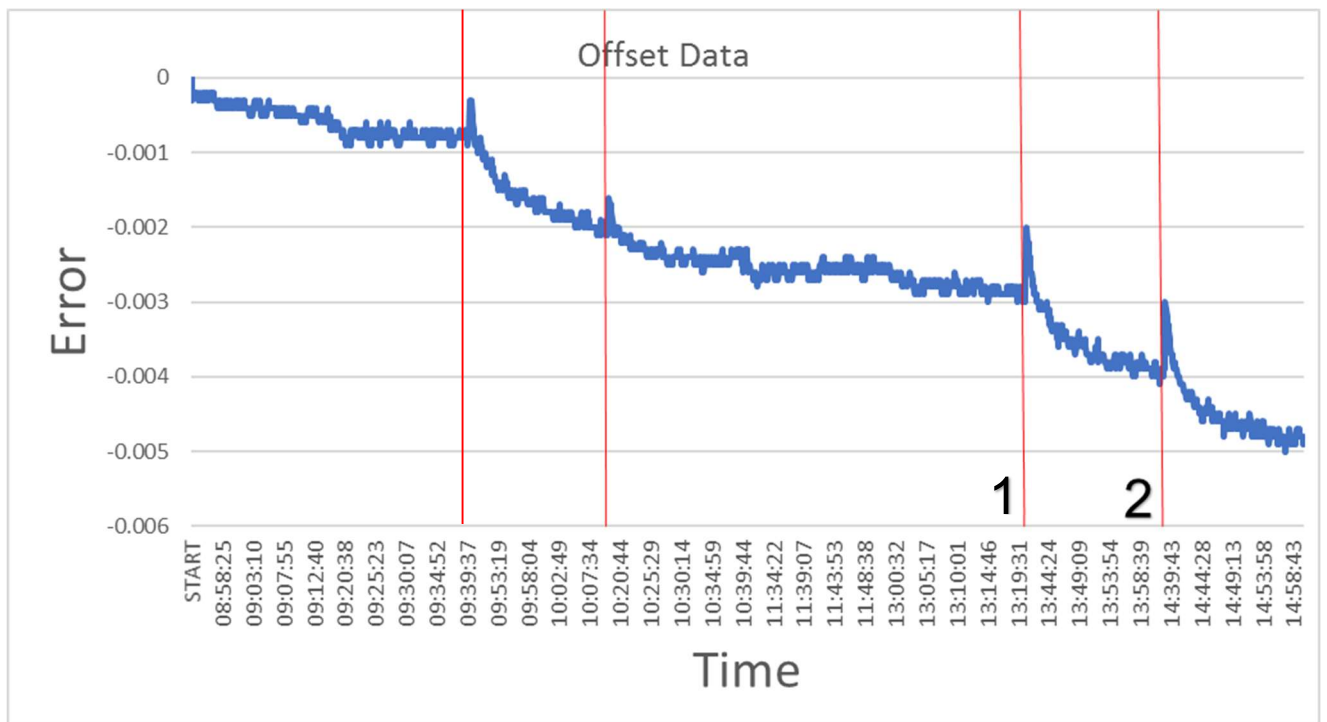


Figure 55 Graph showing change in Z surface measurement from coolant contamination

In Figure 55 peaks can clearly be seen in the data, as indicated by the red vertical lines. These were found to be at the first measured point after the ring had been covered in coolant.

Taking a closer look at the areas around Lines 1 and 2, 20 points were chosen before and after the first measured point where coolant had run onto the ring, to create two graphs of the area of interest. These are Figure 56 and Figure 57 respectively.

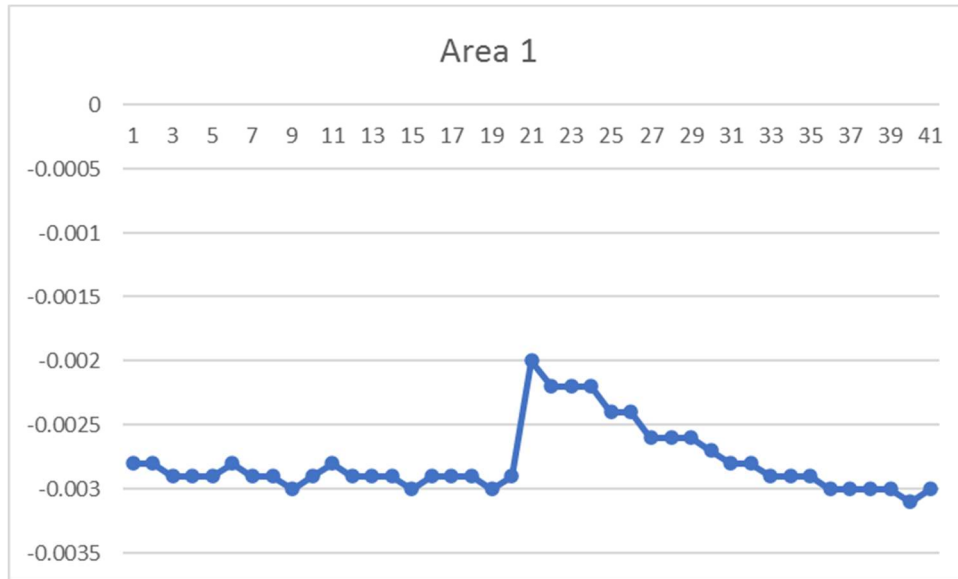


Figure 56 Z surface probe Line 1 -20 / +20 point Graph

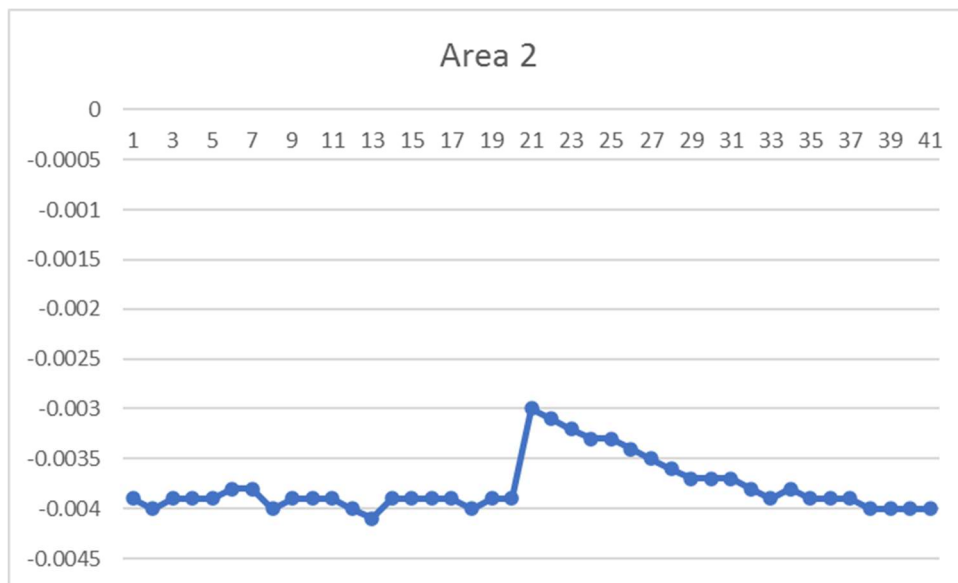


Figure 57 Z surface probe Line 2 -20 / +20 point graph

A shift of $1\mu\text{m}$ can be seen on the graphs of the highlighted areas when coolant contaminates the surface. Due to the coolant only being sat on the surface being measured there is a likelihood of coolant either running off the surface or being dissipated by the probe pressing onto it. This led on to another more controlled experiment, where 20 points were measured dry, 20 points wet, and then 20 points on the surface where coolant had been kept in a “dam” made of blu-tack around the measurement area to prevent the coolant from running off (Figure 58).



Figure 58 Ring gauge with coolant held within dammed area (blu-tack)

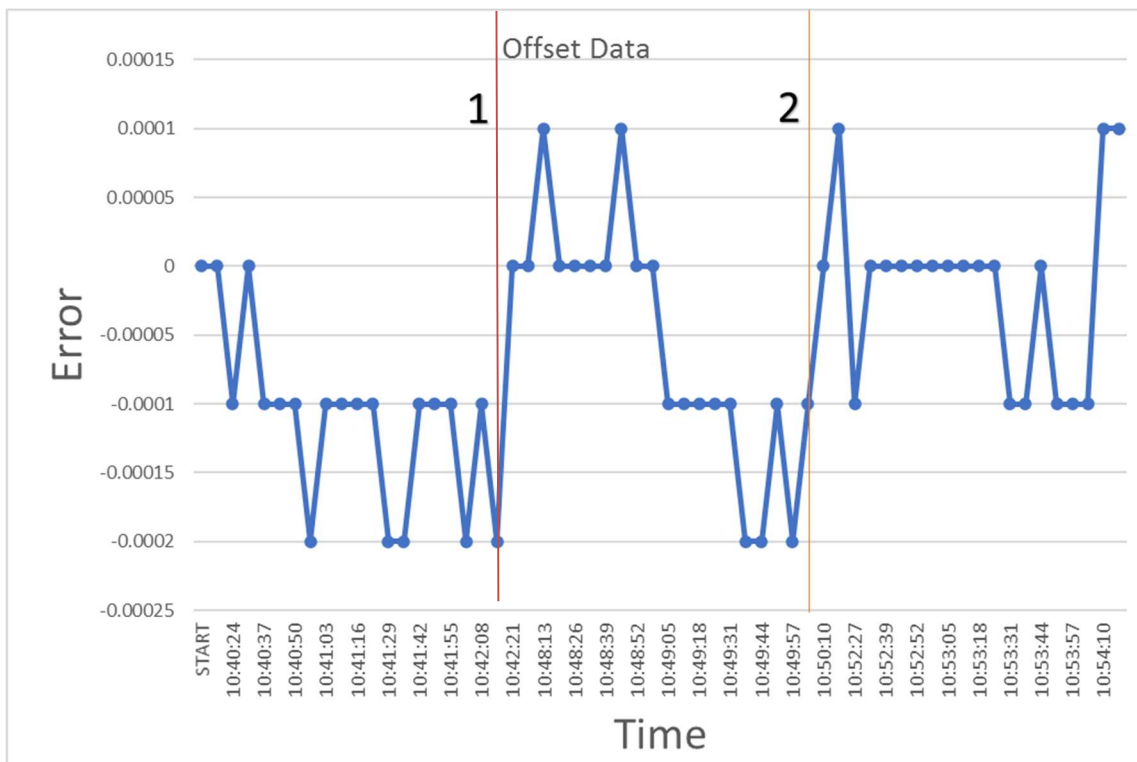


Figure 59 Z surface probe - effect of coolant

In Figure 59 from the start to line 1 the surface of the ring gauge was clean and free from coolant contamination. All measurements are from 0 to $-0.0002\mu\text{m}$. From line 2 onwards when the coolant was held within a dam wall, effectively probing in a puddle, all the readings are from 0 to $0.0001\mu\text{m}$. But between lines 1 and 2 where coolant was sprayed on the surface where it could run off or dissipate, the reading start above 0 as from line 2 but as the coolant dissipates with the probe touching onto the surface the reading starts to go to $-0.0002\mu\text{m}$.

This shows us that if a bore or slot is probed that has not been cleaned of coolant, and where the coolant also has a chance to dissipate there is the possibility of a gradual change if say a plane was being measured. There is also the possibility that with the errors in Figure 59 being submicron that the original $1\mu\text{m}$ shift seen in Figure 55 could be due to stopping the machine to add coolant to the surface and then restarting the test.

It should also be noted that this test used a water-soluble oil coolant mix at 6%. If a higher concentration of oil to water was used or even a 100% cutting oil as used in some modern manufacturing methods, then the thicker medium could influence the readings shown here.

5.3 Machine geometric error influences

5.3.1 Effect of tool change repeatability

The geometry of the spindle and the probe “tool holder” are subject to tolerances in the same way as any other manufactured system. As described in section 2.1.10, different holder geometries give better repeatability of clamping the tool into the spindle. Since calibration of the probe is directly related to the orientation of the tool, this becomes very important.

The HSK high-speed tool holder types E and F are symmetrical in their design, to remove imbalance, but if used with a probe there is no reference to where the spindle Interface will seat rotationally. This means that the probe will have to be calibrated every time a tool change is performed.

Unless the probe can be guaranteed to seat within a specified rotational tolerance then the validity of the existing calibration cannot be guaranteed.

With steep taper tool holders, as in ISO40/50 or BT40/50 for instance [71], which do not incorporate face contact as well as taper then there is also the added possibility of “suck up” where the taper moves up in the spindle nose, this can be due to the heat from the spindle motor and bearings creating heat and causing the spindle nose to expand faster than the tool holder itself, making the taper move upwards in the spindle, likewise with a cold tool holder being placed into a warm spindle. This would manifest itself as a shift in the Z direction, especially if the probe has been used when the machine is cold and then the measurement repeated when the machine has heated up.

5.3.1.1 Tool change repeatability

This test follows the pattern of those quantifying probe repeatability in section 5.2. A single surface measurement was taken and then a tool change cycle implemented, exchanging the spindle probe for another tool and then immediately changing back to the probe, before taking another single surface measurement. This process was repeated for about an hour, taking a measurement after every tool change.

Figure 60 shows an initial shift of 3 μm after the first tool change as the tool had been left in the spindle overnight and not removed before measurement. Once again this shows the 3 μm downwards trend as seen in the previous test with the 300 mm Z axis stroke in Figure 45. When looking at the temperature graph in Figure 61 the same spindle motor temperature trend as Figure 46 can be seen, giving added weight to the spindle motor temperature causing the change in the probed measurements.

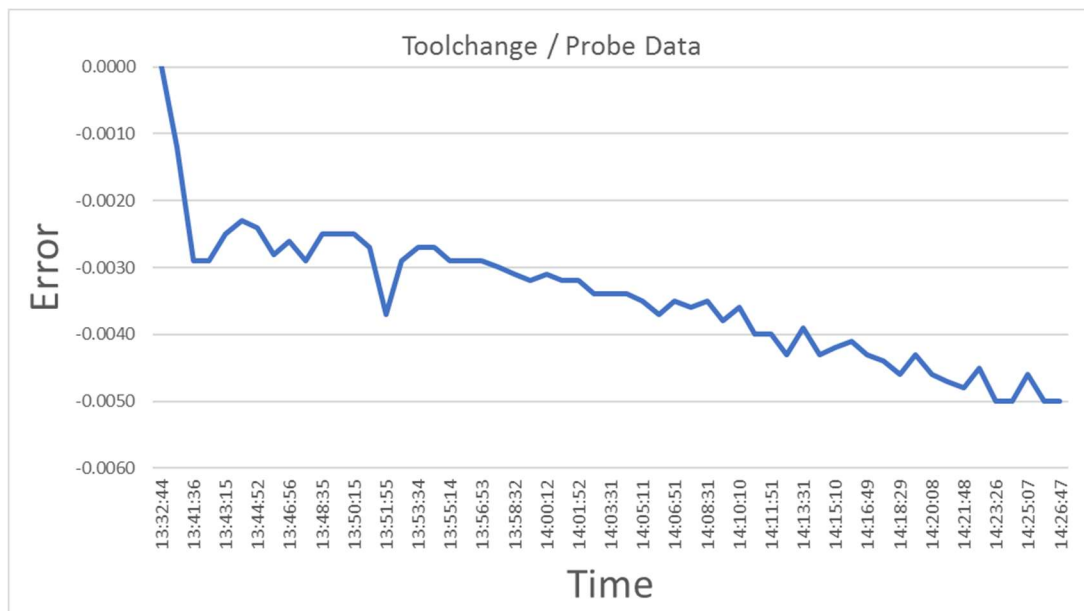


Figure 60 Tool change repeatability graph

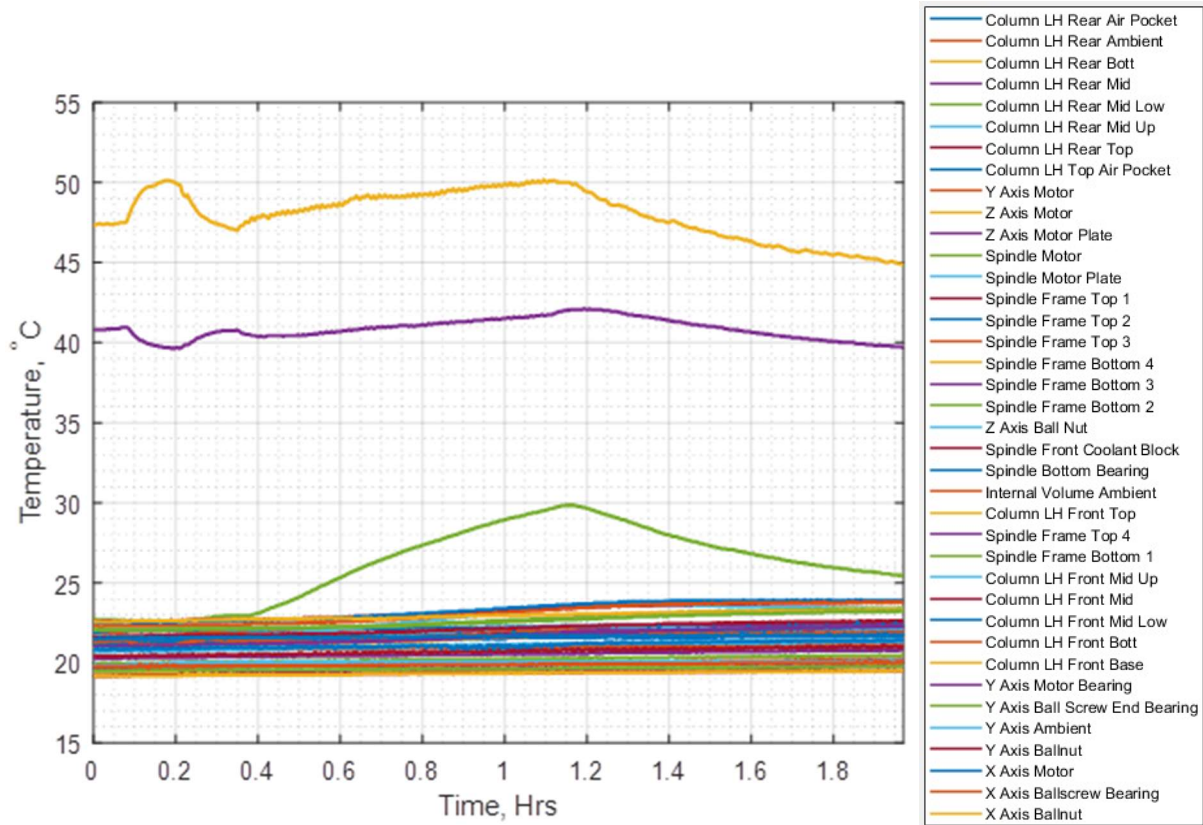


Figure 61 Tool change temperature graph

5.3.2 Geometric error measurements

Geometric error measurements were conducted on Machine A using the XM60 multi-axis calibrator. The results graphs in the preceding sections show the combined 6DoF graphs and then two graphs from the one axis showing how the errors are reported using a different analysis.

As mentioned in section 2.1.8.3 the XM60 multi-axis calibrator is able to measure all six degrees of freedom in one measurement, this not only speeds up the time for the whole measurement and removes any issues of environmental changes from the different measurements but allows all the error profiles to be viewed in one graph and compared as one, this enables the viewer to see quickly how an error component influences another.

In the following graphs the Renishaw format VDI 2617 for axis errors will be used, ISO 230-1 definitions will be placed in brackets.

5.3.2.1 Y Axis XM60 geometric error graphs

When looking at the YRZ (ECY) an error of 8arc seconds can be seen, this would equate to around 40µm/metre of error. In essence, if an arm protruded 1 metre out from the centre of the spindle this would show as 40µm of error at that point on the

graph. Due to the diameter of the machine tool probe ruby being small this error would have very little effect on measurements. However, if a probe stylus with an L shaped configuration was to be used this error would have an influence.

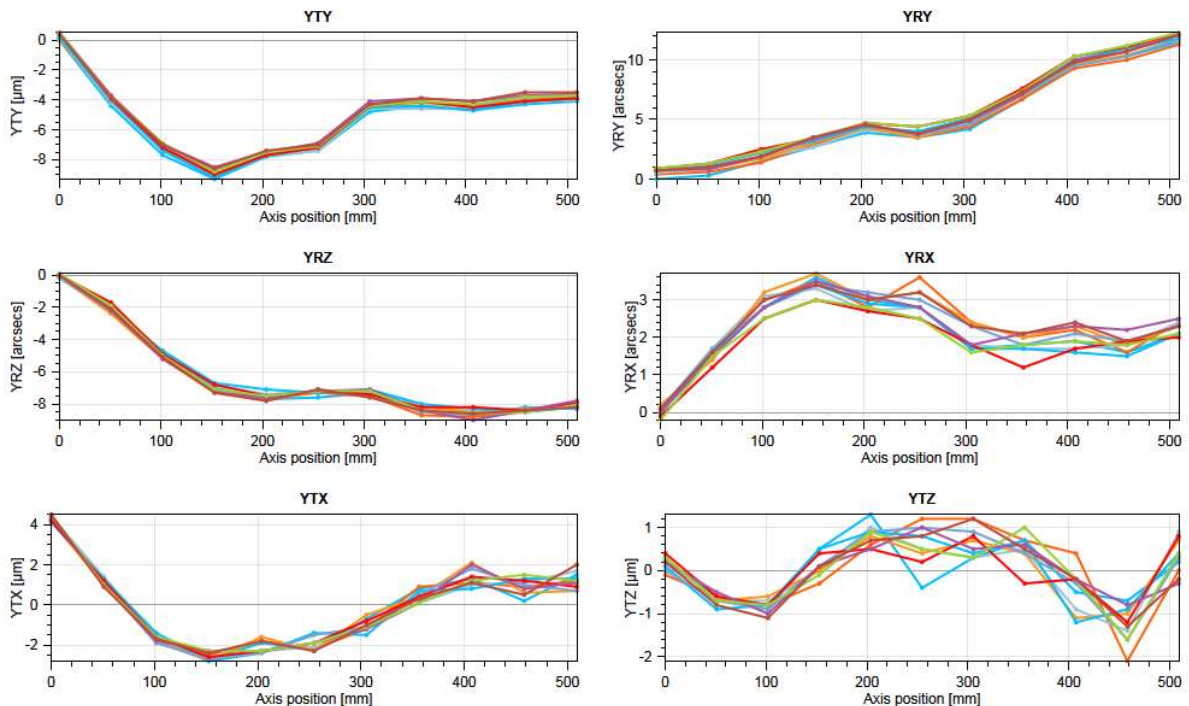


Figure 62 Y axis combined 6DoF graphs

5.3.2.2 X Axis XM60 geometric error graphs

In Figure 63 the largest error here is the linear positioning error XTX (EXX), if the only graph available was the singular XTX graph any person analysing this data may have assumed there was a linear positioning error, but with all six graphs available together, more careful analysis shows that there is a significant pitch error XRY(EBX) consistent with the linear positioning error. In the earlier section 2.1.4 it was discussed the fact that some linear errors are fundamentals of angular errors.

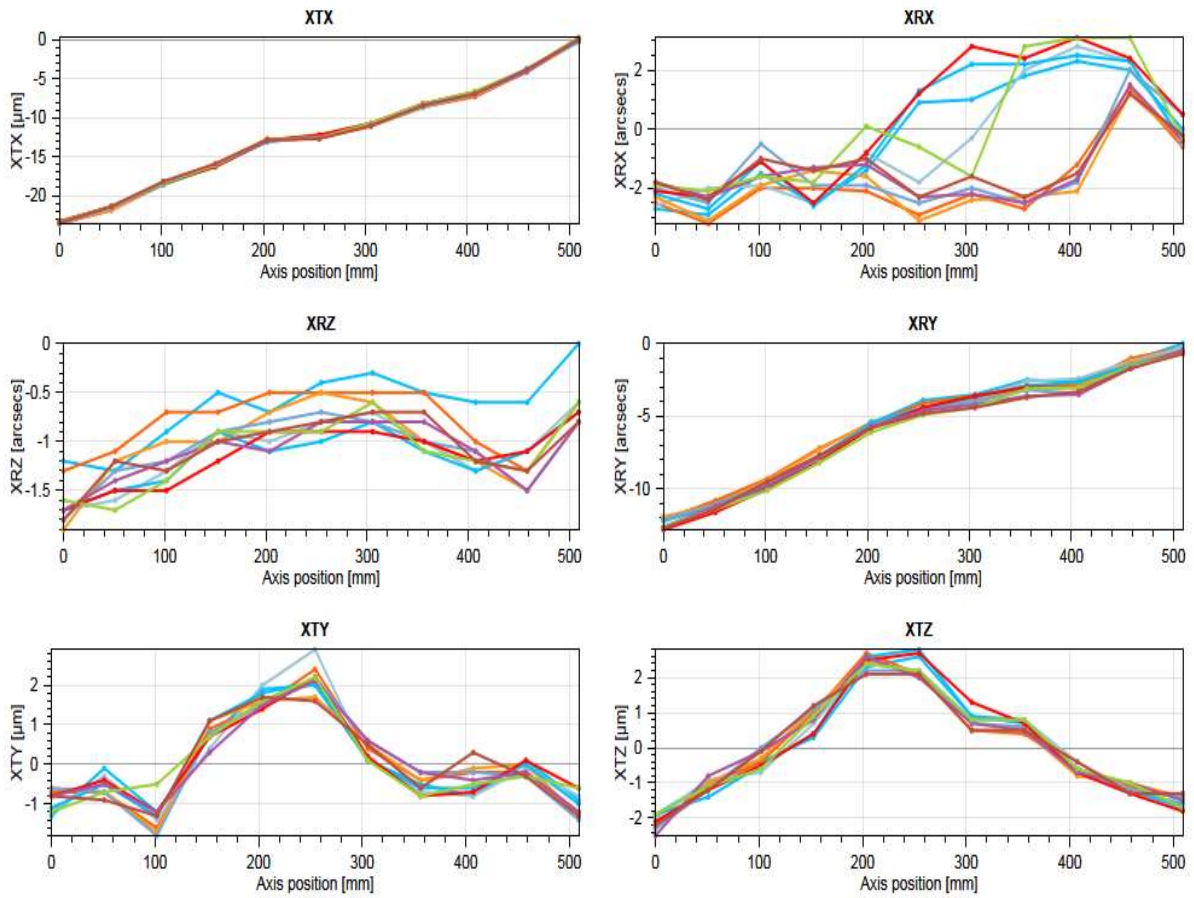


Figure 63 X Axis combined 6DoF graphs 3 axis vertical machining centre

5.3.2.3 Z Axis XM60 geometric error graphs

The ZRX (EAZ) graph in Figure 64 once again matches the ZTZ (EZZ) graph showing the effect of the pitch error on linear positioning, this time a cyclic error in the ZRX graph can also be seen, indicating a possible error in the way the guideways are held in position

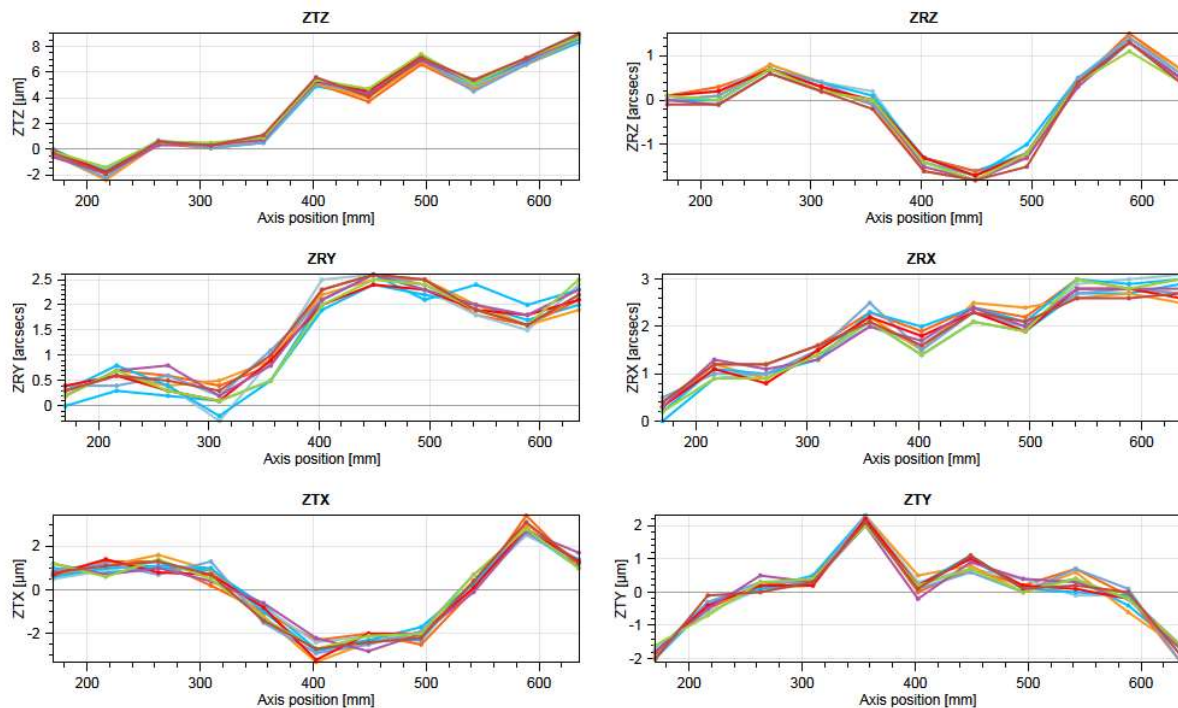


Figure 64 Z Axis combined 6DoF graphs

5.3.2.4 Geometric error graph comparisons

In the XTY (EYX) and XTZ (EZX) graphs of Figure 63 two very pronounced straightness errors can be seen in the Y direction and Z direction respectively, although the magnitude is small. These errors would have varied influence on any parts machined that would not become apparent with on-machine probing until independent measurement was run off the machine. A part datumed at the 0 position on both graphs would have a low point at around the X250 point in the Z plane and a bend in the Y-negative direction. The coordinate frame, when On-machine probing would have the same defect, so would effectively show zero error. If measured independently along the side of the part with off machine measurement the error would be detected.

Conversely, if a straightedge artefact (see section 2.1.8.1.2) was placed at the same positions on the machine and probed using the on-machine probing then it would wrongly show that the straightedge has these errors.

This is a prime reason for quantifying the machine tool before undertaking any kind of on-machine measurements, the errors in this case are small, but could easily have been much larger. For example, $60\mu\text{m}$ as shown for the YTX (EXY) graph in Figure 66. This clear evidence why measuring these errors is so important.

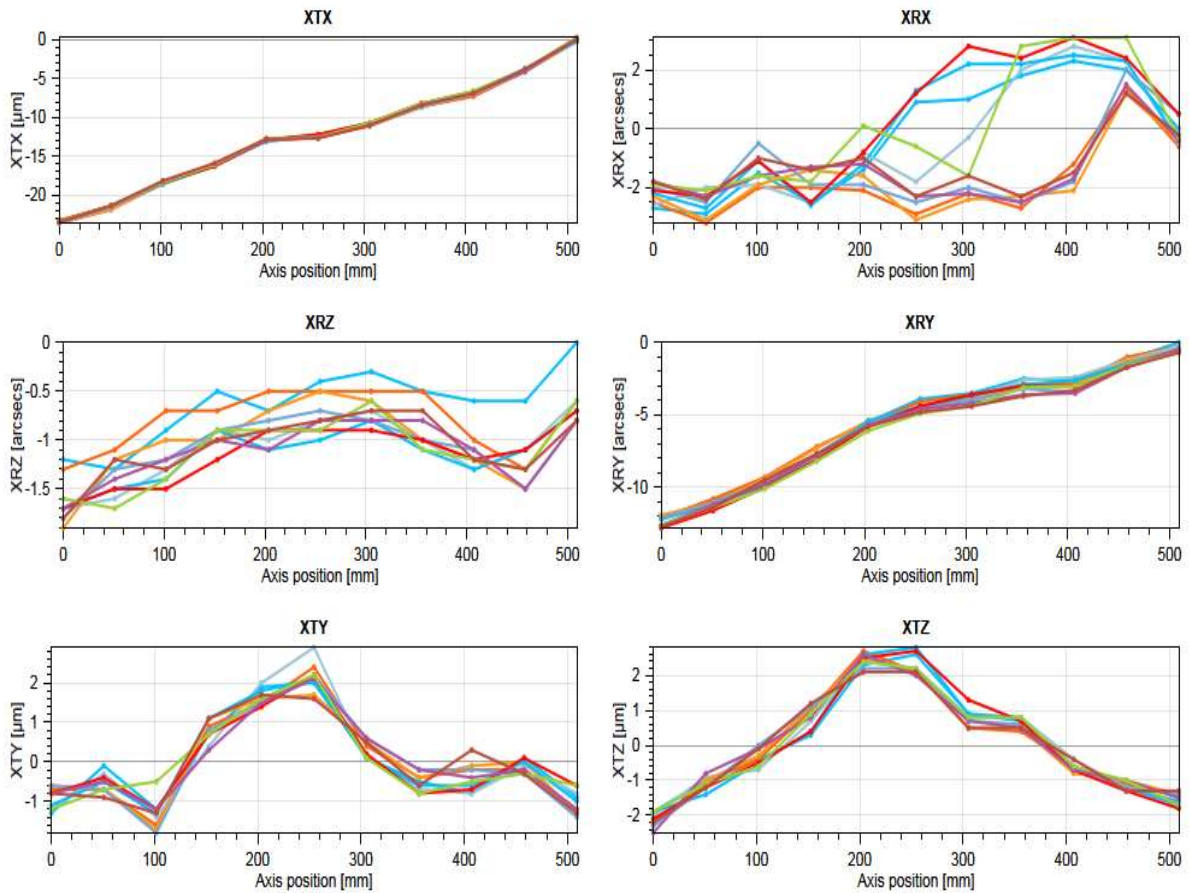


Figure 65 X Axis combined 6DoF graphs 3 axis vertical machining centre (Machine A)

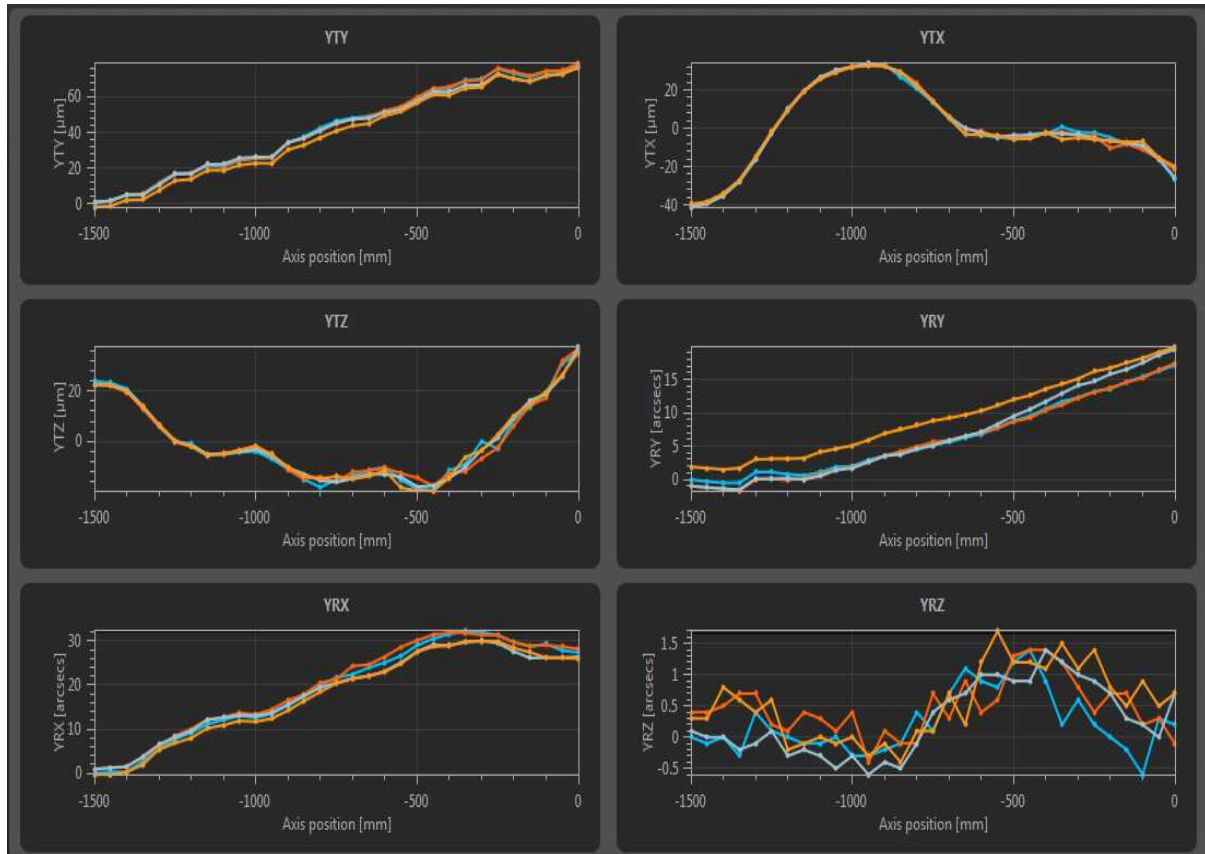


Figure 66 Y Axis combined 6DoF graphs large gantry machine (Machine C)

Figure 67 is a graph of a 5-axis vertical machining centre dominated by thermal error, there is non-repeatability of the linear positioning through the whole of the 5 bidirectional runs indicating thermal growth, but when the graph YRX (EAY) is examined it is clear an angular influence is causing the gradual bend of the head. On further investigation, it was established the chiller coming on and cooling the spindle was causing the head to bend. This test took less than 11 minutes to complete meaning the state of the machine had changed considerably within a short space of time. Accurate and repeatable probing would be difficult to manage on his machine due to the thermal effects, although as previously mentioned some setting operations could still be carried out.

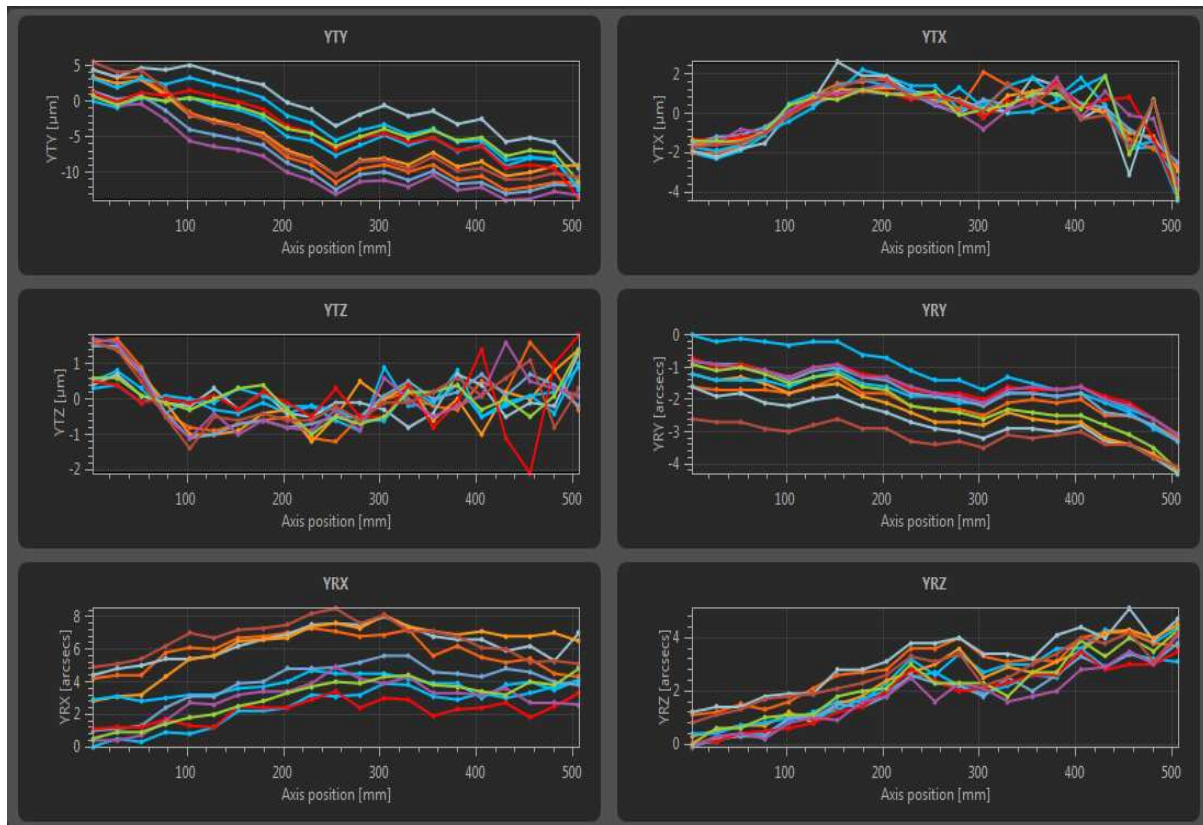


Figure 67 Y Axis combined 6DoF graphs 5 axis vertical machining centre (Machine D)

Looking at the below graphs in Figure 68 a cyclic error can be seen in the YRX graph. This error could be caused by the way the guideways are held onto the machine structure or from an out of alignment or out of round ball screw as the peaks are at regular intervals. Figure 69 shows an expanded version of the same graph for clarity. Aliasing (see section 2.1.8.3) is where measurements are always taken at set intervals that may always be at the high (or low) point of a cyclic error and so do not show up underlying errors that may be offset from those points. If say probing points were taken at the points A and B little difference would be seen in the measurement, but if those same points were recorded at point A and C or B and C, then this would yield a very different result. Just as in the graph XTY graph in Figure 70 a measurement taken at points 180 and 280 would give every different result from a measurement taken at 0 and 230

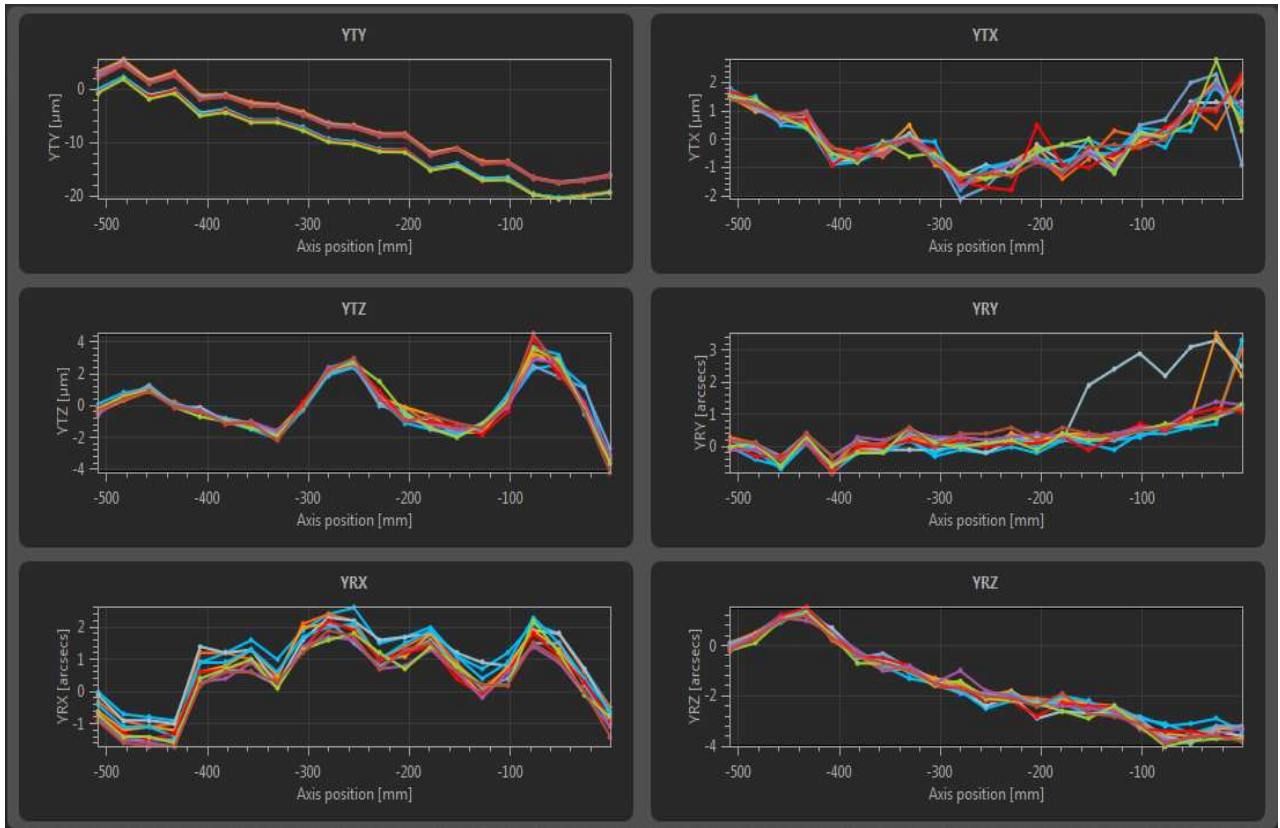


Figure 68 Y Axis combined 6DoF graphs 3 axis vertical machining centre (Machine E)

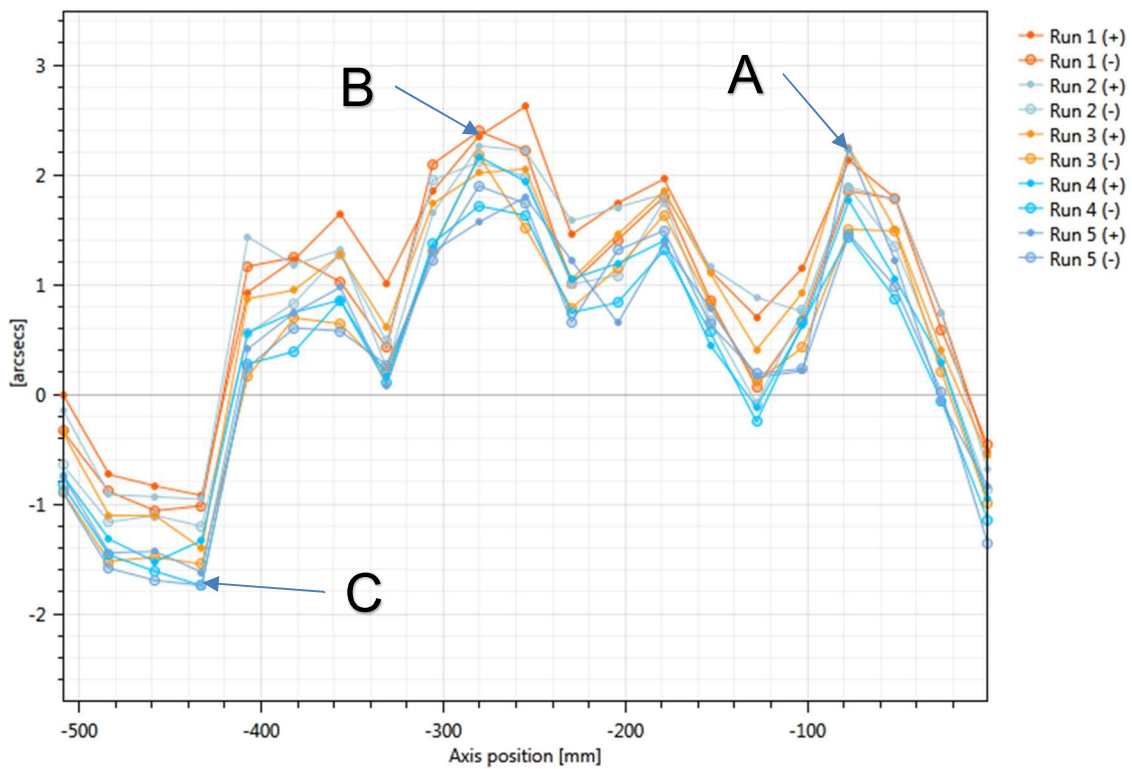


Figure 69 YRX graph from Figure 68 (Machine E)

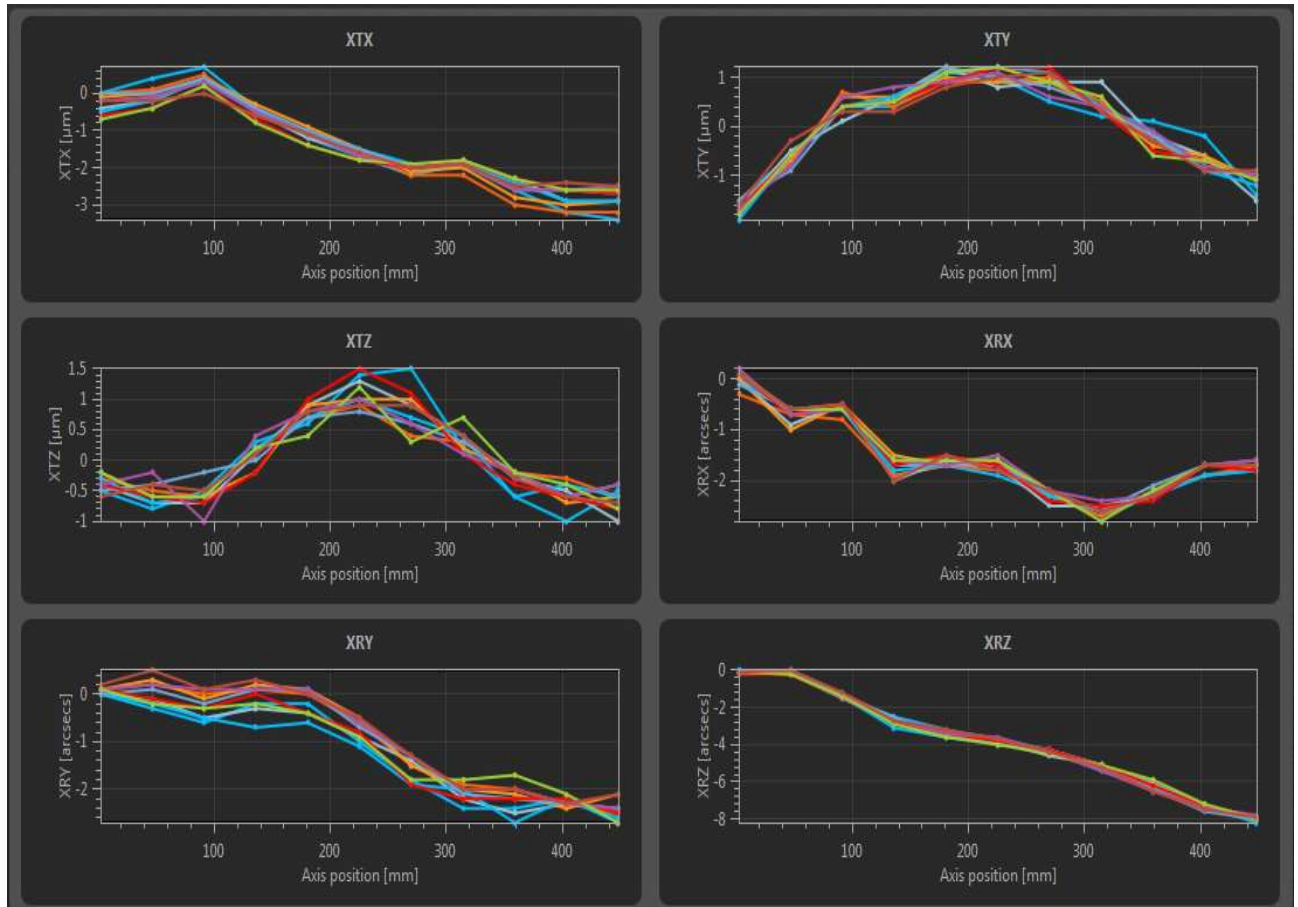


Figure 70 X Axis combined 6DoF graphs 5 axis vertical machining centre (Machine F)

5.3.3 Ball bar results

ball bar measurements are dynamic measurements, the speed at which the tests are run can influence the errors identified, slower speeds would yield results around the geometry of the axes being measured, and faster speeds would show errors directed more towards the drive system itself. For instance, when the machine is running slowly everything is in control, but when the machine speeds up the control, drives and motors are all trying to keep up.

5.3.3.1 *XY Plane*

In the graphs below two error profiles with scales of $2\mu\text{m}$ and $1\mu\text{m}$ respectively are shown. This scale updates automatically within the software depending on the magnitude of the error, sometimes making the error profiles look different. However, if these two graphs are examined closer it becomes evident, they are essentially the same shape.

In Figure 71 there are some backlash spikes that do not present in Figure 72 and the reversal spikes are more than double the magnitude of the slower graph. When the

machine is running at 250mm/min Figure 72 the graph is dominated by the squareness error, but when the machine speeds up to 2500mm/min Figure 71 the squareness error is still there, but as the machine controls and drives start to work harder at keeping control the change of direction at the equator points of the programmed circles start to highlight mechanical backlash and reversal errors.

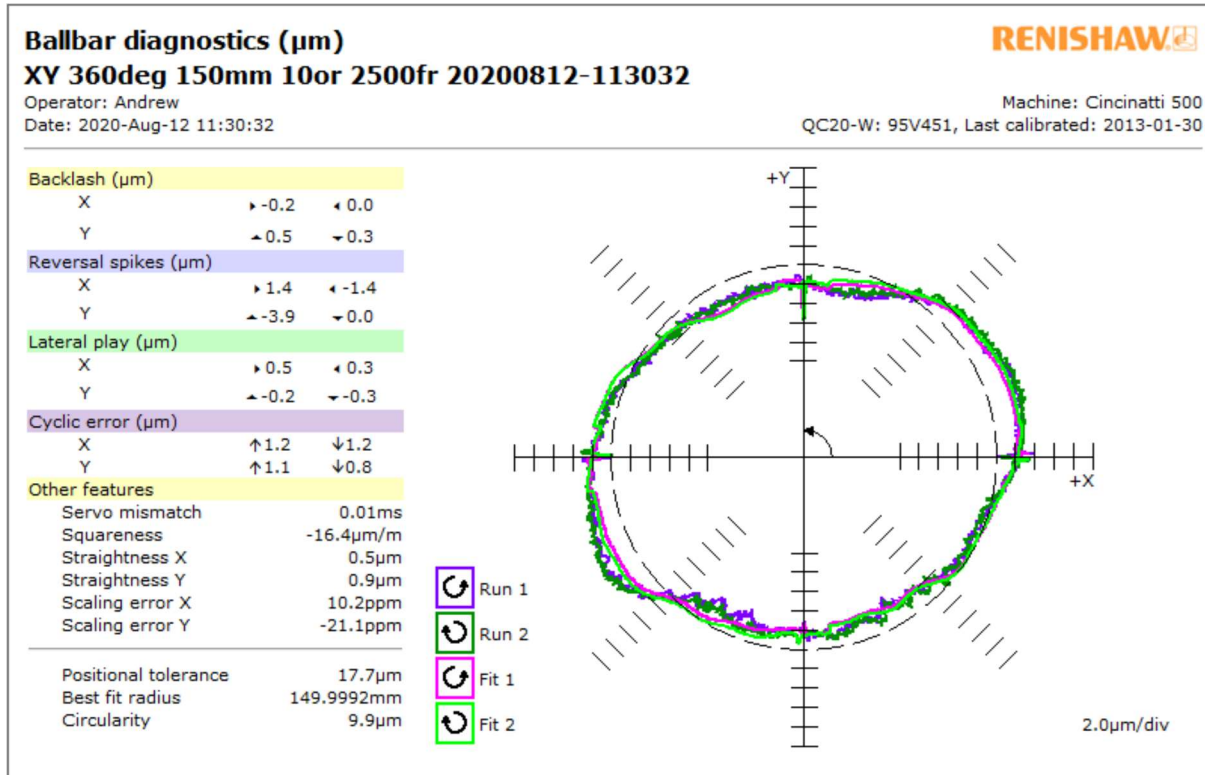


Figure 71 ball bar graph XY 2500mm/min (Machine A)

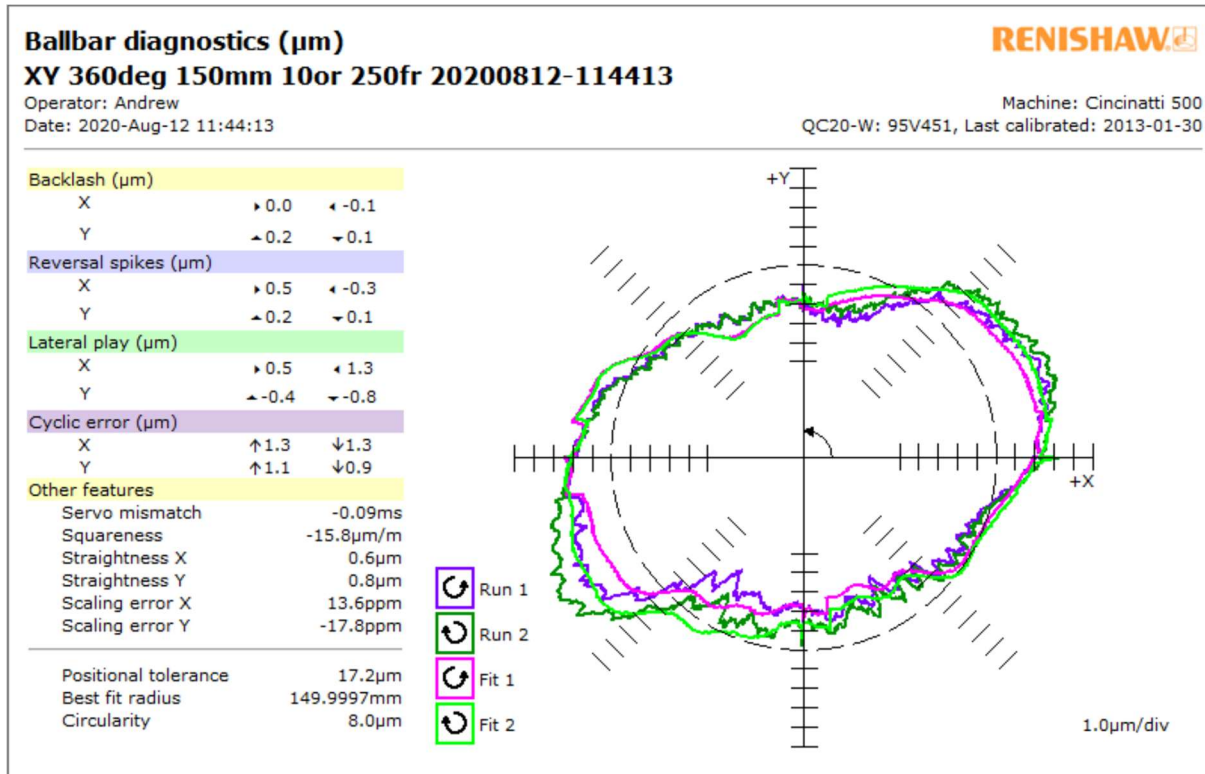


Figure 72 ball bar graph XY 250mm/min (Machine A)

In Figure 73 and Figure 74 there is an increase again in the reversal and backlash errors in the faster speed (Figure 73) but when looking at the other features area of the graphs there is a 54 $\mu\text{m}/\text{m}$ squareness error between the two axes. This could lead to significant positional errors on probing results taken on any parts manufactured by this machine, when taken at differing heights. These errors would not be highlighted until the part was measured independently.

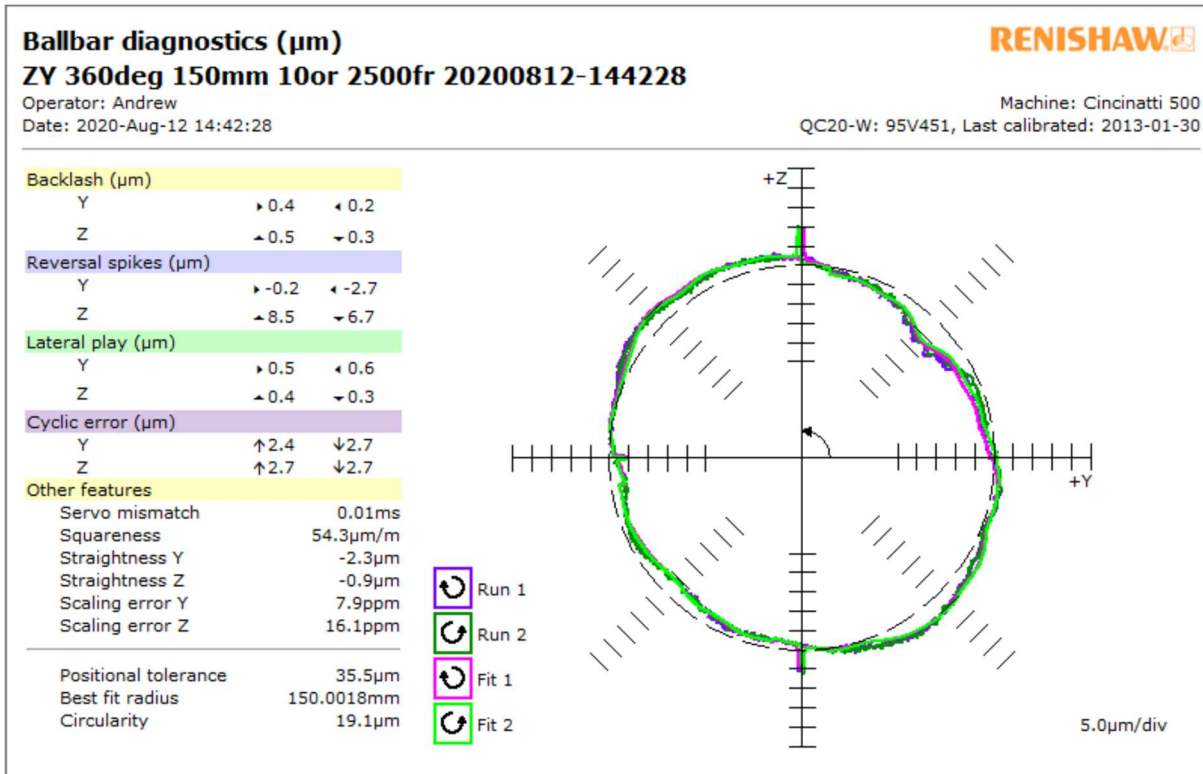


Figure 73 ball bar graph ZX 2500mm (Machine A)

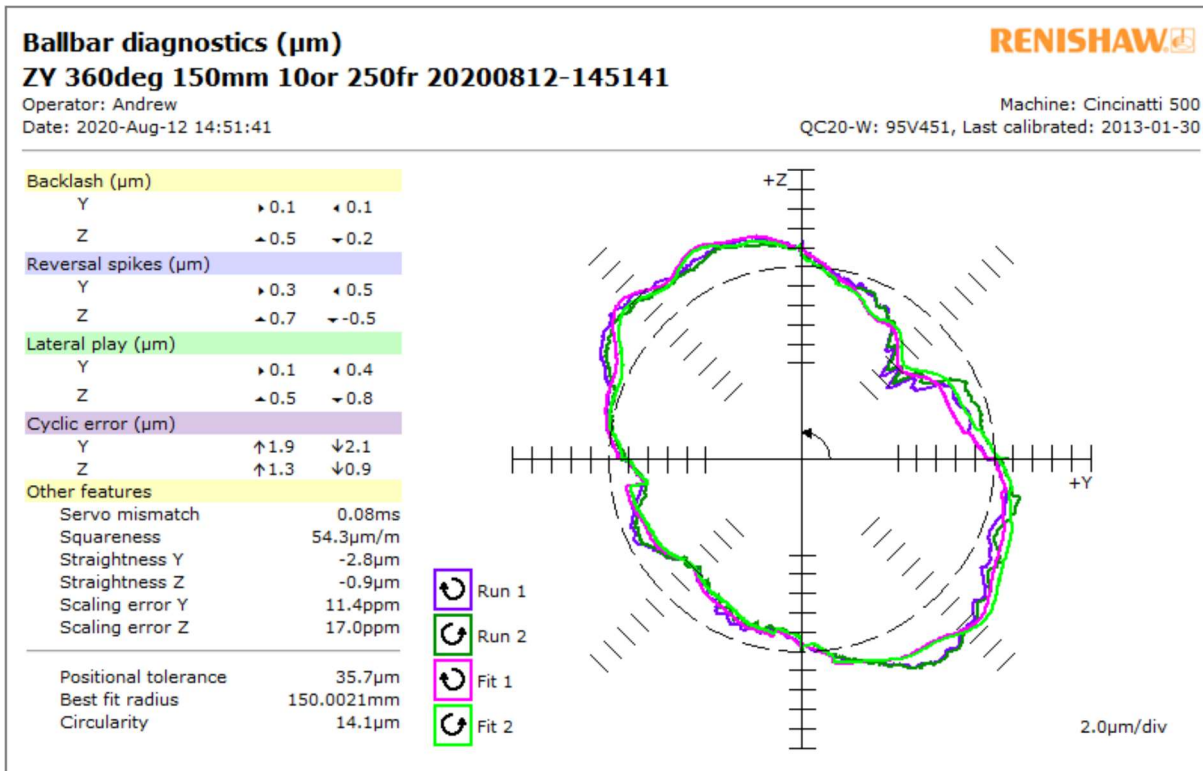


Figure 74 ball bar graph ZX 250mm (Machine A)

5.3.3.2 History graphs from Machine D

The software automatically gives the option to create a history graph of the results as tests are run, this gives the added benefit of creating a benchmark set of results early in the machines life or at a time when the performance of the machine has been established.

In Figure 75 it can be seen early on that there is a peak in the otherwise consistent results, this was due to an error in the setup of the centre offset (operator error).

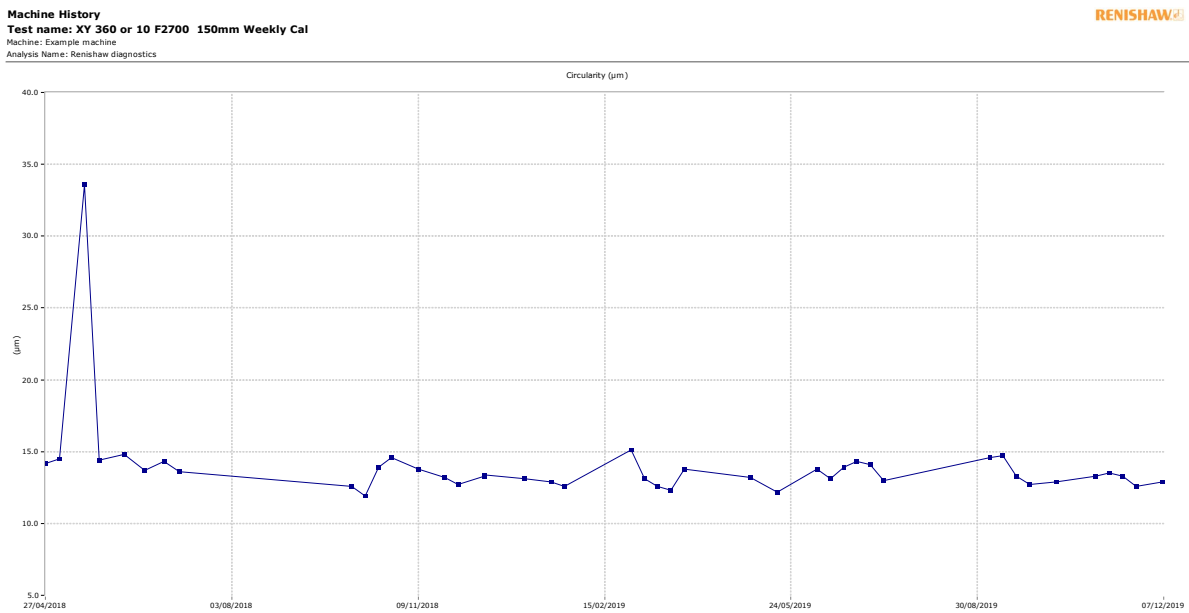


Figure 75 XY plane circularity (Machine D)

As can be seen in the history graph below Figure 76 the results show a consistent trend until an obvious peak in the graph. After investigation it was determined that again this was not due to a machine error but operator error in the setup of the ball bar system, the set up was rectified and the results returned to the previous condition.

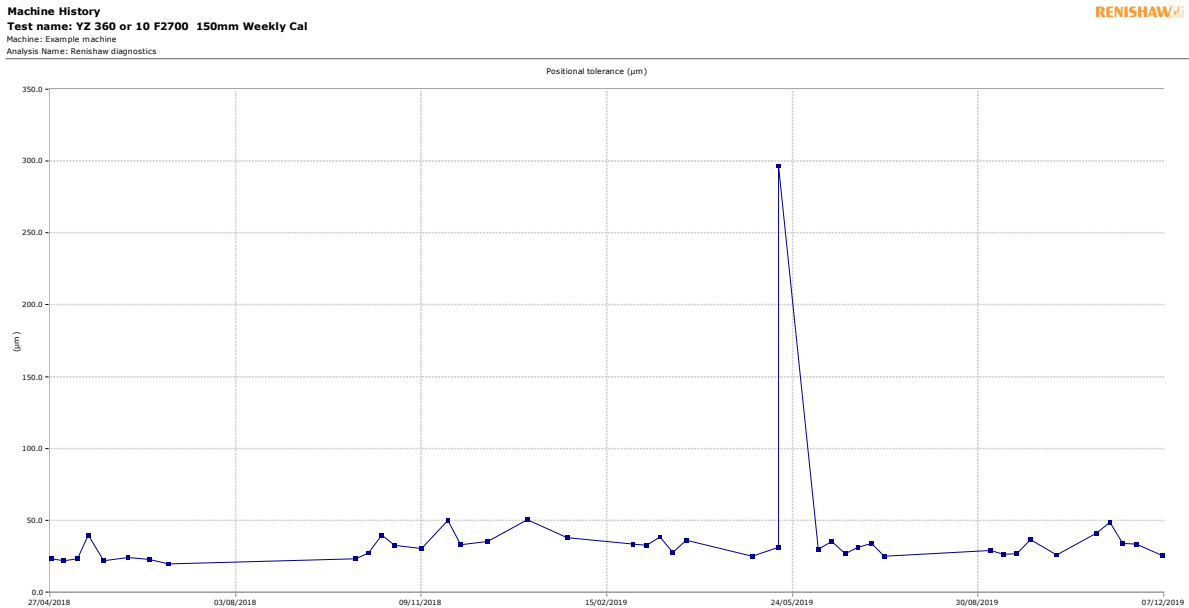


Figure 76 Positional deviation history graph (Machine D)

By checking the history graphs at regular intervals, trends where machines are starting to change shape and their performance reaching tolerance limits would enable companies to rectify issues before impacting on their production. In our history graphs the errors were established to be due to operator error and not machine performance issues, by checking the history graphs as the tests were completed these issues were rectified quickly and without impact. If these graphs had not been checked for some months, then more information would need to be gathered to conclude the reason for the errors, possibly causing halts to production.

5.3.4 Effect of calibration vs probing location

To save time and for ease of operations many machines will have some sort of probing artefact permanently mounted within the working volume but adjacent to the main cutting area to enable probe calibration to be carried out regularly in a repeatable fashion. This could often be a sphere or a ring gauge, but with the artefact being placed under a rotating table (out of the way until it is needed, when it then can be rotated into position) or on a mounting away from fixtures or the part being machined, how does this affect the accuracy?

Assessing the X axis and Y axis graphs in sections 5.3.2.1 and 5.3.2.2, three points of interest were chosen along each of the axes and the ring gauge measured at each nominal point. At the first point the probe was also calibrated in the ring gauge and the calibration data outputted to file. This is the only time the probe is calibrated throughout this test.

The below sketch (Figure 77) and chart of numbers (Figure 78) shows the nominal position and order of the measurements. Only one ring gauge was used to minimise

variation from using different artefacts, so this was moved for each measurement. Position 1 was measured three times during the test, as the first point, then again after the last X measurement and finally after the last Y axis Measurement (1X, 1A, and 1Y) to provide a point of reference and monitor any drift.

At each new position a program is used to find the centre of the ring gauge before measurement.

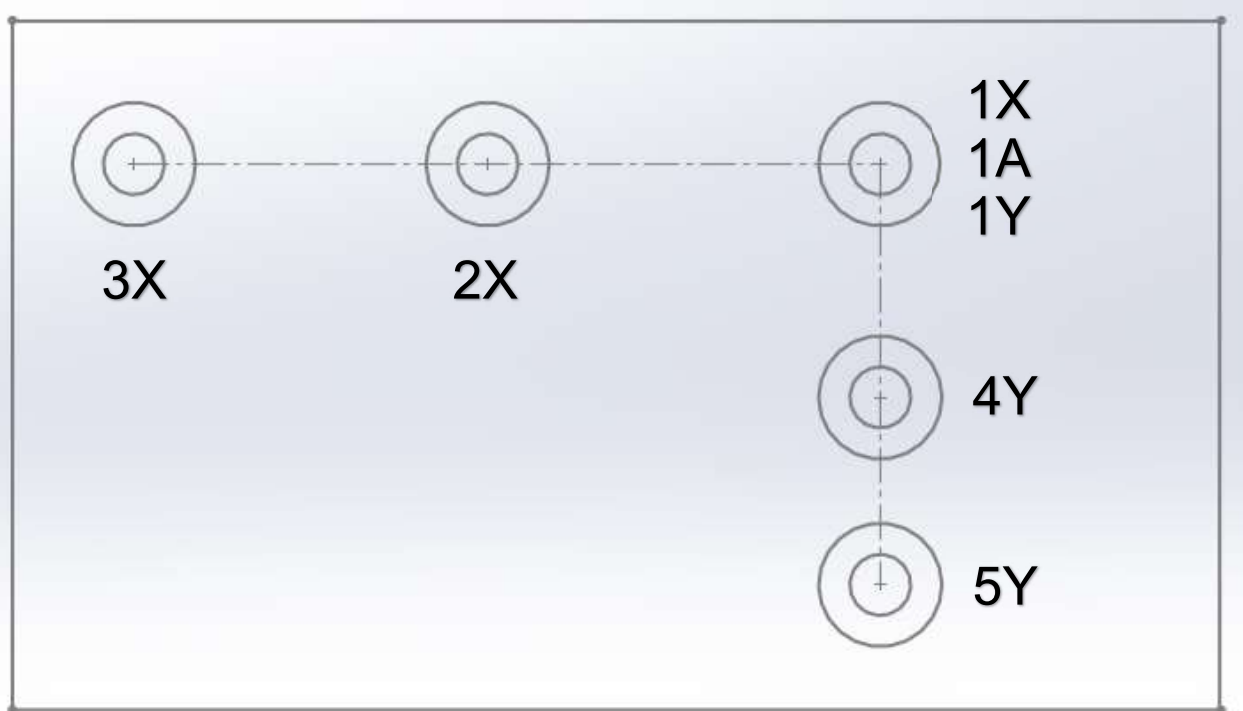


Figure 77 Measurement order of ring gauges

	X	Y	Z
Pos 1X	379.5750	401.8430	16.0000
Pos 2X	229.1450	403.2360	16.0000
Pos 3X	73.3340	399.4850	16.0000
Pos 1A	379.8800	401.9200	16.0000
Pos 4Y	366.7770	254.6970	16.0000
Pos 5Y	365.1990	56.3260	16.0000
Pos 1Y	379.8180	401.8320	16.0000

Figure 78 G55 datum positions for each ring gauge

The graphs below (Figure 79 to Figure 85) show the results from the measurements of the ring gauge in the five positions. Each shows the error magnitude in (a) chart form, (b) a scatter graph of the error magnitude in the X- and Y-axis directions and (c) a polar plot that replicates the ring gauge touch points. A summary chart (Figure 86)

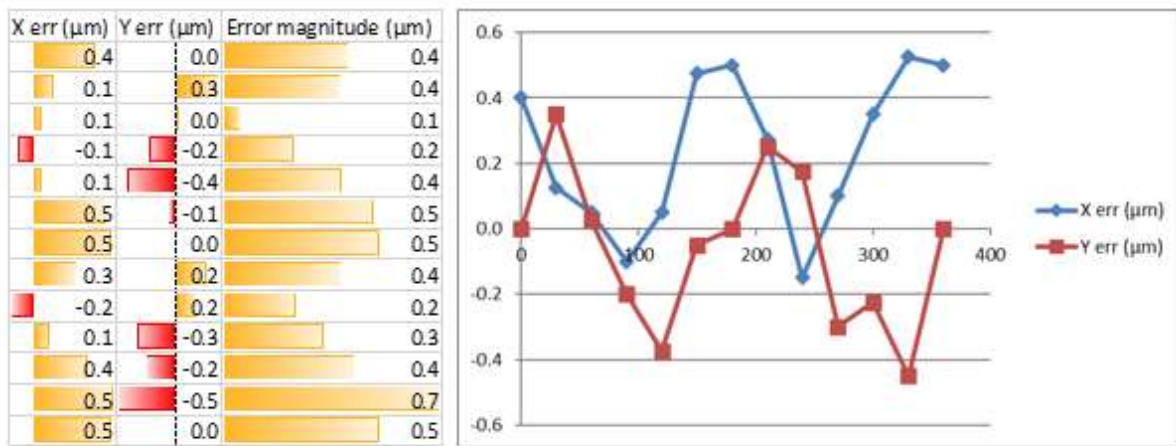
is included with the error magnitudes at each measured touch point on the ring gauge with standard deviation calculated.

The view of the polar plot graph should be taken as looking from above, down through the Z Axis towards the ring gauge.

In Figure 79 the error magnitudes are submicron, as would be expected on a calibrated ring gauge in a position where the probe has been calibrated and nothing moved.

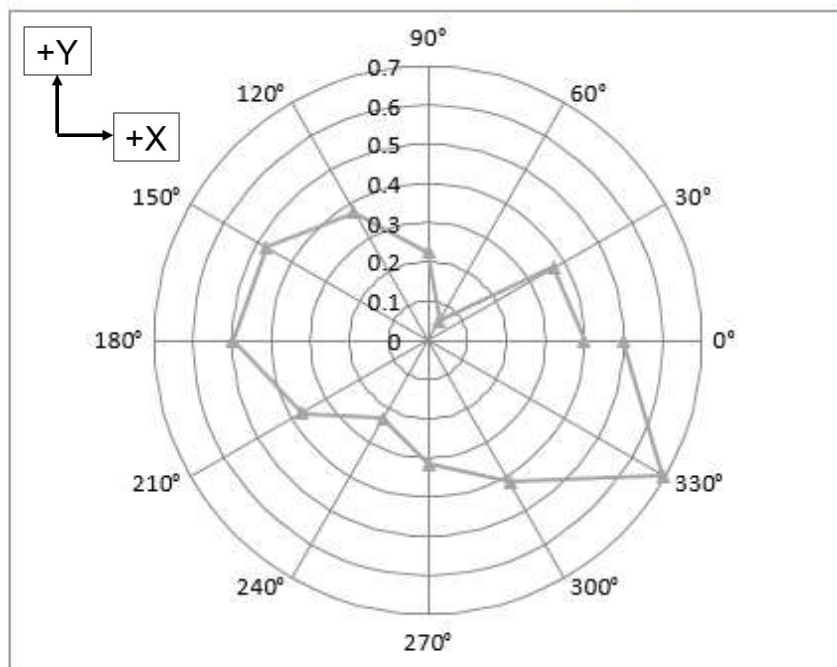
When the ring gauge is moved to the different positions there is very little change in the measured radius at each point on the ring gauge, no more than 2.5 μm , from the measurements at the original calibrated position, but it has to be said that the geometric errors on this machine are very small.

This gives confidence that on this machine a measurement taken at different positions from the calibration position would be good, depending on the tolerance required for conformance.



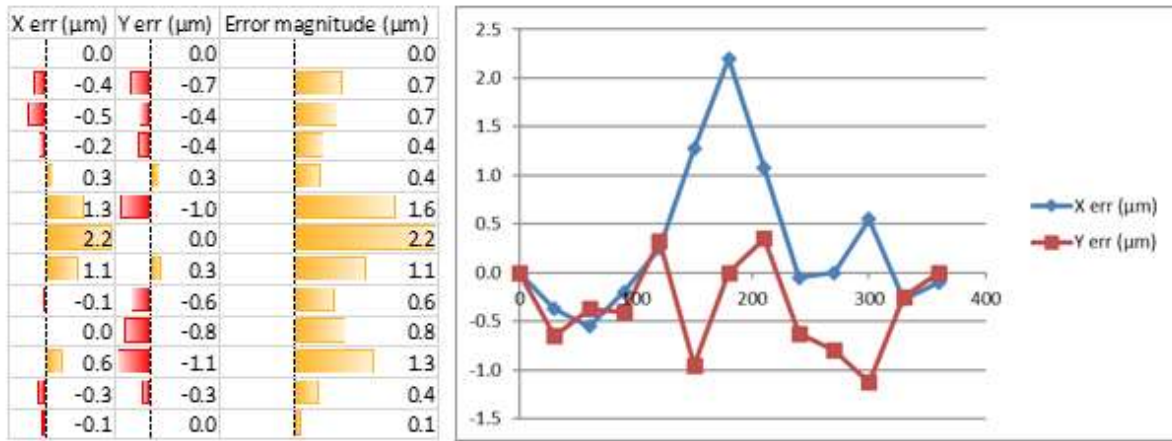
(a)

(b)



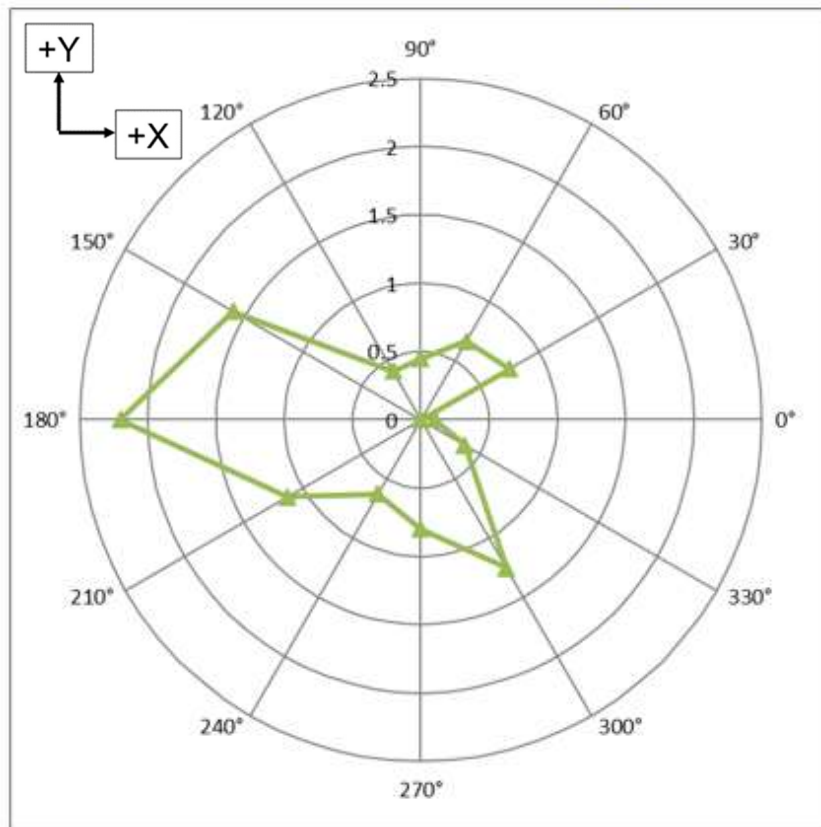
(c)

Figure 79 Measured error magnitude position 1X



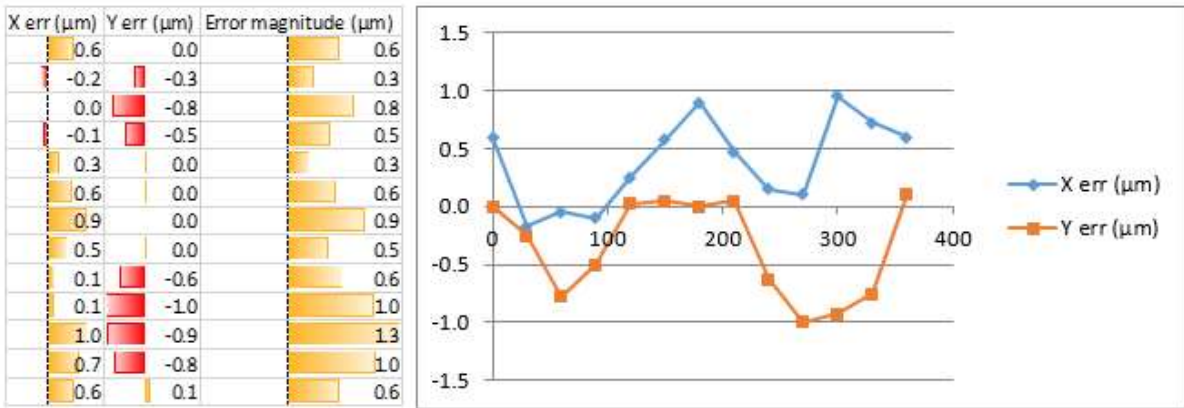
(a)

(b)



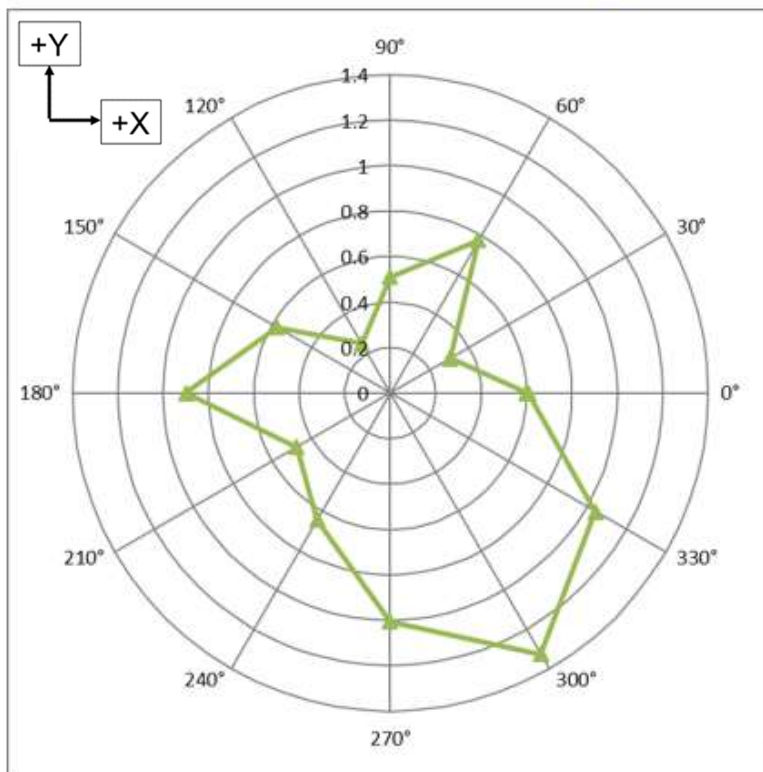
(c)

Figure 80 Measured error magnitude position 2X



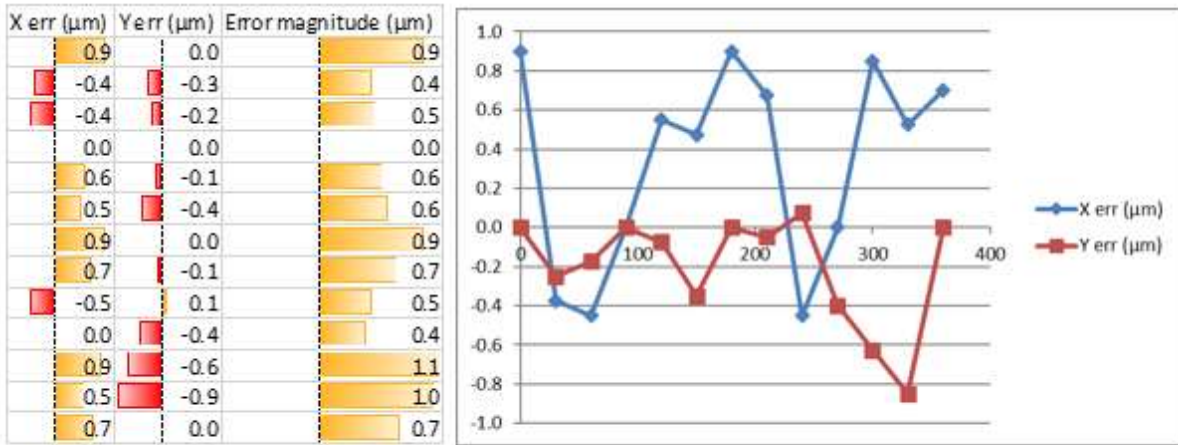
(a)

(b)



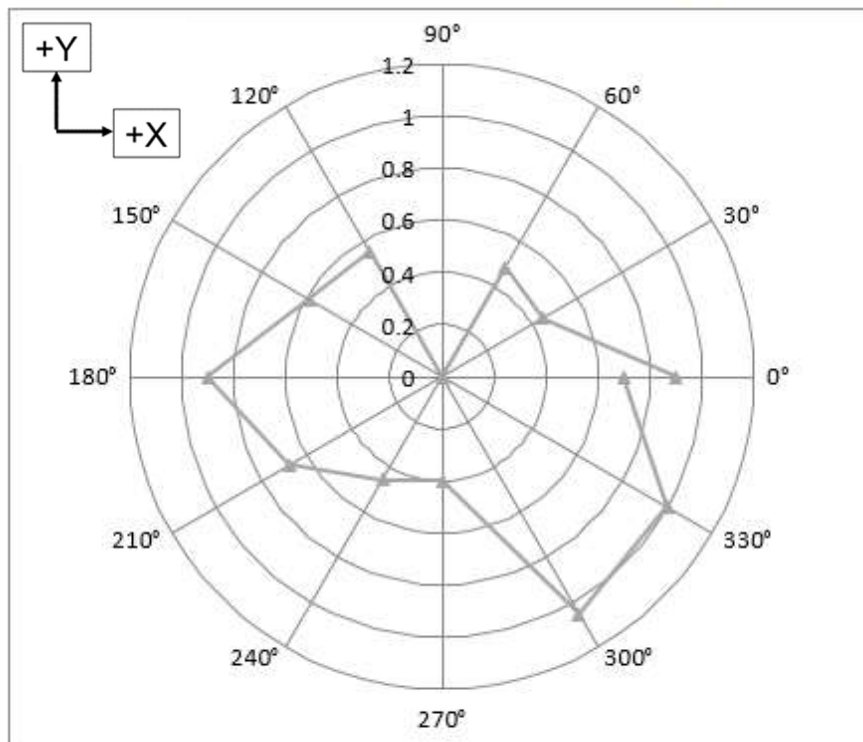
(c)

Figure 81 Measured error magnitude position 3X



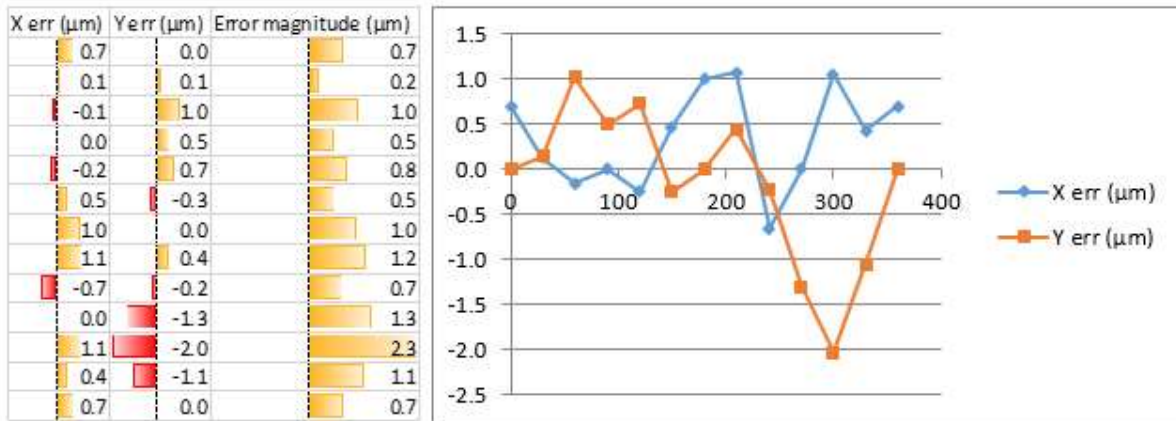
(a)

(b)



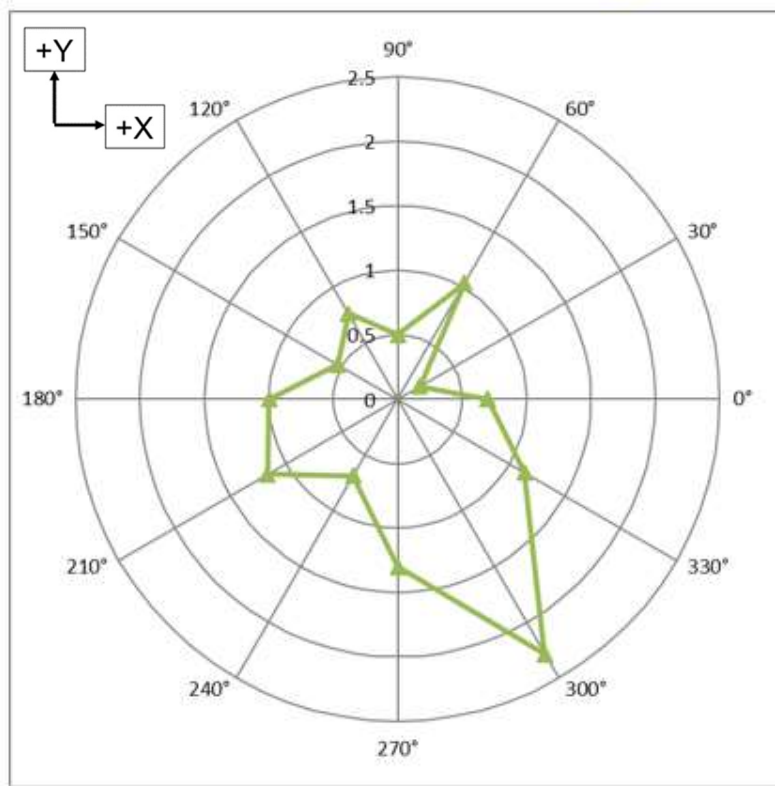
(c)

Figure 82 Measured error magnitude position 1A



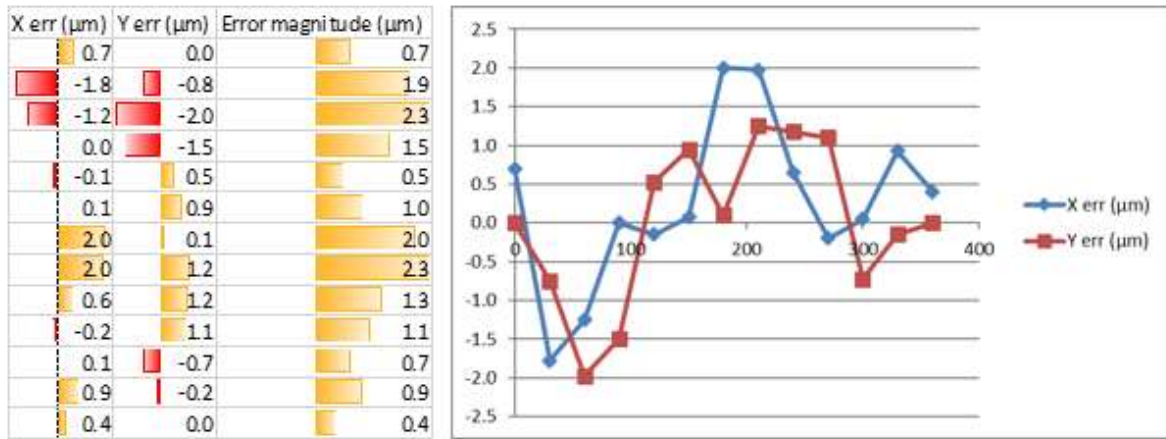
(a)

(b)



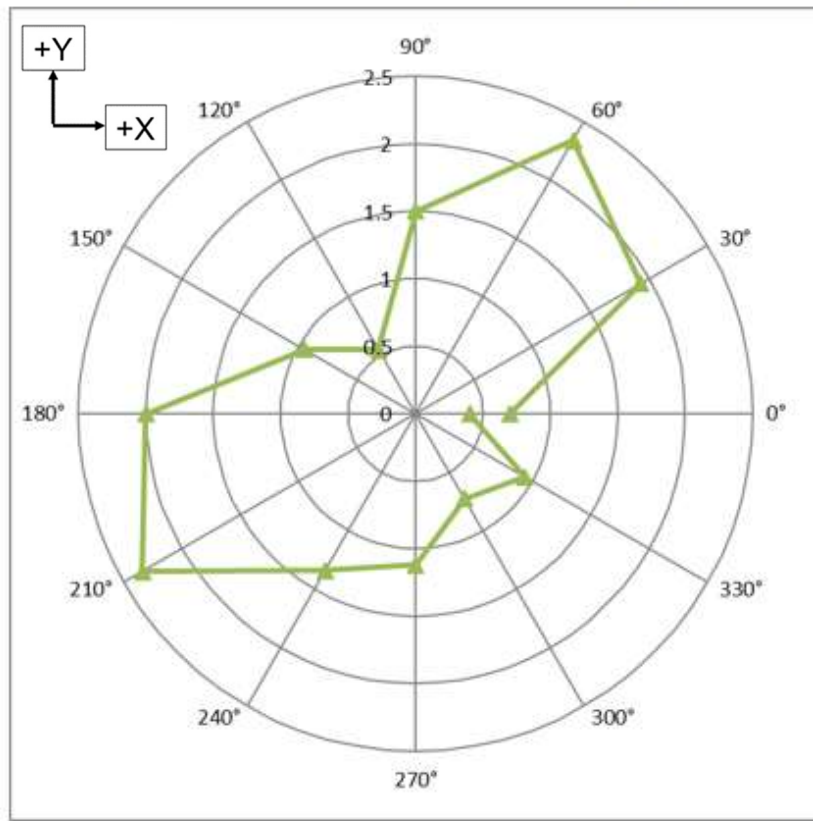
(c)

Figure 83 Measured error magnitude position 4Y



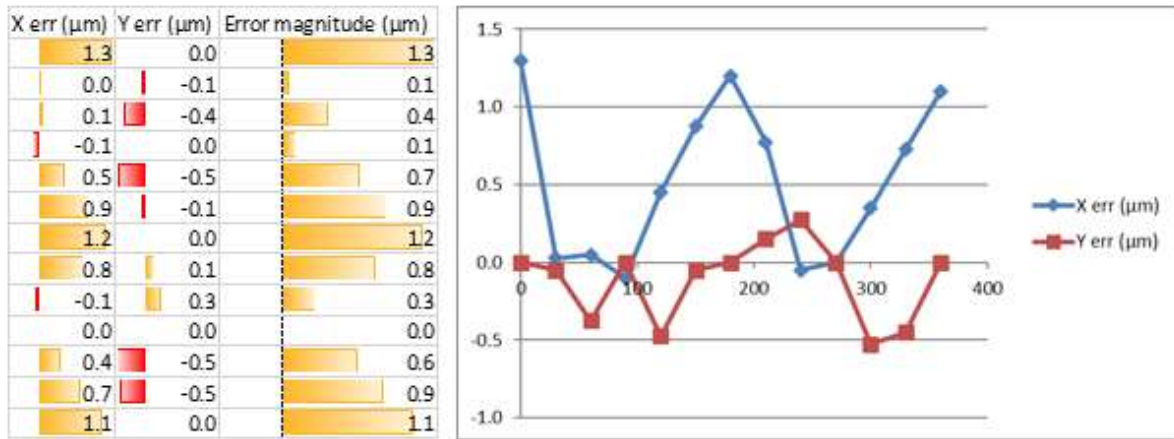
(a)

(b)



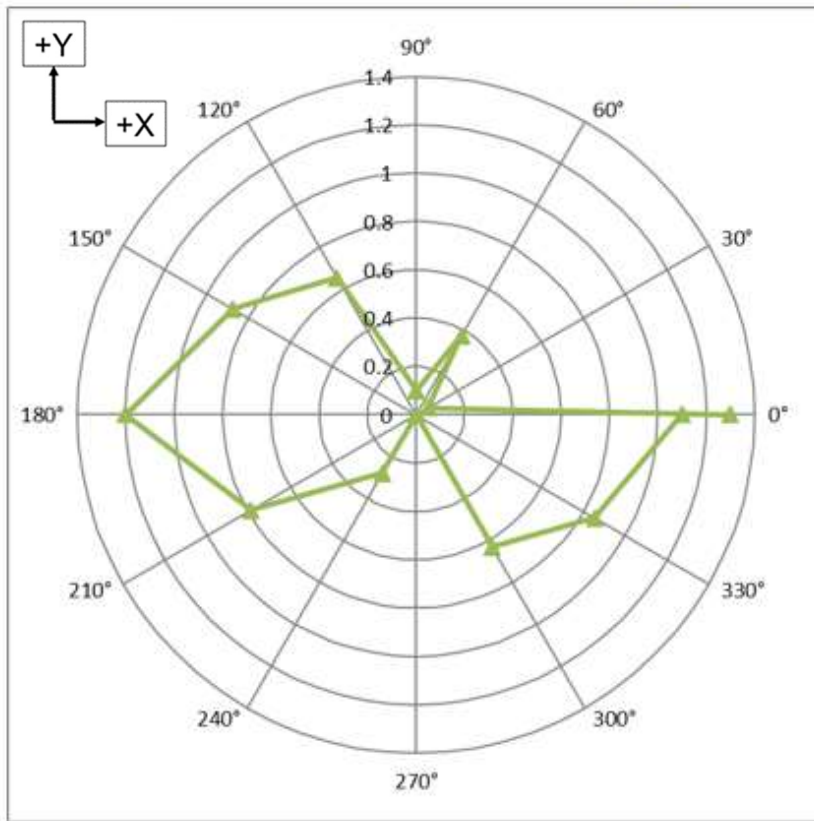
(c)

Figure 84 Measured error magnitude position 5Y



(a)

(b)



(c)

Figure 85 Measured error magnitude position 1Y

deg	Error magnitude (μm)						
	1X	2X	3X	1A	4Y	5Y	1Y
0	0.4	0.0	0.6	0.9	0.7	0.7	1.3
30	0.4	0.7	0.3	0.4	0.2	1.9	0.1
60	0.1	0.7	0.8	0.5	1.0	2.3	0.4
90	0.2	0.4	0.5	0.0	0.5	1.5	0.1
120	0.4	0.4	0.3	0.6	0.8	0.5	0.7
150	0.5	1.6	0.6	0.6	0.5	1.0	0.9
180	0.5	2.2	0.9	0.9	1.0	2.0	1.2
210	0.4	1.1	0.5	0.7	1.2	2.3	0.8
240	0.2	0.6	0.6	0.5	0.7	1.3	0.3
270	0.3	0.8	1.0	0.4	1.3	1.1	0.0
300	0.4	1.3	1.3	1.1	2.3	0.7	0.6
330	0.7	0.4	1.0	1.0	1.1	0.9	0.9
360	0.5	0.1	0.6	0.7	0.7	0.4	1.1
	0.150213	0.590766	0.294757	0.278997	0.491942	0.646027	0.422902

Figure 86 Summary chart of error magnitudes with standard deviation calculated

5.4 Thermal influences

Several machines have been used in this investigation, but two (Machine A and Machine B) are of the same construction as Mian [26] used for detailed analysis of thermal errors. Figure 87 and Figure 88 are reproduced from his thesis, where he notes that the machine can be considered, from a thermal point of view, as being symmetrical and therefore simplified as “*halved CAD models*”.

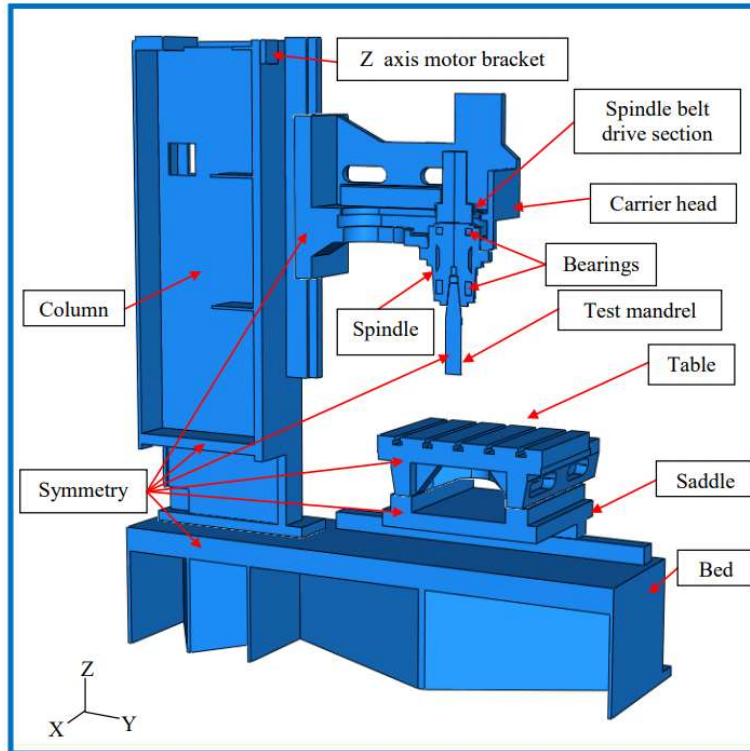


Figure 87 Assembly of the machine (view 1) [26]

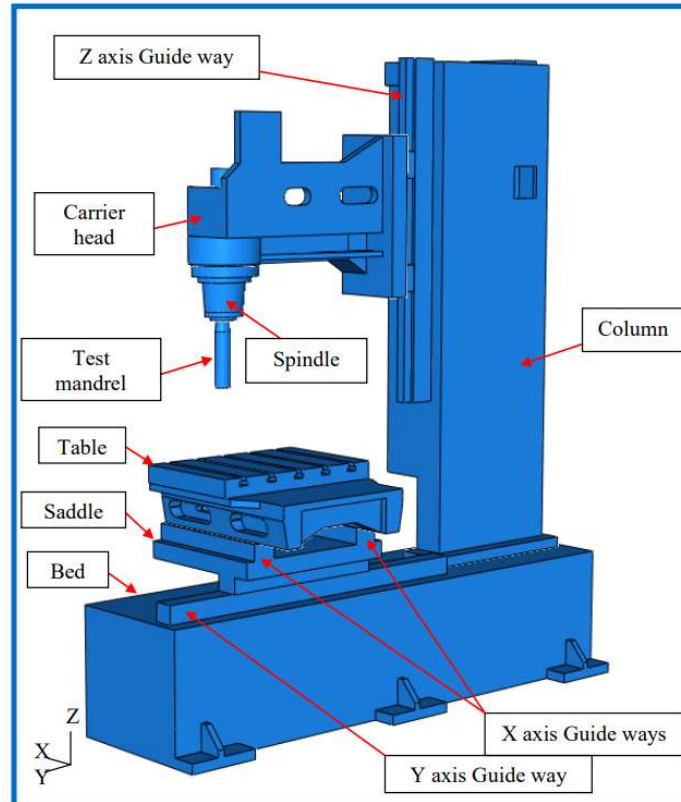


Figure 88 Assembly of the machine view 2 [26]

5.4.1 Laser testing

Laser testing was carried out on Machine B by the method described in section 4.3.5.3, using a Renishaw XL80 laser interferometer measuring the linear positioning error. A standard ISO 230-2:2014 measurement cycle is followed by a succession of rapid axis movements of the axis during the “heating” phase of the test, with a measurement cycle after every ten rapid oscillations. After 75 minutes the “cooling” phase only takes the same periodic measurements and remains static otherwise.

Figure 89, Figure 90 and Figure 91 show the results of the test and the associated temperature graph for the X, Y and Z axes respectively. To interpret the error graph, each line is associated with a target position in millimetres from the datum end of travel. Over time the thermal datum shifts with temperature, this is the “target” trace with the least amount of movement – in Figure 89 the turquoise trace at 500 mm. Over time the heating cycle for the first 75 minutes gives rise to approximately 15 μm of displacement, returning to the original position by the end of the cooling phase. If there were no expansion of the ball screw, or if a glass linear scale were fitted, then all the traces for the other targets would change by the same amount. The divergence between targets 500 mm and 0 mm arises because of the expansion of the ball screw between these two axis positions. The temperature graph associated with each error plot forms the lower part of each figure.

This machine does not have secondary linear encoders but relies on the motor rotary encoder for position control, accounting for the large errors. However, without testing, the user would not know the magnitude of the effect of running each axis in rapid. Here there is over 70 μm of error on each axis from the datum and between 50 μm and 60 μm of error from one end of the axis to the other at the peak deformation. Temperature rises on each of the ball nuts, which transmit heat into the ball screw, are in the order of 3 °C to 5 °C after only one hour of heating.

These results give a very clear picture of the displacements that would be seen on the machine as the result of machining cycles. Perhaps more concerning is the rapidity with which the heat is lost, and distortion “recovers” after 75 minutes. This sharp change would be the sort of phenomenon experienced when translating from machining with high energy cuts, to probing for measurement with more measured feedrate and lower acceleration forces.

These tests provide very rich information but require a laser to be mounted on each axis for two hours sequentially. This represents six hours measurement time per machine, with additional time required for performing the set-up and strip-down of the laser.

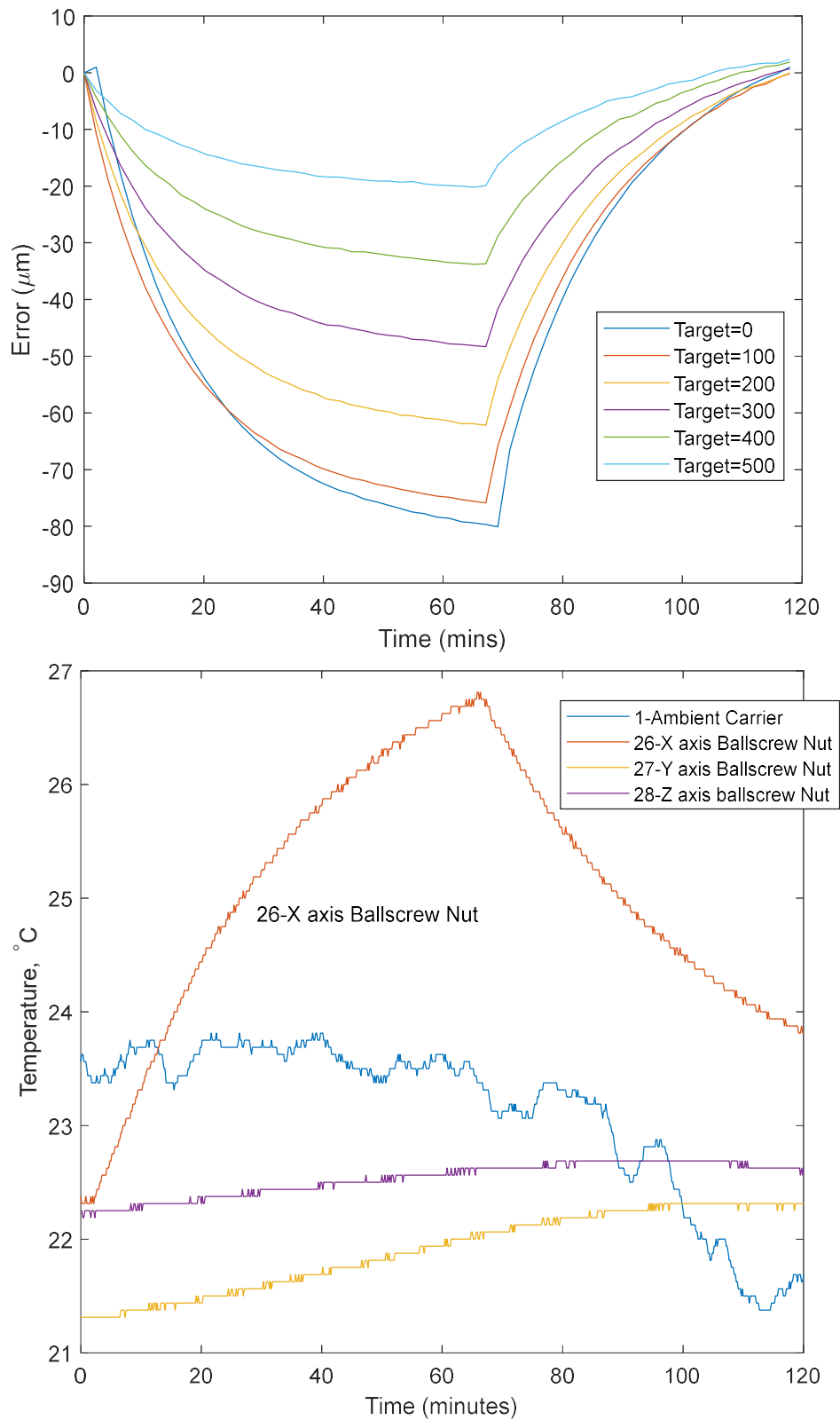


Figure 89 X-axis heating test using laser on Machine B

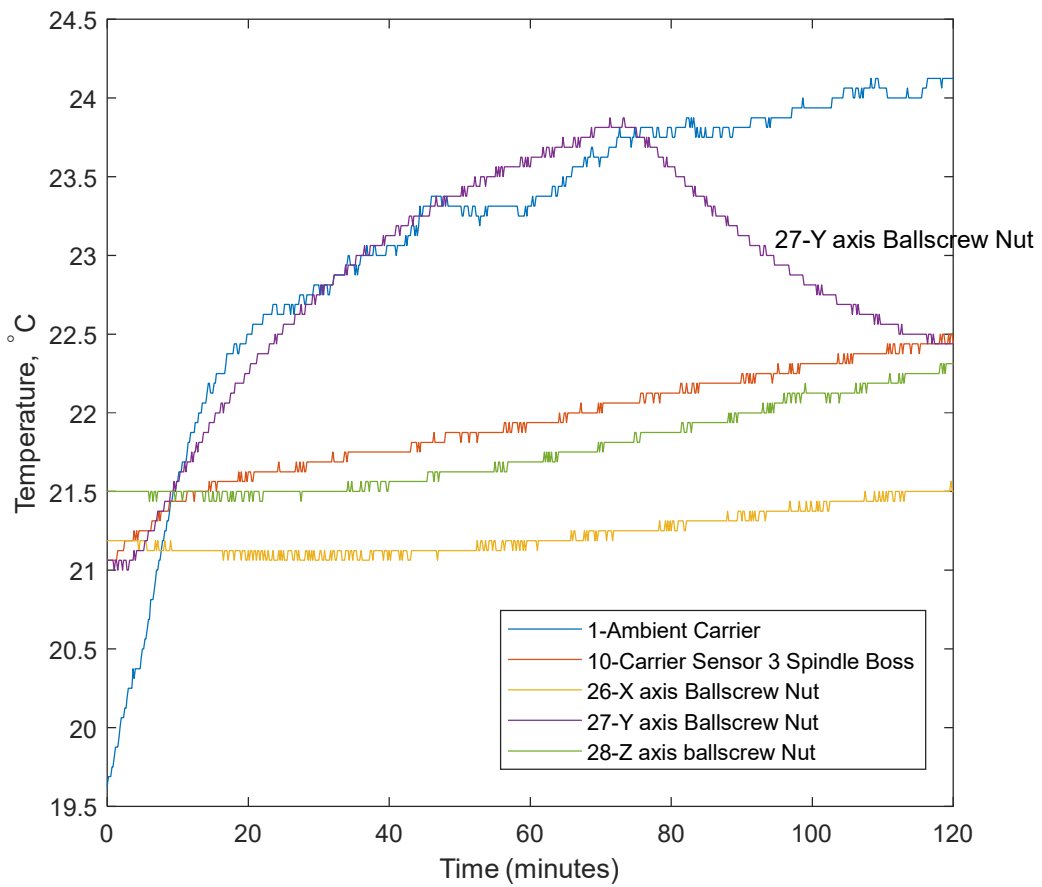
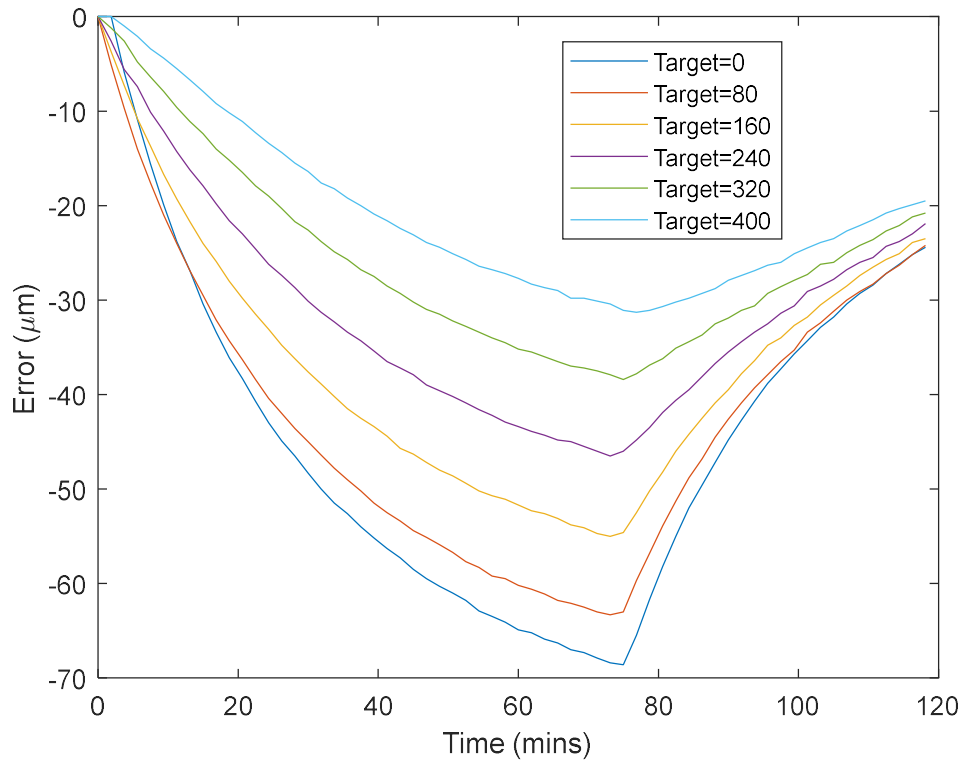


Figure 90 Y-axis heating test using laser on Machine B

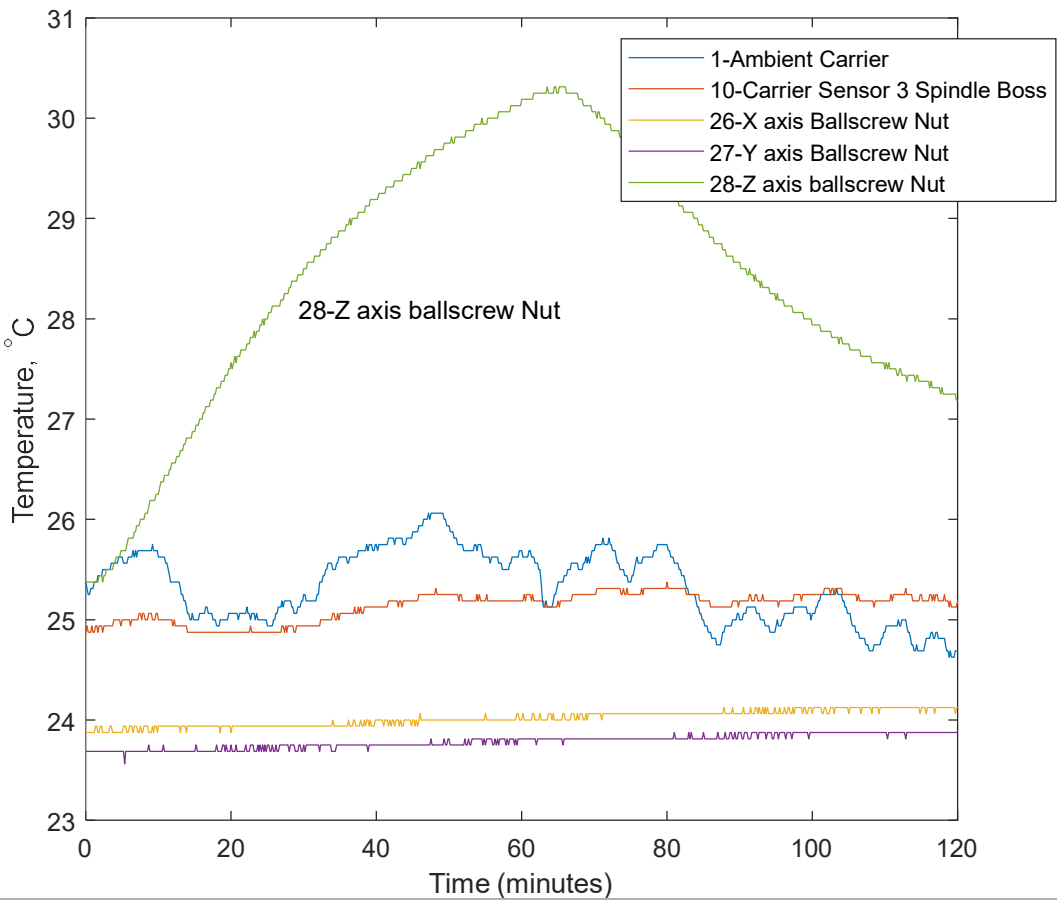
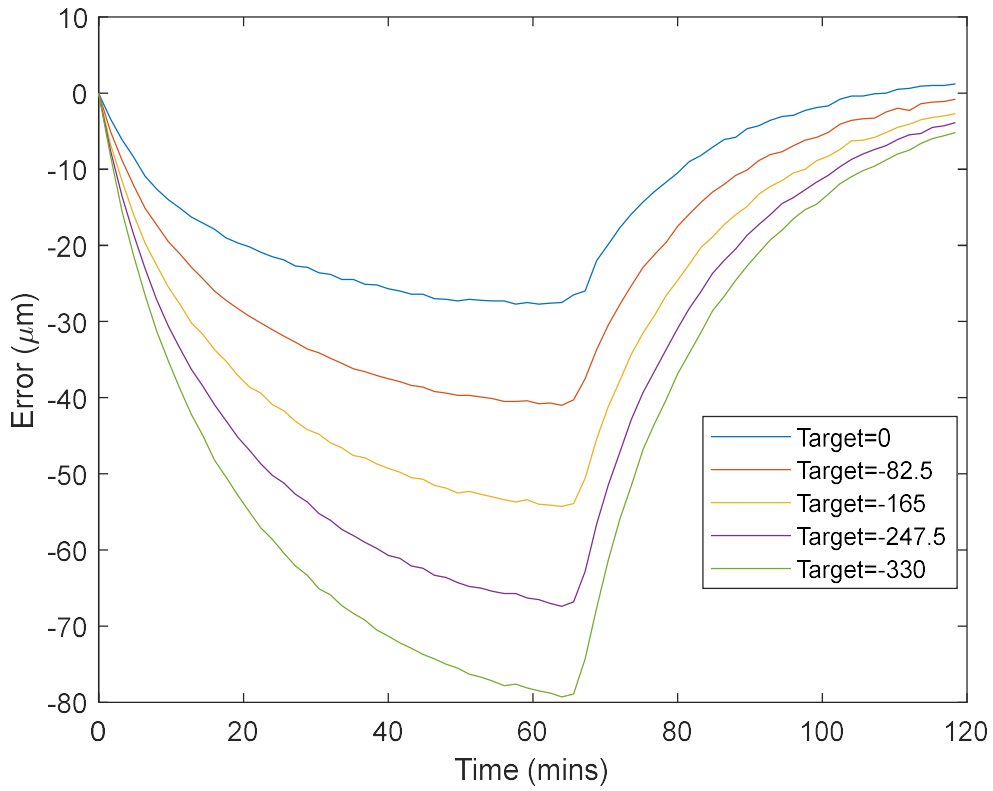


Figure 91 Z-axis heating test using laser on Machine B

5.4.2 Probing testing

The probing points for the tests are comprised of four spheres. The concept for this arose through work on the iTEC thermal compensation system with Dapatech Systems PTE. LTD. and Renishaw plc.

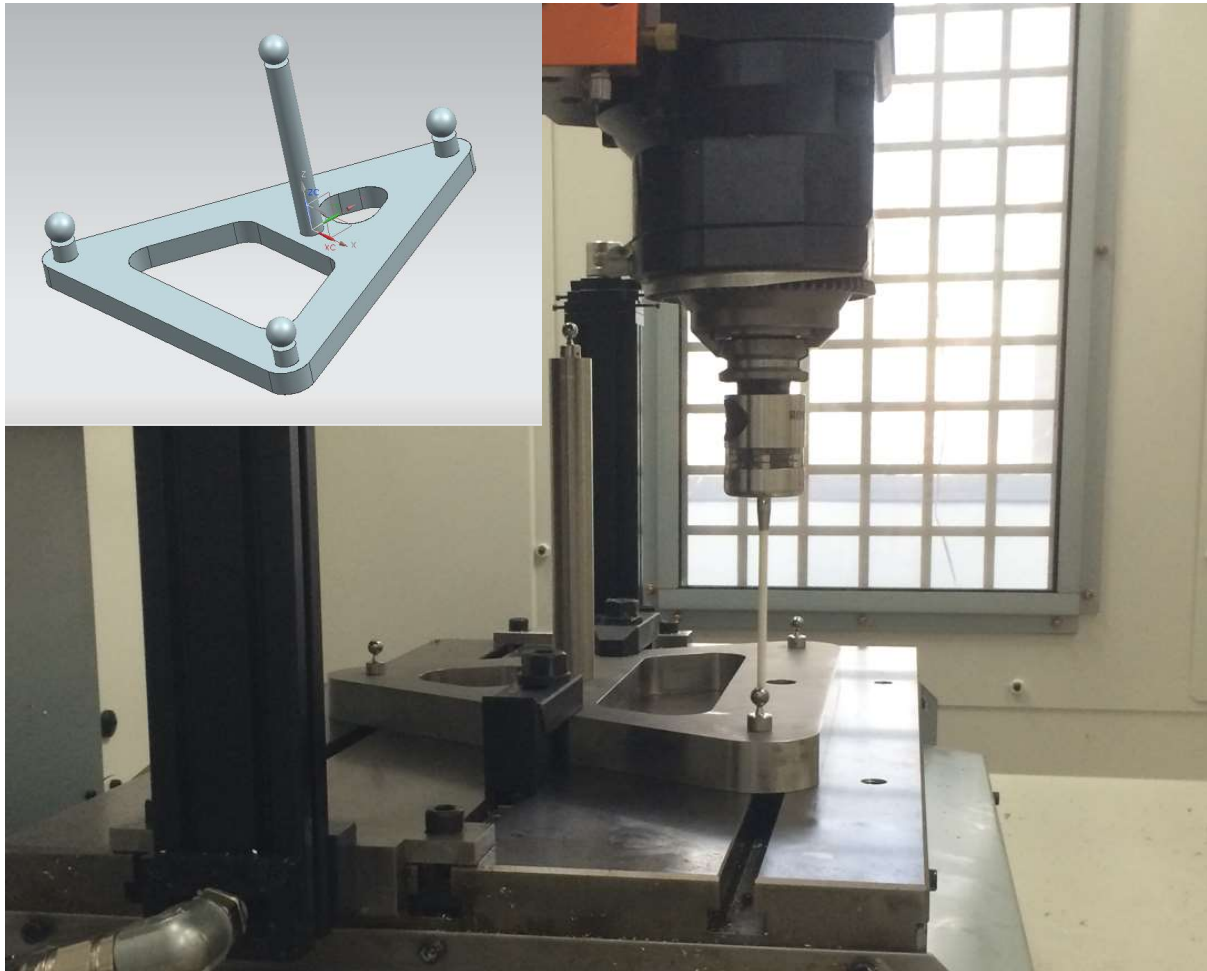


Figure 92 Probing points for thermal tests

5.4.2.1 *Description of analysis*

The spheres (Figure 93) provide information on errors in the X, Y and Z axis directions. The analysis in the graphs related to probing in this section convert the measurements into X, Y and Z errors according to the legend labels in Figure 94. The following explanation of the analysis helps interpretation of the results:

X-axis errors X1 and X2 are given by the X-axis position from sphere 2 and sphere 4 respectively. Change in X1 indicates a position-independent thermal error (PITE) which is an overall shift of the axis. XD is the difference between X1 and X2 (approximately 290 mm apart) and indicates a position-dependent thermal error (PDTE) likely to be expansion of the ball screw or of the scale, Machine A has linear

encoders on each axis, so does not show large PDTE. The machine is nominally symmetrical about the Y-axis, so X-axis thermal errors are relatively small.

Y-axis datum position, Y1, is given by the Y-axis position of Sphere 3. As with the X-axis, this shift can come from a linear expansion of the scale location. However, it is more likely for this configuration of machine to be bending of the spindle carrier head [26]. The second Y-axis location is a virtual sphere mid-way between Sphere 2 and Sphere 4. Therefore, Y2 is an average of the Y-axis positions for these two spheres. YD is the difference between the two locations, approximately 250 mm apart.

The Z-axis datum, Z1, is given as the mean Z-location of the three nominally co-planar spheres (Sphere 2, Sphere 3 and Sphere 4). The second location, Z2, is from the higher Sphere 1 and ZD is the difference over the separation of ~190 mm.

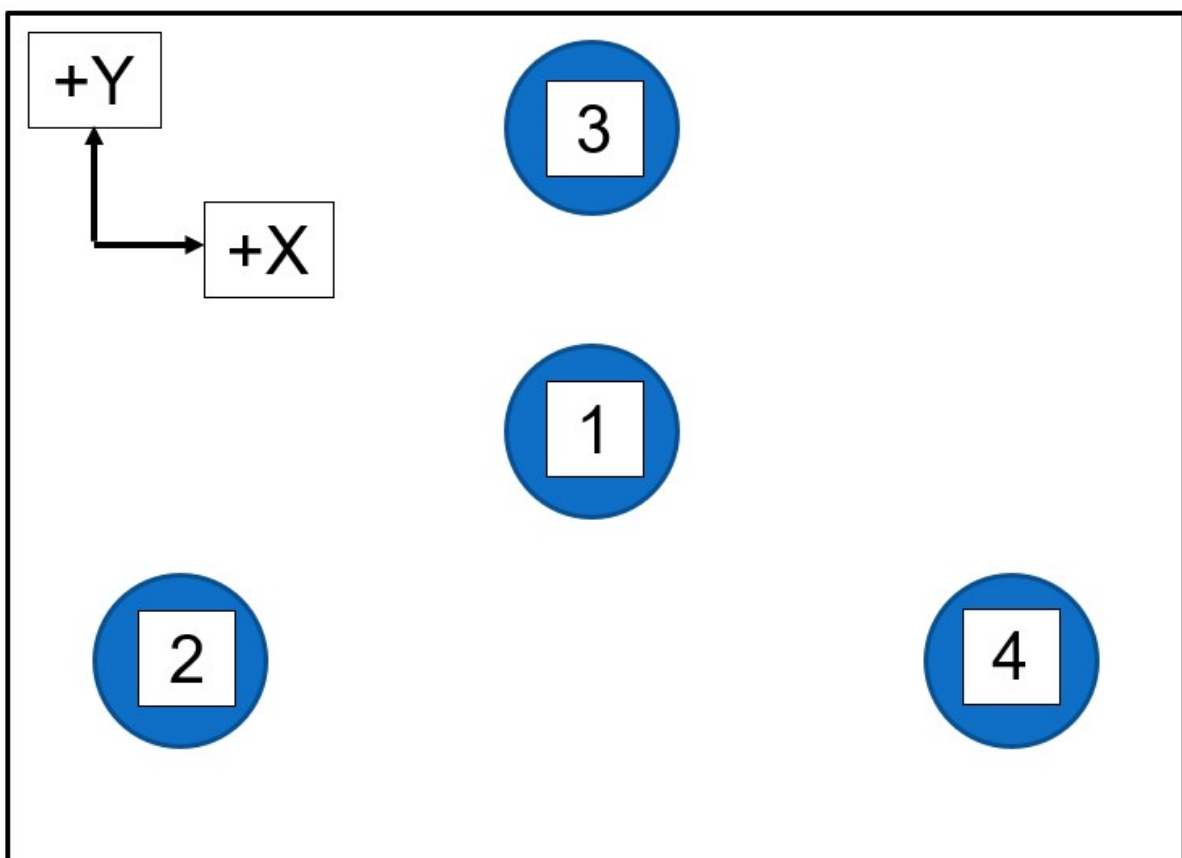


Figure 93 Label convention for probing spheres



Figure 94 Legend used for probe analysis

5.4.3 Typical temperature profile

The sensors used in this work are MAXIM DS18B20 direct-to-digital temperature sensors. They have been used for many years by the research group [92] along with our own logging software, “WinTCal”. Figure 95 shows a plot from the captured data for one sensor. Sample rate and resolution are programmable. The quantisation in the figure derives from this effect. The settings for tests carried out in this work were a sample time of 10 s and a resolution of 0.125 °C.

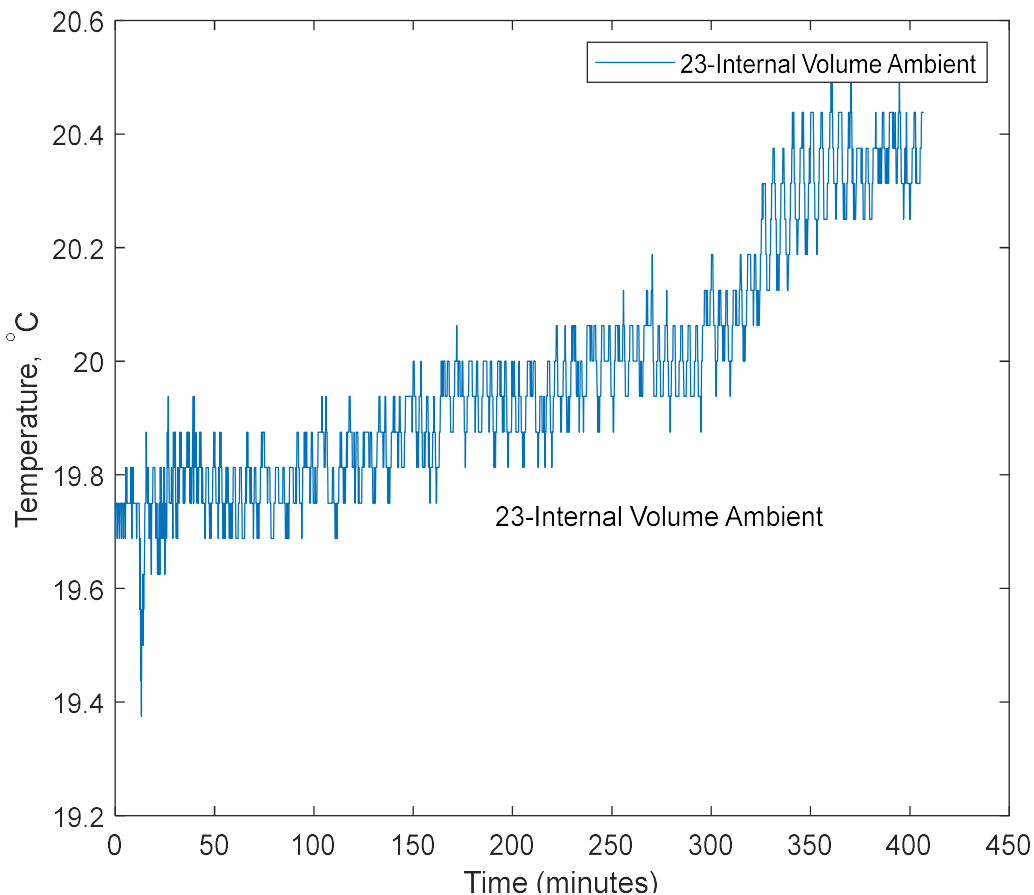


Figure 95 Ambient temperature graph

Sensors were located in a number of places to cover the main elements of the machine, as shown in Table 6.

Clearly, these are many more sensors than would normally be available on a production machine. For the remainder of the analysis the legend for the temperature graph is not provided, since it takes up too much space and the number of lines means that the colour scheme makes visually isolating one sensor too difficult. Figure 96 shows the legend used for all subsequent temperature graphs on Machine A, unless otherwise stated.

Table 6 Location of sensors on Machine A during analysis

Machine column structure	Column LH Front Base
	Column LH Front Bott
	Column LH Front Mid
	Column LH Front Mid Low
	Column LH Front Mid Up
	Column LH Front Top
	Column LH Rear Air Pocket
	Column LH Rear Ambient
	Column LH Rear Bott
	Column LH Rear Mid
	Column LH Rear Mid Low
	Column LH Rear Mid Up
	Column LH Rear Top
	Column LH Top Air Pocket
Ambient inside the machine	Internal Volume Ambient
Spindle and housing	Spindle Bottom Bearing
	Spindle Frame Bottom 1
	Spindle Frame Bottom 2
	Spindle Frame Bottom 3
	Spindle Frame Bottom 4
	Spindle Frame Top 1
	Spindle Frame Top 2
	Spindle Frame Top 3
	Spindle Frame Top 4
	Spindle Front Coolant Block
	Spindle Motor
	Spindle Motor Plate
X-axis	X Axis Ballnut
	X Axis Ballscrew Bearing
	X Axis Motor
Y-axis	Y Axis Ambient
	Y Axis Ball Screw End Bearing
	Y Axis Ballnut

	Y Axis Motor
	Y Axis Motor Bearing
Z-axis	Z Axis Ball Nut
	Z Axis Motor
	Z Axis Motor Plate

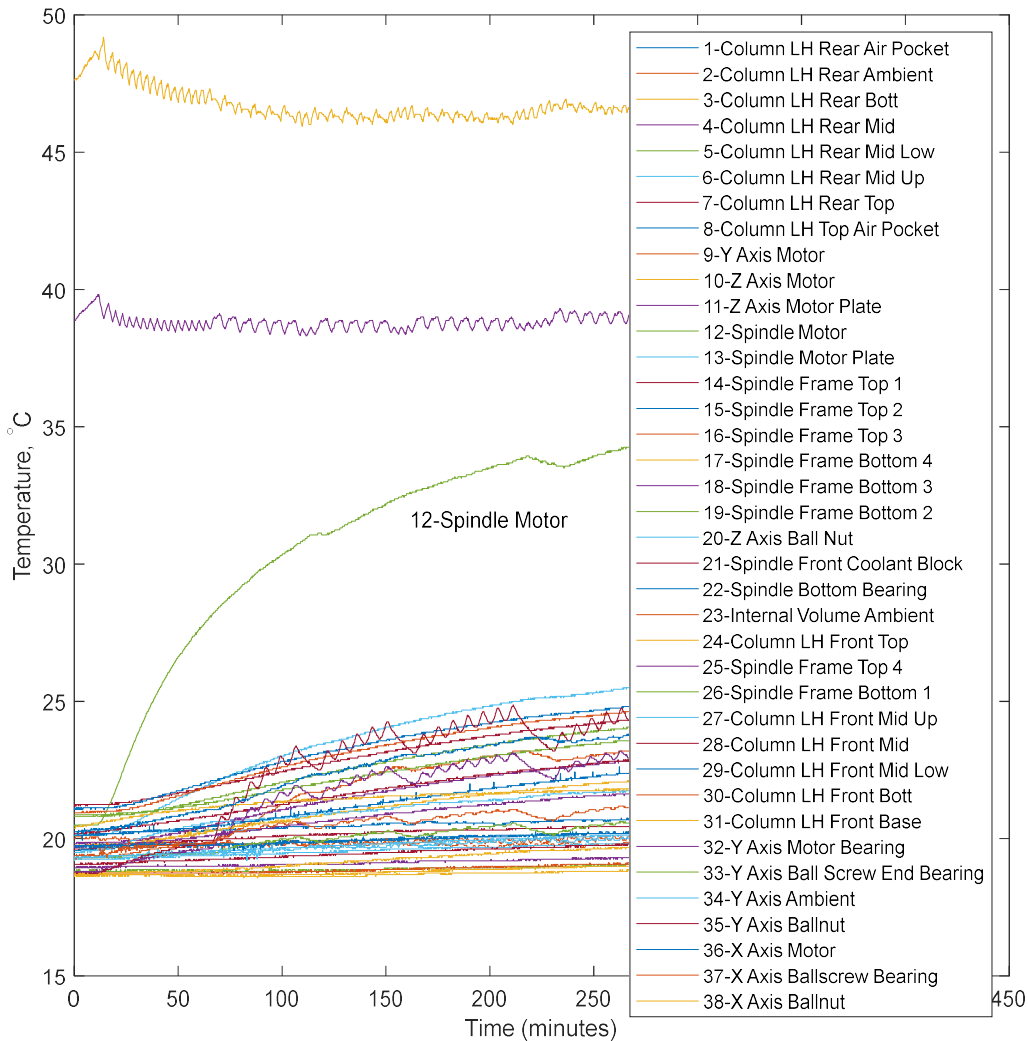


Figure 96 Legend used on following temperature graphs (unless otherwise given)

Figure 97 Shows a typical temperature profile of Machine A over a 21-day period in February. The main body of sensors is affected by the change in ambient temperature. However, it is clear that during testing certain other sensors are affected by induced heat. Figure 98 shows the motor temperatures for each axis and the spindle. Figure 99 isolates the areas around the Z-axis, which is affected by motion of the axis, but also the need to work against gravity whenever the machine drives are energised.

Figure 100 shows how the spindle motor temperature is affected with the spindle running compared to the ambient.

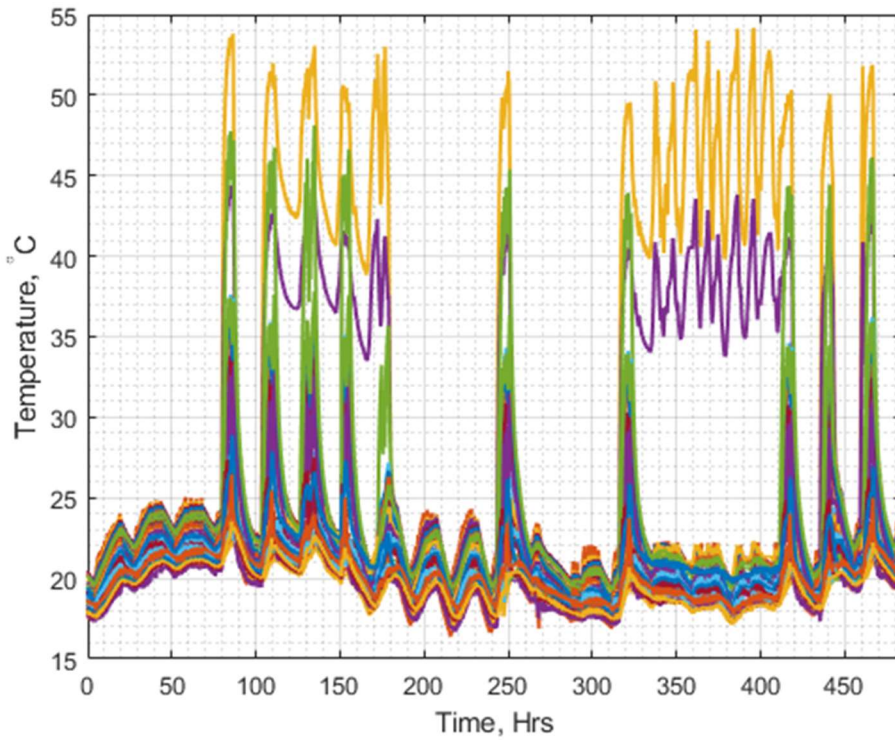


Figure 97 Temperature profile of machine over a 21-day period in February

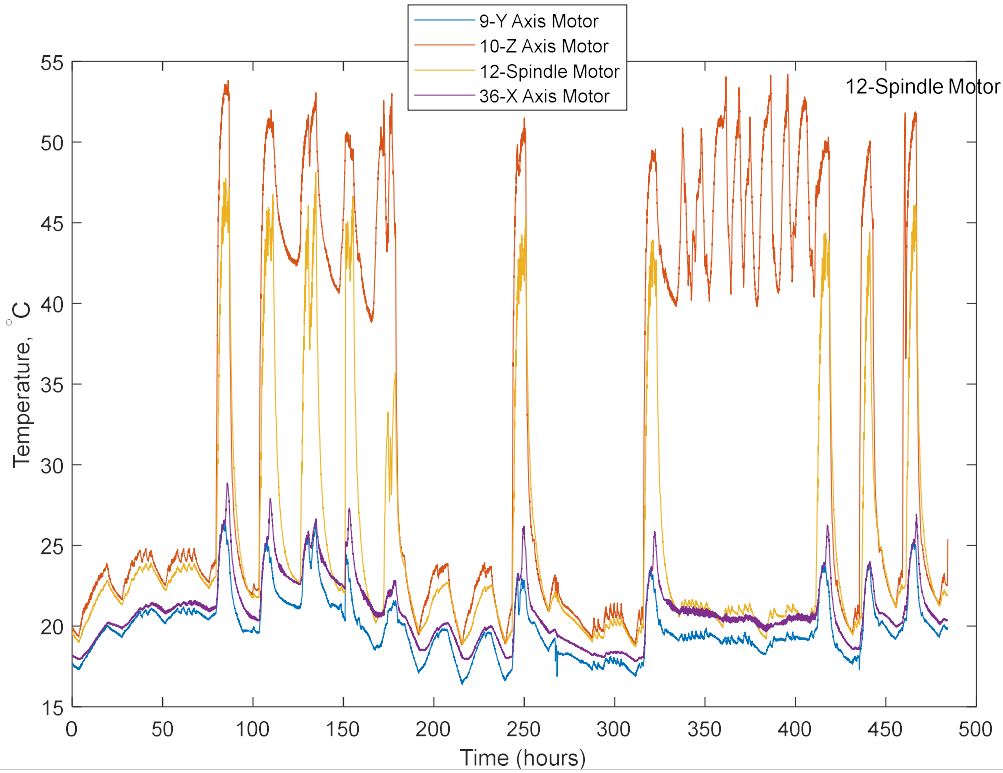


Figure 98 Comparison of axis and spindle motor temperatures

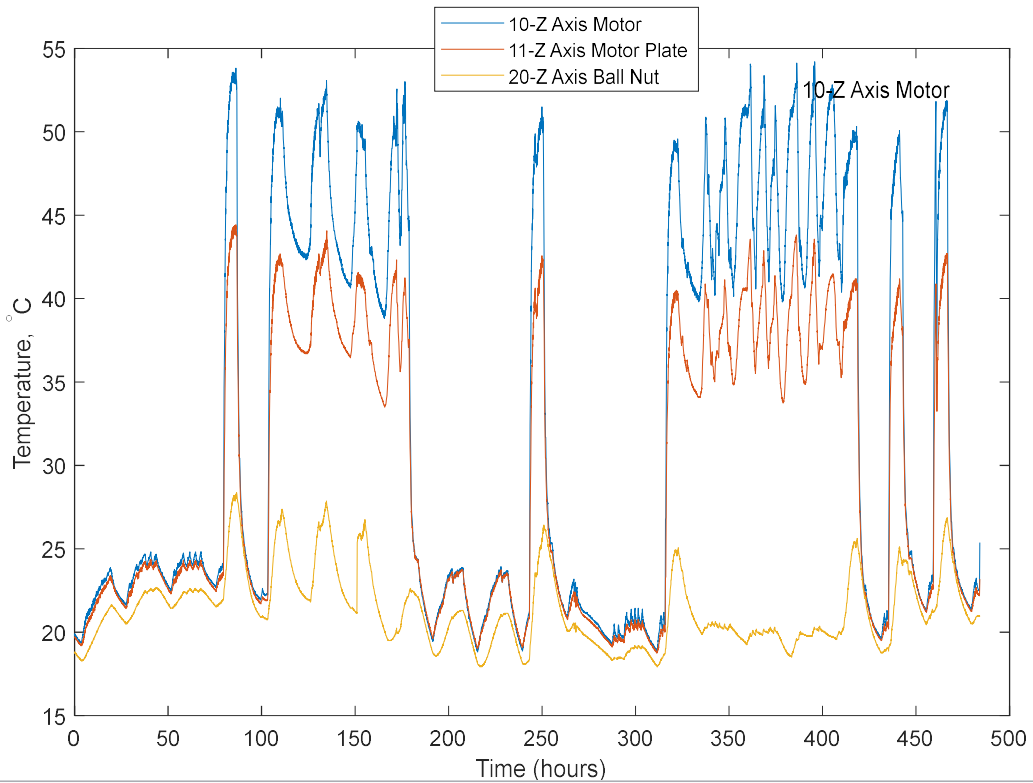


Figure 99 Comparison of different sensors on the Z-axis

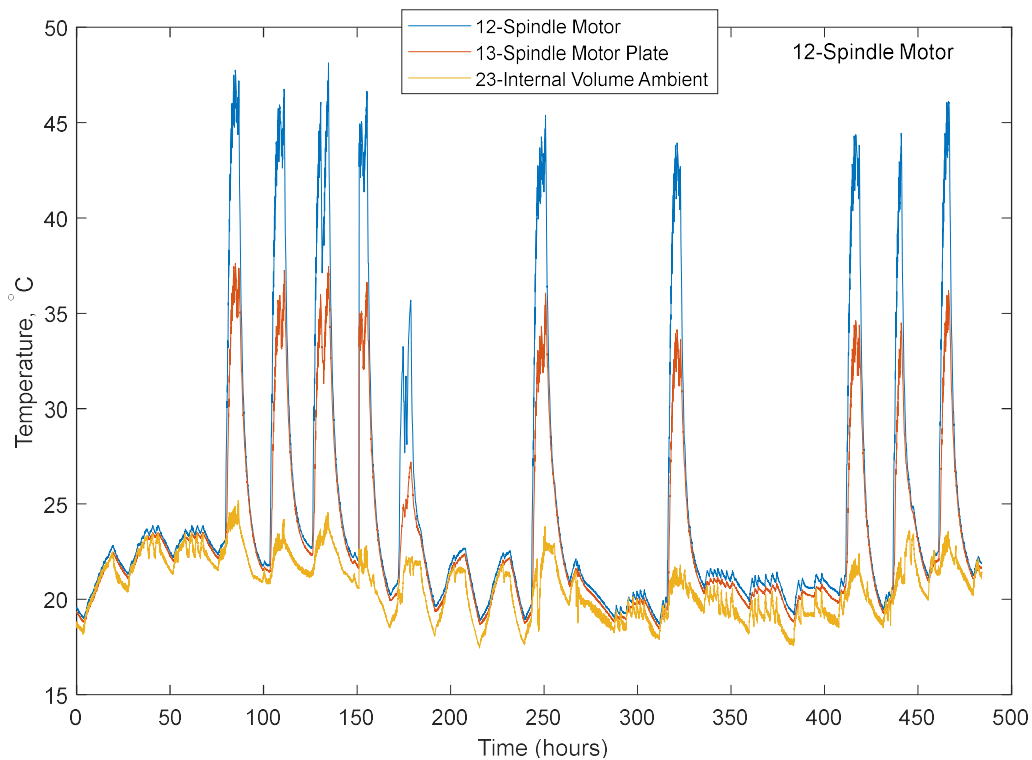


Figure 100 Comparison of spindle temperatures with ambient temperature inside the machine

The following subsections measure the same artefact in different states. The purpose of this work is not to create a new thermal model, which has been the subject of many PhD theses [95,96], but rather to give evidence of the effect of temperature when probing.

5.5 Temperature and probing analysis

5.5.1 Probing when the machine has just been switched on (cold state)

5.5.1.1 *Simulated machining from cold*

Figure 101 shows the temperature effect from three days of simulated machining tests. The areas of interest between the red lines, area A and area B are identical tests using the same parameters run on separate days. They show the rapid rise of the Z axis motor (yellow) and motor mounting plate temperature (purple), and also the spindle motor temperature (green). During the first hour of the test only probing operations are being conducted, the spindle motor temperature rise is due to the spindle orientation, although stationary, being held using the SPOS command. Small, high frequency commands are being sent to the spindle, which is acting like a servo axis in the SPOS mode. This is something often overlooked when assessing the heat sources as the spindle is assumed stationary.

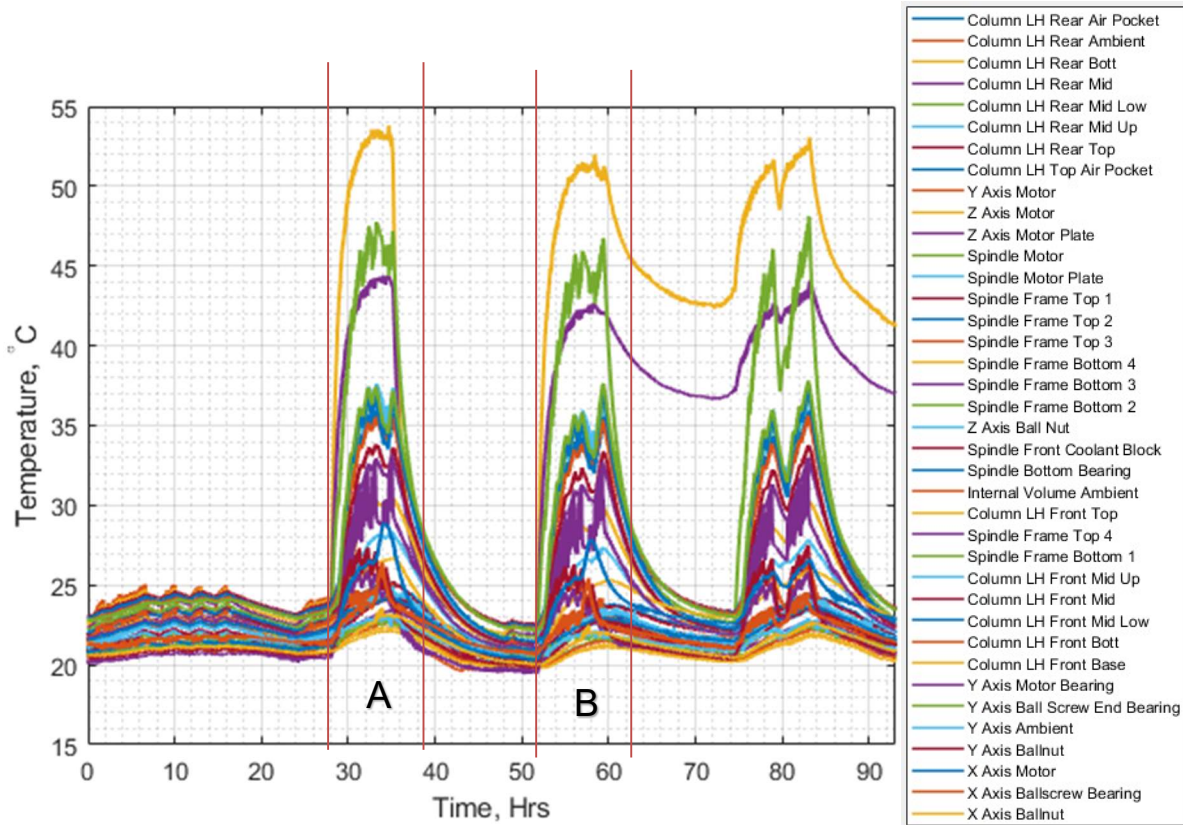


Figure 101 Three-day graph of temperature (simulated machining)

After the first hour has passed the simulated machining cycles begin, as can be seen at hour one in the temperature graphs in Figure 102 and Figure 103 Repeat of test the following day (area of interest B)Figure 103. Spindle temperatures rise further as the spindle is now rotating and axis motors start to generate heat.

When looking at the matched error graphs, the magnitude of the errors and the Y-axis movement with no corresponding heat source from the Y-axis indicate a bend in the head rather than expansion of the scales. The largest error is in the Y axis of 70 μm with the subsequent error in Z of 50 μm associated with bending rather than scale expansion.

A comparison of the graphs from area A and area B shows results repeatable to within 10 μm .

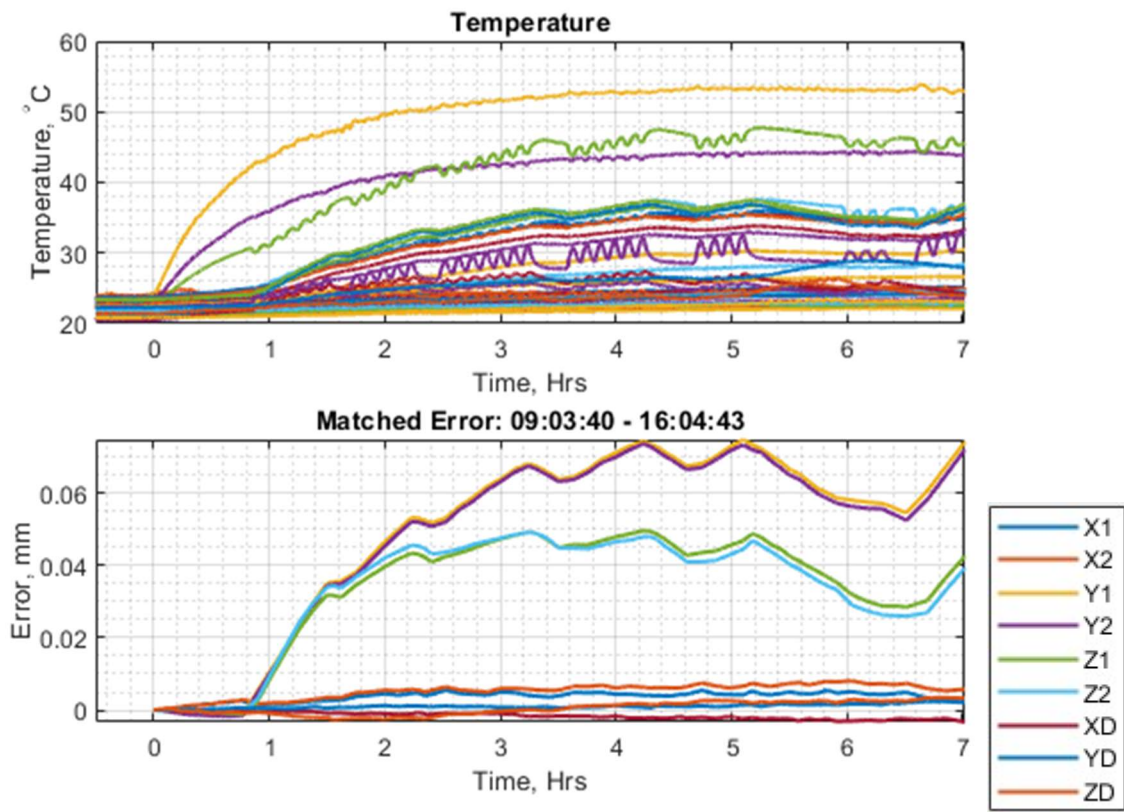


Figure 102 Probing from cold start (area of interest A)

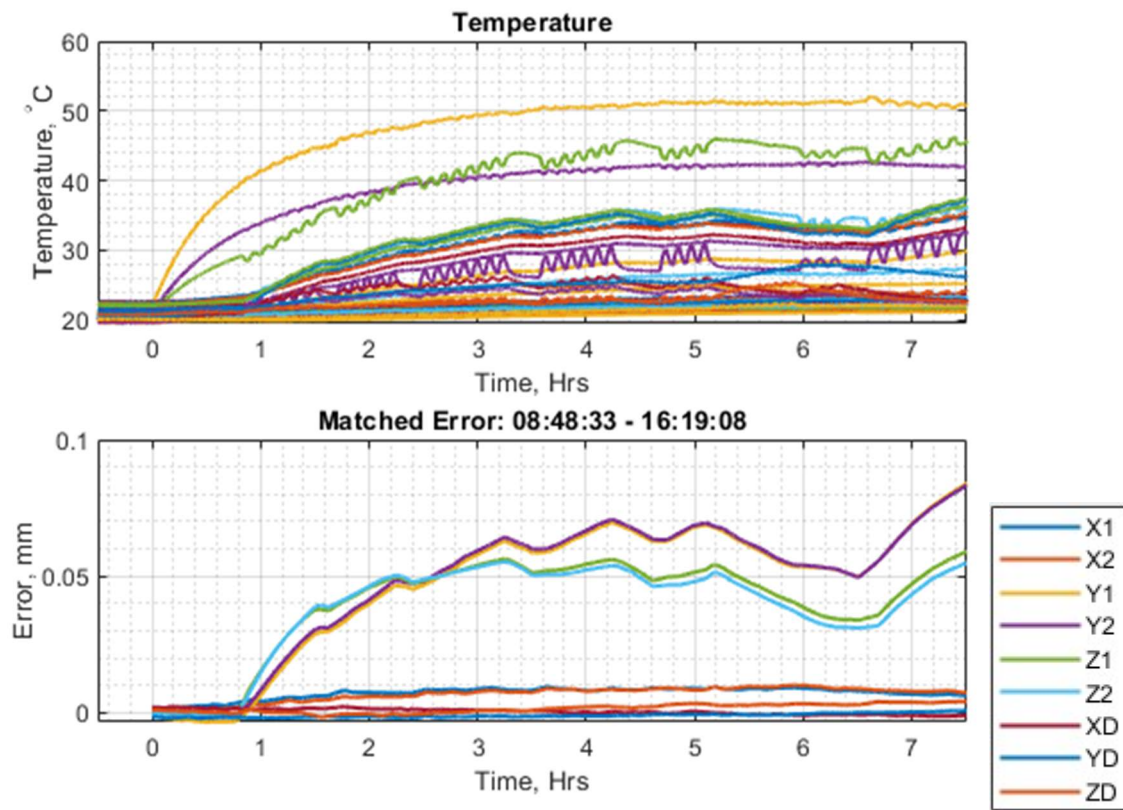


Figure 103 Repeat of test the following day (area of interest B)

5.5.1.2 Test performed on Machine B

For comparison, the same test was run on another machine, Machine B. Unlike Machine A, this machine has rotary encoders on the motor, rather than linear scales, as position feedback. The axis heating for this machine was investigated using a laser interferometer in section 5.4.1. In that case there was a uniform duty cycle. In these experiments the representative velocity spectrum duty cycle shows how rapidly the errors can change. In the Z-axis there is an error difference of over 50 μm and this is over 190 mm, rather than the 330 mm for the laser test, where the maximum displacement between the extremes of travel was in the order of 60 μm .

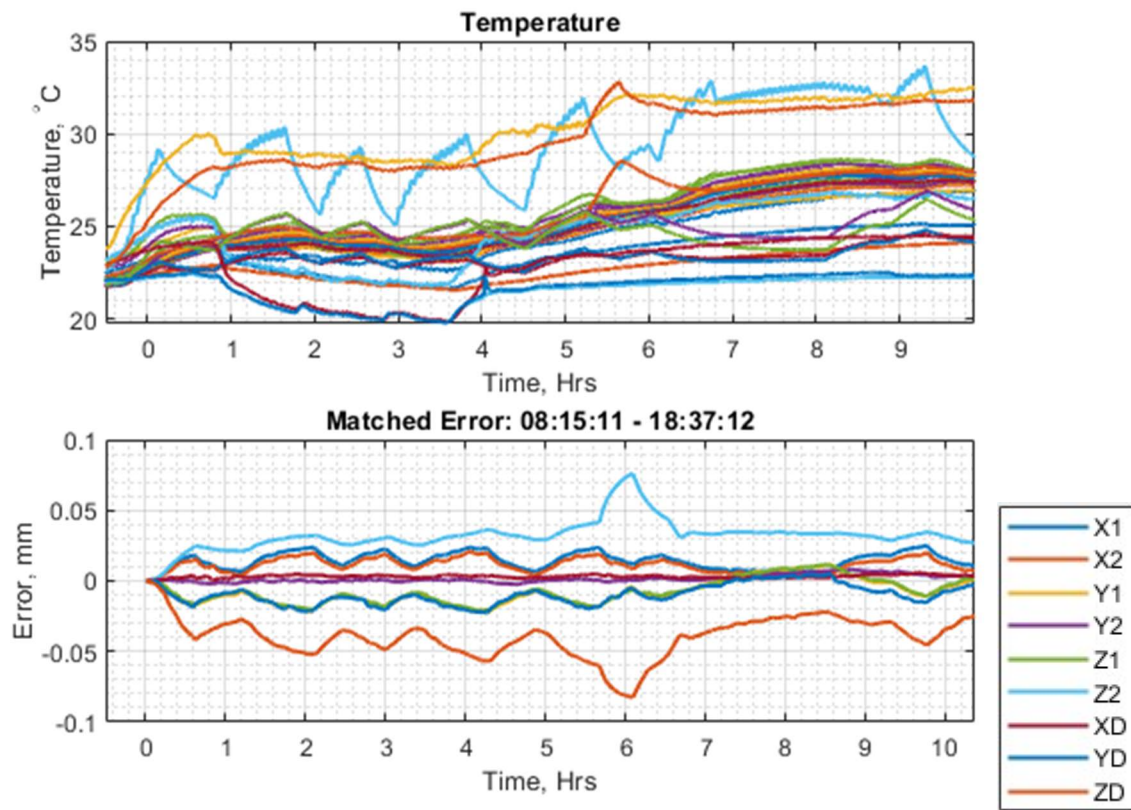


Figure 104 Probing from cold on Machine B

Of particular concern is the significant change in the Z-axis error over the first thirty minutes. Figure 105 shows that over $40\ \mu\text{m}$ of error is generated between Z1 and Z2. This magnitude is not evident at all on the machine with linear scale (Figure 102 and Figure 103).

Converseley, Figure 106 shows that Machine B has relatively low error in the Y-axis direction compared to Machine A. This is because the more open structure of the head carrier does not tend to distribute heat and therefore bend in the same way, reducing the effect in the Y-axis direction.

These results show the validity of using probing to gather data regarding distortion due to temperature change.

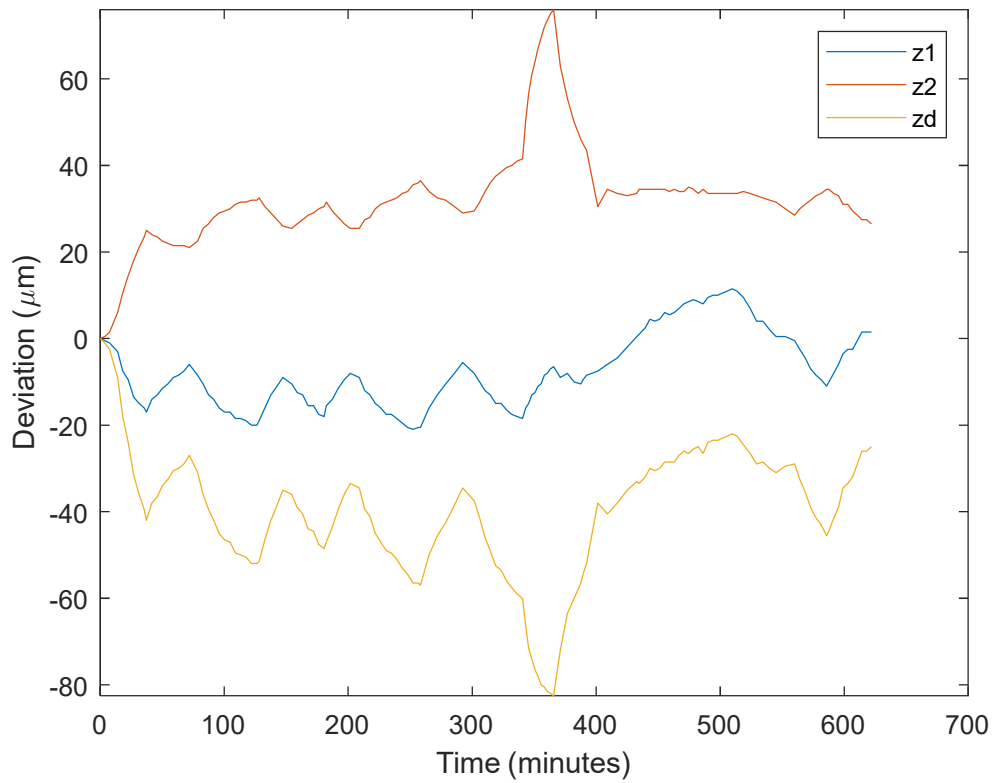


Figure 105 Z-axis error on Machine B (from cold start)

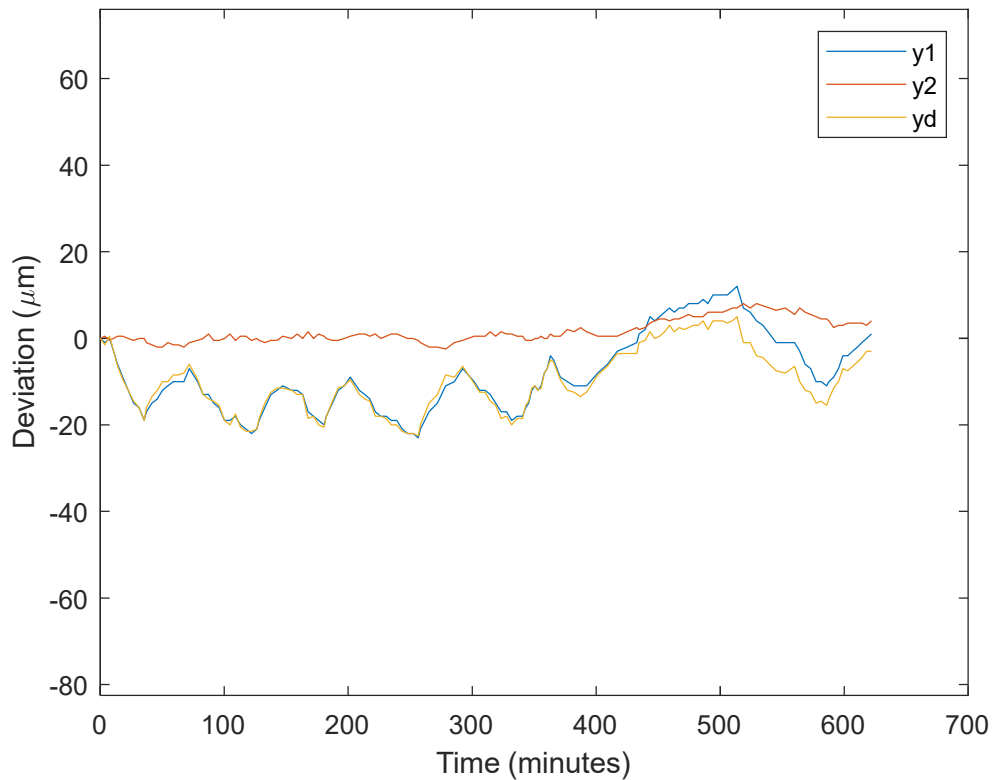


Figure 106 Y-axis error on Machine B (from cold start)

5.5.2 Probing with only machine self-warming

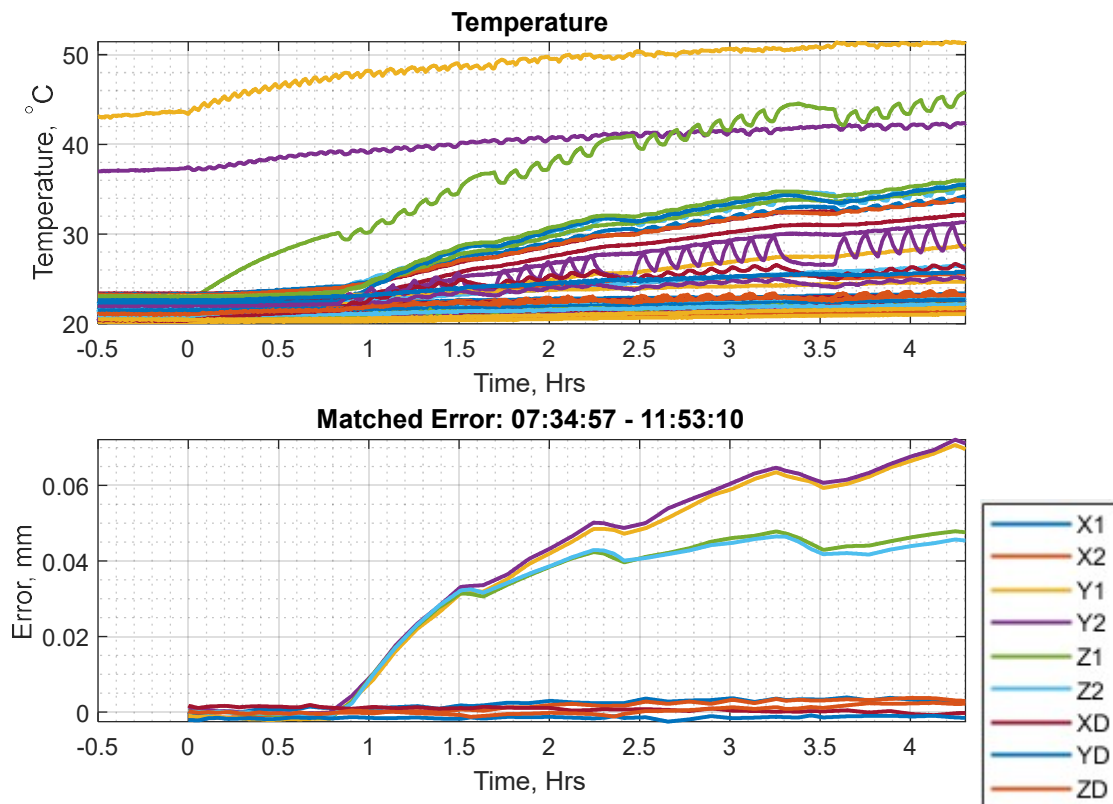


Figure 107 Results for Machine A with Z-axis self-heating already completed

The second half of the test was interrupted because of a probe battery failure. As a result, the machine re-datumed, giving the graph in Figure 108. The data can be partially reconstructed, with Figure 109 showing an example in the Z-axis with an offset applied to the second part of the data. The gap when the machine stood idle waiting for a battery change is very clear. However, this is only an approximation, so if the data were to be used for thermal mapping, the whole test would need to be re-run to reduce uncertainty, rather than the approximation in Figure 110.

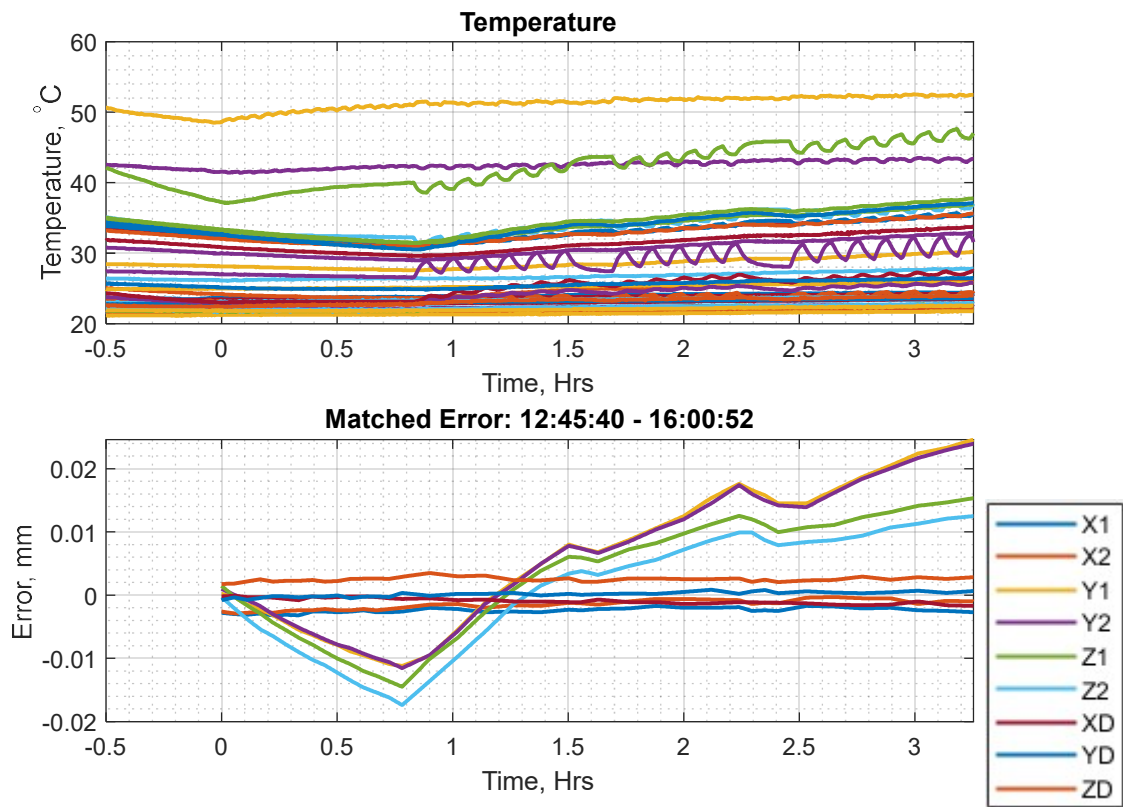


Figure 108 Second half of the test (failed)

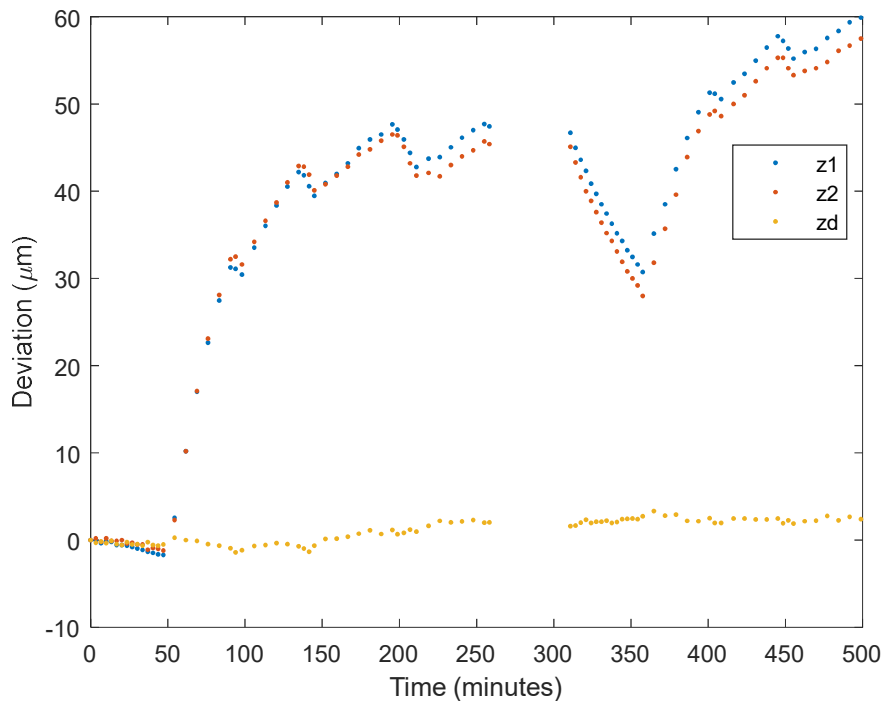


Figure 109 Approximated reconstruction of the test data showing missing data

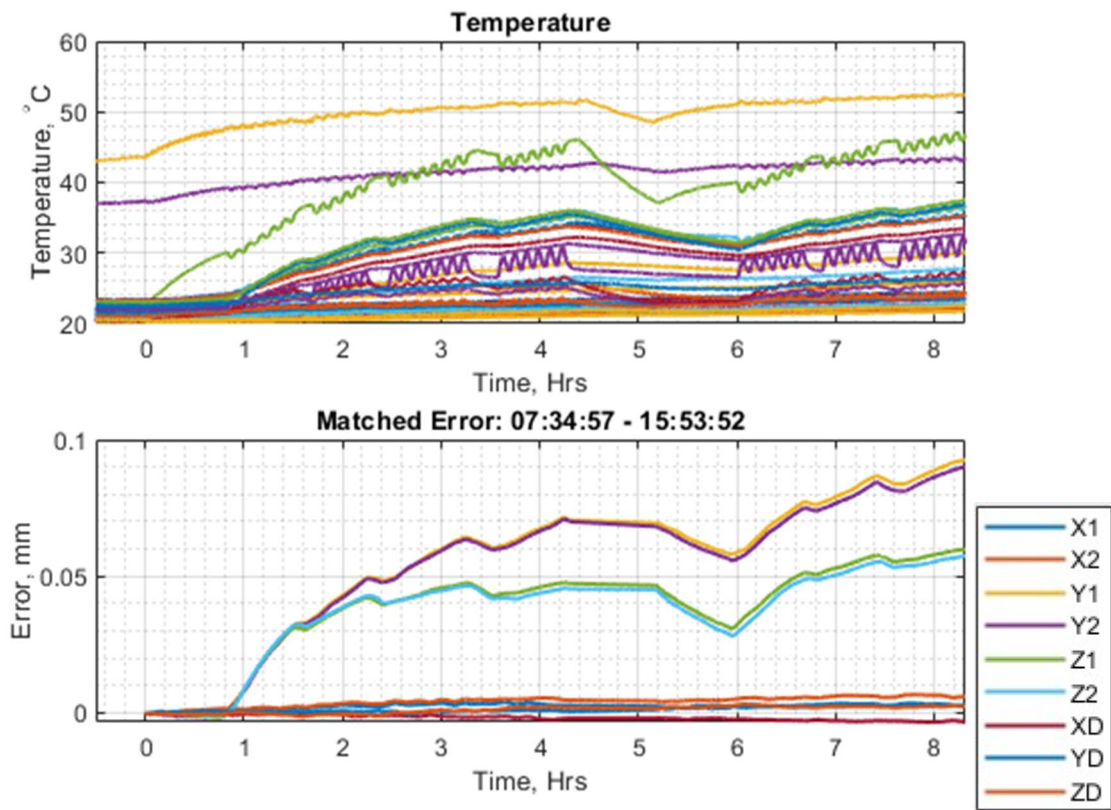


Figure 110 Approximated reconstructed data

5.5.2.1 Test performed on Machine B

For comparison, the same test was run on another machine, Machine B. Unlike Machine A, this machine has rotary encoders on the motor, rather than linear scales, as position feedback. The temperature peak seen at around 5.7 hours in Figure 111 arises from additional excitation of the Z-axis. It can be seen that this affected position between Z1 and Z2 due to ball screw expansion by 55 μm . Clearly, this will affect the reliability of probing results on this machine.

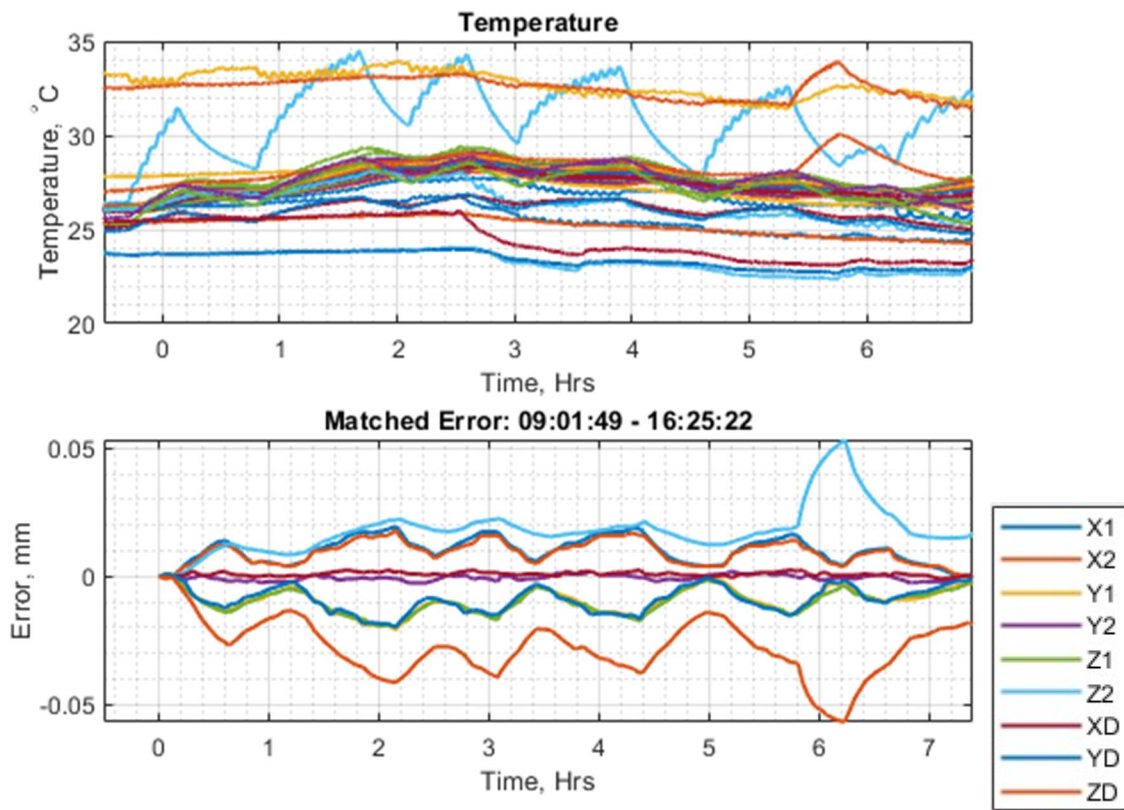


Figure 111 Machine B simulated cycle after self-heating

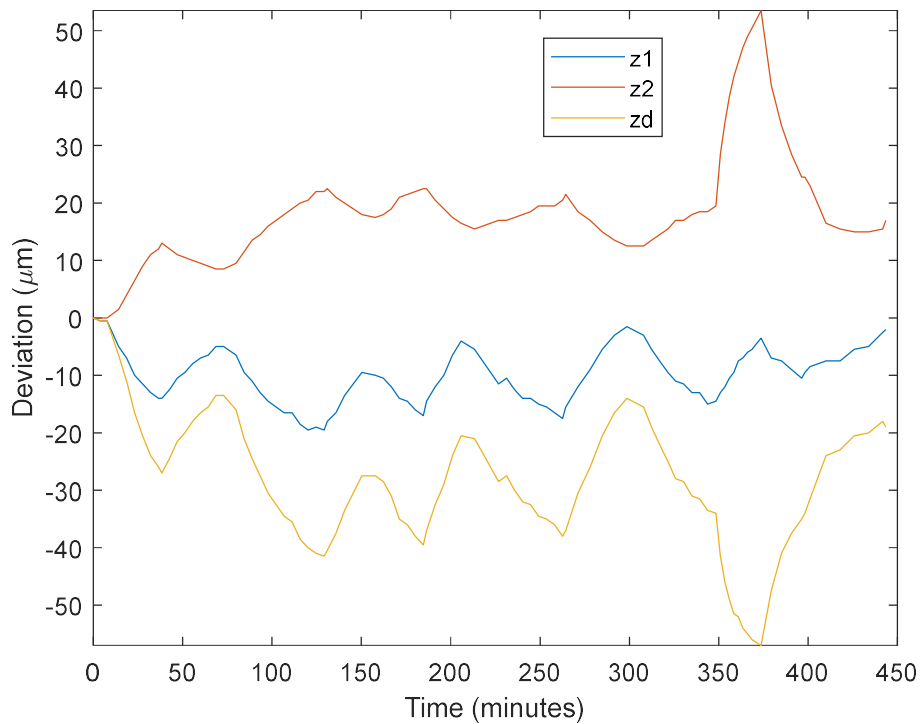


Figure 112 Z-axis error on Machine B

5.5.3 Probing influenced by axis and spindle heating

The test shown in Figure 113 was run to show the effect of a single axis heating up on Machine A. During axis heating, the axis under test is excited by driving the axis through its full length of stroke several predetermined times. Simulating the heating that would occur within production but under controlled conditions. As discussed in section 5.5.1.1 there is some heating of the spindle from the machine holding the probe on the SPOS, which then conducts into the carrier head. Figure 114 shows selected sensors in more detail.

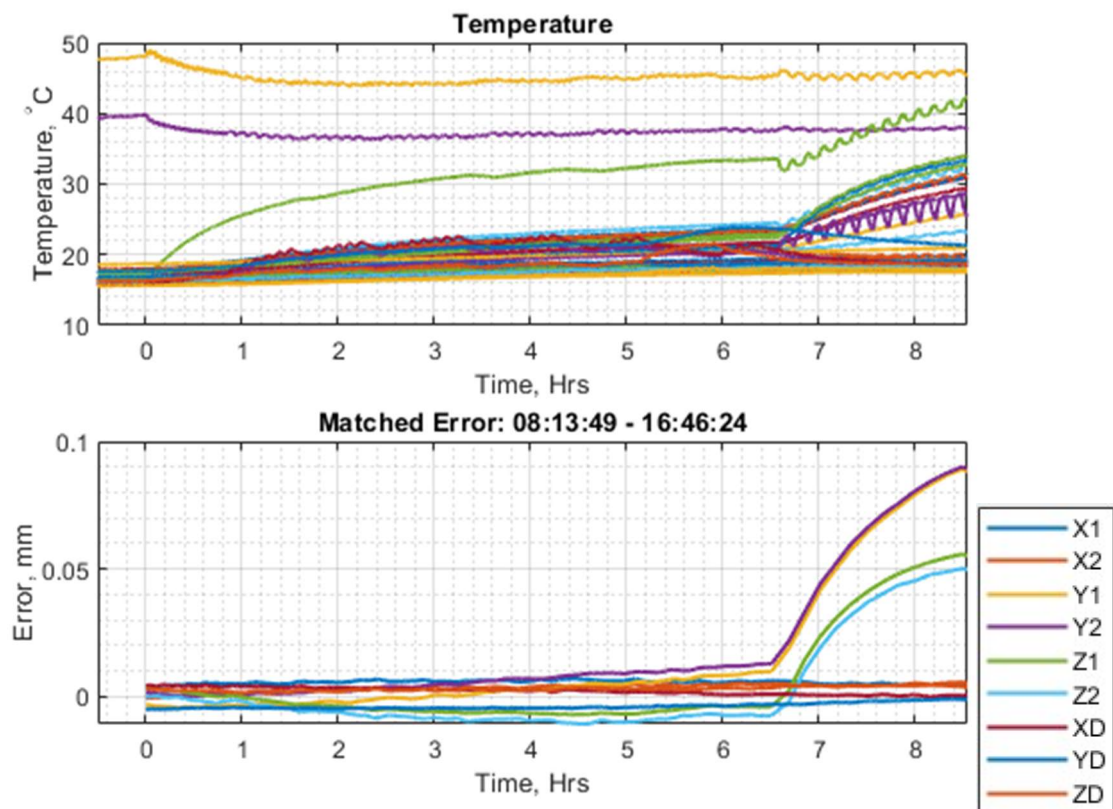


Figure 113 Effect of axis heating only (spindle only running from 6.5hours onwards)

Figure 115 shows the machine, which had its drives energised two hours before testing, being run without the spindle (command S = 0). However, again this data was to some degree contaminated from the SPOS command being active to prevent the probe rotating. This, in itself, induced a rise of 15 °C. This is 10 °C lower than in the full pseudo-machining cycle but will still have an effect. Probing errors of up to 10 µm are shown in Figure 115 from this spindle effect and any heating of the axis.

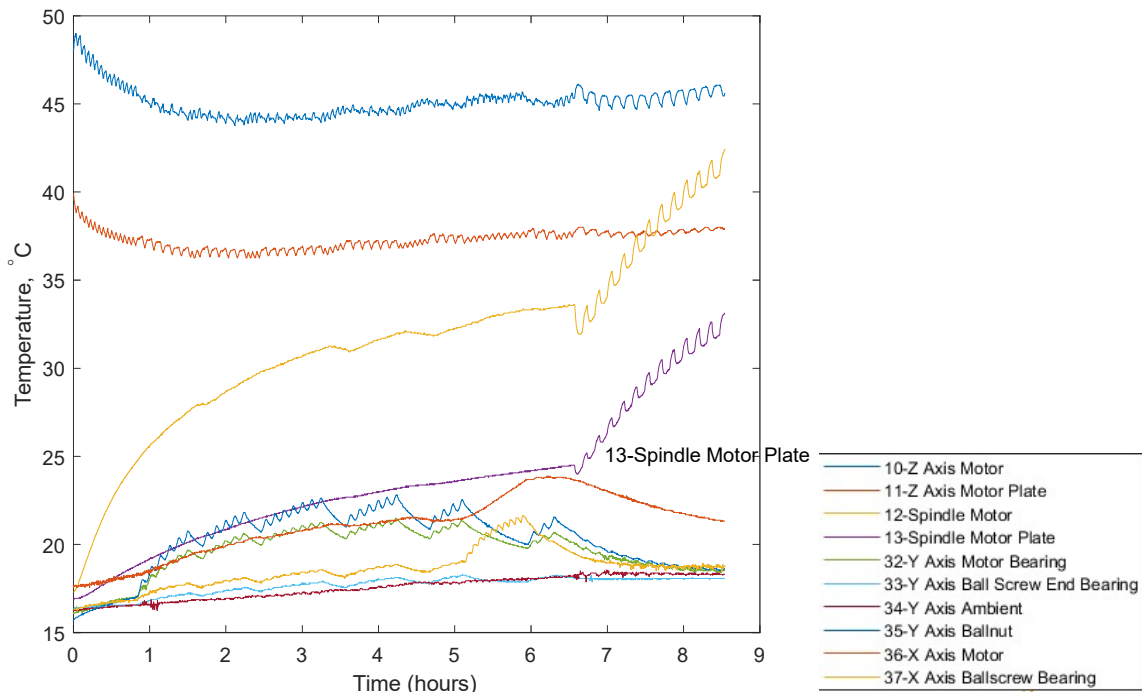


Figure 114 Selected temperatures during “no spindle” test

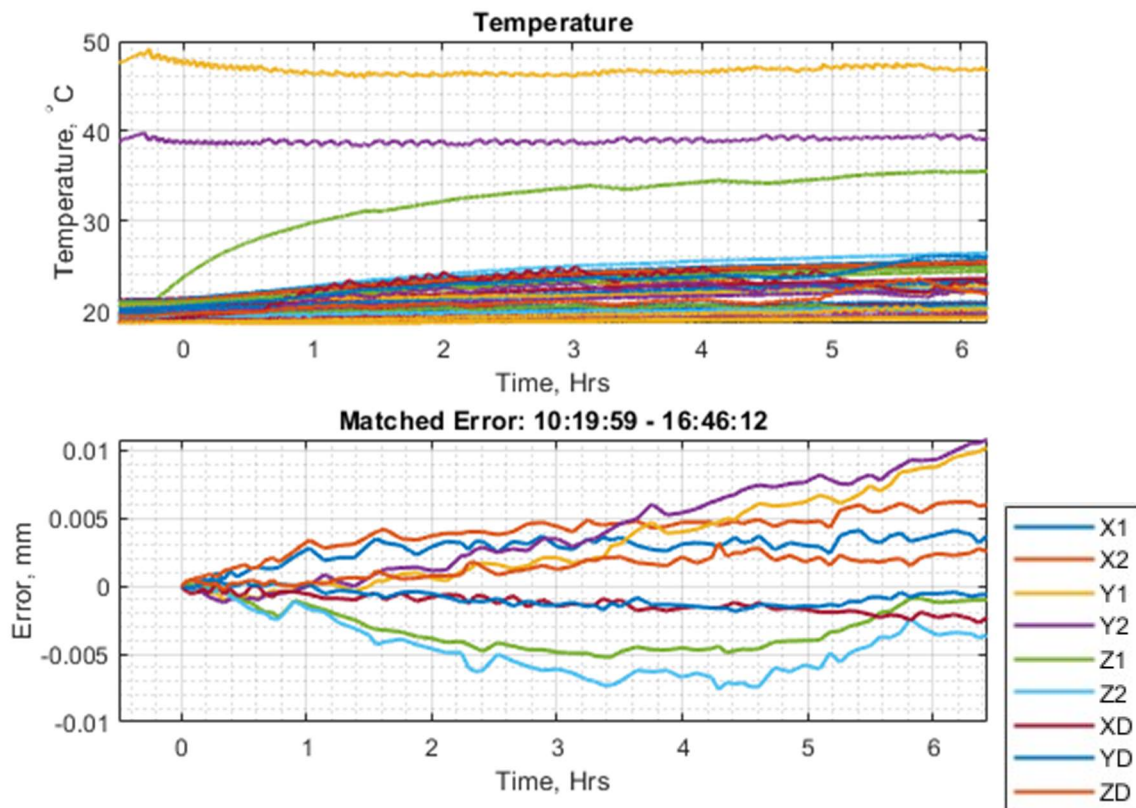


Figure 115 Simulated cycle without spindle

5.5.4 Probing after simulated machining cycle

Figure 116 shows the effects of the machine executing the generic machining cycle. Axis movements are performed in all three axes with the spindle rotating to generate heat typically seen in this kind of machining operation. Different feed rates, spindle speeds and tool-change operations are incorporated to provide a realistic cycle, which is evident from the shape of the temperature graph and the matched error from the probing. The error plot shows almost 100 μm in the Y-axis direction in the second half of the test where the spindle is run at a higher speed.

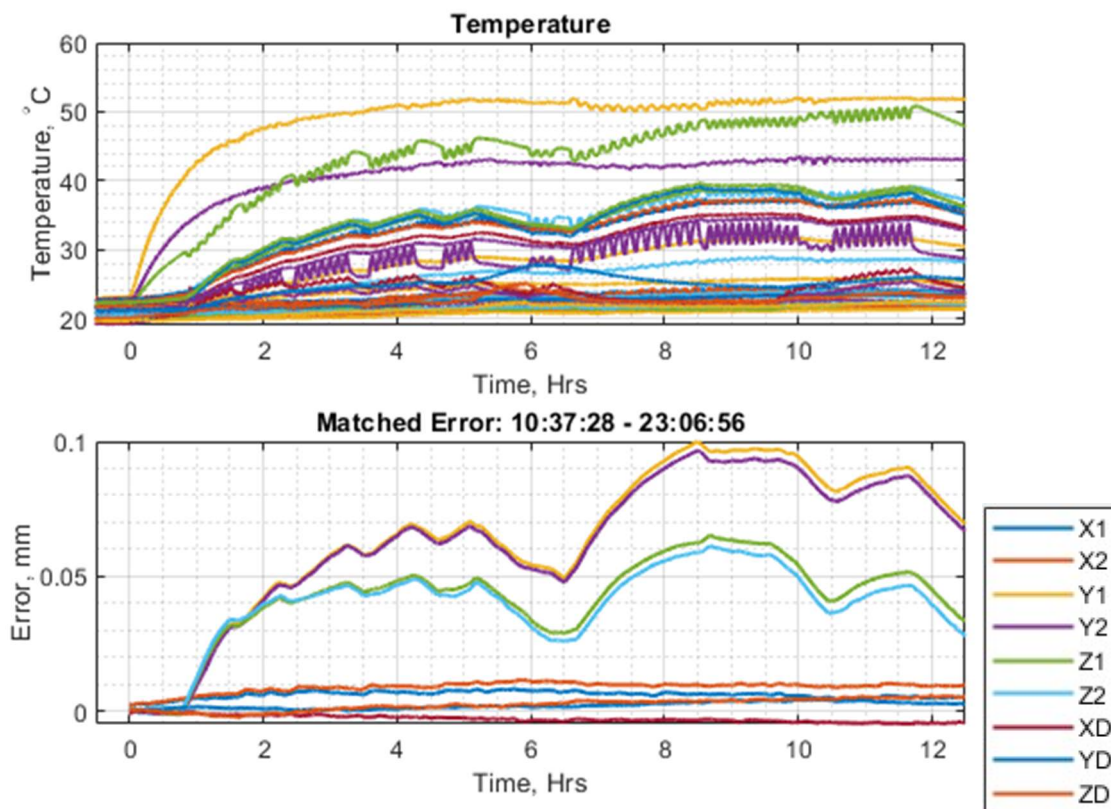


Figure 116 Simulated machining cycle

5.5.5 Probing after machining cycle with coolant

The test was run again to see if there would be any impact from the coolant. The cutting fluid itself is not chilled on this machine, but the action of jetting the fluid over the part and machine has the effect of drawing heat away. Comparing the error plots in Figure 116 and Figure 117, it seems clear that the Y-axis error has been reduced by around 40 μm . While at first glance this appears positive, since the accuracy of the machine has improved, it does show the variability (lack of reproducibility) that arises from different machining strategies. This only serves to reinforce the need for the foundational work of understanding the thermal behaviour of a machine before using it for measurement tasks.

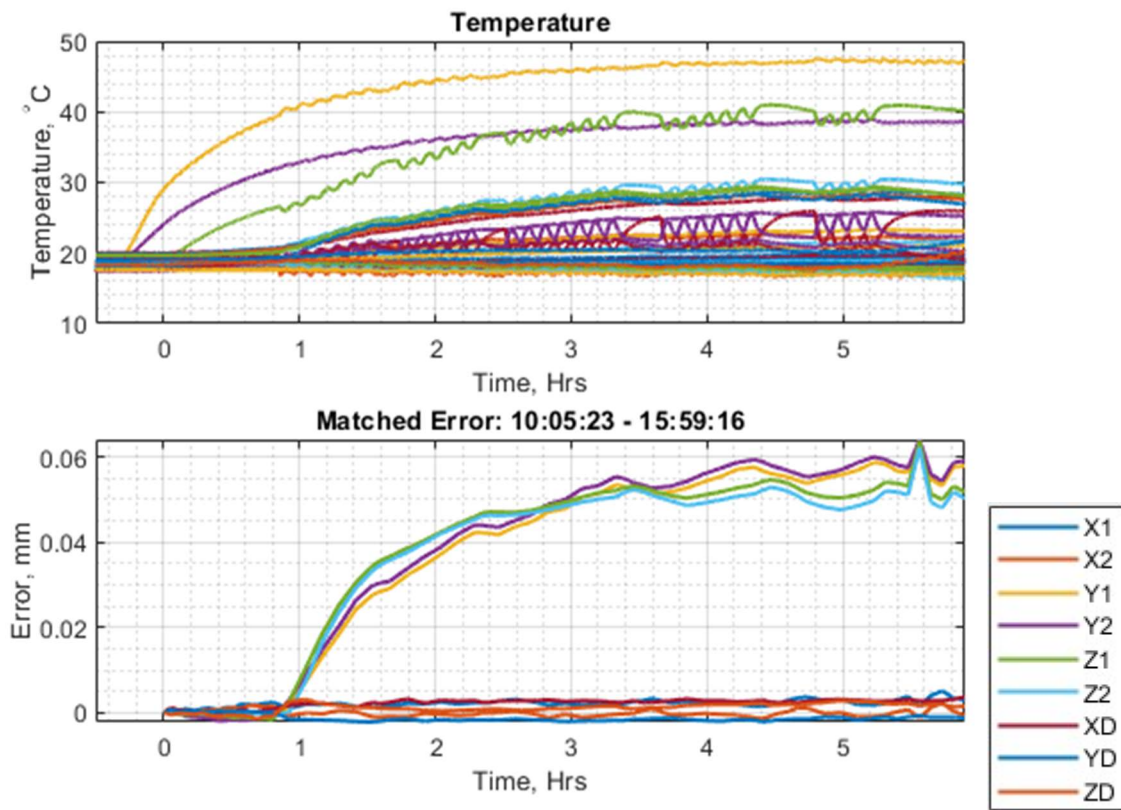


Figure 117 Machining cycle with coolant

5.6 Discussion and summary

This chapter has devised and undertaken a broad range of tests. A set of tests was used to evaluate the repeatability of the spindle-mounted probe, repeatability when moving a distance equivalent to a tool change and finally of a tool change itself.

An investigation into the effect of cutting fluid was devised and conducted. It became clear as the work developed that more controlled methods of measurement were needed than just using the machine in “wet” mode. Although some elements were inconclusive on the tested machine, the learning that contributed to this methodology can now be conducted on other machines to be able to compare results with different probe types, viscosity of fluid, etc.

Similarly, the influence of the profiles from the machine geometry data (XM60 laser measurements) led to a new test to establish the effect of locating a calibration ring or datum position on an axis with geometric errors. The chosen machine did not have large errors, so the efficacy was not fully proven, but the process developed can now be rolled out to other machines as and when time and resources become available.

The flexibility of the parameterised programming method that has been created came into its own when trying the different probing cycles with different feed rates, spindle speeds, durations, travel distances, etc.

Findings included the effect of holding the spindle in position orientation (SPOS) mode on heat generation from the spindle. It had been assumed that when probing there was little or no heat generated, but this was clearly not the case and caused errors of a few microns just from extended probing cycles.

Finally, and perhaps not unexpectedly given the strength of the research group on thermal errors, it became abundantly clear that the thermal problem dominated much of the work. In some cases (Machine A spindle heating, Machine B axis heating) the magnitude was clearly the issue at up to 80 μm . However, the more complex problem was the contamination of other data sets, even with the most cautious approach to establishing thermal stability or inducing temperature rises or gradient. The effect of coolant on the temperature and resultant error profile also provided interesting insight into the effect on reproducibility of probing results if different cutting fluids are used in different ways on a machine.

Chapter 6 Conclusions and further work

6.1 Discussion

This project was borne from experience in industrial settings where on-machine probes were found to be either unused or not well understood beyond very limited purposes. While many machine tool manufacturers sell machine tools fitted with probes and readily advertise the ease of which automation can take place using probing systems, the truth of how well the technology is adopted very much depends on what the end user is trying to achieve.

Spindle-mounted workpiece probes, even when uncalibrated, can give exceptional repeatability, to a degree that is often beyond what is realistically needed for a particular machine operation. However, under some conditions even a calibrated probe used in what is perceived to be the correct way can give varying degrees of accuracy.

This is because users will often look at the repeatability of the probe itself without considering the whole system including the machine tool, its own measuring system and influences from the surrounding environment.

A machine tool using rotary encoders may very well be able to position and measure to within 5µm but as soon as the axes start to be excited by machining operations the ball screws heat and due to expansion, the thermal datum shifts and the distance between two points on the axis changes, meaning any measured results will be compromised (Machine B). Whereas a machine with a closed loop measuring system for the axes (Machine A) may take out any thermal expansion of ball screws, but due to the heat generated by spindle and axis motors bending of the structure will still cause inaccuracies. The case studies in Chapter 5 clearly provided evidence that assumptions about the performance of a machine should not be made, giving value to the proposal in this dissertation that a more formalised approach to thermal evaluation is needed.

One method to deal with thermal issues is to continuously re-datum the part on the same feature thus removing any thermal deviation. But this is an interruption to the production process so some consider this should only be used in high accuracy, high value components. If looking at the machine represented in Figure 67 the thermal effect is changing so rapidly that a user would have to be constantly re-datuming, having a massive negative impact on productivity.

This research has also, through informal conversations, uncovered a widespread misunderstanding of probes and their use, from the operators who do not “trust” the measurements purely because they are scared of getting parts wrong to the operators who blindly believe every result the probe outputs, even when they seem implausible. Having worked in various positions where probing was unavailable, the author has

personally embraced the use of probing and found it to be an invaluable tool within the machining process if used correctly. When machining parts from stock, being able to automate datum setting for first and second operations within the program leaves personnel free to pursue more highly skilled activities than just setting part datums. Because the machines have been calibrated for geometric errors, it is understood what the machines are capable of achieving. Some machines have very good geometry, repeatability and thermal stability and have had machined artefacts compared against CMM results, they have been benchmarked and are tested on a monthly basis. The probe is calibrated at the start of every working and the traceability and procedures that are followed give us confidence in probing results that are obtained from measurements.

Through the measurement of different machines within this research and using data from previous machine measurements it has been concluded that not only the machine geometry, but also thermal errors should be quantified if more advanced probing routines are going to be utilised going forward. A machine in a temperature controlled environment may be thought of as being unaffected by environmental thermal issues but the heat generated by the motors and axes still need to be taken into consideration as seen in section 5.2.1.2 and 5.3.1.1, where the heat from a spindle motor holding in the SPOS command could cause 3 μm of error or the chilled air caused a very accurate glass scale to contract (Figure 9) inducing a $\pm 3 \mu\text{m}$ cyclic error.

However, it is evident how time-consuming the measurements can be. Axis geometry measurement may have reduced significantly to less than 1/2hr for a typical 750mm length axis, but thermal measurements can easily take many hours or even days. Taking a methodical, pragmatic approach where failure modes, and tolerances set on the root cause mechanisms, are related to the modes of operation that are required allows a company to get confidence in the probe for the purpose they wish to use it. At the same time, the “lookahead” allows the company to have the ambition to adopt new functionality if they move on to the next level of testing, or the results that come back are more positive than they had expected.

6.2 Summary and conclusions

Overall, the project has broadly met its stated objectives. It set out to understand the influencing factors that cause failures or create uncertainties in on-machine probing (Objective 1.) This was achieved through the literature review, the scoping sessions with industry and academic partners as part of the FMEA process and during the work undertaken to convert the large amount of feedback relating to causes of failure into an FMEA with a few clear failure modes and effects. Of particular interest was the consideration of commercial impact (lost production time) from either probe failure or from the time taken to conduct the tests that allow the probe to be used.

Breaking the use of machine tool probes down to the three main areas (Evaluating the machine, part setting and in-process/post-process) enabled greater clarity of thought

and “big picture” rather than concentrating too much on any one of the modes of operation. Eleven subcategories then came under this top layer (section 3.2). However, it is not anticipated that this list is exhaustive. There are definitely subcategories a third level down, such as setting rotary axis parameters as part of “evaluating the machine”, but this first step towards breaking the process down into individual value streams for probing has met Objective 2 and will lead to more uses being documented over time. The feedback from those participating in the task was that beforehand they just “used the probe.” Now the different modes of operation can be viewed and treated separately.

Initially, Objectives 3 and 4 were intended to be the separate Chapters 4 and 5; one chapter would be theoretical to create a framework and the other would be practical experiments to validate the process. In fact, the framework was taken down the road of concentrating on the accuracy issues with a machine carrying a probe. This is partly because of the interests of the research group, but also because the FMEA indicated that these were some of the least well understood aspects. Yes, the battery needs to be regularly replaced, but from a research point of view asking how to begin the journey towards traceable on-machine measurement is a more exciting challenge to investigate. As such, the decision flowcharts in Chapter 4 are only part of the framework. The decisions in that same chapter on what to measure and with which tools forms part of the framework too. However, the development did not stop there; testing of the “expected” factors in Chapter 5 found many other things that needed addressing, with thermal influences and controller nuances providing additional challenges. This has helped to build a set of tests (Appendix A), summarised in section 5.6, that can be deployed as part of the framework, with foreknowledge of likely pitfalls and measurement expectations.

Perhaps just as importantly, the research showed the importance of the parameterised programming methodology that was adopted. This dissertation contains less than a tenth of the data gathered from the machines by varying the duty cycles when probing. This would not have been possible with traditional “hard-coded” part programs. It has already become the de facto standard in the research group for our laser measurements, and now is being extended to evaluation by on-machine probing of artefacts.

Finally, testing of several machines showed that geometric errors do play a role, while monitoring them with current tools raises some issues of data quality versus time required. The probe has excellent repeatability, the machines tested also had very good repeatability and the absolute geometric error was both measurable and controllable. Ultimately, though, the unpredictability of thermal behaviour is likely to cause the greatest problems for on-machine probing, with a full understanding being required for reproducibility of measurement results from a machine tool.

6.3 Further work

On-machine probing is a vast subject that this research project has only just scratched the surface of. The following future work arises from this dissertation, listed in order of importance.

6.3.1 In-depth investigation of geometry and thermal effects

Further work would look at how the machine tool geometry, and changes due to thermal effects, affects more of the standard measurements. Projects are already underway into the use of high-fidelity digital twins to be able to understand the influencing factors for machining.

FW1: The output of this research work is to conclude that the tools be developed to provide “virtual” on-machine measurement.

Similarly, thermal modelling of machine tools has been a subject of research for decades and continues to fill the pages of esteemed journals, due to its complexity and the foreseeable improvements in newer self-learning modelling techniques. A complexity is making compensating actions during machining. However, probing is a measurement process and, as with coordinate measuring machines (CMMs), the data can be compensated post-measurement.

FW2: Thermal modelling for evaluating measurement uncertainty or applying correction to on-machine probing should be investigated.

6.3.2 Other machine configurations

While completing this dissertation a literature review revealed a paper by Sepahi-Boroujeni, Mayer and Khamenaifar [93] specifically investigating the repeatability of on-machine probing on a five-axis machine tool. This publication is evidence that research into this area of work is still ongoing. In fact, the publication deals only with a single five-axis machine with a horizontal spindle where the rotational axes carry the workpiece. From a probing point of view, the configuration where the spindle, and hence the probe, is carried on the rotary axes is more complex and will have additional uncertainties from the changing gravitational effects. This will become even more important if applying to articulated robots, where there is not a unique solution for the axes when measuring a single point.

FW3: Expand the research to more configurations of machine tools and robots

6.3.3 Expansion of the logic and “industrialising” the process

The work proposed above would refine the findings from this master’s dissertation, enabling the flow charts to be expanded to create a full strategy for all situations and all the identified causes of failure. For this to be industrially exploited a software tool, such as an expert system, should be developed with the end-user in mind.

FW4: Create a software tool suitable for industry to help inform the decision process

6.3.4 Tool measurement probes

This work has concentrated on the commonly available spindle-mounted workpiece probe. An in-depth piece of work is required to better understand the same influences on the machine-mounted tool measurement systems, their possible modes of operation and how they relate to the workpiece probes and to independent tool pre-setting systems.

FW5: Conduct similar in-depth analysis into the use of on-machine tool measurement probes.

6.3.5 Artefact

Gauge R&R is standard procedure when evaluating measurement processes for robustness on CMMs but is a less accepted method on machine tools. In many cases when an artefact is produced for such purposes it will either be exactly the same, or strongly mimic, the part being produced and usually be situated in the same position as machining takes place.

It has been noted through this research, there is a strong case for an artefact that could be used on multiple machine configurations to establish probe capability.

FW6: Design and manufacture an artefact for probe capability gauge R&R on machine tools.

References

1. Canadian Measurement-Metrology Inc. (2021). *The History of Coordinate Measuring Machines* | CMMXYZ. <https://blog.cmmxyz.com/blog/the-history-of-coordinate-measuring-machines>
2. Renishaw plc. (2021). <https://www.renishaw.com/en/sir-david-mcmurtry--42054>
3. Renishaw plc. (2021). <https://www.renishaw.com/en/about-renishaw--6432>
4. Rolls Royce plc. (2021). <https://www.rolls-royce.com/contact-us/rolls-royce-headquarters.aspx>
5. de Sausmarez, s. (2014). Heritage Concorde. <https://www.heritageconcorde.com/concorde-olympus-593-mk610-engines>
6. Blum Novotest. <https://www.blum-novotest.com/en/company.html>
7. Marposs. <https://www.marposs.com/eng/address/united-kingdom>

8. Heidenhain. https://www.heidenhain.co.uk/en_UK/products/
9. M&H. <https://www.hexagonmi.com/products/machine-tool-probes>
10. Future Market Insights (2018) "Machine Tool Touch Probe Market to Top US\$ 75.6 Bn by 2028 as Automated Manufacturing Processes Take Over" Market Research Report <https://www.prnewswire.co.uk/news-releases/machine-tool-touch-probe-market-to-top-us-756-bn-by-2028-as-automated-manufacturing-processes-take-over-690706491.html>
11. Renishaw PLC. (2018). *Discover RENGAGE™ technology – high-accuracy machine tool probes with market-leading performance* [PDF Brochure]. Renishaw PLC.
12. Longstaff, A. P., Fletcher, S., Parkinson, S. and Myers, A. (2013) The role of measurement and modelling of machine tools in improving product quality, *Int. J. Metrol. Qual. Eng.* 4, 177–184 DOI: 10.1051/ijmqe/2013054
13. ISO 230-10:2016(en) Test code for machine tools — Part 10: Determination of the measuring performance of probing systems of numerically controlled machine tools
14. Forbes, A. (2006) Measurement uncertainty and optimized conformance assessment, *Measurement* 39, 808–814
15. BIPM, IEC, IFCC, ISO, IUPAC, IUPAP and OIML (2008) Guide to the Expression of Uncertainty in Measurement (International Organisation for Standardisation, Geneva)
16. BS EN ISO 14253-1:2017 Geometrical product specifications (GPS). Inspection by measurement of workpieces and measuring equipment. Decision rules for verifying conformity or nonconformity with specifications
17. VERMA, M. R. (2016). *An Investigation Into Enabling Industrial Machine Tools As Traceable Measurement Systems* [PhD Thesis, The University of bath]. https://purehost.bath.ac.uk/ws/portalfiles/portal/191603805/An_Investigation_into_Enabling_Industrial_Machine_Tools_as_Traceable_Measurement_Systems_Final_Version_MRV.pdf
18. Renishaw plc. *Transform your manufacturing*. Retrieved from <http://www.renishaw.com/en/transform-your-manufacturing--32600> April 2020
19. Renishaw plc. Manufacturing Process Timeline. Retrieved from [https://resources.renishaw.com/en/details/Manufacturing%20process%20timeline\(42392\)](https://resources.renishaw.com/en/details/Manufacturing%20process%20timeline(42392)) February 2021
20. Renishaw plc. *Process foundation*. Retrieved from <https://www.renishaw.com/en/process-foundation--14157> April 2020
21. Fanuc Corporation. (2010). *FANUC Series 30i/31i/32i/35i-MODEL B*. Retrieved from [https://www.fanuc.co.jp/en/product/catalog/pdf/cnc/FS30i-B\(E\)-09.pdf](https://www.fanuc.co.jp/en/product/catalog/pdf/cnc/FS30i-B(E)-09.pdf) April 2020
22. BS ISO (2012). *Test code for machine tools. Geometric accuracy of machines operating under no-load or quasi-static conditions* (BS ISO 230-1:2012).
23. Ibaraki, S, & Knapp, W. (2012). Indirect measurement of volumetric accuracy for three-axis and five-axis machine tools. *A review. International Journal of Automation Technology*, 6, 110-124.
24. Schwenke, H., Knapp, W., Haitjema, H., Weckenmann, A., Schmitt, R., & Delbressine, F. (2008). Geometric error measurement and compensation of machines—An update. *CIRP Annals, Volume 57*(Issue 2), Pages 60-675.

25. Mayr, J., Jedrzejewski, J., Uhlmann, E., Donmez, M., Knapp, W. o., Härtig, F. Wegener, K. (2012). Thermal issues in machine tools. *CIRP Annals - Manufacturing Technology*, 61, 771–791.
26. Kent CNC. (2018). *Spindle Chiller – Does your VMC need it?*. Retrieved from <https://kentcnc.com/does-your-cnc-machine-need-spindle-chiller/>
27. Patil, P. and Mudholkar R.R. (2016). Cooling Techniques for a Spindle of Machine Tool. *International Journal Of Engineering And Computer Science*, 5(12), 19653-19656.
28. DMG/Mori. *dmu_dmc_portal_uk*. Retrieved from https://media.dmgmori.com/media/epaper/dmu_dmc_portal_uk/index.html#0 May 2020
29. Fudali, P., Witkowski, W., & Wydrzyński, D. (2013). COMPARISON OF GEOMETRIC PRECISION OF PLASTIC COMPONENTS MADE BY SUBTRACTIVE AND ADDITIVE METHODS. *Advances in Science and Technology Research Journal*, 7(19), 36–40. <https://doi.org/10.5604/20804075.1062353>
30. Swanton Welding Company. (2020). *Horizontal vs. Vertical Milling: Which Is Best For Your Metalwork Job?*. [https://blog.swantonweld.com/horizontal-vs.-vertical-milling#:~:text=Vertical%20Mills%20features%20spindles%20\(cutting,is%20parallel%20to%20the%20ground.](https://blog.swantonweld.com/horizontal-vs.-vertical-milling#:~:text=Vertical%20Mills%20features%20spindles%20(cutting,is%20parallel%20to%20the%20ground.)
31. BS ISO . (1998). *Test conditions for machining centres. Geometric tests for machines with integral indexable or continuous universal heads (vertical Z-axis)* (BS ISO 10791-3:1998).
32. Lin, M. T., Lee, Y. T., Jywe, W. Y., & Chen, J. A. (2011). Analysis and compensation of geometric error for five-axis CNC machine tools with titling rotary table. *IEEE/ASME (AIM) International Conference on Advanced Intelligent Mechatronics*, Budapest, Hungary, <https://doi.org/10.1109/AIM.2011.6027136>
33. Postlethwaite, S. R. (1992). *Electronic based accuracy enhancement of CNC machine tools* [PhD Thesis, University of Huddersfield]. t <http://eprints.hud.ac.uk/id/eprint/4663/>
34. Postlethwaite S.R. and Ford, D.G. (1997) Geometric error analysis software for CNC machine tools. *Transactions on Engineering Sciences* vol 16, page 305-316 WIT Press
35. Ozkirimli, O., Fletcher, S., Kite, J., Longstaff, A.P., McVey, S., Ozturk, E., (2017), Modelling and visualisation of machine tool and process related form errors, 6th International Conference on Virtual Machining Process Technology (VMPT), Montréal, May 29th – June 2nd, 2017
36. Longstaff, A. P., Fletcher, S., Myers, A., (2005). Volumetric error compensation through a Siemens controller. *Proceedings of the 7th International Conference and Exhibition on Laser Metrology, Machine Tool, CMM & Robotic Performance*, , 422-431. <https://doi.org/http://eprints.hud.ac.uk/id/eprint/1298/>
37. Longstaff, A., Fletcher, S., Myers, A., (2005). Volumetric compensation for precision manufacture through a standard CNC controller. *Proceedings of the 20th Annual ASPE Meeting*, ASPE 2005.
38. Ford, D. G. (2003). Machine tool performance: past and present research contributions from the Centre for Precision Technologies. *Transactions on Engineering Sciences*, 44, <https://doi.org/https://www.witpress.com/Secure/elibrary/papers/LAMDAMAP03/LAMDAMAP03035FU.pdf>
39. Mian, N. S., Fletcher, S., Longstaff, A. P., & Myers, A. (2015). FEA-based design study for optimising nonrigid error detection on machine tools. *Laser Metrology and Machine Performance XI*,

- https://doi.org/http://eprints.hud.ac.uk/id/eprint/24282/1/NSMIAN_LAMDAMAP2015-FINAL_SUBMITTED-Corrected.pdf
40. Miller, J., Fletcher, S., Longstaff, A., & Parkinson, S. (2020). Simultaneous Constant Velocity Measurement of the Motion Errors of Linear Axes. *Int. J. Automation Technol*, 14(3), 417-428. <https://doi.org/https://doi.org/10.20965/ijat.2020.p0417>
 41. NPL. (2019). *Introduction to Measurement and Metrology*. The National Physical Laboratory <https://training.npl.co.uk/course/introduction-to-metrology/>
 42. CNC Cookbook. (2018). *Dial Test Indicators & Dial Indicators (DTI, Dial Gauge, Digital Dial Indicator, Digital Dial Gauge)*. CNC Cookbook. <https://www.cnccookbook.com/dial-indicators-dial-test-indicators-easy-guide-2018/>
 43. BSI. (2007). *Engineers' squares (including cylindrical and block squares). Specification* (BS 939:2007).
 44. Machine tool metrology training course, delivered by the Centre for Precision Technologies and machine Tool Technologies at the University of Huddersfield 2012
 45. Atkins, A., & Escudier, M. (2019). *A Dictionary of Mechanical Engineering* (2nd ed.). Oxford University Press.
 46. Verdirame, J. (2016). "Airy Points, Bessel Points, Minimum Gravity Sag, and Vibration Nodal Points of Uniform Beams". *Mechanics and Machines*. Retrieved from <https://mechanicsandmachines.com/?p=330>.
 47. Evans, C.J., Hocken, R.J., Estler, W.T., (1996) Self-Calibration: Reversal, Redundancy, Error Separation, and 'Absolute Testing', *CIRP Annals*, Volume 45, Issue 2, Pages 617-634, doi: 10.1016/S0007-8506(07)60515-0.
 48. Renishaw PLC. (2016). *XL-80 laser measurement system* [PDF Brochure].
 49. BS ISO 230-2:2014+A1:2016: Test code for machine tools. Determination of accuracy and repeatability of positioning of numerically controlled axes. *BSI*.
 50. Parkinson, S., & Longstaff, A. P. (2015). Multi-objective optimisation of machine tool error mapping using automated planning. *Expert Systems with Applications*, 42, 3005-3015. <https://doi.org/https://doi.org/10.1016/j.eswa.2014.11.066>
 51. Hariharan, P. (2006). *Basics of Interferometry* (2nd ed.). Elsevier Science & Technology.
 52. Edlén, B. (1966). The Refractive Index of Air. *Metrologia*, 2(2), 71-80.
 53. Birch, K. P., & Downs, M. J. (1993). An Updated Edlén Equation for the Refractive Index of Air. *Metrologia*, 30(3), 155-.
 54. Birch, K. P., & Downs, M. J. (1993). Correction to the Updated Edlén Equation for the Refractive Index of Air. *Metrologia*, 31(4), 315-.
 55. Hexagon DEU01 GmbH. (2020). *ETALON LASERTRACER-NG*. www.etalonproducts.com. <https://www.etalonproducts.com/en/products/lasertracer/>
 56. Muralikrishnan, B., Phillips, S., & Sawyer, D. (2015). Laser Trackers for Large Scale Dimensional Metrology: A Review. *Precision Engineering*, 44, <https://doi.org/10.1016/j.precisioneng.2015.12.001>.
 57. Hexagon Manufacturing Intelligence. (2021). *Super Cat Eye Reflector The Ultra-Wide Acceptance Angle Reflector*. <https://www.hexagonmi.com/en-gb/products/laser-tracker-systems/accessories-for-laser-tracker-systems/super-cateye-reflector>

58. Aguado , S., Santolaria , J., Samper , D., & Aguilar, J. J. (2013). Influence of Measurement Noise and Laser Arrangement on Measurement Uncertainty of Laser Tracker Multilateration in Machine Tool Volumetric Verification. *Precision Engineering*, 37, 929-943.
59. Geotab Inc. (2021). *What is GPS?*. <https://www.geotab.com/blog/what-is-gps/>
60. Marek , J. (2020). *Geometric Accuracy, Volumetric Accuracy and Compensation of CNC Machine Tools*. www.intechopen.com. <https://www.intechopen.com/online-first/geometric-accuracy-volumetric-accuracy-and-compensation-of-cnc-machine-tools>
61. BNP Media. (2007). *Quality 101: Laser Tracking Fundamentals*. Quality Magazine. <https://www.qualitymag.com/articles/85066-quality-101-laser-tracking-fundamentals>
62. Creaform. (2016). *THE HISTORY OF METROLOGY FROM GALILEO TO OPTICAL SYSTEMS*. Creaform Blog. <https://www.creaform3d.com/blog/the-history-of-metrology-from-galileo-to-optical-systems/>
63. Insphere. *Baseline*. <https://insphereltd.com/baseline/>
64. Erkan, T., René Mayer, J. R., & Dupont , Y. (2011). Volumetric distortion assessment of a five-axis machine by probing a 3D reconfigurable uncalibrated master ball artefact. *Precision Engineering*, 35(1), 116-125. <https://doi.org/https://doi.org/10.1016/j.precisioneng.2010.08.003>.
65. Zimmermann, N., & Ibaraki, S. (2020). Self-calibration of rotary axis and linear axes error motions by an automated on-machine probing test cycle. *Int J Adv Manuf Technol* , 107, 2107–2120. <https://doi.org/https://doi.org/10.1007/s00170-020-05105-3>
66. Choi, P., Min, B. K., & Lee, S. J. (2004). Reduction of machining errors of a three-axis machine tool by on-machine measurement and error compensation system. *Journal of Materials Processing Technology*, 155–156, 2056-2064. <https://doi.org/https://doi.org/10.1016/j.jmatprotec.2004.04.402>
67. Inora. *SPATIAL REFERENCE SYSTEM (SRS)*. <https://www.inora.com/product/inora-spatial-reference-system-srs/>
68. Renishaw PLC. (2021). *QC20-W ball bar system* [PDF Brochure].
69. Wright, D. (2011). *Introduction of a Semi Automatic Quality Control Process into an SME* [MRes Dissertation, University of Huddersfield]. <http://eprints.hud.ac.uk/id/eprint/17554/>
70. Big Daishowa Seiki Co Ltd. (2021). https://www.big-daishowa.com/big-plus_index.php
71. (2020). *Difference Between BT and HSK Tool Holders*. Tool holder Exchange. <https://toolholderexchange.com/difference-bt-hsk-tool-holders/>
72. Renishaw plc. *OMP600 Data Sheet retrieved April 2021*. <https://www.renishaw.com/en/omp600-high-accuracy-machine-probe--31250>
73. GAŚKA, P., GAŚKA, A., GRUZA, M., OSTROWSKA, K., & SŁADEK, J. (2017). Assessment of impact of stylus length on measurement accuracy for 5-axis coordinate measuring systems. *Mechanik*, 90(11), <https://doi.org/https://doi.org/10.17814/mechanik.2017.11.170>
74. Woz´niak, A., & Meczyn´ska, K. (2020). Measurement hysteresis of touch-trigger probes for CNC machine tools. *Measurement*, 156, <https://doi.org/https://doi.org/10.1016/j.measurement.2020.107568>

75. Renishaw PLC. (2014). *RMP60 – radio machine probe* [PDF Brochure].
76. Cristea, G., & Constantinescu, D. M. (2017). A comparative critical study between FMEA and FTA risk analysis methods. *IOP Conference Series: Materials Science and Engineering*, 252, <https://doi.org/https://iopscience.iop.org/article/10.1088/1757-899X/252/1/012046>
77. Ruijters, E., & Stoelinga, M. (2015). Fault tree analysis: A survey of the state-of-the-art in modelling, analysis and tools. *Computer Science Review*, 15-16, 29-62. <https://doi.org/https://doi.org/10.1016/j.cosrev.2015.03.001>
78. BS EN IEC 60812:2018 Failure modes and effects analysis (FMEA and FMECA)
79. https://www.weibull.com/pubs/2014_RAMS_fundamentals_of_fmeas.pdf
80. Hexagon manufacturing Intelligence. (2021). *LS-C-5.8 Machine Tool Laser Sensor Complete solution for laser scanning directly on the machine tool*. <https://www.hexagonmi.com/en-gb/products/machine-tool-probes/machine-tool-laser-scanning/ls-c-5-8-machine-tool-laser-sensor>
81. Renishaw plc (2021). *SPRINT™ technology*. <https://www.renishaw.com/en/sprint-technology-20908>
82. Papananias, M. (2019). *Combined Numerical And Statistical Modelling For In-Depth Uncertainty Evaluation Of Comparative Coordinate Measurement* [PhD Thesis, University of Huddersfield]. <http://eprints.hud.ac.uk/id/eprint/34836>
83. Sangeeth, V., & Saravanan, P. (2016). An innovated method using Failure mode and effects analysis for improving quality of the. *International Journal of Advanced Research in Computer and Communication Engineering*, 5(1), <https://doi.org/https://ijarcce.com/wp-content/uploads/2016/02/IJARCCE-33.pdf>
84. Enrico, Z. (2007). Introduction To The Basics Of Reliability And Risk Analysis, An. *World Scientific Publishing Company*, , <https://doi.org/https://ebookcentral.proquest.com/lib/HUD/detail.action?docID=312287>
85. https://www.bipm.org/documents/20126/2071204/JCGM_200_2012.pdf/f0e1ad45-d337-bbeb-53a6-15fe649d0ff1?version=1.8&download=true
86. Anandan, P., Nahata, S., & Ozdoganlar, O. B. (2012). Implementation Of Donaldson Reversal Technique To Measure Error Motions Of Ultra-High-Speed Spindles. *American Society of Precision Engineering*, San Diego, CA,
87. <https://www.blum-novotest.com/en/products/measuring-components/lasercontrol/lc50-digilog.html>
88. Lion precision. (2021). *Spindle Error Analyzer (SEA) Components*. <https://www.lionprecision.com/spindle-error-analyzer-components/>
89. BS ISO. (2006). *Geometric accuracy of axes of rotation (230-7:2006)*.
90. Flack, D (2014) Measurement Good Practice Guide No. 41 CMM measurement strategies, *Queen's Printer and Controller of HMSO*, ISSN 1368-6550. Retrieved from: [https://www.npl.co.uk/special-pages/guides/gpg41_cmm.pdf?ext=.](https://www.npl.co.uk/special-pages/guides/gpg41_cmm.pdf?ext=)
91. <https://metrology.news/measuring-on-machine-tools-correlates-with-cmm/>
92. White, A.J., Postelthwaite, S.R. and Ford, D.G. (2001) Measuring and modelling thermal distortion on CNC machine tools. *Transactions on Engineering Sciences* vol34, pages 69-79, WIT Press

93. Sepahi-Boroujeni, S., Mayer, J. R. R., & Khameneifar, F. (2020). Repeatability of on-machine probing by a five-axis machine tool. *International Journal of Machine Tools and Manufacture*, 152, <https://doi.org/https://doi.org/10.1016/j.ijmachtools.2020.103544>
94. Shagluf, a., Parkinson, S., Longstaff, A. P., & Fletcher, S. (2014). Towards an Optimization Calculation for Preventative and Reactive Calibration Strategies. *KES Transactions on Sustainable Design and Manufacturing*, Cardiff, 83-94.
95. Abdulshahed, A. (2015). *The Application of ANN and ANFIS Prediction Models for Thermal Error Compensation on CNC Machine Tools* [PhD Thesis, University of Huddersfield]. <http://eprints.hud.ac.uk/id/eprint/27946/>
96. Mian, N. (2010). *Efficient machine tool thermal error modelling strategy for accurate offline assessment* [PhD Thesis, University of Huddersfield]. <http://eprints.hud.ac.uk/id/eprint/11054/>
97. Burdick, R. K., Borrer, C., Montgomery, D. C., Czitrom, V., & Spagon, P. (1987). *Design and Analysis of Gauge R&R Studies: Making Decisions with Confidence Intervals in Random and Mixed ANOVA Models* 10.1137/1.9780898718379

Appendix A Test list for a 3-axis machine

- Axis geometry
 - X axis
 - Linear position error of linear motions EXX
 - Straightness of linear motion errors EYX, EZX
 - angular deviations of linear motions EAX, EBX, ECX
 - Y axis Laser
 - Linear position error of linear motions EYY
 - Straightness of linear motion errors EXY, EZY
 - angular deviations of linear motions EAY, EBY, ECY
 - Z Axis Laser
 - Linear position error of linear motions EZZ
 - Straightness of linear motion errors EXZ, EYZ
 - angular deviations of linear motions EAZ, EBZ, ECZ
 - Squareness between axes
 - XY Plane
 - XZ Plane
 - YZ Plane
- Ball bar
 - XY Plane in multiple locations
 - XZ Plane in multiple locations
 - YZ Plane in multiple locations
- Spindle
 - Parallelism between the spindle axis and the Z Axis motion
 - Parallelism between the spindle axis and Z-Axis motion in the YZ plane
 - Parallelism between the spindle axis and Z-Axis motion in the XZ plane
 - Spindle Run out
- Tool change repeatability
- Thermal
 - Environmental ETVE
 - Spindle thermal distortion evaluation
 - Axis thermal distortion evaluation
- Probe
 - Repeatability of probing
 - Position of calibration Vs Measurement location
 - Effect of contamination
 - Coolants and oils

Appendix B Machine descriptions

B.1 Machine A Cincinnati

Machine A is a C frame 3 axis vertical Spindle machining centre with Siemens 840D Sinumerik controller and a closed loop glass scale measurement feedback system.

Axis Strokes

- X axis 500mm
- Y Axis 500mm
- Z Axis 630mm

Utilising a Renishaw RMP600 probing system

B.2 Machine B Robodrill

Machine B is a C frame 3 axis vertical Spindle machining centre with Fanuc 18i Controller and a rotary encoder measurement feedback system.

Axis Strokes

- X axis 500mm
- Y Axis 400mm
- Z Axis 330mm

Utilising a Renishaw RMP40 probing system

B.3 Machine C Geiss

Machine C is a gantry style 5 axis head/head style machining centre with Siemens 840D solution line Controller and a closed loop glass scale measurement feedback system.

Axis Strokes

- X axis 500mm
- Y Axis 400mm
- Z Axis 330mm

Utilising a Renishaw RMP40 probing system

B.4 Machine D Hurco

Machine C is a C frame 5 axis vertical Spindle machining centre, trunnion mounted rotary axes with Winmax controller and a closed loop glass scale measurement feedback system.

Axis Strokes

- X axis 760mm
- Y Axis 508mm
- Z Axis 520mm
- A Axis +30/-110
- C Axis Continuous

Utilising a Renishaw OMP600 probing system

B.5 Machine E Huron VX10

Machine E is a C frame 3 axis vertical Spindle machining centre with Siemens 828D controller and a closed loop glass scale measurement feedback system.

Axis Strokes

- X axis 1020mm
- Y Axis 510mm
- Z Axis 510mm

Utilising a Renishaw RMP600 probing system

B.6 Machine F Hermle C22

Machine F is a C frame 5 axis vertical Spindle machining centre, trunnion mounted rotary axes with Heidenhain TNC640 controller and a closed loop glass scale measurement feedback system.

Axis Strokes

- X axis 450mm
- Y Axis 600mm
- Z Axis 330mm
- A Axis +135/-135
- C Axis Continuous

Utilising a Renishaw OMP600 probing system

Appendix C Part programs

C.1 Main variable Probing Program

```
;FULL VALIDATION PROGRAM FOR SIEMENS
;USING PROBING OF 4 SPHERES WITH INTERMITTANT SIMULATED
MACHINING AND AXIS HEATING
;*****
DEF REAL PROB1 = 15 ;NO OF FIRST PROBING CYCLES
DEF REAL TIPROB1 = 2 ; TIME BETWEEN FIRST PROBES
DEF REAL MASP100 = 9000 ; 100PC MACH SPINDLE SPEED
DEF REAL NOMAC1 = 6 ;NO OF FIRST MACHINING CYCLES
DEF REAL PROB2 = 2 ; NO OF SECOND PROBING CYCLES
DEF REAL TIPROB2 = 45 ; TIME BETWEEN SECOND PROBE
DEF REAL NOMAC2 = 5 ; NO OF SECOND MACHINING CYCLES
DEF REAL PROB3 = 3 ; NO OF THIRD PROBING CYCLES
DEF REAL TIPROB3 = 15 ; TIME BETWEEN THIRD PROBING CYCLES
DEF REAL NOMAC3 = 7 ; NO OF THIRD MACHINING CYCLES
DEF REAL PROB4 = 4 ; NO OF FOURTH PROBING CYCLES
DEF REAL TIPROB4 = 45 ; TIME BETWEEN FOURTH PROBES
DEF REAL NOMAC4 = 6 ; NO OF FOURTH MACHINING CYCLES
DEF REAL PROB5 = 6 ; NO OF FIFTH PROBING CYCLES
DEF REAL TIPROB5 = 30 ; TIME BETWEEN FIFTH PROBES
DEF REAL NOMAC5 = 4 ; NO OF FIFTH MACHINING CYCLES
DEF REAL AXHEAT1 = 10 ; FIRST AXIS HEATING CYCLES
DEF REAL PCMACH50 = 3 ; NO OF 50PC MACHINING CYCLES
DEF REAL PCPROBE50 = 3 ; NO OF 50PC PROBING CYCLES
DEF REAL TIPROB50 = 60 ;TIME BETWEEN 50PC COOLING PROBES
DEF REAL SPHEATTI1 = 360 ; TIME OF FIRST SPINDLE HEATS
DEF REAL NOSPHEAT1 = 12 ; NO OF FIRST SPINDLE HEAT CYCLES
DEF REAL SPHEATTI2 = 180 ; TIME OF SECOND SPINDLE HEATS
DEF REAL NOSPHEAT2 = 9 ; NO OF SECOND HEAT CYCLES
```

```
DEF REAL PCMACH75 = 3 ; NO OF 75PC MACHINING CYCLES
DEF REAL PCMACH30 = 3 ; NO OF 30PC MACHINING CYCLES
DEF REAL NOMACFI = 10 ; NO OF FINAL MACHINING CYCLES
DEF REAL PROBFI = 15 ; NO OF FINAL PROBE CYCLES
DEF REAL TIPROBEFI = 2 ; TIME BETWEEN FINAL PROBES
DEF REAL FEED100 = 12000 ; 100PC MACHINING FEEDRATE
DEF REAL PROBSP = 10000 ; PROBE MOVEMENT SPEED
DEF REAL AXISHEFE = 12000 ; AXIS HEAT FEEDRATE
DEF REAL AXISRUN = 12 ; NUMBER OF AXIS HEAT RUNS
;*****
;DO NOT TOUCH BELOW HERE
;*****

; PROBE VARIABLES
DEF real tempx1
DEF real tempy1
DEF real tempz1
DEF real tempx1a
DEF real tempy1a
DEF real tempz1a
DEF real tempx2
DEF real tempy2
DEF real tempz2
DEF real tempx3
DEF real tempy3
DEF real tempz3
DEF real tempx4
DEF real tempy4
DEF real tempz4
DEF REAL hourstart
DEF REAL minstart
```

```
DEF REAL secstart
DEF REAL hourend
DEF REAL minend
DEF REAL secend

; FILE STORAGE
EXTERN FWRITE (STRING[160],STRING[200])
DEF STRING[200] msgtxt=" "
DEF STRING[160] FNAME="VARISIM_RESULTS1"

;R VARIABLE SETUP
;CALCULATIONS
R50=0
R51=PROB1
R52=TIPROB1
R53=MASP100
R54=NOMAC1
R55=PROB2
R56=TIPROB2
R57=NOMAC2
R58=PROB3
R59=TIPROB3
R60=NOMAC3
R61=PROB4
R62=TIPROB4
R63=NOMAC4
R64=PROB5
R65=TIPROB5
R66=NOMAC5
R67=AXHEAT1
R68=PCMACH50
```

```
R69=PCPROBE50
R70=TIPROB50
R71=SPHEATTI1
R72=NOSPHEAT1
R73=SPHEATTI2
R74=NOSPHEAT2
R75=PCMACH75
R76=PCMACH30
R77=NOMACFI
R78=PROBFI
R79=TIPROBEFI
R80=FEED100
R90=10
R91=9
R92=8
R93=7
R94=6
R95=5
;*****
;*****

; Load probe and set datum on tallest sphere center line g54
T21 ; Load T21 Machine tool Probe
M6
G54
M19

;SET DATUM G54
M19
G1 Z100 F5000
M75 ; Probe on
```



```
G04F0.5
L9800          ;   Clear global R parameters
R24=0 R25=0 R9=5000
L9810          ;   protected move to sphere centre
R26=50 R9=3000
L9810          ;   Protected move 50mm above sphere top
R7=9.5 R26=-3.0 R18=5 R19=1 ; set sphere centre datum g54
L9814          ;   Probe cycle for boss centre line
R24=RENC[35] R25=RENC[36]      ; Move to sphere top centre
L9810          ;Protected move
R26=4.75 R19=1 R17=8 ; set sphere centreline datum g54
L9811          ;Probe cycle for Z0

;end of datum set and start of variable program

;MAIN PROGRAM START
;create file header
msgtxt=<<"D, "<<"ST, "<<"X1, "<<"X2, "<<"X3, "<<"X4, "<<"X1, "<<"Y1, "
<<"Y2, "<<"Y3, "<<"Y4, "<<"Y1, "<<"Z1, "<<"Z2, "<<"Z3, "<<"Z4, "<<"Z1,
"<<"ET, ";
FWRITE (FNAME,msgtxt)

R99=10

;COOLING PROBE
LABEL0010:
G54
T21
M6

VARISIM_PROBE_SUB
```

```
;msgtxt=<<$A_DAY<<"/"<<$A_MONTH<<"/"<<$A_YEAR<<","<<(hourstart
)<<":"<<(minstart)<<":"<<(secstart)<<","<<(tempx1)<<","<<(temp
x2)<<","<<(tempx3)<<","<<(tempx4)<<","<<(tempx1a)<<","<<(tempy
1)<<","<<(tempy2)<<","<<(tempy3)<<","<<(tempy4)<<","<<(tempy1a
)<<","<<(tempz1)<<","<<(tempz2)<<","<<(tempz3)<<","<<(tempz4)<
<","<<(tempz1a)<<","<<(hourend)<<":"<<(minend)<<":"<<(secend)
;FWRITE(FNAME,msgtxt)
```

M5

G0 Z100

G04F=R52

R51=R51-1

IF R51>R50 GOTOB LABEL0010

;MACHINING CYCLE

LABEL0020:

G54

T1

M6

S=MASP100

F=FEED100

VARISIM_MACH_POS

T21

M6

G54

VARISIM_PROBE_SUB

M5

G0 Z100

R54=R54-1

IF R54>R50 GOTOB LABEL0020

```
;JUMP LOOPS FOR MACHINING CYCLES
```

```
IF R99==R90 GOTO LABEL0050
```

```
IF R99==R91 GOTO LABEL0060
```

```
IF R99==R92 GOTO LABEL0070
```

```
IF R99==R93 GOTO LABEL0080
```

```
IF R99==R94 GOTO LABEL0090
```

```
LABEL0050:
```

```
R99=R99-1
```

```
R51=R55
```

```
R52=R56
```

```
R54=R57
```

```
GOTOB LABEL0010
```

```
LABEL0060:
```

```
R99=R99-1
```

```
R51=R58
```

```
R52=R58
```

```
R54=R60
```

```
GOTOB LABEL0010
```

```
LABEL0070:
```

```
R99=R99-1
```

```
R51=R61
```

```
R52=R62
```

```
R54=R63
```

```
GOTOB LABEL0010
```

```
LABEL0080:
```

```
R99=R99-1
```

```
R51=R64
```

R52=R65

R54=R66

GOTOB LABEL0010

;AXIS HEATING

LABEL0090:

STOPRE

G54

VARISIM_AXIS_HEATING_SUB

T21

M6

G54

VARISIM_PROBE_SUB

R67=R67-1

IF R67>R50 GOTOB LABEL0090

;MACHINING CYCLE 50PC

LABEL0100:

T1

M6

S=R53/2 M3

F=R80/2

VARISIM_MACH_POS

M5

G0 Z100

T21

M6

G54

VARISIM_PROBE_SUB

R68=R68-1

IF R68>R50 GOTOB LABEL0100

;COOLING CYCLE FOR 50PC MACHINING

LABEL0110:

T21

M6

VARISIM_PROBE_SUB

G04F=R70

R69=R69-1

IF R69>R50 GOTOB LABEL0110

;FIRST SPINDLE HEATING

LABEL120:

G54

T1

M06

G1 X0 Y0

S9000 M3

G04F=R71

M5

T21 ; Load T21 Machine tool Probe

M6

G54

VARISIM_PROBE_SUB

M5

G0 Z100

R72=R72-1

IF R72>R50 GOTOB LABEL120

IF R99==R95 GOTO LABEL0140

;SECOND SPINDLE HEATING

LABEL130:

R99=R99-1

R71=R73

R72=R74

GOTOB LABEL0110

;MACHINING CYCLE 75PC

LABEL0140:

T1

M6

S=R53/4*3 M3

F=R80/4*3

VARISIM_MACH_POS

M5

G0 Z100

T21

M6

G54

VARISIM_PROBE_SUB

```
R75=R75-1  
IF R75>R50 GOTOB LABEL0140
```

```
;MACHINING CYCLE 30PC
```

```
LABEL0150:
```

```
T1
```

```
M6
```

```
S=R53/100*30 M3
```

```
F=R80/100*30
```

```
VARISIM_MACH_POS
```

```
M5
```

```
G0 Z100
```

```
T21
```

```
M6
```

```
G54
```

```
VARISIM_PROBE_SUB
```

```
R76=R76-1
```

```
IF R76>R50 GOTOB LABEL0150
```

```
;MACHINING CYCLE FINAL
```

```
LABEL0160:
```

```
G54
```

```
T1
```

```
M6
```

```
S=MASP100
```

```
F=FEED100
```

```
VARISIM_MACH_POS
```

M5

G54

T21

M6

VARISIM_PROBE_SUB

M5

G0 Z100

R77=R77-1

IF R77>R50 GOTOB LABEL0160

;COOLING PROBE END

LABEL0170:

G54

T21

M6

VARISIM_PROBE_SUB

M5

G0 Z100

G04F=R79

R78=R78-1

IF R78>R50 GOTOB LABEL0170

M30

C.2 Probing Subroutine

```
;VARISIM PROBE SUBROUTINE 4 SPHERES
;store measurement start time
hourstart=$A_HOUR
minstart=$A_MINUTE
secstart=$A_SECOND

M19
M75 ; PROBE ON
G04F0.5

;Sphere 1
L9800          ; Clear global R parameters
R24=0 R25=0 R9=PROBSP
L9810          ; protected move to sphere centre
R26=50 R9=PROBSP
L9810          ; Protected move 50mm above sphere top
R7=9.5 R26=-3.0 R18=5
L9814          ; Probe cycle for boss centre line
R24=RENC[35] R25=RENC[36] ; Move to sphere top centre
L9810          ;Protected move
R26=0
L9811          ;Probe cycle for Z0
tempx1=RENC[35]
tempy1=RENC[36]
tempz1=RENC[37]-4.75
L9800

;sphere 2
R24=-233.962 R25=-199.519 R9=PROBSP
L9810          ; protected move to post 2 centre
```

```
R26=-130 R9=PROBSP
L9810          ; Protected move 25mm above sphere top
R7=9.5 R26=-188.466 R18=5
L9814          ; Probe cycle for boss centre line
R24=RENC[35] R25=RENC[36]      ; Move to post top position
L9810          ;Protected move
R26=-184.5
L9811          ;Probe cycle for Z0
tempx2=RENC[35]
tempy2=RENC[36]
tempz2=RENC[37]-4.75
L9800
R26=100 R9=PROBSP
L9810          ; Protected move safe travel height

;sphere 3
R24=1.727 R25=200.650 R9=PROBSP
L9810          ; protected move to post 3 centre
R26=-130 R9=PROBSP
L9810          ; Protected move 25mm above sphere top
R7=9.5 R26=-188.23 R18=5
L9814          ; Probe cycle for boss centre line
R24=RENC[35] R25=RENC[36]      ; Move to post top position
L9810          ;Protected move
R26=-184.5
L9811          ;Probe cycle for Z0
tempx3=RENC[35]
tempy3=RENC[36]
tempz3=RENC[37]-4.75
L9800
R26=100 R9=PROBSP
```

```
L9810          ; Protected move safe travel height

;sphere 4
R24=234.711 R25=-199.477 R9=PROBSP
L9810          ; protected move to post 4 centre
R26=-130 R9=PROBSP
L9810          ; Protected move 25mm above sphere top
R7=9.5 R26=-188.75 R18=5
L9814          ; Probe cycle for boss centre line
R24=RENC[35] R25=RENC[36]      ; Move to post top position
L9810          ;Protected move
R26=-184.5
L9811          ;Probe cycle for Z0
tempx4=RENC[35]
tempy4=RENC[36]
tempz4=RENC[37]-4.75
L9800
R26=100 R9=PROBSP
L9810          ; Protected move safe travel height

;sphere 1a
L9800          ; Clear global R parameters
R24=0 R25=0 R9=PROBSP
L9810          ; protected move to sphere centre
R26=50 R9=PROBSP
L9810          ; Protected move 50mm above sphere top
R7=9.5 R26=-3.0 R18=5
L9814          ; Probe cycle for boss centre line
R24=RENC[35] R25=RENC[36]      ; Move to sphere top centre
L9810          ;Protected move
R26=0
```

```
L9811          ;Probe cycle for Z0
tempx1a=RENC[35]
tempy1a=RENC[36]
tempz1a=RENC[37]-4.75
L9800

;store measurement end time
hourend=$A_HOUR
minend=$A_MINUTE
secend=$A_SECOND

;rounding function
tempx1=(ROUND(tempx1*10000))/10000
tempy1=(ROUND(tempy1*10000))/10000
tempz1=(ROUND(tempz1*10000))/10000
tempx2=(ROUND(tempx2*10000))/10000
tempy2=(ROUND(tempy2*10000))/10000
tempz2=(ROUND(tempz2*10000))/10000
tempx3=(ROUND(tempx3*10000))/10000
tempy3=(ROUND(tempy3*10000))/10000
tempz3=(ROUND(tempz3*10000))/10000
tempx4=(ROUND(tempx4*10000))/10000
tempy4=(ROUND(tempy4*10000))/10000
tempz4=(ROUND(tempz4*10000))/10000
tempx1a=(ROUND(tempx1a*10000))/10000
tempy1a=(ROUND(tempy1a*10000))/10000
tempz1a=(ROUND(tempz1a*10000))/10000

msgtxt=<<$A_DAY<<"/"<<$A_MONTH<<"/"<<$A_YEAR<<","<<(hourstart)
<<":"<<(minstart)<<":"<<(secstart)<<","<<(tempx1)<<","<<(tempx
2)<<","<<(tempx3)<<","<<(tempx4)<<","<<(tempx1a)<<","<<(tempy1
)<<","<<(tempy2)<<","<<(tempy3)<<","<<(tempy4)<<","<<(tempy1a)
```

```
<<" , "<<(tempz1)<<" , "<<(tempz2)<<" , "<<(tempz3)<<" , "<<(tempz4)<<  
" , "<<(tempz1a)<<" , "<<(hourend)<<":"<<(minend)<<":"<<(secend)  
FWRITE (FNAME,msgtxt)
```

M75

M17

C.3 Machining Positions

```
;MACHINING POSITIONS
```

```
;START POSITIONS OF SIMULATED MACHINING OPERATIONS
```

```
TRANS X-150.0Y100.0
```

```
VARISIM_MACH_SUB
```

```
TRANS X150.0Y100.0
```

```
VARISIM_MACH_SUB
```

```
TRANS X150.0Y-100.0
```

```
VARISIM_MACH_SUB
```

```
TRANS X-150.0Y-100.0
```

```
VARISIM_MACH_SUB
```

```
TRANS
```

M17

C.4 Axis Heating

```
;AXIS HEATING SUBPROGRAM
```

```
;PROGRAM FOR X AXIS
```

```
STOPRE
```

```
R81=AXISRUN
```

```
T1
```

M6

```
G54
G0X240.0 Y-100.

LABEL0510:
F=AXISHEFE
G1 X-240.
X240.
R81=R81-1
IF R81>R50 GOTO LABEL0510
G1 Z100
M17
```

C.5 Z Repeat

```
;THIS PROGRAM REPEATS THE Z MEASURMENT AND WRITES THE VALUES TO
FILE
```

```
DEF REAL repeats = 200 ;no of repeat measurements
DEF REAL wait = 5. ; no of seconds between measurments
```

```
;*****
****
```

```
DEF REAL zero = 0
DEF REAL hourstart
DEF REAL minstart
DEF REAL secstart
```

```
;*****
****
```

```
EXTERN FWRITE (STRING[160],STRING[200])
DEF STRING[200] msgtxt=" "
DEF STRING[160] FNAME="Z_POS_DATA"
```

```
msgtxt=<<"DATE"<<" "<<"START"<<" "<<"ZPOS"
FWRITE (FNAME,msgtxt)

G17 T21
M6
G40 G90
G55 G0 X-20 Y-20
Z100
SPOS=0
M75;turns probe on
G04F0.5
L9800

R26=5 R9=5000
L9810

LABEL10:
;store measurement start time
hourstart=$A_HOUR
minstart=$A_MINUTE
secstart=$A_SECOND

R26=0
L9811

msgtxt=<<$A_DAY<<"/"<<$A_MONTH<<"/"<<$A_YEAR<<"
"<<(hourstart)<<":"<<(minstart)<<":"<<(secstart)<<"
"<<((ROUND(RENC[37]*10000))/10000)
FWRITE (FNAME,msgtxt)

R26=5
```

```
L9810
G04F=wait

repeats=repeats-1
IF repeats>0 GOTOB LABEL10

R26=100 R9=5000
L9810
M75
M5
M30
```

C.6 Z repeat with tool change

```
;THIS PROGRAM REPEATS THE Z MEASURMENT AND WRITES THE VALUES TO
FILE
```

```
DEF REAL repeats = 200 ;no of repeat measurements
DEF REAL wait = 5. ; no of seconds between measurments
```

```
;*****
****
```

```
DEF REAL zero = 0
DEF REAL hourstart
DEF REAL minstart
DEF REAL secstart
```

```
;*****
****
```

```
EXTERN FWRITE (STRING[160],STRING[200])
DEF STRING[200] msgtxt=" "
DEF STRING[160] FNAME="Z_POS_DATA_HIGH"
```



```
msgtxt=<<"DATE"<<" "<<"START"<<" "<<"ZPOS"  
FWRITE (FNAME,msgtxt)  
  
LABEL10:  
G17 T21  
M6  
G40 G90  
G55 G0 X-10 Y-10  
Z100  
SPOS=0  
  
M75 ;turns probe on  
G04F0.5  
L9800  
  
R26=5 R9=5000  
L9810  
  
;store measurement start time  
hourstart=$A_HOUR  
minstart=$A_MINUTE  
secstart=$A_SECOND  
  
R26=0  
L9811  
  
msgtxt=<<$A_DAY<<"/"<<$A_MONTH<<"/"<<$A_YEAR<<"  
"<<(hourstart)<<":"<<(minstart)<<":"<<(secstart)<<"  
"<<((ROUND(RENC[37]*10000))/10000)  
FWRITE (FNAME,msgtxt)  
  
R26=300 R9=5000
```

```
L9810
G04F=wait

T20
M6
G04F=wait

repeats=repeats-1
IF repeats>0 GOTOB LABEL10

R26=300 R9=5000
L9810
M75
M5
M30
```

C.7 Probe Calibrate 19mm ring

```
;THIS PROGRAM CALIBRATES OMP600 PROBE AND RECORDS THE OFFSET
VALUES TO FILE
;PROGRAM 9806 DOES THE 180 SPINDLE ROTATION TO FIND CENTRE OF
BORE
;19MM RING GAUGE
;USES G55

DEF REAL repeats = 100 ;no of repeat measurements

;*****
****

DEF REAL zero
DEF REAL runs
DEF REAL ZTEMP
```

```
DEF REAL hourstart
DEF REAL minstart
DEF REAL secstart
DEF REAL hourend
DEF REAL minend
DEF REAL secend
;*****
****

EXTERN FWRITE (STRING[160],STRING[200])
DEF STRING[200] msgtxt=" "
DEF STRING[160] FNAME="CALIBRATION_DATA191"

msgtxt=<<"DATE  "<<"START  "<<"XSTYLUSOS  "<<"YSTYLUSOS  "<<"XR
"<<"YR  "<<"30R  "<<"60R  "<<"120R  "<<"150R  "<<"210R  "<<"240R
"<<"300R  "<<"330R  "<<"END"

FWRITE (FNAME,msgtxt)

runs=repeats

G17 T21
M6
G40 G90
G55 G0 X0 Y0
Z100
SPOS=0
M75;turns probe on
G04F0.5
L9800

R26=10 R9=1500
L9810
```

R26=-10 R9=1500

L9810

R7=19.

R19=2

L9806

LABEL10:

;store measurement start time

hourstart=\$A_HOUR

minstart=\$A_MINUTE

secstart=\$A_SECOND

R24=0 R25=0

L9810

R7=18.999

L9802

R7=18.999

L9804

;store measurement end time

hourend=\$A_HOUR

minend=\$A_MINUTE

secend=\$A_SECOND

msgtxt=<<\$A_DAY<<"/"<<\$A_MONTH<<"/"<<\$A_YEAR<<"
"<<(hourstart)<<":"<<(minstart)<<":"<<(secstart)<<"
"<<((ROUND(RENP[2]*10000))/10000)<<"
"<<((ROUND(RENP[3]*10000))/10000)<<"

```
"<< ( (ROUND (RENP [0] *10000) ) /10000) <<"
"<< ( (ROUND (RENP [1] *10000) ) /10000) <<" "
msgtxt=<<msgtxt<< ( (ROUND (RENP [10] *10000) ) /10000) <<"
"<< ( (ROUND (RENP [11] *10000) ) /10000) <<"
"<< ( (ROUND (RENP [12] *10000) ) /10000) <<"
"<< ( (ROUND (RENP [13] *10000) ) /10000) <<"
"<< ( (ROUND (RENP [14] *10000) ) /10000) <<"
"<< ( (ROUND (RENP [15] *10000) ) /10000) <<"
"<< ( (ROUND (RENP [16] *10000) ) /10000) <<"
"<< ( (ROUND (RENP [17] *10000) ) /10000) <<"
"<<(hourend) <<": "<<(minend) <<": "<<(secend)
FWRITE (FNAME,msgtxt)

runs=runs-1
IF runs>zero GOTOB LABEL10

R26=100
L9810
M75
M5
M30
```

C.8 Probe Calibrate 44mm ring

```
;THIS PROGRAM CALIBRATES OMP600 PROBE AND RECORDS THE OFFSET
VALUES TO FILE
;PROGRAM 9806 DOES THE 180 SPINDLE ROTATION TO FIND CENTRE OF
BORE
;44MM RING GAUGE
;USES G55

DEF REAL repeats = 100 ;no of repeat measurements

;*****
***
```

```
DEF REAL zero
DEF REAL runs
DEF REAL ZTEMP
DEF REAL hourstart
DEF REAL minstart
DEF REAL secstart
DEF REAL hourend
DEF REAL minend
DEF REAL secend
;*****
****

EXTERN FWRITE (STRING[160],STRING[200])
DEF STRING[200] msgtxt=" "
DEF STRING[160] FNAME="CALIBRATION_DATA441"

msgtxt=<<"DATE  " <<"START  " <<"XSTYLUSOS  " <<"YSTYLUSOS  " <<"XR
" <<"YR  " <<"30R  " <<"60R  " <<"120R  " <<"150R  " <<"210R  " <<"240R
" <<"300R  " <<"330R  " <<"END"

FWRITE (FNAME,msgtxt)

runs=repeats

G17 T21
M6
G40 G90
G55 G0 X0 Y0
Z100
SPOS=0
M75;turns probe on
G04F0.5
L9800
```

R26=10 R9=1500

L9810

R26=-10 R9=1500

L9810

R7=44.

R19=2

L9806

LABEL10:

;store measurement start time

hourstart=\$A_HOUR

minstart=\$A_MINUTE

secstart=\$A_SECOND

R24=0 R25=0

L9810

R7=43.999

L9802

R7=43.999

L9804

;store measurement end time

hourend=\$A_HOUR

minend=\$A_MINUTE

secend=\$A_SECOND

```
msgtxt=<<$A_DAY<<"/"<<$A_MONTH<<"/"<<$A_YEAR<<"
"<<(hourstart)<<":"<<(minstart)<<":"<<(secstart)<<"
"<<((ROUND(RENP[2]*10000))/10000)<<"
"<<((ROUND(RENP[3]*10000))/10000)<<"
"<<((ROUND(RENP[0]*10000))/10000)<<"
"<<((ROUND(RENP[1]*10000))/10000)<<" "
msgtxt=<<msgtxt<<((ROUND(RENP[10]*10000))/10000)<<"
"<<((ROUND(RENP[11]*10000))/10000)<<"
"<<((ROUND(RENP[12]*10000))/10000)<<"
"<<((ROUND(RENP[13]*10000))/10000)<<"
"<<((ROUND(RENP[14]*10000))/10000)<<"
"<<((ROUND(RENP[15]*10000))/10000)<<"
"<<((ROUND(RENP[16]*10000))/10000)<<"
"<<((ROUND(RENP[17]*10000))/10000)<<"
"<<(hourend)<<":"<<(minend)<<":"<<(secend)
FWRITE(FNAME,msgtxt)

runs=runs-1
IF runs>zero GOTOB LABEL10

R26=100
L9810
M75
M5
M30
```


Appendix D Failure mechanisms in probing

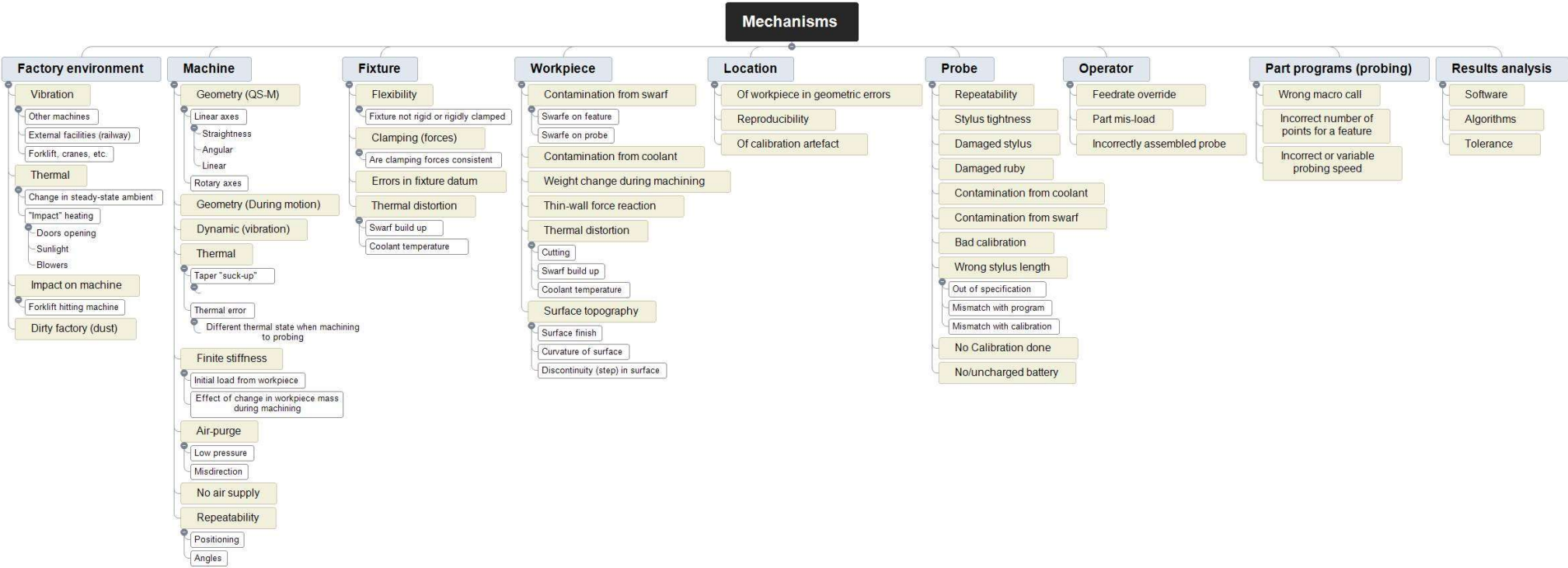


Figure 118 Mind map showing the different failure mechanisms in probing

Appendix E Probe calibration repeatability data

E.1 44 mm diameter ring

START	XSTYLUSOS	YSTYLUSOS	XR	YR	30R	60R	120R	150R	210R	240R	300R	330R	END
09:50:33	-0.0102	-0.0052	2.9928	2.992	2.993	2.9922	2.9921	2.9924	2.9928	2.9923	2.9925	2.993	09:51:54
09:51:54	-0.0101	-0.0054	2.9929	2.9922	2.9932	2.9924	2.9924	2.9926	2.9928	2.9922	2.9922	2.9928	09:53:15
09:53:15	-0.01	-0.0055	2.9929	2.9922	2.993	2.9924	2.9923	2.9925	2.9929	2.9924	2.9922	2.9926	09:54:35
09:54:36	-0.0101	-0.0054	2.9928	2.9922	2.9931	2.9925	2.9924	2.9928	2.9929	2.9923	2.9921	2.9929	09:55:56
09:55:56	-0.01	-0.0054	2.9929	2.9921	2.9931	2.9925	2.9924	2.9924	2.9929	2.9922	2.9922	2.9926	09:57:17
09:57:17	-0.0101	-0.0054	2.9929	2.9921	2.993	2.9926	2.9924	2.9925	2.9928	2.9923	2.9921	2.9927	09:58:38
09:58:38	-0.01	-0.0054	2.9929	2.9921	2.9931	2.9925	2.9924	2.9926	2.9929	2.9921	2.9921	2.9928	09:59:58
09:59:59	-0.01	-0.0054	2.9928	2.9921	2.9931	2.9923	2.9925	2.9927	2.9927	2.9923	2.9921	2.9926	10:01:19
10:01:19	-0.01	-0.0053	2.9929	2.9921	2.993	2.9925	2.9923	2.9926	2.9927	2.9921	2.9922	2.9927	10:02:40
10:02:40	-0.01	-0.0054	2.9929	2.9921	2.9931	2.9925	2.9923	2.9925	2.9929	2.9923	2.9922	2.9926	10:04:01
10:04:01	-0.0099	-0.0053	2.9928	2.9921	2.9932	2.9924	2.9924	2.9925	2.9928	2.9921	2.9921	2.9926	10:05:22
10:05:22	-0.0101	-0.0053	2.9928	2.9921	2.993	2.9924	2.9925	2.9925	2.9928	2.9921	2.9921	2.9925	10:06:42
10:06:43	-0.0101	-0.0052	2.9929	2.9921	2.9932	2.9923	2.9923	2.9926	2.9928	2.9923	2.9921	2.9926	10:08:03
10:08:03	-0.0101	-0.0051	2.9929	2.992	2.9932	2.9923	2.9924	2.9925	2.9928	2.9922	2.9922	2.9927	10:09:24
10:09:24	-0.0101	-0.0051	2.9928	2.992	2.9931	2.9925	2.9923	2.9924	2.9929	2.9922	2.9922	2.9926	10:10:45
10:10:45	-0.0101	-0.005	2.9928	2.992	2.9932	2.9925	2.9925	2.9925	2.9927	2.9921	2.9921	2.9926	10:12:06
10:12:06	-0.0101	-0.005	2.9928	2.9921	2.9931	2.9924	2.9924	2.9926	2.9929	2.9922	2.9921	2.9925	10:13:26
10:13:27	-0.0102	-0.005	2.9928	2.992	2.9932	2.9924	2.9921	2.9923	2.9927	2.992	2.9922	2.9928	10:14:47
10:14:47	-0.0102	-0.0049	2.9929	2.9921	2.9933	2.9923	2.9922	2.9923	2.9928	2.9922	2.9922	2.9926	10:16:08
10:16:08	-0.0103	-0.005	2.9928	2.9921	2.9932	2.9924	2.9924	2.9926	2.9927	2.9922	2.992	2.9924	10:17:29

10:17:29	-0.0103	-0.0049	2.9929	2.9921	2.9933	2.9925	2.9924	2.9925	2.9926	2.9921	2.9921	2.9929	10:18:50
10:18:50	-0.0102	-0.0048	2.9927	2.9921	2.9931	2.9923	2.9923	2.9925	2.9927	2.9922	2.9922	2.9927	10:20:10
10:20:11	-0.0102	-0.0048	2.9927	2.9921	2.9931	2.9924	2.9923	2.9927	2.9928	2.9922	2.9921	2.9926	10:21:31
10:21:31	-0.0103	-0.0047	2.9928	2.9921	2.9932	2.9923	2.9923	2.9926	2.9928	2.9923	2.9922	2.9927	10:22:52
10:22:52	-0.0103	-0.0048	2.9929	2.9922	2.9932	2.9924	2.9923	2.9925	2.9928	2.992	2.9921	2.9927	10:24:13
10:24:13	-0.0103	-0.0048	2.9928	2.992	2.9932	2.9923	2.9922	2.9925	2.9927	2.9922	2.9921	2.9925	10:25:33
10:25:34	-0.0103	-0.0048	2.9929	2.992	2.9931	2.9924	2.9923	2.9926	2.9927	2.9922	2.9922	2.9926	10:26:54
10:26:54	-0.0103	-0.0049	2.9929	2.9921	2.993	2.9925	2.9924	2.9925	2.9928	2.992	2.992	2.9925	10:28:15
10:28:15	-0.0102	-0.0048	2.9929	2.9921	2.9932	2.9924	2.9923	2.9926	2.9927	2.9923	2.9922	2.9926	10:29:36
10:29:36	-0.0102	-0.0048	2.9927	2.9921	2.9931	2.9925	2.9923	2.9925	2.9927	2.9921	2.9919	2.9925	10:30:56
10:30:57	-0.0102	-0.0048	2.9929	2.9921	2.9932	2.9925	2.9924	2.9925	2.9928	2.9921	2.9922	2.9925	10:32:17
10:32:18	-0.0104	-0.0048	2.9929	2.9921	2.9931	2.9924	2.9924	2.9926	2.9929	2.9922	2.9919	2.9925	10:33:38
10:33:38	-0.0102	-0.0048	2.9929	2.9921	2.993	2.9925	2.9924	2.9927	2.9928	2.9922	2.992	2.9925	10:34:59
10:34:59	-0.0102	-0.0048	2.9928	2.9921	2.9931	2.9924	2.9923	2.9925	2.9928	2.992	2.992	2.9925	10:36:20
10:36:20	-0.0102	-0.005	2.9928	2.9922	2.9929	2.9923	2.9923	2.9924	2.9929	2.9922	2.9923	2.9926	10:37:41
10:37:41	-0.0104	-0.005	2.9928	2.9921	2.9932	2.9923	2.9923	2.9926	2.9927	2.9922	2.9921	2.9928	10:39:01
10:39:02	-0.0103	-0.0049	2.9928	2.9921	2.9932	2.9923	2.9924	2.9925	2.9928	2.9922	2.9923	2.9926	10:40:22
10:40:22	-0.0104	-0.0051	2.9928	2.9921	2.9931	2.9925	2.9924	2.9926	2.9927	2.9921	2.992	2.9925	10:41:43
10:41:43	-0.0105	-0.0051	2.9927	2.9921	2.9931	2.9924	2.9922	2.9925	2.9928	2.9921	2.9923	2.9926	10:43:03
10:43:04	-0.0104	-0.005	2.9929	2.992	2.9931	2.9924	2.9923	2.9926	2.9927	2.9921	2.9922	2.9925	10:44:24
10:44:25	-0.0104	-0.0052	2.9928	2.9921	2.9932	2.9922	2.9922	2.9925	2.993	2.9922	2.9922	2.9925	10:45:45

10:45:45	-0.0104	-0.0052	2.9928	2.992	2.9932	2.9924	2.9923	2.9925	2.9927	2.9921	2.9922	2.9926	10:47:06
10:47:06	-0.0105	-0.0052	2.9928	2.992	2.9931	2.9923	2.9922	2.9925	2.9927	2.9923	2.9922	2.9925	10:48:27
10:48:27	-0.0104	-0.0052	2.9928	2.992	2.9931	2.9924	2.9922	2.9926	2.9927	2.9922	2.9922	2.9927	10:49:47
10:49:48	-0.0105	-0.0053	2.9929	2.992	2.9932	2.9925	2.9924	2.9925	2.9926	2.992	2.992	2.9926	10:51:08
10:51:09	-0.0105	-0.0053	2.9928	2.992	2.993	2.9923	2.9922	2.9925	2.9927	2.9922	2.9923	2.9926	10:52:29
10:52:29	-0.0104	-0.0053	2.9929	2.9919	2.9932	2.9923	2.9922	2.9925	2.9927	2.9922	2.9923	2.9927	10:53:50
10:53:50	-0.0105	-0.0052	2.9928	2.992	2.993	2.9923	2.9924	2.9925	2.9929	2.9922	2.9922	2.9925	10:55:11
10:55:11	-0.0105	-0.0054	2.9928	2.992	2.993	2.9923	2.9922	2.9925	2.9928	2.9923	2.9921	2.9927	10:56:31
10:56:32	-0.0105	-0.0053	2.9929	2.992	2.993	2.9924	2.9925	2.9926	2.9927	2.9923	2.9922	2.9925	10:57:52
10:57:52	-0.0105	-0.0054	2.9928	2.992	2.9931	2.9924	2.9923	2.9925	2.9927	2.9921	2.9922	2.9927	10:59:13
10:59:13	-0.0106	-0.0054	2.9928	2.9921	2.9929	2.9923	2.9922	2.9926	2.9928	2.9923	2.9923	2.9926	11:00:34
11:00:34	-0.0105	-0.0054	2.9928	2.9921	2.9931	2.9924	2.9923	2.9926	2.9929	2.9923	2.9922	2.9926	11:01:55
11:01:55	-0.0107	-0.0054	2.9928	2.992	2.993	2.9923	2.9922	2.9925	2.9928	2.9922	2.9923	2.9925	11:03:15
11:03:16	-0.0106	-0.0056	2.9929	2.9921	2.9929	2.9923	2.9923	2.9925	2.9928	2.9922	2.9921	2.9926	11:04:36
11:04:36	-0.0106	-0.0056	2.9928	2.9921	2.993	2.9925	2.9923	2.9925	2.9926	2.9921	2.9922	2.9926	11:05:57
11:05:57	-0.0107	-0.0056	2.9928	2.9921	2.993	2.9924	2.9923	2.9926	2.9928	2.9922	2.9921	2.9925	11:07:18
11:07:18	-0.0107	-0.0056	2.9928	2.992	2.9931	2.9924	2.9924	2.9924	2.9927	2.9922	2.9923	2.9926	11:08:38
11:08:39	-0.0108	-0.0056	2.9928	2.9919	2.9932	2.9925	2.9924	2.9926	2.9927	2.9923	2.9922	2.9926	11:09:59
11:09:00	-0.0107	-0.0056	2.9929	2.992	2.993	2.9924	2.9923	2.9924	2.9929	2.9922	2.9922	2.9925	11:11:20
11:11:20	-0.0107	-0.0057	2.9929	2.992	2.9929	2.9924	2.9923	2.9925	2.9928	2.9923	2.9923	2.9927	11:12:41
11:12:41	-0.0108	-0.0058	2.9929	2.9919	2.993	2.9923	2.9923	2.9925	2.9929	2.9923	2.9922	2.9926	11:14:02

11:14:02	-0.0107	-0.0057	2.9928	2.992	2.993	2.9925	2.9923	2.9925	2.9928	2.9922	2.9922	2.9927	11:15:23
11:15:23	-0.0107	-0.0057	2.9928	2.9921	2.9931	2.9924	2.9923	2.9925	2.9928	2.9921	2.9923	2.9926	11:16:43
11:16:44	-0.0107	-0.0059	2.9928	2.9921	2.993	2.9924	2.9924	2.9925	2.9927	2.9921	2.9921	2.9924	11:18:04
11:18:05	-0.0108	-0.0059	2.9929	2.992	2.9931	2.9925	2.9921	2.9923	2.9926	2.9923	2.9923	2.9927	11:19:25
11:19:25	-0.0108	-0.006	2.9928	2.9921	2.9929	2.9924	2.9923	2.9924	2.9928	2.9922	2.9922	2.9927	11:20:46
11:20:46	-0.0107	-0.0061	2.9928	2.992	2.993	2.9925	2.9924	2.9924	2.9928	2.9923	2.9921	2.9925	11:22:07
11:22:07	-0.0107	-0.0061	2.9928	2.992	2.9931	2.9924	2.9923	2.9925	2.9928	2.9921	2.9922	2.9925	11:23:27
11:23:28	-0.0107	-0.0062	2.9928	2.9919	2.993	2.9925	2.9924	2.9926	2.9927	2.9922	2.9921	2.9925	11:24:48
11:24:49	-0.0107	-0.0062	2.9928	2.992	2.9929	2.9925	2.9924	2.9925	2.9928	2.9922	2.9921	2.9926	11:26:09
11:26:09	-0.0107	-0.0062	2.9929	2.9921	2.9931	2.9925	2.9924	2.9925	2.9928	2.9921	2.9921	2.9926	11:27:30
11:27:30	-0.0108	-0.0062	2.9928	2.992	2.9931	2.9925	2.9923	2.9925	2.9928	2.9921	2.9921	2.9925	11:28:51
11:28:51	-0.0108	-0.0063	2.9928	2.992	2.993	2.9925	2.9923	2.9925	2.9928	2.9921	2.9922	2.9926	11:30:12
11:30:12	-0.0107	-0.0063	2.9928	2.992	2.9929	2.9924	2.9922	2.9924	2.9927	2.9923	2.9922	2.9926	11:31:32
11:31:33	-0.0107	-0.0065	2.9928	2.992	2.9929	2.9924	2.9923	2.9925	2.9927	2.9921	2.9923	2.9924	11:32:53
11:32:53	-0.0107	-0.0065	2.9929	2.992	2.993	2.9924	2.9924	2.9925	2.9927	2.9921	2.9921	2.9925	11:34:14
11:34:14	-0.0107	-0.0065	2.9928	2.992	2.9928	2.9924	2.9924	2.9927	2.9928	2.9922	2.9922	2.9925	11:35:35
11:35:35	-0.0106	-0.0066	2.9928	2.992	2.993	2.9925	2.9924	2.9924	2.9927	2.9922	2.9922	2.9927	11:36:56
11:36:56	-0.0106	-0.0067	2.9928	2.992	2.993	2.9925	2.9924	2.9925	2.9928	2.9922	2.9921	2.9926	11:38:16
11:38:17	-0.0106	-0.0067	2.9928	2.992	2.9933	2.9926	2.9924	2.9924	2.9927	2.9921	2.9921	2.9927	11:39:37
11:39:37	-0.0105	-0.0069	2.9928	2.992	2.9929	2.9926	2.9924	2.9925	2.9927	2.9921	2.9921	2.9926	11:40:58
11:40:58	-0.0106	-0.007	2.9927	2.992	2.9931	2.9925	2.9925	2.9925	2.9928	2.992	2.9921	2.9925	11:42:19

11:42:19	-0.0106	-0.007	2.9928	2.9921	2.9931	2.9926	2.9925	2.9926	2.9928	2.9922	2.9919	2.9925	11:43:40
11:43:40	-0.0106	-0.0071	2.9928	2.9921	2.9931	2.9926	2.9925	2.9924	2.9927	2.992	2.992	2.9927	11:45:00
11:45:01	-0.0105	-0.0072	2.9928	2.9921	2.993	2.9925	2.9925	2.9925	2.9928	2.9923	2.9921	2.9926	11:46:21
11:46:21	-0.0105	-0.0073	2.9928	2.9921	2.9931	2.9925	2.9925	2.9924	2.9929	2.9922	2.9919	2.9925	11:47:42
11:47:42	-0.0106	-0.0075	2.9928	2.9921	2.9931	2.9926	2.9925	2.9926	2.9928	2.9921	2.9919	2.9924	11:49:03
11:49:03	-0.0105	-0.0075	2.9928	2.9921	2.993	2.9926	2.9925	2.9925	2.9928	2.9921	2.992	2.9926	11:50:23
11:50:24	-0.0105	-0.0075	2.9928	2.992	2.993	2.9925	2.9923	2.9924	2.9927	2.9921	2.9922	2.9927	11:51:44
11:51:44	-0.0105	-0.0077	2.9927	2.992	2.9929	2.9926	2.9925	2.9927	2.9928	2.9921	2.9919	2.9925	11:53:05
11:53:05	-0.0105	-0.0079	2.9928	2.9921	2.9931	2.9925	2.9925	2.9925	2.9927	2.9921	2.9919	2.9925	11:54:26
11:54:26	-0.0105	-0.0078	2.9928	2.9921	2.9929	2.9925	2.9924	2.9926	2.9927	2.9921	2.992	2.9926	11:55:46
11:55:47	-0.0104	-0.008	2.9928	2.992	2.9929	2.9926	2.9926	2.9927	2.9928	2.992	2.992	2.9925	11:57:07
11:57:08	-0.0104	-0.0081	2.9929	2.9921	2.9932	2.9924	2.9923	2.9924	2.9927	2.9921	2.992	2.9927	11:58:28
11:58:28	-0.0105	-0.0081	2.9928	2.992	2.993	2.9925	2.9924	2.9926	2.9928	2.992	2.9919	2.9924	11:59:49
11:59:49	-0.0105	-0.0082	2.9928	2.9921	2.993	2.9923	2.9925	2.9925	2.9928	2.992	2.992	2.9926	12:01:10
12:01:10	-0.0105	-0.0083	2.9928	2.992	2.9931	2.9925	2.9923	2.9924	2.9927	2.9921	2.992	2.9925	12:02:30
12:02:31	-0.0106	-0.0083	2.9928	2.9921	2.9931	2.9926	2.9923	2.9926	2.9927	2.992	2.992	2.9925	12:03:51
12:03:51	-0.0105	-0.0084	2.9927	2.992	2.9931	2.9924	2.9923	2.9925	2.9928	2.9921	2.992	2.9926	12:05:12

E.2 19 mm diameter ring

START	XSTYLUSOS	YSTYLUSOS	XR	YR	30R	60R	120R	150R	210R	240R	300R	330R	END
14:03:43	-0.0089	-0.0056	2.9909	2.9908	2.991	2.9907	2.9912	2.9909	2.9908	2.9908	2.9909	2.9908	14:04:56
14:04:57	-0.0086	-0.0057	2.9909	2.9906	2.9907	2.9907	2.9911	2.9909	2.9907	2.9909	2.9906	2.9907	14:06:10
14:06:10	-0.0087	-0.0057	2.9912	2.9907	2.991	2.991	2.9913	2.991	2.9906	2.9907	2.9907	2.9907	14:07:24
14:07:24	-0.0087	-0.0056	2.9911	2.9907	2.991	2.9908	2.9913	2.9908	2.9909	2.9909	2.9907	2.9907	14:08:37
14:08:37	-0.0085	-0.0056	2.9909	2.9907	2.991	2.9907	2.9912	2.9907	2.9907	2.9909	2.9908	2.9906	14:09:51
14:09:51	-0.0087	-0.0056	2.9909	2.9907	2.991	2.9909	2.9914	2.9907	2.9908	2.9907	2.9907	2.9906	14:11:05
14:11:05	-0.0085	-0.0056	2.9909	2.9907	2.991	2.9909	2.9911	2.9907	2.9908	2.9907	2.9909	2.9909	14:12:18
14:12:19	-0.0084	-0.0055	2.9909	2.9907	2.991	2.9908	2.9912	2.9906	2.9908	2.9908	2.9908	2.9907	14:13:32
14:13:32	-0.0085	-0.0055	2.991	2.9908	2.9909	2.9908	2.9913	2.9907	2.9906	2.9908	2.9908	2.9908	14:14:46
14:14:46	-0.0086	-0.0055	2.9911	2.9907	2.991	2.9909	2.9912	2.9908	2.9907	2.9907	2.9909	2.9908	14:16:00
14:16:00	-0.0085	-0.0055	2.991	2.9907	2.991	2.9909	2.9912	2.9907	2.9907	2.9908	2.9908	2.9908	14:17:13
14:17:14	-0.0085	-0.0054	2.991	2.9907	2.9911	2.9908	2.9912	2.9907	2.9907	2.9908	2.9909	2.9908	14:18:27
14:18:27	-0.0085	-0.0053	2.9911	2.9907	2.9911	2.9909	2.9911	2.9906	2.9907	2.9908	2.9908	2.9909	14:19:41
14:19:41	-0.0085	-0.0052	2.991	2.9908	2.991	2.9909	2.9913	2.9909	2.9906	2.9908	2.9907	2.9907	14:20:54
14:20:55	-0.0085	-0.0052	2.991	2.9907	2.9911	2.9908	2.9913	2.9907	2.9906	2.9908	2.9908	2.9907	14:22:08
14:22:08	-0.0085	-0.0052	2.991	2.9907	2.991	2.9908	2.9912	2.9908	2.9907	2.9907	2.9909	2.9906	14:23:22
14:23:22	-0.0085	-0.0051	2.991	2.9907	2.991	2.9909	2.9912	2.9907	2.9908	2.9908	2.9908	2.9908	14:24:35
14:24:36	-0.0085	-0.0051	2.9909	2.9907	2.9909	2.9908	2.9911	2.9908	2.9906	2.9908	2.9907	2.9906	14:25:49
14:25:49	-0.0085	-0.005	2.991	2.9908	2.991	2.9909	2.9913	2.9908	2.9907	2.9907	2.9909	2.9907	14:27:03
14:27:03	-0.0085	-0.0051	2.9909	2.9908	2.9909	2.9909	2.9913	2.9909	2.9908	2.9908	2.9909	2.9908	14:28:17
14:28:17	-0.0084	-0.0049	2.9909	2.9907	2.9909	2.9908	2.9911	2.9908	2.9906	2.9908	2.9909	2.9908	14:29:30
14:29:31	-0.0086	-0.005	2.991	2.9907	2.991	2.9909	2.9912	2.9908	2.9906	2.9908	2.9908	2.9907	14:30:44
14:30:44	-0.0084	-0.005	2.9909	2.9907	2.9909	2.9908	2.9913	2.9909	2.9907	2.9908	2.9907	2.9907	14:31:58
14:31:58	-0.0084	-0.0049	2.9909	2.9907	2.991	2.9907	2.9913	2.9907	2.9907	2.9909	2.991	2.9908	14:33:12

14:33:12	-0.0084	-0.0049	2.991	2.9908	2.991	2.9908	2.9912	2.9906	2.9907	2.9907	2.9908	2.9909	14:34:25
14:34:26	-0.0084	-0.0049	2.9909	2.9908	2.991	2.9909	2.9914	2.9906	2.9906	2.9907	2.9908	2.9908	14:35:39
14:35:39	-0.0085	-0.0048	2.9909	2.9908	2.991	2.9908	2.9913	2.9907	2.9907	2.9907	2.9908	2.9908	14:36:53
14:36:53	-0.0084	-0.0048	2.991	2.9908	2.9909	2.9909	2.9913	2.9909	2.9906	2.9908	2.9908	2.9907	14:38:06
14:38:07	-0.0084	-0.0049	2.991	2.9908	2.991	2.9909	2.9915	2.9908	2.9908	2.9908	2.9909	2.9908	14:39:20
14:39:20	-0.0083	-0.005	2.991	2.9907	2.991	2.9908	2.9911	2.9907	2.9908	2.9908	2.9909	2.991	14:40:34
14:40:34	-0.0083	-0.0049	2.9909	2.9908	2.991	2.9909	2.9911	2.9907	2.9908	2.9907	2.9908	2.9908	14:41:48
14:41:48	-0.0084	-0.0048	2.991	2.9907	2.991	2.9908	2.9913	2.9906	2.9906	2.9907	2.9908	2.9909	14:43:01
14:43:01	-0.0083	-0.0049	2.991	2.9907	2.9911	2.9909	2.9914	2.9908	2.9906	2.9907	2.9907	2.9907	14:44:15
14:44:15	-0.0084	-0.0049	2.991	2.9908	2.9909	2.9909	2.9912	2.9907	2.9908	2.9908	2.9909	2.9908	14:45:29
14:45:29	-0.0084	-0.0049	2.991	2.9908	2.9909	2.9908	2.9913	2.991	2.9908	2.9908	2.9907	2.9908	14:46:42
14:46:43	-0.0083	-0.0049	2.991	2.9907	2.991	2.9909	2.9913	2.9907	2.9907	2.9907	2.9907	2.9907	14:47:56
14:47:56	-0.0083	-0.0048	2.9909	2.9907	2.9909	2.9908	2.9912	2.9906	2.9908	2.9908	2.9908	2.9907	14:49:10
14:49:10	-0.0084	-0.0049	2.991	2.9907	2.9908	2.9908	2.9912	2.9908	2.9907	2.9908	2.9908	2.9909	14:50:23
14:50:24	-0.0084	-0.0048	2.991	2.9908	2.991	2.9908	2.9911	2.9905	2.9906	2.9906	2.9907	2.9909	14:51:37
14:51:38	-0.0084	-0.0049	2.9909	2.9907	2.9909	2.9907	2.9911	2.9907	2.9907	2.9909	2.9908	2.9907	14:52:51
14:52:51	-0.0084	-0.0049	2.991	2.9907	2.9909	2.9907	2.991	2.9907	2.9907	2.9908	2.9909	2.9908	14:54:04
14:54:05	-0.0084	-0.005	2.991	2.9907	2.991	2.9908	2.9912	2.9907	2.9906	2.9908	2.9907	2.9908	14:55:18
14:55:19	-0.0083	-0.005	2.9909	2.9907	2.9909	2.9908	2.9912	2.9907	2.9907	2.9907	2.9907	2.9907	14:56:32
14:56:32	-0.0084	-0.005	2.9909	2.9907	2.9911	2.9909	2.9911	2.9907	2.9907	2.9908	2.9909	2.9909	14:57:46
14:57:46	-0.0083	-0.005	2.9911	2.9907	2.991	2.9908	2.9912	2.9908	2.9907	2.9908	2.9907	2.9907	14:58:59
14:59:00	-0.0083	-0.005	2.9909	2.9907	2.991	2.9908	2.9911	2.9907	2.9908	2.9908	2.9908	2.9907	15:00:13
15:00:13	-0.0084	-0.0051	2.991	2.9907	2.9909	2.9907	2.9912	2.9908	2.9907	2.9909	2.9909	2.9908	15:01:27
15:01:27	-0.0083	-0.0051	2.991	2.9908	2.991	2.9908	2.9912	2.9908	2.9907	2.9908	2.9908	2.9907	15:02:40
15:02:41	-0.0083	-0.0051	2.991	2.9907	2.991	2.9909	2.9913	2.9907	2.9906	2.9907	2.9908	2.9907	15:03:54
15:03:54	-0.0083	-0.0051	2.9909	2.9908	2.991	2.9909	2.9911	2.9907	2.9906	2.9908	2.9908	2.9907	15:05:08
15:05:08	-0.0083	-0.0052	2.991	2.9907	2.9911	2.9908	2.9912	2.9908	2.9907	2.9907	2.9908	2.9908	15:06:21

15:06:22	-0.0083	-0.0052	2.991	2.9908	2.9909	2.9907	2.9911	2.9907	2.9907	2.9908	2.9909	2.9908	15:07:35
15:07:35	-0.0083	-0.0053	2.9909	2.9907	2.991	2.9908	2.9911	2.9906	2.9906	2.9909	2.9909	2.9907	15:08:49
15:08:49	-0.0083	-0.0053	2.991	2.9907	2.991	2.9909	2.9913	2.9908	2.9907	2.9907	2.9907	2.9907	15:10:03
15:10:03	-0.0083	-0.0052	2.991	2.9906	2.991	2.9908	2.9911	2.9907	2.9907	2.9907	2.9907	2.9906	15:11:16
15:11:17	-0.0083	-0.0053	2.991	2.9908	2.9909	2.9908	2.9911	2.9907	2.9907	2.9908	2.9908	2.9908	15:12:30
15:12:30	-0.0084	-0.0054	2.9909	2.9908	2.991	2.9907	2.9911	2.9908	2.9908	2.991	2.9909	2.9907	15:13:44
15:13:44	-0.0083	-0.0053	2.9909	2.9908	2.9909	2.9908	2.9911	2.9908	2.9908	2.9908	2.9908	2.9907	15:14:57
15:14:58	-0.0083	-0.0054	2.9911	2.9907	2.9909	2.9908	2.9912	2.9908	2.9907	2.9908	2.9908	2.9906	15:16:11
15:16:11	-0.0083	-0.0054	2.9909	2.9907	2.991	2.9908	2.9911	2.9909	2.9907	2.9909	2.9909	2.9906	15:17:25
15:17:25	-0.0083	-0.0054	2.991	2.9907	2.9911	2.9909	2.9912	2.9908	2.9907	2.9908	2.9908	2.9908	15:18:38
15:18:39	-0.0083	-0.0055	2.991	2.9907	2.991	2.9906	2.9911	2.9907	2.9908	2.9908	2.9908	2.9907	15:19:52
15:19:53	-0.0084	-0.0055	2.9909	2.9907	2.991	2.9908	2.9912	2.9909	2.9907	2.9908	2.9907	2.9907	15:21:06
15:21:06	-0.0084	-0.0054	2.991	2.9906	2.9909	2.9908	2.9911	2.9908	2.9907	2.9907	2.9907	2.9906	15:22:20
15:22:20	-0.0084	-0.0054	2.991	2.9907	2.9909	2.9907	2.9911	2.9907	2.9907	2.9907	2.9907	2.9906	15:23:33
15:23:34	-0.0084	-0.0054	2.9908	2.9907	2.9911	2.9909	2.9913	2.9907	2.9906	2.9908	2.9907	2.9907	15:24:47
15:24:48	-0.0085	-0.0054	2.991	2.9906	2.991	2.9909	2.9911	2.9908	2.9907	2.9908	2.9908	2.9907	15:26:01
15:26:01	-0.0084	-0.0054	2.9909	2.9906	2.991	2.9908	2.9911	2.9909	2.9907	2.9907	2.9907	2.9907	15:27:15
15:27:15	-0.0084	-0.0054	2.9909	2.9907	2.991	2.9907	2.9911	2.9909	2.9907	2.9908	2.9907	2.9907	15:28:28
15:28:28	-0.0084	-0.0054	2.9909	2.9907	2.991	2.9908	2.991	2.9908	2.9906	2.9907	2.9907	2.9907	15:29:42
15:29:42	-0.0085	-0.0054	2.991	2.9907	2.991	2.9907	2.9912	2.9909	2.9907	2.9908	2.9908	2.9906	15:30:56
15:30:56	-0.0085	-0.0053	2.9909	2.9906	2.991	2.9907	2.9912	2.9908	2.9907	2.9907	2.9908	2.9906	15:32:09
15:32:10	-0.0085	-0.0054	2.991	2.9907	2.991	2.9909	2.9912	2.9907	2.9906	2.9907	2.9909	2.9907	15:33:23
15:33:23	-0.0085	-0.0054	2.991	2.9906	2.9911	2.9907	2.9911	2.9908	2.9907	2.9908	2.9908	2.9906	15:34:37
15:34:37	-0.0085	-0.0053	2.9909	2.9907	2.9911	2.9907	2.9911	2.9908	2.9906	2.9908	2.9908	2.9907	15:35:50
15:35:51	-0.0086	-0.0054	2.9909	2.9907	2.991	2.9909	2.991	2.9907	2.9906	2.9907	2.9908	2.9907	15:37:04
15:37:05	-0.0086	-0.0054	2.991	2.9908	2.9911	2.9909	2.9911	2.9908	2.9905	2.9907	2.9908	2.9908	15:38:18
15:38:18	-0.0085	-0.0054	2.9909	2.9907	2.9911	2.9908	2.991	2.9907	2.9906	2.9908	2.9908	2.9907	15:39:32

15:39:32	-0.0084	-0.0054	2.9909	2.9908	2.9911	2.9907	2.991	2.9907	2.9906	2.9909	2.9909	2.9907	15:40:45
15:40:46	-0.0085	-0.0053	2.9909	2.9907	2.9912	2.9908	2.9911	2.991	2.9906	2.9908	2.9906	2.9907	15:41:59
15:41:59	-0.0084	-0.0055	2.9909	2.9907	2.991	2.9908	2.9912	2.9909	2.9906	2.9909	2.9906	2.9906	15:43:13
15:43:13	-0.0085	-0.0055	2.991	2.9908	2.9909	2.9907	2.9911	2.9909	2.9908	2.9908	2.9908	2.9906	15:44:26
15:44:27	-0.0085	-0.0055	2.991	2.9907	2.9909	2.9907	2.9911	2.9907	2.9907	2.9909	2.9909	2.9907	15:45:40
15:45:41	-0.0085	-0.0055	2.991	2.9907	2.991	2.9907	2.9911	2.9908	2.9906	2.9908	2.9907	2.9908	15:46:54
15:46:54	-0.0084	-0.0055	2.9909	2.9908	2.991	2.9907	2.9911	2.9907	2.9905	2.9908	2.9907	2.9906	15:48:08
15:48:08	-0.0085	-0.0055	2.991	2.9907	2.991	2.9906	2.9912	2.9909	2.9908	2.9907	2.9907	2.9907	15:49:21
15:49:22	-0.0084	-0.0056	2.9909	2.9907	2.9909	2.9908	2.9912	2.9909	2.9906	2.9908	2.9908	2.9906	15:50:35
15:50:35	-0.0084	-0.0054	2.991	2.9907	2.9909	2.9908	2.9911	2.9908	2.9906	2.9908	2.9908	2.9907	15:51:49
15:51:49	-0.0085	-0.0055	2.991	2.9907	2.9909	2.9908	2.9911	2.9909	2.9906	2.9908	2.9908	2.9907	15:53:02
15:53:03	-0.0084	-0.0056	2.9911	2.9907	2.9911	2.9908	2.9912	2.9909	2.9907	2.9908	2.9907	2.9906	15:54:16
15:54:17	-0.0084	-0.0056	2.9909	2.9907	2.991	2.9907	2.9911	2.9909	2.9907	2.9908	2.9908	2.9906	15:55:30
15:55:30	-0.0084	-0.0057	2.9908	2.9907	2.991	2.9908	2.9909	2.9907	2.9906	2.9908	2.9908	2.9909	15:56:44
15:56:44	-0.0084	-0.0057	2.991	2.9907	2.991	2.9907	2.9911	2.9908	2.9908	2.9908	2.9907	2.9906	15:57:57
15:57:58	-0.0084	-0.0057	2.991	2.9907	2.991	2.9908	2.9912	2.9909	2.9906	2.9907	2.9907	2.9907	15:59:11
15:59:11	-0.0084	-0.0057	2.991	2.9907	2.9908	2.9908	2.9911	2.9909	2.9907	2.9908	2.9907	2.9907	16:00:25
16:00:25	-0.0085	-0.0058	2.991	2.9907	2.991	2.9908	2.9911	2.9909	2.9906	2.9908	2.9909	2.9909	16:01:39
16:01:39	-0.0083	-0.0058	2.991	2.9906	2.9911	2.9908	2.9911	2.9909	2.9906	2.9908	2.9908	2.9906	16:02:52
16:02:53	-0.0084	-0.0058	2.9909	2.9907	2.9911	2.9909	2.9912	2.9909	2.9905	2.9908	2.9907	2.9907	16:04:06
16:04:06	-0.0083	-0.0058	2.991	2.9907	2.9909	2.9907	2.9911	2.9908	2.9909	2.9908	2.9909	2.9908	16:05:20
16:05:20	-0.0083	-0.006	2.9909	2.9907	2.991	2.9909	2.9911	2.9909	2.9906	2.9909	2.9908	2.9908	16:06:33